Supplementary Materials for

Catalytic olefin metathesis in blood

Igor Nasibullin, Hiromasa Yoshioka, Akari Mukaimine, Akiko Nakamura, Yuriko Kusakari, Tsung-Che Chang, Katsunori Tanaka

Correspondence to: chang.t.ac@m.titech.ac.jp (T.-C. C.) and kotzenori@riken.jp (K. T.)

This PDF file includes:

General information. General reagents and buffer components were purchased from Sigma-Aldrich, Fisher Scientific, Alfa Aesar, TCI, or Wako Chemicals without further purification. Human Serum Albumin (lyophilized powder, essentially fatty acid free) was purchased from Sigma-Aldrich (Prod# A1887). Sheep blood in Alsevers was purchased from Funakoshi (Rockland Immunochemicals, Inc.) (Prod# R311-0100). All experiments dealing with air- and moisture-sensitive compounds were conducted under an atmosphere of dry nitrogen. Anhydrous solvents were used as received, which include tetrahydrofuran (anhydrous; FUJIFILM Wako Pure Chemical), dichloromethane (anhydrous; FUJIFILM Wako Pure Chemical), benzene (anhydrous; FUJIFILM Wako Pure Chemical), 1,4-dioxane (anhydrous; FUJIFILM Wako Pure Chemical), acetone (anhydrous; FUJIFILM Wako Pure Chemical), *N,N*-dimethylformamide (anhydrous; FUJIFILM Wako Pure Chemical) and chloroform (anhydrous; FUJIFILM Wako Pure Chemical). TLC analyses (F-254) were performed with 60 Å silica gel from Merck. Ultrapure water used for all synthetic experiments described in this paper was obtained from a Milli-Q Advantage® A10 Water Purification System sold by Merck Millipore (Burlington, USA). In addition, Amicon® Ultra Centrifugal Filters (30 kDa) and Durapore PVDF 0.45 μm® filters were also purchased from by Merck Millipore (Burlington, USA). All animal procedures were performed in accordance with the Guidelines for Care and Use of Laboratory Animals of RIKEN and approved by the Animal Ethics Committee of RIKEN (W2019-2-049).

Nuclear magnetic resonance (NMR) spectroscopy. ^{1}H, ^{19}F and ^{13}C NMR spectra were measured on JNM-ECZ400 (399 MHz) instrument or JNM-ECX400 (392 MHz) or JNM-ECZ600R/S1 (600 MHz) instrument with the solvent peaks as internal standards: δH 0.00 for TMS, δH 7.26 and δC 77.16 for $CDCl_3$.

Mass spectrometry (MS). For chemical synthesis, high-resolution mass spectra (HRMS) were measured on a Bruker MicroTOF-QIII spectrometer by electron spray ionization time-of-flight (ESI-TOF-MS) or a JMS-T100GCV (JEOL) spectrometer by electron ionization time-of-flight mass spectrometer (EI-TOF-MS) or JMS-T100GCV (JEOL) by field desorption time-of-flight mass spectrometer FD-TOF-MS). High weight mass characterizations (i.e. proteins) were done using matrix-assisted laser desorption ionization (MALDI-TOF) mass spectrometry analysis on a Shimadzu Benchtop Linear MALDI-8020 Mass Spectrometer. Sample preparations used sinapic acid as a matrix.

HPLC analysis. To identify compounds from reaction mixtures, reverse-phase HPLC was used with a Shimadzu system consisting of two LC-20AP pumps, an SPD-20AV photodiode array detector. The column was an analytical 4.6 × 250 mm Cosmosil 5C18-AR-300 from Nacalai Tesque. Samples were eluted using a combination of mobile phases A (H_2O with or w/o 0.1% TFA) and B (acetonitrile with or w/o 0.1% TFA). Normal-phase HPLC analysis was used with a Shimadzu system consisting of two LC-20AD pumps, an SPD-20AV photodiode array detector, a CTO-20A column oven. The column was an analytical Inert sil Diol 3 μm, 4.6 × 250 mm from GL sciences. Samples were eluted using a combination of mobile phase C (hexane for HPLC grade) and D (ethanol for HPLC grade). For absorbance, the detector was set to 220 and 254 nm. The HPLC methods outlined in Table S1-2 were used to identify products. Product peaks were identified by retention times and mass spectrometry analysis. Products peaks were integrated and then compared with calibration curves (Fig. S6-42) to quantify HPLC yields. Example HPLC traces of reaction mixtures, along with their corresponding product and substrate standards are shown in Fig. S43-80.

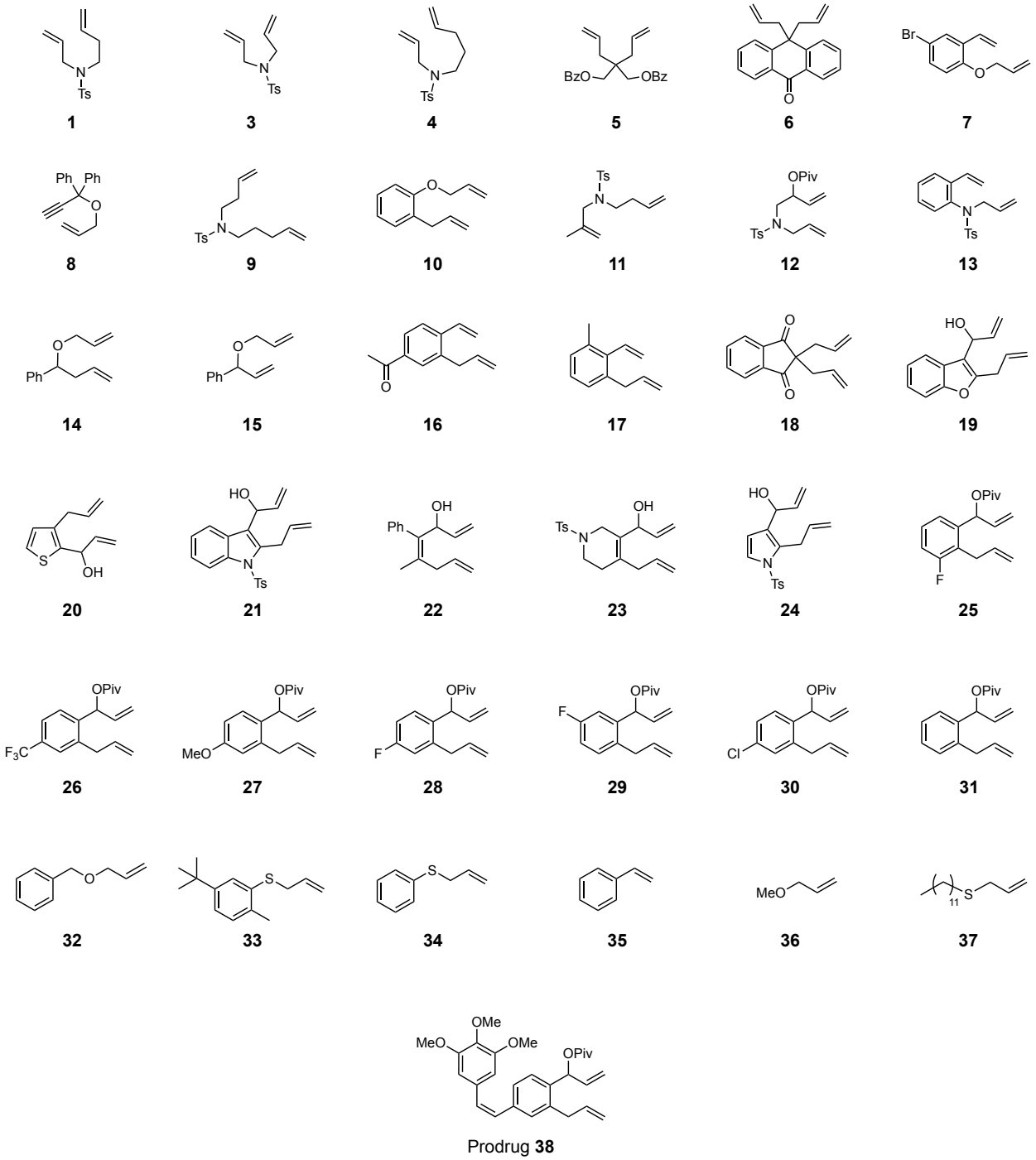

Fig. S1. The list of substrates used in the study.

Preparation of substrates

The substrates used in the study were depicted in Fig. S1. Substrates **1**[1], **3-5**[1], **6**[2], **7**[3], **8**[1], **9**[4], **10**[5], **11**[6], **13**[7], **14**[8], **15**[9], **16-17**[10], **18**[11], **19-22**[12], **31**[12], **32**[13], **37**[14], and prodrug **38**[12] were prepared according to these previous references. Substrates **34-36** were purchased from Tokyo chemical industry CO., Ltd. (**34**: Prod# A1442; **35**: Prod# S0095; **36**: Prod# A1983). Substrates **12**, **23-30**, and **33** were synthesized by the following protocols.

General protocols for synthesis of substrates 12 and 23-30.

General method A for protection with trimethyl orthoformate

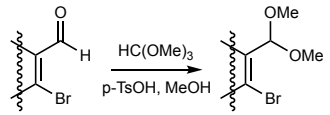

A two-necked round-bottom flask was charged with an aromatic aldehyde (1.0 eq) in anhydrous MeOH (Concentration based on the aldehyde compound: 0.25 M) and $HC(OMe)_3$ (10.0 eq) under N_2 atmosphere, followed by addition of *p*-TsOH·H_2O (1 mol%). The reaction mixture was stirred at room temperature for 2 hours. After that, the reaction mixture was quenched with sat. aq. $NaHCO_3$ solution and the solvent was removed under vacuum. The obtained residue was dissolved in a water/EtOAc (1/1) mixture, and the aqueous layer was extracted with EtOAc three times. The combined organic layers were washed with brine, dried over Na_2SO_4, and concentrated under vacuum. The crude product was purified by silica gel column chromatography using a hexane/EtOAc eluent mixture to give the desired dimethyl acetal compound.

General method B for allylation via Suzuki-Miyaura cross-coupling

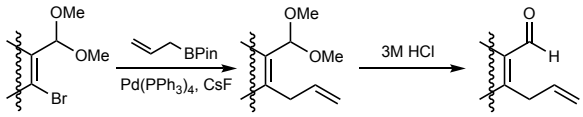

In a dried two-necked round-bottom flask, CsF (4.0 eq) and $Pd(PPh_3)_4$ (10 mol%) were dissolved in anhydrous 1,4-dioxane (Concentration based on the acetal compound: 0.05 M) under N_2 atmosphere, followed by dropwise adding a mixture solution of bromo dimethyl acetal (1.0 eq) and allylboronic acid pinacol ester (2.0 eq) dissolved in anhydrous 1,4-dioxane. The resulting yellow reaction mixture was refluxed for 15 hours. After that, the reaction mixture was diluted with EtOAc, and the resulting suspension was filtered through a short silica gel pad. The obtained filtrate was concentrated under vacuum and purified by silica gel column chromatography using a hexane/EtOAc eluent mixture to give the desired allylated product.

For acetal deprotection, allylated product was dissolved in THF (Concentration based on the allylated product: 0.1 M) and treated with 3 M aqueous solution of HCl. The mixture was stirred for 2 hours at room temperature, followed by quenching slowly with saturated $NaHCO_3$ aqueous solution. The obtained solution was diluted with water and extracted with EtOAc three times. The organic layers were combined and washed with brine, dried over Na_2SO_4 and concentrated to dryness under vacuum. The obtained aldehyde was used for the next step without additional purification.

General method C for Grignard reaction

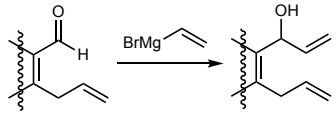

In a dried round-bottom flask, the aldehyde (1.0 eq) was dissolved in anhydrous THF (Concentration based on the aldehyde: 0.2 M) and cooled down to –20 °C. The vinyl magnesium bromide (1.5 eq, 1.0 M in THF) was added in dropwise fashion under N_2 atmosphere and the mixture was stirred at room temperature for 3 hours. The reaction mixture was then quenched with saturated NH_4Cl aqueous solution, followed by extracting with EtOAc three times. The combined organic layers were washed with brine, dried over Na_2SO_4, concentrated under vacuum. The residue was purified by silica gel column chromatography using a hexane/EtOAc eluent mixture to give the desired hydroxyl compound.

General method D for pivalate esters synthesis

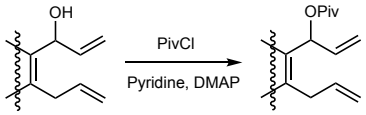

A two-necked round-bottom flask was charged with hydroxyl compound (1.0 eq) in anhydrous CH_2Cl_2, followed by addition of DMAP (0.2 eq) and pyridine (1.0 eq) at r.t. under an N_2 atmosphere. Then, pivaloyl chloride (2.3 eq) was added in dropwise fashion at 0 °C. After that, the reaction mixture was refluxed for overnight (50 °C of oil bath). After cooling down to r.t., the solvent of reaction mixture was removed under vacuum. The residue was redissolved in a mixture of EtOAc/1 M HCl aqueous solution. The aqueous layer was extracted three times with EtOAc, then combined organic fractions was neutralized with saturated $NaHCO_3$ aqueous solution, followed by washing with brine, and dried over Na_2SO_4. The crude product was purified by silica gel column chromatography using a Hexane/EtOAc eluent mixture to give the desired ester compound.

Preparation of 12

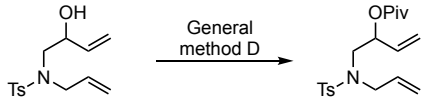

S1 **12**

1-((N-allyl-4-tosyl)but-3-en-2-yl pivalate 12. Substrate **12** was prepared according to general method D using the reported compounds **S1**[15] (97.0 mg, 0.34 mmol)**,** pivaloyl chloride (94 mg, 0.78 mmol), pyridine (27 mg, 0.34 mmol) and DMAP (8.3 mg, 0.07 mmol). The crude product was purified by silica gel column chromatography using a hexane/EtOAc gradient from 9:1 to 8:2 to afford **12** (70 mg, 56%) as a colorless oil.

^{1}H NMR (392 MHz, $CDCl_3$): δ 7.69 (dt, J = 8.5, 1.8 Hz, 2H), 7.30 (d, J = 8.1 Hz, 2H), 5.77 (ddd, J = 16.9, 10.8, 5.8 Hz, 1H), 5.53 (ddt, J = 17.1, 10.3, 6.7 Hz, 1H), 5.45–5.40 (m, 1H), 5.29 (dt, J = 17.2, 1.2 Hz, 1H), 5.23 (dt, J = 10.5, 1.2 Hz, 1H), 5.21–5.14 (m, 2H), 3.95–3.81 (m, 2H), 3.41 (dd, J = 14.6, 8.3 Hz, 1H), 3.26 (dd, J = 14.6, 4.7 Hz, 1H), 2.43 (s, 3H), 1.21 (s, 9H).

^{13}C NMR (99 MHz, $CDCl_3$): δ 177.6, 143.5, 137.2, 133.9, 132.6, 129.9, 127.3, 119.7, 118.3, 71.8, 51.4, 49.7, 38.9, 27.3, 21.6.

HRMS (ESI): m/z $[M+H]^+$ calcd for $C_{19}H_{28}NO_4S^+$: 366.1734; found 366.1705.

Preparation of 23

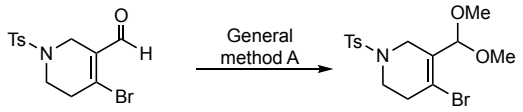

S2 **S3**

4-bromo-5-(dimethoxymethyl)-1-tosyl-1,2,3,6-tetrahydropyridine S3. Compound **S3** was prepared according to general method A using the reported aldehyde[16] (310 mg, 0.9 mmol, 1.0), $HC(OMe)_3$ (954 mg, 9.0 mmol) and *p*-TsOH·H_2O (2 mg, 0.009 mmol). The crude product was purified by silica gel column chromatography using a hexane/EtOAc gradient from 9:1 to 8:2 to afford **S3** as a colorless oil (374 mg, quant.).

^{1}H NMR (392 MHz, $CDCl_3$): δ 7.67 (d, J = 8.5 Hz, 2H), 7.32 (d, J = 8.5 Hz, 2H), 5.14 (s, 1H), 3.71 (t, J = 2.5 Hz, 2H), 3.37 (s, 6H), 3.23 (t, J = 5.8 Hz, 2H), 2.67 (tt, J = 5.8, 2.7 Hz, 2H), 2.43 (s, 3H).

^{13}C NMR (100 MHz, $CDCl_3$): δ 143.9, 133.3, 130.6, 129.9, 127.8, 119.6, 104.9, 55.3, 44.9, 44.1, 36.1, 21.6.

HRMS (FD): m/z $[M]^+$ calcd. for $C_{15}H_{20}BrNO_4S^+$: 389.0296; found 389.0298.

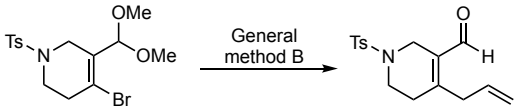

S3 **S4**

4-allyl-1-tosyl-1,2,5,6-tetrahydropyridine-3-carbaldehyde S4. Compound **S4** was prepared according to general method B using **S3** (374 mg, 0.96 mmol), allylBPin (322 mg, 1.92 mmol), $Pd(PPh_3)_4$ (111 mg, 0.096 mmol) and CsF (580 mg, 3.84 mmol). The allylated product was purified by silica gel column chromatography using a hexane/EtOAc gradient from 75/25 to 60/40. After deprotection step, desired aldehyde **S4** was obtained as a colorless oil (227 mg, 77%).

^{1}H NMR (399 MHz, $CDCl_3$): δ 10.0 (s, 1H), 7.69 (d, J = 8.2 Hz, 2H), 7.33 (d, J = 8.2 Hz, 2H), 5.73 (ddt, J = 16.9, 10.1, 6.5 Hz, 1H), 5.12 (dd, J = 10.1, 0.9 Hz, 1H), 5.06 (dd, J = 17.2, 1.1 Hz, 1H), 3.73 (s, 2H), 3.28 (d, J = 6.4 Hz, 2H), 3.16 (t, J = 5.7 Hz, 2H), 2.48–2.45 (m, 2H), 2.43 (s, 3H).

^{13}C NMR (100 MHz, $CDCl_3$): δ 188.3, 154.5, 144.0, 133.8, 132.8, 130.7, 129.9, 127.9, 118.1, 43.1, 42.3, 35.7, 31.3, 21.6.

HRMS (ESI): m/z $[M+Na]^+$ calcd. for $C_{16}H_{19}NNaO_3S^+$: 328.0978; found 328.0983.

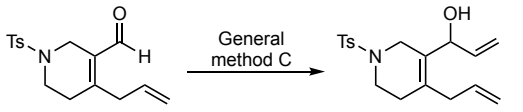

S4 **23**

1-(4-allyl-1-tosyl-1,2,5,6-tetrahydropyridin-3-yl)prop-2-en-1-ol 23. Substrate **23** was prepared according to general method C using **S4** (225 mg, 0.74 mmol), vinyl magnesium bromide 1 M solution (1.1 mL, 1.11 mmol). The crude product was purified by silica gel column chromatography using a hexane/EtOAc gradient from 70/30 to 60/40 to afford **23** as a colorless oil (210 mg, 85%).

^{1}H NMR (392 MHz, $CDCl_3$): δ 7.67 (dd, J = 6.3, 1.8 Hz, 2H), 7.31 (d, J = 7.6 Hz, 2H), 5.82 (ddd, J = 17.3, 10.5, 5.2 Hz, 1H), 5.65 (ddt, J = 16.6, 10.3, 6.4 Hz, 1H), 5.30 (dt, J = 17.2, 1.6 Hz, 1H), 5.18 (dt, J = 10.3, 1.3 Hz, 1H), 5.12–5.10 (m, 1H), 5.00–4.96 (m, 2H), 3.68 (d, J = 16.2 Hz, 1H), 3.53 (d, J = 16.2 Hz, 1H), 3.12 (ddq, J = 25.6, 11.7, 5.8 Hz, 2H), 2.81 (ddd, J = 33.2, 15.3, 6.3 Hz, 2H), 2.42 (s, 3H), 2.26–2.11 (m, 2H), 1.72 (d, J = 3.1 Hz, 1H).
^{13}C NMR (99 MHz, $CDCl_3$): δ 143.6, 137.7, 135.1, 133.4, 130.3, 129.7, 128.8, 127.9, 116.2, 115.5, 70.4, 43.4, 43.1, 36.7, 29.4, 21.6.
HRMS (ESI): m/z $[M+H]^+$ calcd. for $C_{18}H_{24}NO_3S^+$: 334.1471; found 334.1476.

Preparation of 24

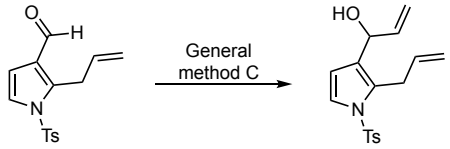

S5 **24**

1-(2-allyl-1-tosyl-1H-pyrrol-3-yl)prop-2-en-1-ol 24. Substrate **24** was prepared according to general method C using the reported aldehyde **S5**[17] (37 mg, 0.13 mmol), vinyl magnesium bromide 1 M solution (200 μL, 0.20 mmol). The crude product was purified by silica gel column chromatography using a hexane/EtOAc gradient from 70/30 to 60/40 to afford **24** as a colorless oil (34 mg, 84%).
^{1}H NMR (392 MHz, $CDCl_3$): δ 7.65 (dt, J = 8.5, 1.9 Hz, 2H), 7.29 (d, J = 3.6 Hz, 1H), 7.27 (d, J = 8.5 Hz, 2H), 6.29 (d, J = 3.6 Hz, 1H), 5.97 (ddd, J = 17.1, 10.3, 5.4 Hz, 1H), 5.79–5.69 (m, 1H), 5.25 (dt, J = 17.2, 1.6 Hz, 1H), 5.13 (dt, J = 10.3, 1.3 Hz, 1H), 5.08–5.06 (m, 1H), 4.89 (dq, J = 10.0, 1.5 Hz, 1H), 4.81 (dq, J = 17.1, 1.6 Hz, 1H), 3.57 (dt, J = 5.8, 1.8 Hz, 2H), 2.40 (s, 3H), 1.78 (d, J = 3.6 Hz, 1H).
^{13}C NMR (99 MHz, $CDCl_3$): δ 145.1, 139.2, 136.4, 135.5, 130.1, 128.8, 128.5, 127.1, 122.3, 115.9, 115.0, 110.3, 67.9, 29.0, 21.7.
HRMS (ESI): m/z $[M+Na]^+$ calcd. for $C_{17}H_{19}NNaO_3S^+$: 340.0978; found 340.0993.

Preparation of 25

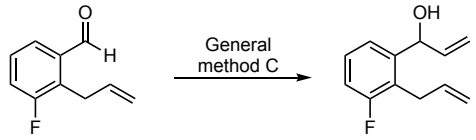

S6 **S7**

1-(2-allyl-3-fluorophenyl)prop-2-en-1-ol S7. Compoudn **S7** was prepared according to general method C using the reported **S6**[18] (344.7 mg, 2.1 mmol), vinyl magnesium bromide 1 M solution (3.2 mL, 3.2 mmol). The crude product was purified by silica gel column chromatography using a hexane/EtOAc gradient from 95/5 to 85/15 to afford **S7** as a colorless oil (342 mg, 85%).
^{1}H NMR (399 MHz, $CDCl_3$): δ 7.27–7.20 (m, 2H), 6.99 (ddd, J = 9.6, 7.4, 2.2 Hz, 1H), 6.08–5.92 (m, 2H), 5.44–5.41 (m, 1H), 5.34 (dt, J = 17.2, 1.5 Hz, 1H), 5.23 (dt, J = 10.4, 1.4 Hz, 1H), 5.05 (dq, J = 10.2, 1.6 Hz, 1H), 4.97–4.92 (m, 1H), 3.57 (ddq, J = 16.0, 5.7, 1.8 Hz, 1H), 3.46 (ddq, J = 15.8, 6.0, 1.9 Hz, 1H), 1.95 (d, J = 3.9 Hz, 1H).
^{13}C NMR (100 MHz, $CDCl_3$): δ 161.3 (d, J_{C-F} = 244.7 Hz), 143.1 (d, J_{C-F} = 3.9 Hz), 139.6, 136.1, 128.1 (d, J_{C-F} = 9.6 Hz), 124.5 (d, J_{C-F} = 16.4 Hz), 122.4 (d, J_{C-F} = 3.9 Hz), 115.8, 115.6, 114.8 (d, J_{C-F} = 23.1 Hz), 71.3 (d, J_{C-F} = 2.9 Hz), 28.9 (d, J_{C-F} = 4.8 Hz).

^{19}F NMR (376 MHz, $CDCl_3$): δ –117.2.
HRMS (EI): m/z $[M]^+$ calcd. for $C_{12}H_{13}FO^+$: 192.0950; found 192.0949.

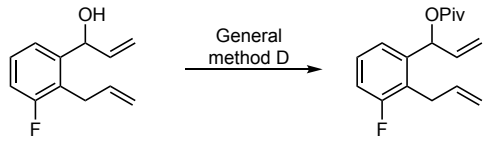

S7 **25**

1-(2-allyl-3-fluorophenyl)allyl pivalate 25. Substrate **25** was prepared according to general method D using **S7** (116 mg, 0.6 mmol), pivaloyl chloride (166 mg, 1.38 mmol), pyridine (48 mg, 0.6 mmol) and DMAP (15 mg, 0.12 mmol). The crude product was purified by silica gel column chromatography using a hexane/EtOAc gradient from 9:1 to 8:2 to afford **25** (86 mg, 52%) as a colorless oil.
^{1}H NMR (392 MHz, $CDCl_3$): δ 7.24–7.16 (m, 2H), 6.99 (ddd, J = 9.9, 8.0, 1.7 Hz, 1H), 6.40 (dt, J = 4.9, 1.6 Hz, 1H), 6.00–5.90 (m, 2H), 5.24 (dt, J = 6.6, 1.5 Hz, 1H), 5.20 (d, J = 1.3 Hz, 1H), 5.05 (dq, J = 10.2, 1.6 Hz, 1H), 5.00–4.94 (m, 1H), 3.61–3.49 (m, 2H), 1.22 (s, 9H).
^{13}C NMR (99 MHz, $CDCl_3$): δ 177.3, 161.2 (d, $J_{C–F}$ = 245.2 Hz), 140.0 (d, $J_{C–F}$ = 3.8 Hz), 136.2, 135.5, 127.9 (d, $J_{C–F}$ = 9.4 Hz), 125.1 (d, $J_{C–F}$ = 16.0 Hz), 123.0 (d, $J_{C–F}$ = 2.8 Hz), 116.7, 116.0, 114.9 (d, $J_{C–F}$ = 22.5 Hz), 72.1, 38.9, 29.2 (d, $J_{C–F}$ = 4.7 Hz), 27.2.
^{19}F NMR (376 MHz, $CDCl_3$): δ –116.8.
HRMS (ESI): m/z $[M+Na]^+$ calcd. for $C_{17}H_{21}FNaO_2^+$: 299.1418; found 299.1422.

Preparation of 26

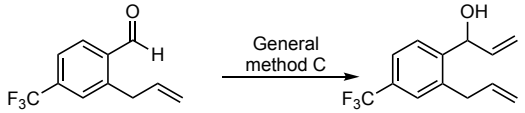

S8 **S9**

1-(2-allyl-4-(trifluoromethyl)phenyl)prop-2-en-1-ol S9. Compound **S9** was prepared according to general method C using the reported **S8**[19] (362 mg, 1.69 mmol) and vinyl magnesium bromide 1 M solution (2.5 mL, 2.5 mmol). The crude product was purified by silica gel column chromatography using a hexane/EtOAc gradient from 95/5 to 80/20 to afford **S9** as a colorless oil (343 mg, 84%).
^{1}H NMR (392 MHz, $CDCl_3$): δ 7.61 (d, J = 8.1 Hz, 1H), 7.51 (d, J = 8.5 Hz, 1H), 7.43 (s, 1H), 6.06–5.93 (m, 2H), 5.50–5.47 (m, 1H), 5.33 (dt, J = 17.1, 1.3 Hz, 1H), 5.24 (dt, J = 10.3, 1.3 Hz, 1H), 5.14 (dq, J = 10.2, 1.5 Hz, 1H), 5.02 (dq, J = 17.2, 1.7 Hz, 1H), 3.56–3.45 (m, 2H), 1.99 (d, J = 3.9 Hz, 1H).
^{13}C NMR (99 MHz, $CDCl_3$): δ 144.4, 139.2, 138.0, 136.3, 130.1 (q, $J_{C–F}$ = 31.9 Hz), 127.2, 126.8 (q, $J_{C–F}$ = 3.8 Hz), 124.3 (q, $J_{C–F}$ = 272.2 Hz), 123.8 (q, $J_{C–F}$ = 3.8 Hz), 117.1, 116.2, 71.2, 36.6.
^{19}F NMR (376 MHz, $CDCl_3$): δ –62.5.
HRMS (EI): m/z $[M]^+$ calcd. for $C_{13}H_{13}F_3O^+$: 242.0919; found 242.0914.

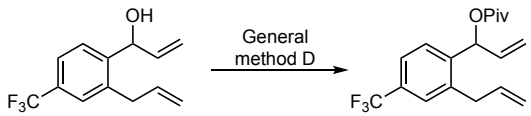

S9 **26**

1-(2-allyl-4-(trifluoromethyl)phenyl)allyl pivalate 26. Substrate **26** was prepared according to general method D using **S9** (40 mg, 0.17 mmol)**,** pivaloyl chloride (46 mg, 0.38 mmol), pyridine (12 mg, 0.17 mmol) and DMAP (4 mg, 0.03 mmol). The crude product was purified by silica gel column chromatography using a hexane/EtOAc gradient from 9:1 to 8:2 to afford **26** (35 mg, 63%) as a colorless oil.

^{1}H NMR (392 MHz, $CDCl_3$): δ 7.49 (s, 2H), 7.44 (s, 1H), 6.44 (d, J = 5.5 Hz, 1H), 6.02–5.91 (m, 2H), 5.25 (dd, J = 6.6, 1.3 Hz, 1H), 5.22 (dt, J = 13.1, 1.3 Hz, 1H), 5.15 (dq, J = 10.2, 1.4 Hz, 1H), 5.06 (dq, J = 17.2, 1.6 Hz, 1H), 3.63–3.51 (m, 2H), 1.23 (s, 9H).

^{13}C NMR (99 MHz, $CDCl_3$): δ 177.3, 141.4, 138.5, 135.8, 135.7, 130.3 (d, J_{C-F} = 31.8 Hz), 127.7, 126.7 (d, J_{C-F} = 3.5 Hz), 124.2 (q, J_{C-F} = 269.7 Hz), 123.7 (q, J_{C-F} = 3.5 Hz), 117.4, 117.3, 72.0, 39.0, 36.8, 27.2.

^{19}F NMR (376 MHz, $CDCl_3$): δ –62.5.

HRMS (ESI): m/z $[M+Na]^+$ calcd. for $C_{18}H_{21}F_3NaO_2^+$: 349.1386; found 349.1354.

Preparation of 27

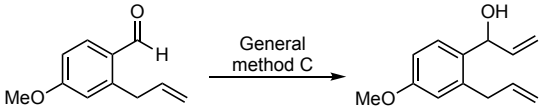

S10 **S11**

1-(2-allyl-4-methoxyphenyl)prop-2-en-1-ol S11. Compound **S11** was prepared according to general method C using the reported **S10**[20] (480.6 mg, 2.73 mmol) and vinyl magnesium bromide 1 M solution (4.1 mL, 4.1 mmol). The crude product was purified by silica gel column chromatography using a hexane/EtOAc gradient from 90/10 to 70/30 to afford **S11** as a yellow oil (480 mg, 86%).

^{1}H NMR (399 MHz, $CDCl_3$): δ 7.35 (d, J = 8.7 Hz, 1H), 6.79 (dd, J = 8.7, 2.7 Hz, 1H), 6.73 (d, J = 2.7 Hz, 1H), 6.09–5.94 (m, 2H), 5.41–5.39 (m, 1H), 5.33 (dt, J = 17.2, 1.5 Hz, 1H), 5.20 (dt, J = 10.2, 1.5 Hz, 1H), 5.09 (dq, J = 10.1, 1.5 Hz, 1H), 5.02 (dq, J = 17.0, 1.7 Hz, 1H), 3.79 (s, 3H), 3.47 (td, J = 6.0, 3.2 Hz, 2H), 1.85 (d, J = 3.7 Hz, 1H).

^{13}C NMR (100 MHz, $CDCl_3$): δ 159.3, 140.1, 139.0, 137.4, 132.9, 128.3, 116.3, 115.7, 114.8, 112.0, 71.1, 55.4, 37.0.

HRMS (EI): m/z $[M]^+$ calcd. for $C_{13}H_{16}O_2^+$: 204.1150; found 204.1147.

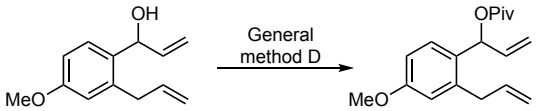

S11 **27**

1-(2-allyl-4-methoxyphenyl)allyl pivalate 27. Substrate **27** was prepared according to general method D using **S11 (**139 mg, 0.68 mmol), pivaloyl chloride (187 mg, 1.56 mmol), pyridine (52 mg, 0.68 mmol) and DMAP (17 mg, 0.14 mmol). The crude product was purified by silica gel column chromatography using a hexane/EtOAc gradient from 9:1 to 8:2 to afford **27** (92 mg, 47%) as a colorless oil.

^{1}H NMR (392 MHz, $CDCl_3$): δ 7.29 (d, J = 8.5 Hz, 1H), 6.78 (dd, J = 8.5, 2.9 Hz, 1H), 6.72 (d, J = 2.7 Hz, 1H), 6.38 (dt, J = 5.4, 1.6 Hz, 1H), 6.01–5.91 (m, 2H), 5.20 (dt, J = 6.9, 1.6 Hz, 1H), 5.17 (d, J = 1.8 Hz, 1H), 5.09 (dq, J = 8.3, 1.6 Hz, 1H), 5.04 (dq, J = 17.1, 1.7 Hz, 1H), 3.79 (s, 3H), 3.54 (dd, J = 16.0, 6.7 Hz, 1H), 3.79 (s, 3H), 3.57–3.41 (m, 2H), 1.21 (s, 9H).

^{13}C NMR (99 MHz, $CDCl_3$): δ 177.4, 159.4, 139.4, 136.80, 136.77, 129.6, 129.0, 116.5, 115.9, 115.2, 112.1, 72.4, 55.3, 38.9, 37.1, 27.3.
HRMS (ESI): m/z $[M+Na]^+$ calcd. for $C_{18}H_{24}NaO_3^+$: 311.1618; found 311.1619.

Preparation of 28

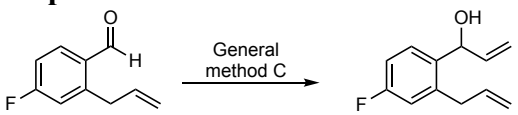

S12 **S13**

1-(2-allyl-4-(trifluoromethyl)phenyl)prop-2-en-1-ol S13. Compound **S13** was prepared according to general method C using the reported **S12**[19] (362 mg, 1.69 mmol) and vinyl magnesium bromide 1 M solution (2.5 mL, 2.5 mmol). The reaction mixture was purified by silica gel column chromatography using a hexane/EtOAc gradient from 95/5 to 80/20 to afford **S13** as a colorless oil (343 mg, 84%).
^{1}H NMR (399 MHz, $CDCl_3$): δ 7.42 (dd, J = 8.7, 5.9 Hz, 1H), 6.96–6.87 (m, 2H), 6.07–5.91 (m, 2H), 5.42–5.40 (m, 1H), 5.32 (dt, J = 17.2, 1.5 Hz, 1H), 5.22 (dt, J = 10.3, 1.4 Hz, 1H), 5.12 (dq, J = 10.1, 1.5 Hz, 1H), 5.02 (dq, J = 17.2, 1.7 Hz, 1H), 3.46 (d, J = 6.2 Hz, 2H), 1.88 (dd, J = 3.9, 1.1 Hz, 1H).
^{13}C NMR (99 MHz, $CDCl_3$): δ 1162.4 (d, J_{C-F} = 246.2 Hz), 139.9 (d, J_{C-F} = 7.5 Hz), 139.8, 136.6, 136.3 (d, J_{C-F} = 3.8 Hz), 128.7 (d, J_{C-F} = 8.5 Hz), 116.8, 116.6 (d, J_{C-F} = 21.6 Hz), 115.4, 113.7 (d, J_{C-F} = 20.7 Hz), 71.0, 36.6.
^{19}F NMR (376 MHz, $CDCl_3$): δ –114.8.
HRMS (EI): m/z $[M]^+$ calcd. for $C_{12}H_{13}FO^+$: 192.0950; found 192.0948.

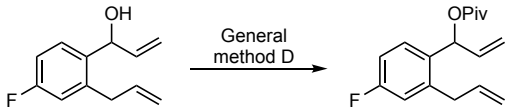

S13 **28**

1-(2-allyl-4-fluorophenyl)allyl pivalate 28. Substrate **28** was prepared according to general method D using **S13** (115 mg, 0.6 mmol), pivaloyl chloride (166 mg, 1.38 mmol), pyridine (48 mg, 0.6 mmol) and DMAP (15 mg, 0.12 mmol). Crude reaction mixture was purified by silica gel column chromatography using a hexane/EtOAc gradient from 9:1 to 8:2 to afford **28** (61 mg, 36%) as a colorless oil.
^{1}H NMR (392 MHz, $CDCl_3$): δ 7.34 (dd, J = 8.5, 5.8 Hz, 1H), 6.95–6.88 (m, 2H), 6.39 (dt, J = 5.1, 1.5 Hz, 1H), 6.00–5.89 (m, 2H), 5.23–5.21 (m, 1H), 5.18 (dt, J = 9.9, 1.3 Hz, 1H), 5.12 (dq, J = 10.2, 1.5 Hz, 1H), 5.04 (dq, J = 17.1, 1.6 Hz, 1H), 3.57–3.43 (m, 2H), 1.21 (s, 9H).
^{13}C NMR (99 MHz, $CDCl_3$): δ 177.4, 162.5 (d, J_{C-F} = 247.1 Hz), 140.3 (d, J_{C-F} = 7.5 Hz), 136.4, 136.1, 133.2 (d, J_{C-F} = 2.8 Hz), 129.3 (d, J_{C-F} = 8.5 Hz), 117.1, 116.5, 116.4 (d, J_{C-F} = 21.6 Hz), 113.7 (d, J_{C-F} = 21.6 Hz), 72.0, 38.9, 36.8, 27.2.
^{19}F NMR (376 MHz, $CDCl_3$): δ –114.3.
HRMS (ESI): m/z $[M+Na]^+$ calcd. for $C_{17}H_{21}FNaO_2^+$: 299.1418; found 299.1422.

Preparation of 29

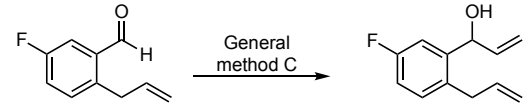

S14 **S15**

1-(2-allyl-5-fluorophenyl)prop-2-en-1-ol S15. The compound **S15** was prepared according to general method C using the known aldehyde **S14**[21] (350.5 mg, 2.14 mmol) and vinyl magnesium bromide 1 M solution (3.2 mL, 3.2 mmol). Reaction mixture was purified by silica gel column chromatography using a hexane/EtOAc gradient from 90/10 to 75/25 to afford **S15** as a colorless oil (334 mg, 81%).

^{1}H NMR (399 MHz, $CDCl_3$): δ 7.20 (d, J = 10.1 Hz, 1H), 7.12 (t, J = 7.0 Hz, 1H), 6.92 (t, J = 8.2 Hz, 1H), 6.04–5.91 (m, 2H), 5.42–5.40 (m, 1H), 5.33 (dd, J = 16.9, 1.4 Hz, 1H), 5.23 (dd, J = 10.3, 1.1 Hz, 1H), 5.09 (dt, J = 10.2, 1.6 Hz, 1H), 4.97 (dt, J = 17.1, 1.7 Hz, 1H), 3.42 (d, J = 5.9 Hz, 2H), 1.98 (d, J = 1.8 Hz, 1H).

^{13}C NMR (100 MHz, $CDCl_3$): δ 162.0 (d, J_{C-F} = 244.7 Hz), 142.7 (d, J_{C-F} = 6.7 Hz), 139.3, 137.3, 132.6 (d, J_{C-F} = 2.9 Hz), 131.6 (d, J_{C-F} = 7.7 Hz), 116.3, 115.8, 114.7 (d, J_{C-F} = 21.2 Hz), 113.5 (d, J_{C-F} = 22.2 Hz), 71.1, 36.1.

^{19}F NMR (376 MHz, $CDCl_3$): δ –115.7.

HRMS (EI): m/z $[M]^+$ calcd. for $C_{12}H_{13}FO^+$: 192.0950; found 192.0947.

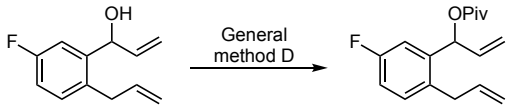

S15 **29**

1-(2-allyl-5-fluorophenyl)allyl pivalate 29. Substrate **29** was prepared according to general method D using **S15** (110 mg, 0.57 mmol)**,** pivaloyl chloride (160 mg, 1.32 mmol), pyridine (45 mg, 0.57 mmol) and DMAP (14 mg, 0.11 mmol). The crude product was purified by silica gel column chromatography using a hexane/EtOAc gradient from 9:1 to 8:2 to afford **29** (130 mg, 82%) as a colorless oil.

^{1}H NMR (392 MHz, $CDCl_3$): δ 7.13 (dd, J = 8.5, 5.8 Hz, 1H), 7.08 (dd, J = 10.1, 2.9 Hz, 1H), 6.93 (td, J = 8.3, 2.7 Hz, 1H), 6.40–6.38 (m, 1H), 6.00–5.89 (m, 2H), 5.24 (dt, J = 4.5, 1.4 Hz, 1H), 5.21 (dt, J = 2.7, 1.4 Hz, 1H), 5.09 (dq, J = 10.1, 1.5 Hz, 1H), 5.00 (dq, J = 17.1, 1.6 Hz, 1H), 3.52–3.41 (m, 2H), 1.23 (s, 9H).

^{13}C NMR (99 MHz, $CDCl_3$): δ 177.2, 161.8 (d, J_{C-F} = 244.3 Hz), 139.6 (d, J_{C-F} = 7.5 Hz), 136.7, 135.9, 133.1 (d, J_{C-F} = 2.8 Hz), 131.5 (d, J_{C-F} = 8.5 Hz), 117.0, 116.5, 115.0 (d, J_{C-F} = 20.7 Hz), 113.9 (d, J_{C-F} = 22.5 Hz), 72.0, 38.9, 36.2, 27.2.

^{19}F NMR (376 MHz, $CDCl_3$): δ –115.9.

HRMS (ESI): m/z $[M+Na]^+$ calcd. for $C_{17}H_{21}FNaO_2^+$: 299.1418; found 299.1422.

Preparation of 30

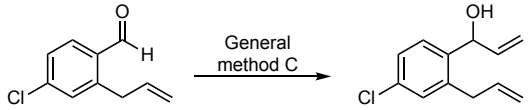

S16 **S17**

1-(2-allyl-4-chlorophenyl)prop-2-en-1-ol S17. Compound **S17** was prepared according to general method C using the reported **S16**[22] (295 mg, 1.63 mmol) and vinyl magnesium bromide

1 M solution (2.4 mL, 2.4 mmol). The crude product was purified by silica gel column chromatography using a hexane/EtOAc gradient from 95/5 to 80/20 to afford **S17** as a colorless oil (260 mg, 76%).

^{1}H NMR (399 MHz, $CDCl_3$): δ 7.40 (d, J = 8.3 Hz, 1H), 7.22 (dd, J = 8.3, 2.2 Hz, 1H), 7.17 (d, J = 2.3 Hz, 1H), 6.05–5.91 (m, 2H), 5.41 (dt, J = 5.2, 1.9 Hz, 1H), 5.32 (dt, J = 17.2, 1.4 Hz, 1H), 5.22 (dt, J = 10.4, 1.4 Hz, 1H), 5.12 (dq, J = 10.1, 1.5 Hz, 1H), 5.02 (dq, J = 17.1, 1.7 Hz, 1H), 3.45–3.43 (m, 2H), 1.89 (d, J = 3.9 Hz, 1H).

^{13}C NMR (100 MHz, $CDCl_3$): δ 139.5, 139.2, 139.0, 136.5, 133.7, 129.9, 128.3, 127.1, 116.9, 115.7, 71.1, 36.5.

HRMS (EI): m/z $[M]^+$ calcd. for $C_{12}H_{13}ClO^+$: 208.0655; found 208.0627.

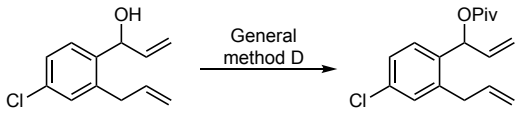

S17 **30**

1-(2-allyl-4-chlorophenyl)allyl pivalate 30. Substrate **30** was prepared according to general method D using **S17** (82 mg, 0.4 mmol), pivaloyl chloride (108 mg, 0.9 mmol), pyridine (32 mg, 0.4 mmol) and DMAP (10 mg, 0.08 mmol). The crude product was purified by silica gel column chromatography using a hexane/EtOAc gradient from 9:1 to 8:2 to afford **30** (63 mg, 55%) as a colorless oil.

^{1}H NMR (392 MHz, $CDCl_3$): δ 7.30 (d, J = 8.5 Hz, 1H), 7.21 (dd, J = 8.5, 2.2 Hz, 1H), 7.18 (d, J = 1.8 Hz, 1H), 6.37 (dt, J = 5.4, 1.6 Hz, 1H), 5.99–5.89 (m, 2H), 5.23 (dt, J = 3.1, 1.5 Hz, 1H), 5.19 (dt, J = 9.3, 1.5 Hz, 1H), 5.12 (dq, J = 10.3, 1.5 Hz, 1H), 5.04 (dq, J = 17.1, 1.6 Hz, 1H), 3.56–3.41 (m, 2H), 1.21 (s, 9H).

^{13}C NMR (99 MHz, $CDCl_3$): δ 177.3, 139.7, 136.1, 136.04, 135.99, 133.9, 129.8, 128.9, 127.0, 117.1, 116.8, 72.0, 38.9, 36.7, 27.2.

HRMS (ESI): m/z $[M+Na]^+$ calcd. for $C_{17}H_{21}ClNaO_2^+$: 315.1122; found 315.1145.

Prepartion of 33

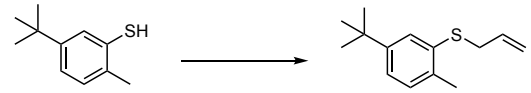

S18 **33**

allyl (5-(*tert*-butyl)-2-methylphenyl)sulfane (33). To a solution of commerical avaiable 5-(*tert*-butyl)-2-methylbenzenethiol **S18** (0.88 g, 4.9 mmol) in THF (9.8 mL) were added by Et_3N (1.2 g, 12 mmol) and allyl bromide (1.1 mL, 12 mmol) at 0 °C. The reaction mixture was warmed to room temperature and stirred for 16 hours, and then quenched with 1 N HCl (3.0 mL). The mixture was extracted with ethyl acetate three times. The combined organic layers were washed with brine, dried over Na_2SO_4, filtered, and concentrated under vaccum. The crude product was purified by flash column chromatography (hexane only) to give **33** (1.0 g, 93%) as a colorless oil.

^{1}H NMR (392 MHz, $CDCl_3$) δ: 7.33 (d, J = 1.6 Hz, 1H), 7.13 (dd, J = 8.0, 1.8 Hz, 1H), 7.10 (d, J = 7.8 Hz, 1H), 5.90 (ddt, J = 16.7, 10.0, 6.9 Hz, 1H), 5.15 (dq, J = 16.9, 1.4 Hz, 1H), 5.08 (dq, J = 10.0, 1.2 Hz, 1H), 3.54 (d, J = 6.7 Hz, 2H), 2.35 (s, 3H), 1.30 (s, 9H).

^{13}C NMR (99 MHz, $CDCl_3$) δ: 149.3, 135.2, 134.6, 134.0, 129.9, 126.6, 123.3, 117.7, 36.8, 34.7, 31.5, 20.0.

HRMS (EI): m/z $[M]^+$ calcd. for $C_{14}H_{20}S^+$: 220.1285 found 220.1286.

Preparation of Ru-I catalyst.

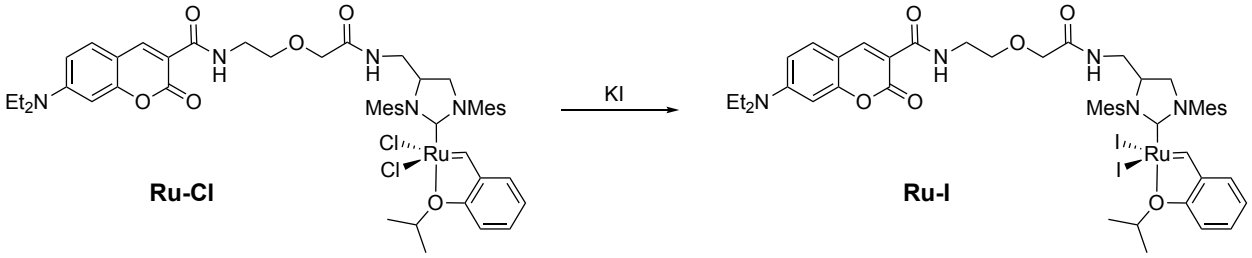

Ru-I. In a round-bottom flask, the reported **Ru-Cl**[1] (16 mg, 16 μmol) and KI (74 mg, 0.45 mmol) were dissolved in the degassed and anhydrous MeOH (4.0 mL). The resulting mixture was stirred at room temperature for 3 hours under N_2 atmosphere. Then, the reaction mixture was evaporated to dryness under vacuum and the obtained residue was suspended in CH_2Cl_2 (2.0 mL). The resulting suspension was filtered through celite with CH_2Cl_2 washing. The filtrate was evaporated dryness under vacuum and the obtained solid was dissolved in the degassed and anhydrous MeOH (4.0 mL), followed by adding KI (74 mg). The mixture solution was reacted for additional 4 h at room temperature. Then, the reaction mixture was evaporated to dryness under vacuum and the obtained residue was precipitated with CH_2Cl_2/Hexane to give **Ru-I** (12 mg, 63%) as a green solid.

^{1}H NMR (400 MHz, $CDCl_3$) δ: 15.64–15.56 (m, 1H), 9.10–9.05 (m, 1H), 8.69–8.66 (m, 1H), 7.54–7.41 (m, 2H), 7.19–6.93 (m, 5H), 6.85–6.80 (m, 2H), 6.68–6.63 (m, 1H), 6.53–6.49 (m, 1H), 5.07–4.97 (m, 1H), 4.89–4.66 (m, 1H), 4.33–4.27 (m, 1H), 4.07–3.91 (m, 3H), 3.87–3.73 (m, 2H), 3.70–3.59 (m, 5H), 3.50–3.42 (m, 5H), 2.91 (s, 2H), 2.71–2.67 (m, 2H), 2.60–2.58 (m, 4H), 2.54–2.52 (m, 3H), 2.42–2.41 (m, 3H), 2.31–2.30 (m, 3H), 1.52–1.38 (m, 6H), 1.27–1.24 (m, 6H).

^{13}C NMR (100 MHz, $CDCl_3$) δ: 299.7, 299.0, 217.0, 216.1, 170.9, 170.2, 170.0, 163.5, 163.4(x2), 163.2, 163.0, 162.6, 157.8, 153.1, 153.0, 152.9, 152.8, 152.6, 148.2, 148.1, 145.4, 145.2, 139.8, 139.3, 139.1, 139.0, 138.9, 138.7, 138.2, 138.1, 138.0, 137.5, 137.2, 136.5, 135.2, 134.0, 131.4, 131.3, 131.2, 130.8, 130.6(x3), 130.3, 130.0, 109.9, 108.4, 96.7(x2), 96.6, 75.8, 75.7, 70.6, 70.5(x2), 70.4(x2), 68.5, 64.0, 63.2, 57.1, 55.8, 52.0, 45.3, 45.2(x2), 42.0, 41.6, 39.5, 39.2, 39.1, 38.7, 35.7, 35.1, 27.1, 27.0(x2), 26.4(x2), 26.2, 24.9, 24.0, 23.5, 23.3, 22.0, 21.9, 21.8, 21.7, 21.5, 21.2, 21.1(x2), 20.7, 20.5, 20.2, 12.6(x2), 12.5.

HRMS (ESI): m/z $[M–HI]^+$ calcd. for $C_{50}H_{61}N_5O_6IRu^+$: 1056.2705; found 1056.2816.

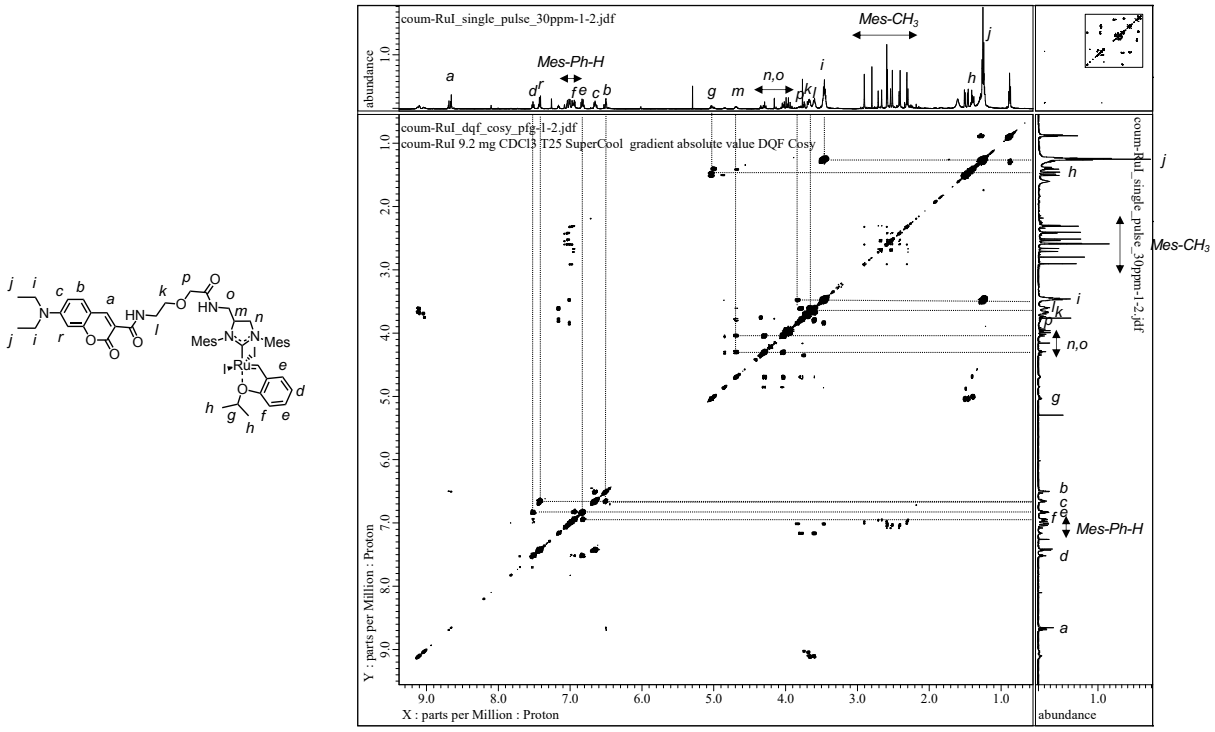

Fig. S2. ^{1}H-^{1}H COSY NMR spectrum (600 MHz, $CDCl_3$, chemical shift from 0.5 to 9.5 ppm) of **Ru-I**

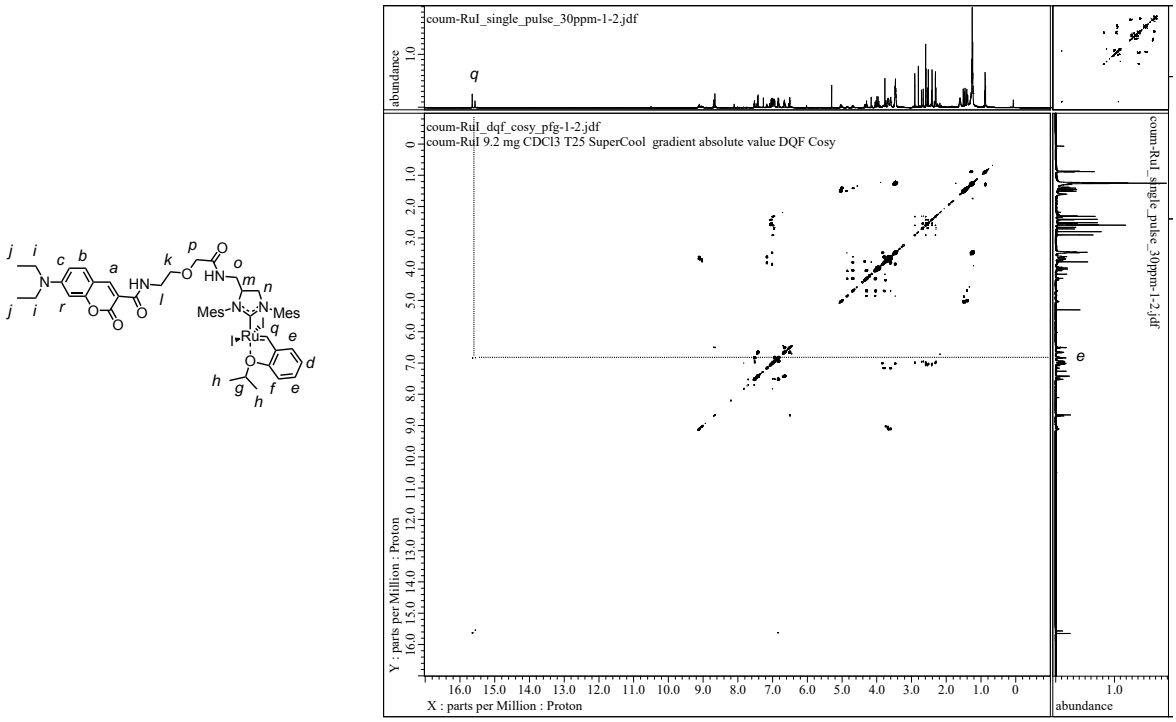

Fig. S3. ^{1}H-^{1}H COSY NMR spectrum (600 MHz, $CDCl_3$, chemical shift from -1.0 to 17.0 ppm) of **Ru-I**

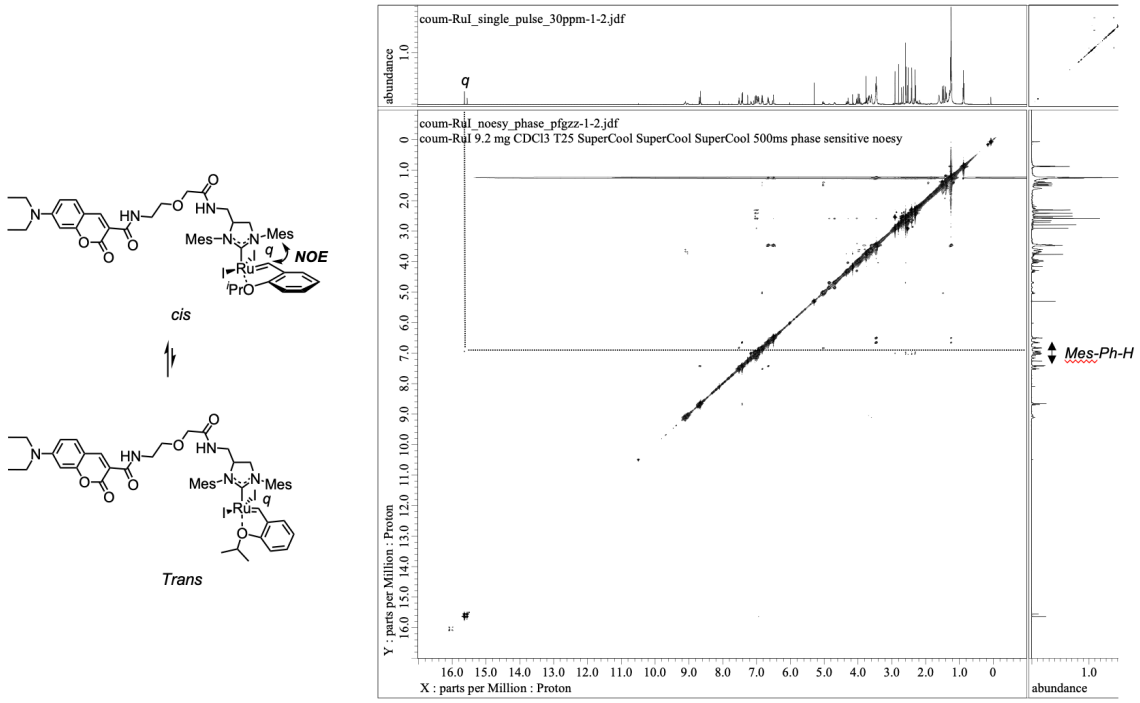

Fig. S4. 1H-NOESY NMR spectrum (600 MHz, $CDCl_3$) of **Ru-I**

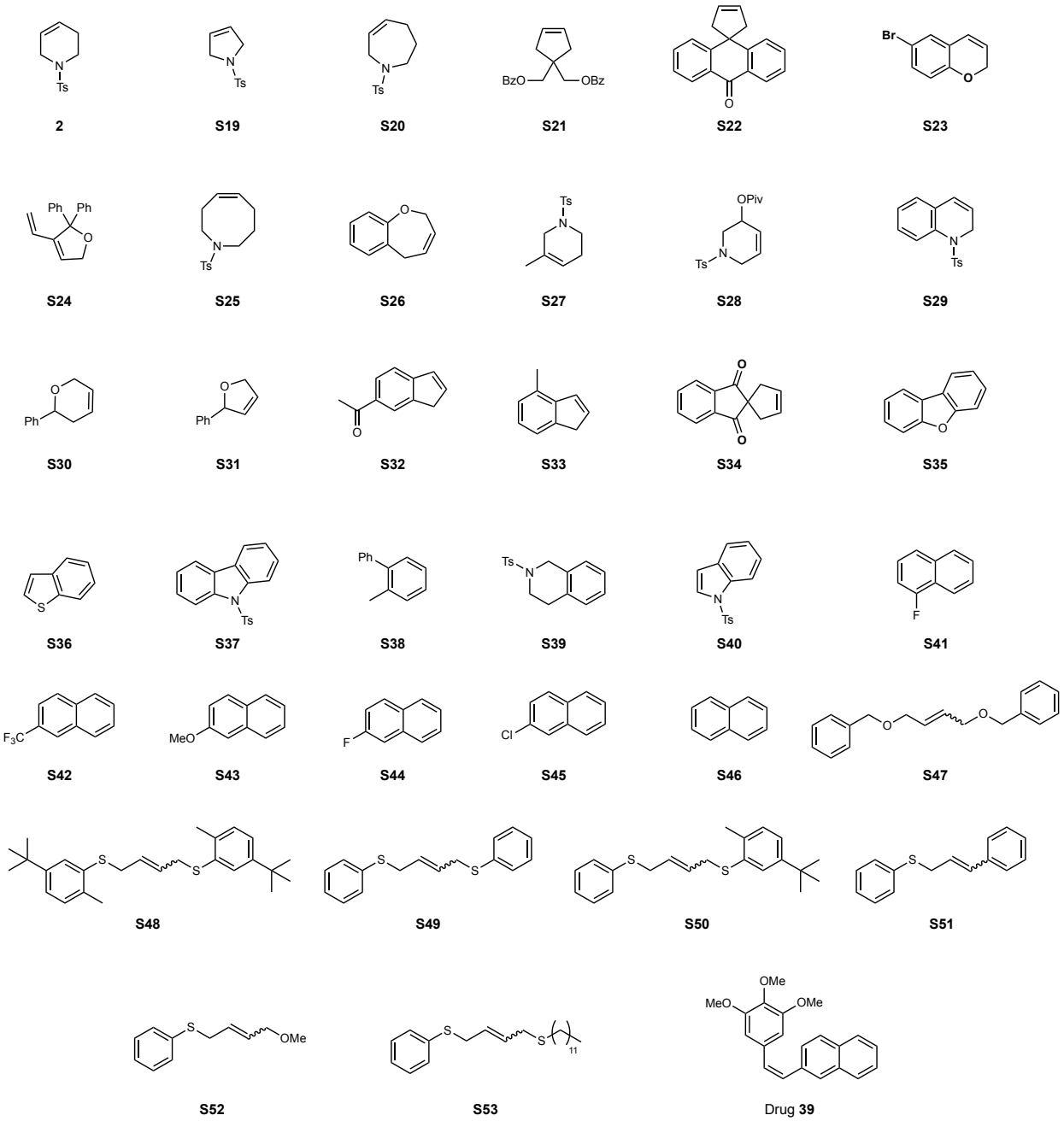

Fig. S5. The list of olefin metathesis products in the study.

Prepartion of olefin metathesis products generated from substrates

To determine yields through HPLC analysis, olefin metathesis products **2**, **S19-53**, and drug **39** (Fig. S5) were synthesized according to the following methods.

General method E for preparing products **2**, **S19-46**, and drug **39**

A substrate (0.05 mmol, 1.0 eq) dissolved in anhydrous CH_2Cl_2 (1 mL), followed by addition of Hoveyda-Grubbs catalyst 2nd generation (1 mol%). The resulting reaction mixture was stirred at room temperature for 2-15 hours, and then reaction progress was monitored by TLC (commonly a hexane/EtOAc mixture (4:1)). After completion, reaction mixture was purified by a silica gel column chromatography using a hexane/EtOAc gradient from 10:1 to 1:1 to afford cylization product.

General method F for preparing products **S47-49**

To a solution of a substrate (0.91 mmol, 1.0 eq) in anhydrous toluene (9.0 mL) were added by Grubbs Catalyst 2nd generation (0.027 mmol, 3 mol%). The reaction mixture was reacted at 80 °C for 4 h. After cooling down to r.t., the mixture was concentrated under vaccum, and the crude product was purified by a silica gel column chromatography using a cyclohexane/CH_2Cl_2 gradient from 10:0 to 9:1 to afford a homodimerization product.

Products **2**[1], **S19-21**[1], **S22**[23], **S23**[3], **S24**[1], **S25**[24], **S26-27**[6], **S29**[25], **S30-31**[6], **S32-33**[10], **S34**[23], **S35**[26], **S36**[27], **S37**[26], **S38**[28], **S39**[29], **S40**[30], **S41**[31], **S42**[32], **S43**[33], **S44**[34], **S45**[35], **S46**[36], **S47**[13], **S49**[13] and drug **39**[12] were reported compounds and characterization data matched these reported references.

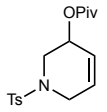

S28

1-tosyl-1,2,3,6-tetrahydropyridin-3-yl pivalate S28. According the general method E, the yield of **S28** (a white solid) was 91%.

^{1}H NMR (399 MHz, $CDCl_3$) δ: 7.68 (d, *J* = 8.2 Hz, 2H), 7.33 (d, *J* = 8.1 Hz, 2H), 5.97–5.87 (m, 1H), 5.79 (ddt, *J* = 10.1, 4.2, 2.2 Hz, 1H), 5.22 (br.s, 1H), 3.84–3.73 (m, 1H), 3.47 (dd, *J* = 16.8, 2.6 Hz, 1H), 3.36 (dd, *J* = 12.5, 4.6 Hz, 1H), 3.20 (dd, *J* = 12.5, 4.1 Hz, 1H), 2.43 (s, 3H), 1.20 (s, 9H).

^{13}C NMR (99 MHz, $CDCl_3$) δ: 178.2, 143.9, 133.7, 129.9, 128.0, 127.7, 124.3, 65.1, 46.6, 44.6, 38.9, 27.2, 21.7

HRMS (ESI): m/z $[M+H]^+$ calcd. for $C_{17}H_{24}NO_4S^+$: 338.1421; found 338.1434.

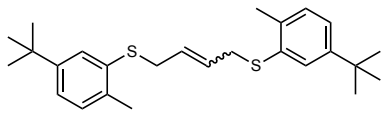

S48

(4-(*tert*-butyl)-2-methylphenyl)(4-((5-(*tert*-butyl)-2-methylphenyl)thio)but-2-en-1-yl)sulfane S48. According the general method F, the yield of **S48** (a white solid) was 28%.

^{1}H NMR (392 MHz, $CDCl_3$) δ: 7.28 (s, 2H), 7.11 (q, *J* = 6.9 Hz, 4H), 5.67–5.64 (m, 2H), 3.47 (d, *J* = 5.4 Hz, 4H), 2.32 (s, 6H), 1.29 (s, 18H)

^{13}C NMR (99 MHz, $CDCl_3$) δ: 149.4, 135.3, 134.6, 129.9, 128.9, 126.7, 123.4, 35.7, 34.6, 31.5, 20.0.
HRMS (EI): m/z $[M]^+$ calcd. for $C_{26}H_{36}S_2^+$: 412.2258; found 412.2257.

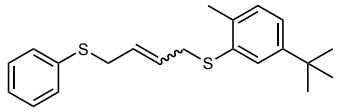

S50

(4-(*tert*-butyl)-2-methylphenyl)(4-(phenylthio)but-2-en-1-yl)sulfane S50. To a solution of **34** (480 mg, 2.63 mmol) and **33** (290 mg, 1.32 mmol) in CH_2Cl_2 (20 mL) were added Hoveyda-Grubbs catalyst 2nd generation (41 mg, 0.066 mmol). The reaction mixture was reacted at 40 °C for 3 hours. The mixture was concentrated under vaccum and the crude product was purified by a silica gel column chromatography using a cyclohexane/CH_2Cl_2 gradient from 10:0 to 10:1 to afford **S50** (40 mg, 8.9%) as a colorless oil.
^{1}H NMR (392 MHz, $CDCl_3$) δ: 7.28–7.08 (m, 8H), 5.64–5.62 (m, 2H), 3.47 (d, J = 4.9 Hz, 4H), 2.32 (s, 3H), 1.28 (s, 9H).
^{13}C NMR (99 MHz, $CDCl_3$) δ: 149.3, 136.0, 135.3, 134.5, 130.04, 129.96, 128.9, 128.7, 126.5, 126.4, 123.4, 36.2, 35.5, 34.7, 31.5, 20.0.
HRMS (EI): m/z $[M]^+$ calcd. for $C_{21}H_{26}S_2^+$: 342.1476; found 342.1481.

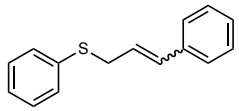

S51

Phenyl (3-phenylallyl)sulfane S51. To a solution of **34** (200 mg, 1.33 mmol) and styrene **35** (139 mg, 1.33 mmol) in CH_2Cl_2 (20 mL) were added Hoveyda-Grubbs catalyst 2nd generation (25 mg, 0.040 mmol). The reaction mixture was reacted at 40 °C for 3 hours. The mixture was concentrated under vaccum and the crude product was purified by a silica gel column chromatography using a cyclohexane/CH_2Cl_2 gradient from 100:0 to 90:10 to afford **S51** (105 mg, 36%) as a white solid.
^{1}H NMR (392 MHz, $CDCl_3$) δ: 7.39–7.35 (m, 2H), 7.32–7.25 (m, 6H), 7.23–7.17 (m, 2H), 6.42 (d, J = 15.7 Hz, 1H), 6.29–6.21 (m, 1H), 3.71 (d, J = 7.2 Hz, 2H)
^{13}C NMR (99 MHz, $CDCl_3$) δ: 136.9, 135.9, 132.9, 130.4, 129.0, 128.7, 127.7, 126.6, 126.5, 125.2, 37.3.
HRMS (EI): m/z $[M]^+$ calcd. For $C_{15}H_{14}S^+$: 226.0816; found 226.0820.

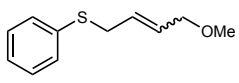

S52

(4-methoxybut-2-en-1-yl)(phenyl)sulfane S52. To a solution of **34** (100 mg, 0.66 mmol) and allyl methyl ether **36** (480 mg, 6.6 mmol) in CH_2Cl_2 (15 mL) were added Hoveyda-Grubbs catalyst 2nd generation (21 mg, 0.033 mmol). The reaction mixture was reacted at 40 °C for 3 hours. The mixture was concentrated under vaccum and the crude product was purified by a silica gel column chromatography using a hexane/EtOAc gradient from 20:0 to 20:1 to afford **S52** (37 mg, 29%) as a colorless oil.
^{1}H NMR (392 MHz, $CDCl_3$) δ: 7.37–7.27 (m, 4H), 7.17 (t, J = 6.5 Hz, 1H), 5.80–5.73 (m, 1H), 5.66–5.60 (m, 1H), 3.85 (d, J = 5.8 Hz, 2H), 3.55 (d, J = 7.2 Hz, 2H), 3.23 (s, 3H).

^{13}C NMR (99 MHz, $CDCl_3$) δ: 135.9, 130.0, 129.9, 129.0, 128.7, 126.4, 72.4, 57.9, 36.1.
HRMS (EI): m/z $[M]^+$ calcd. for $C_{11}H_{14}OS^+$: 194.0765; found 194.0765.

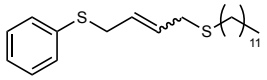

S53

dodecyl(4-(phenylthio)but-2-en-1-yl)sulfane S53. To a solution of **34** (110 mg, 0.45 mmol) and allyl(dodecyl)sulfane **37** (68 mg, 0.45 mmol) in CH_2Cl_2 (10 mL) were added Hoveyda-Grubbs catalyst 2nd generation (8.5 mg, 0.014 mmol). The reaction mixture was reacted at 40 °C for 3.5 hours. The mixture was concentrated under vaccum and the crude product was purified by a silica gel column chromatography using from 90:10 to 85:15 to afford **S53** (20 mg, 12%) as a white solid.
^{1}H NMR (392 MHz, $CDCl_3$) δ: 7.33–7.25 (m, 3H), 7.18 (t, *J* = 7.9 Hz, 1H), 5.57–5.53 (m, 2H), 3.55 (d, *J* = 5.8 Hz, 2H), 3.05 (d, *J* = 5.8 Hz, 2H), 2.28 (t, *J* = 7.4 Hz, 2H), 1.51–1.44 (m, 2H), 1.26 (s, 18H), 0.88 (t, *J* = 6.7 Hz, 3H).
^{13}C NMR (99 MHz, $CDCl_3$) δ: 135.9, 130.1, 129.9, 129.0, 127.9, 126.4, 36.0, 33.4, 32.1, 30.6, 29.82, 29.79, 29.76, 29.69, 29.5, 29.4, 29.0, 22.8, 14.3.
HRMS (EI): m/z $[M]^+$ calcd. For $C_{22}H_{36}S_2$: 346.2258; found 364.2249.

HPLC product standard curves and calibration

To determine yields through HPLC analysis, calibration curves were constructed using product standards of known amounts (shown in Fig. S6-42). The used HPLC methods were showed in Tables S1-2.

Reverse-phase HPLC	Flow rate (ml/min)	Time (min)	%A (H_2O with or w/o 0.1% TFA)	%A (CH_3CN with or w/o 0.1% TFA)
Method 1	1.0	0	50	50
		20	10	90
		30	10	90
		31	50	50
		38	50	50
Method 2	1.0	0	70	30
		20	10	90
		22	10	90
		22.5	30	70
		30	70	30
Method 3	1.0	0	80	20
		30	10	90
		35	80	20
Method 4	1.0	0	50	50
		20	10	90
		30	10	90
		31	50	50
		38	50	50

Table S1.

Gradient profiles for reverse-phase HPLC analysis

Normal-phase HPLC	Flow rate (ml/min)	Column temperature	Time (min)	%C (hexane)	%D (ethanol)
Method 5	1.0	Ambient temperature	0	99	1
			20	50	50
			23	50	50
			27	99	1
			30	99	1
Method 6	1.0	50 °C	0	99.5	0.5
			10	99.5	0.5
			20	50	50
			23	50	50
			27	99.5	0.5
			30	99.5	0.5

Table S2.

Gradient profiles for normal-phase HPLC analysis

HPLC Method		Calibration Curve
Method 1		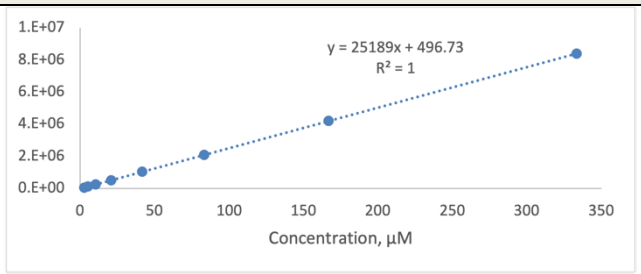
Slope	25189	
Intercept	496.73	
R^2	0.99999	

HPLC trace:

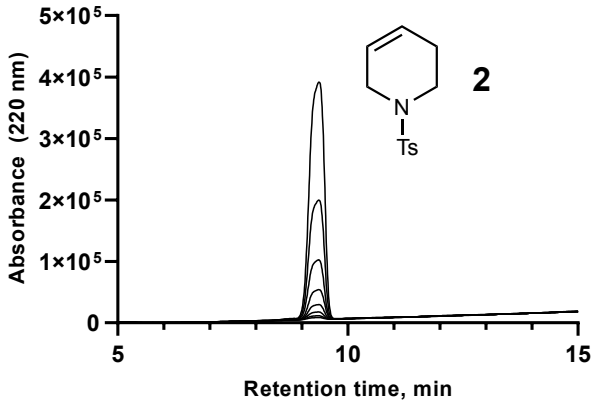

Fig. S6. HPLC calibration curve of product **2**

HPLC Method		Calibration Curve
Method 1		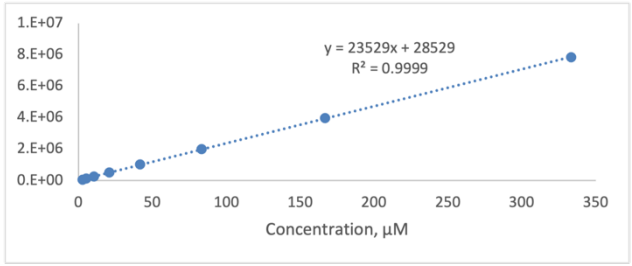
Slope	23529	
Intercept	28528	
R^2	0.99999	

HPLC trace:

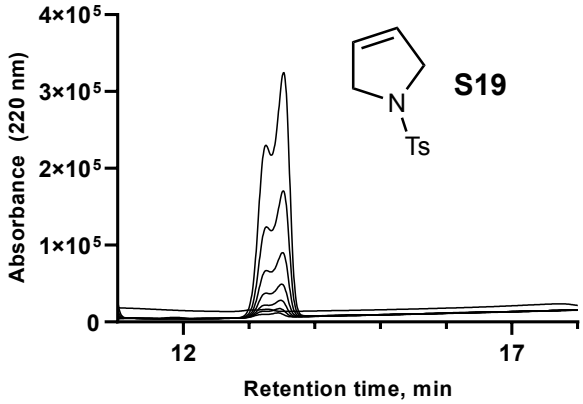

Fig. S7. HPLC calibration curve of product **S19**

HPLC Method	
Method 1	
Slope	19898
Intercept	19462
R^2	0.9999

Calibration Curve

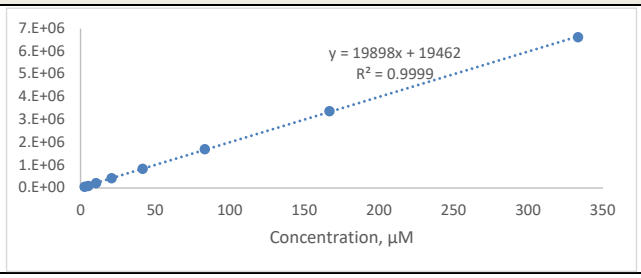

HPLC trace:

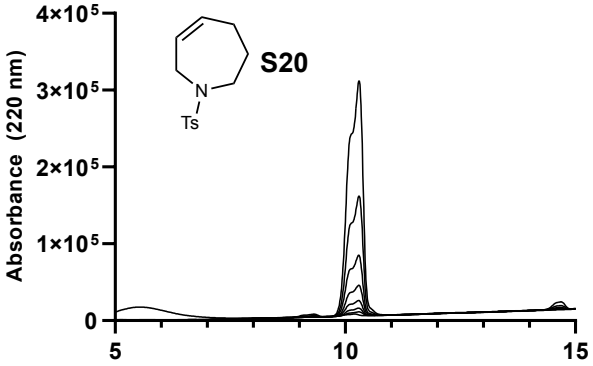

Fig. S8. HPLC calibration curve of product **S20**

HPLC Method		Calibration Curve
Method 1		
Slope	41576	
Intercept	96242	
R^2	0.9995	

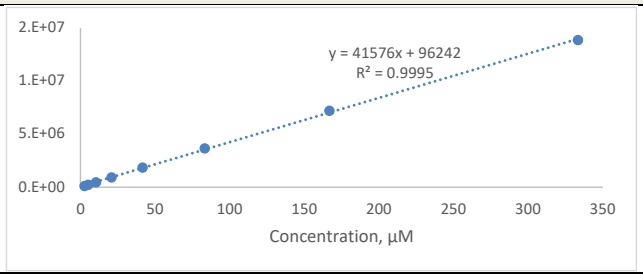

HPLC trace:

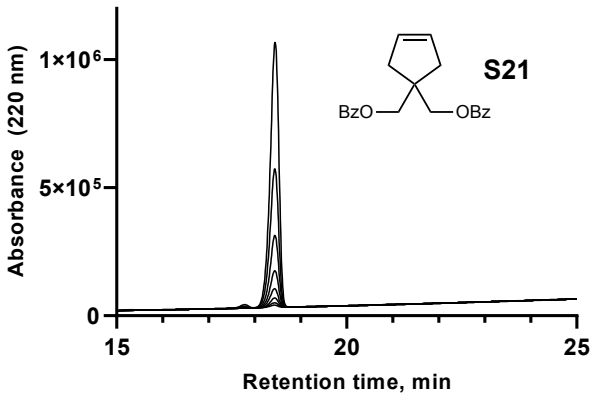

Fig. S9. HPLC calibration curve of product **S21**

HPLC Method		Calibration Curve
Method 1		
Slope	48076	
Intercept	173494	
R^2	0.9987	

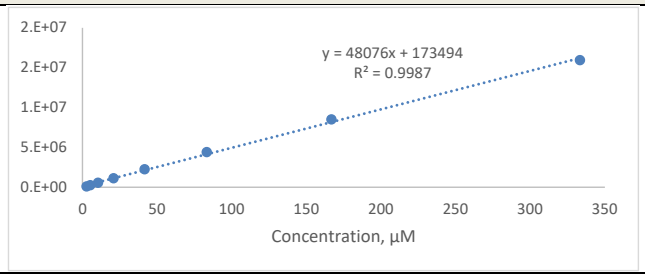

HPLC trace:

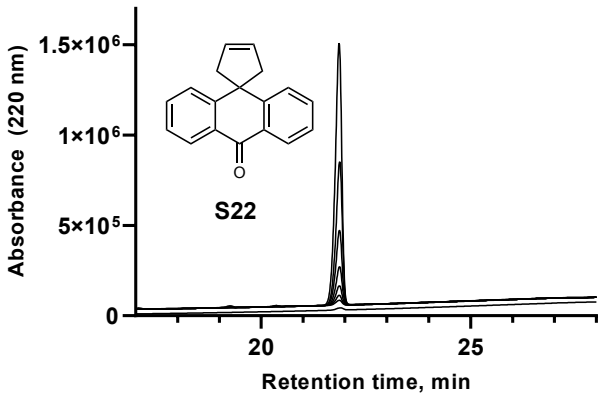

Fig. S10. HPLC calibration curve of product **S22**

HPLC Method		Calibration Curve
Method 2		
Slope	52108	
Intercept	84393	
R^2	0.9998	

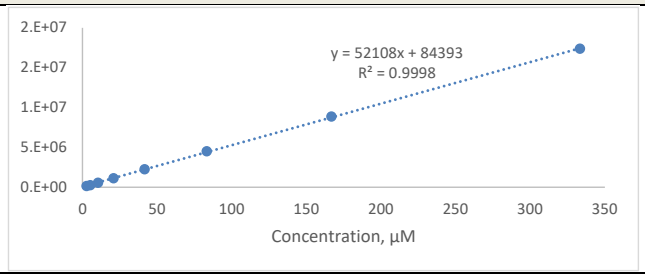

HPLC trace:

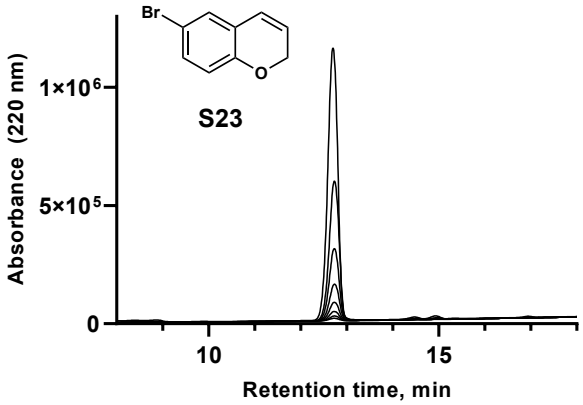

Fig. S11. HPLC calibration curve of product **S23**

HPLC Method		Calibration Curve
Method 1		
Slope	42793	
Intercept	85565	
R^2	0.9997	

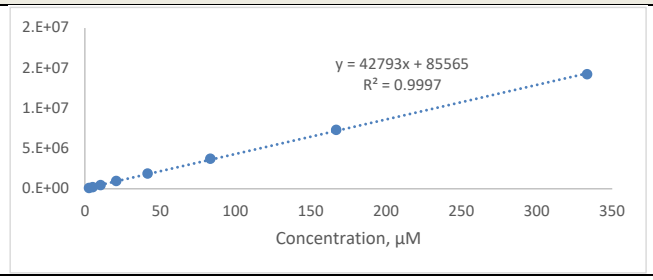

HPLC trace:

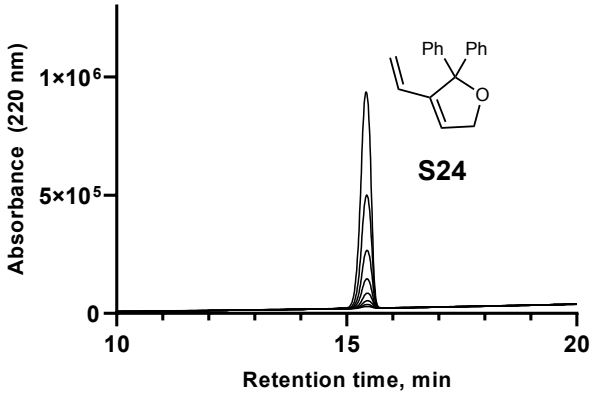

Fig. S12. HPLC calibration curve of product **S24**

HPLC Method		Calibration Curve
Method 1		
Slope	17870	
Intercept	31908	
R^2	0.9999	

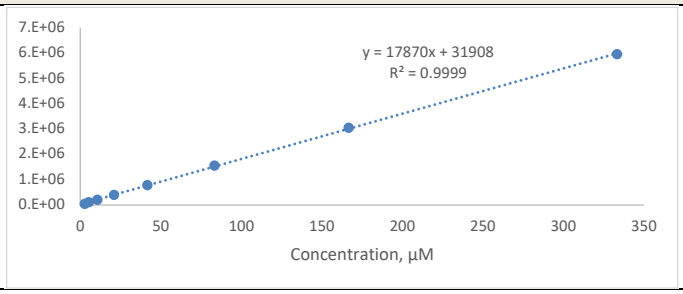

HPLC trace:

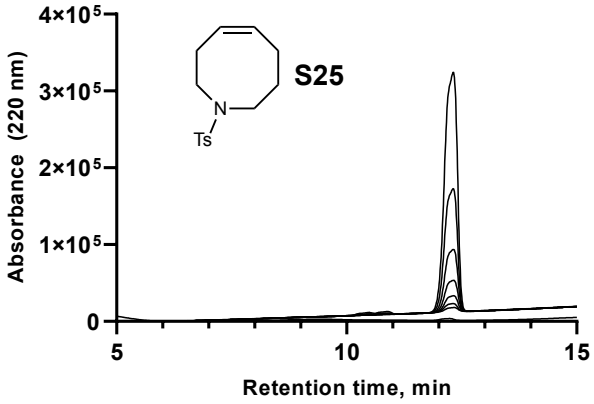

Fig. S13. HPLC calibration curve of product **S25**

HPLC Method		Calibration Curve
Method 2		
Slope	8207	
Intercept	13206	
R^2	0.9998	

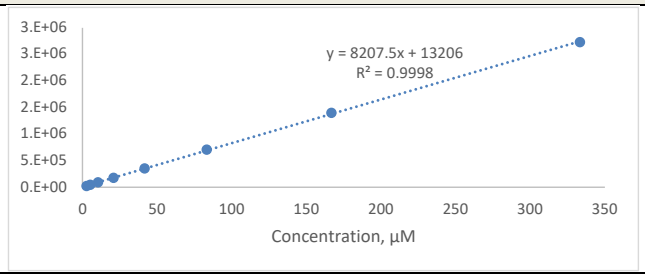

HPLC trace:

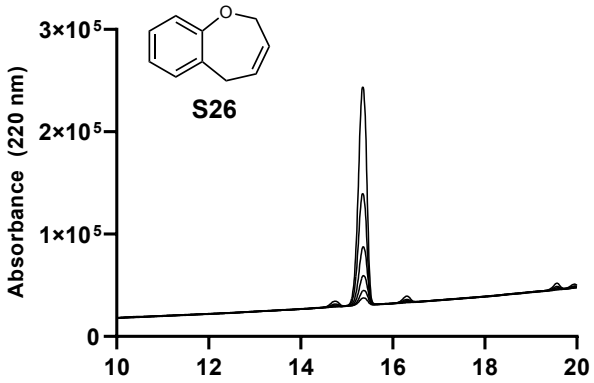

Fig. S14. HPLC calibration curve of product **S26**

HPLC Method		Calibration Curve
Method 1		
Slope	20869	
Intercept	28371	
R^2	0.9998	

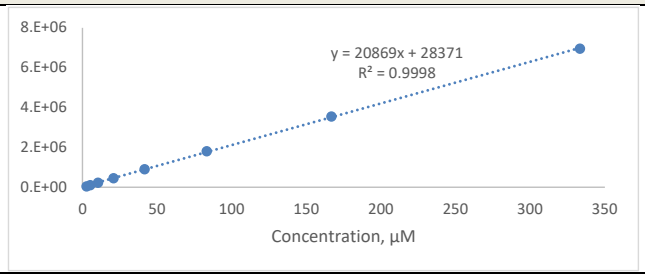

HPLC trace:

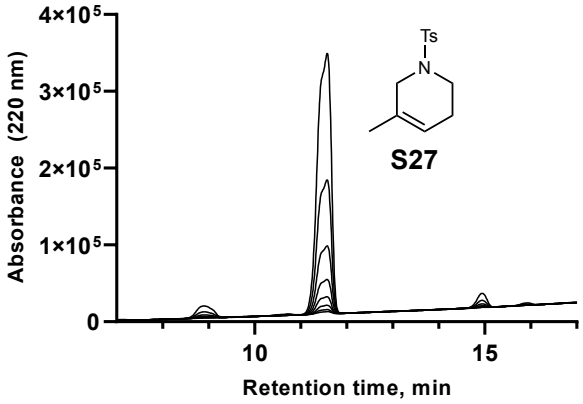

Fig. S15. HPLC calibration curve of product **S27**

HPLC Method		Calibration Curve
Method 1		
Slope	22241	
Intercept	38118	
R^2	0.9998	

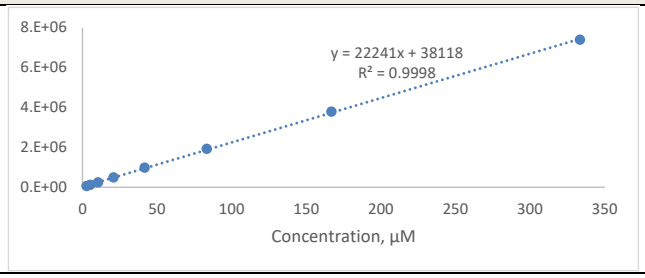

HPLC trace:

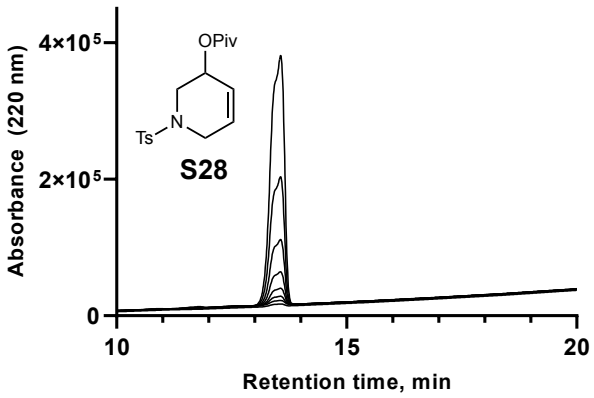

Fig. S16. HPLC calibration curve of product **S28**

HPLC Method		Calibration Curve
Method 2		
Slope	69947	
Intercept	143867	
R^2	0.9997	

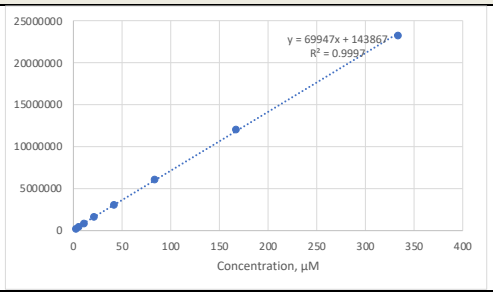

HPLC trace:

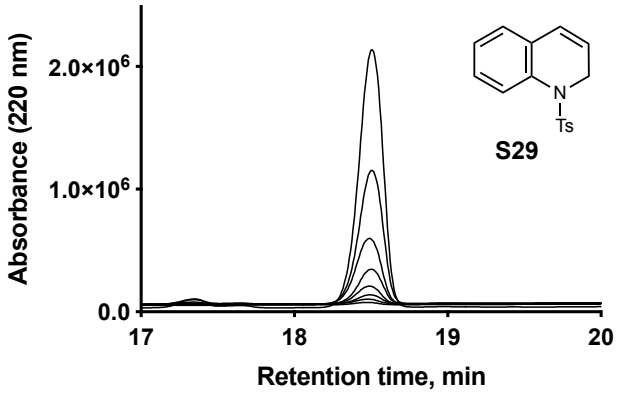

Fig. S17. HPLC calibration curve of product **S29**

HPLC Method		Calibration Curve
Method 2		
Slope	4335	
Intercept	19372	
R^2	0.9994	

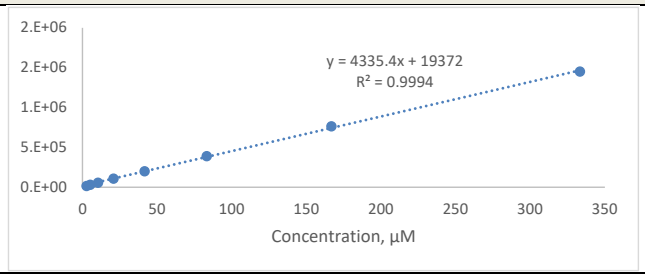

HPLC trace:

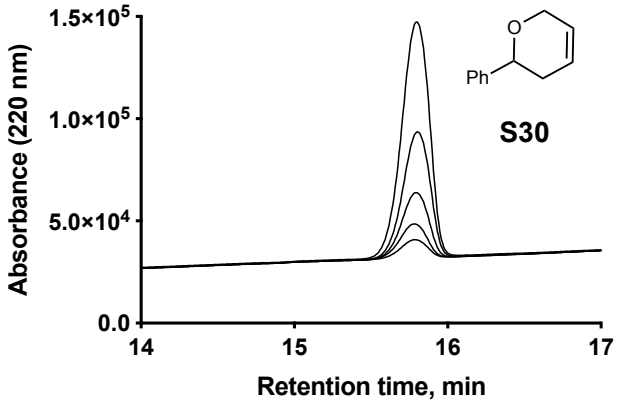

Fig. S18. HPLC calibration curve of product **S30**

HPLC Method		Calibration Curve
Method 2		
Slope	7006	
Intercept	4367	
R^2	1	

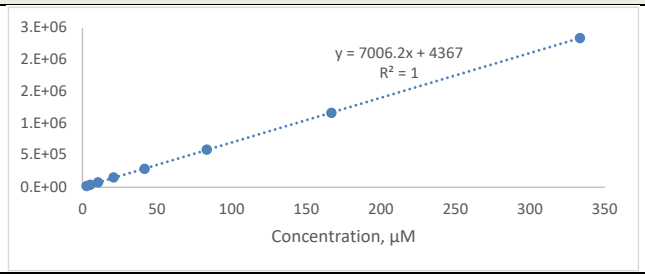

HPLC trace:

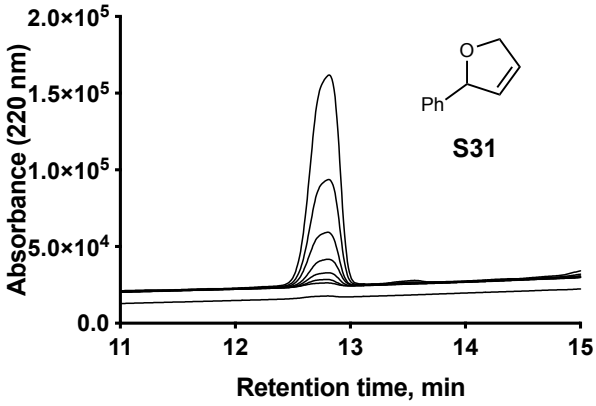

Fig. S19. HPLC calibration curve of product **S31**

HPLC Method		Calibration Curve
Method 2		
Slope	14177	
Intercept	20.288	
R^2	0.9999	

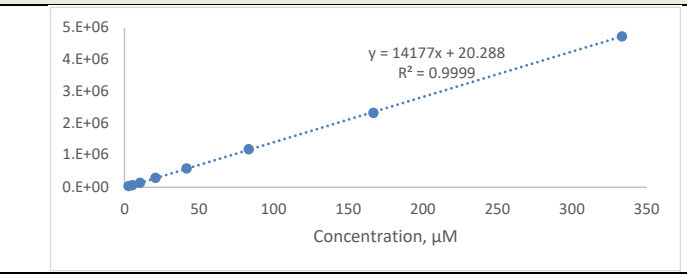

HPLC trace:

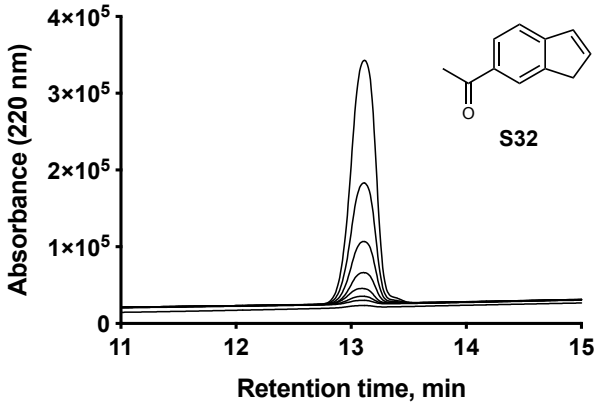

Fig. S20. HPLC calibration curve of product **S32**

HPLC Method		Calibration Curve
Method 2		
Slope	26125	
Intercept	89271	
R^2	0.9987	

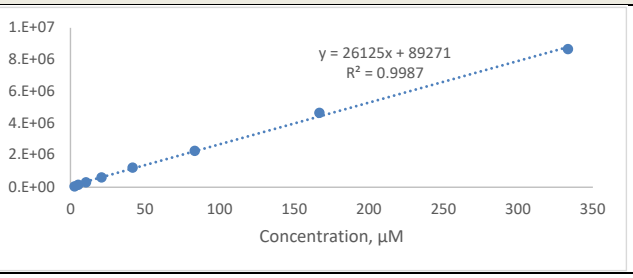

HPLC trace:

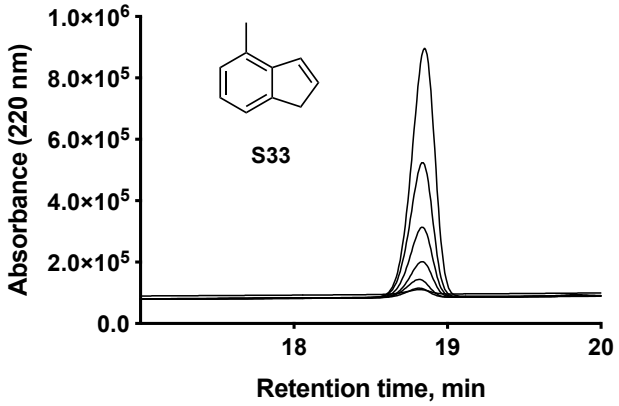

Fig. S21. HPLC calibration curve of product **S33**

HPLC Method		Calibration Curve
Method 2		
Slope	87658	
Intercept	389512	
R^2	0.9982	

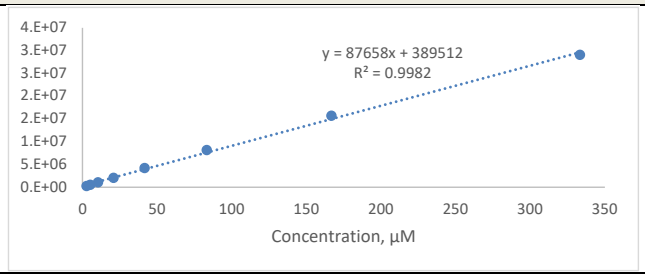

HPLC trace:

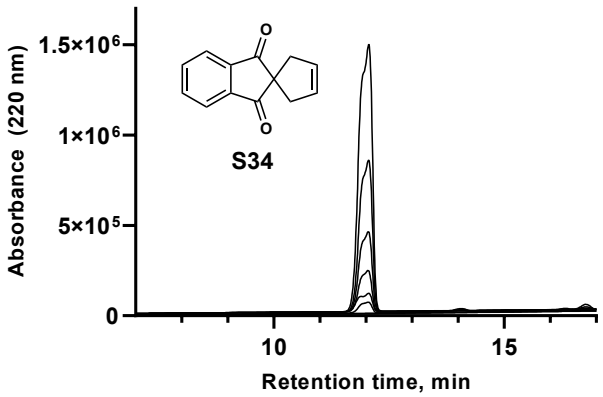

Fig. S22. HPLC calibration curve of product **S34**

HPLC Method		Calibration Curve
Method 2		
Slope	91436	
Intercept	115093	
R^2	0.9996	

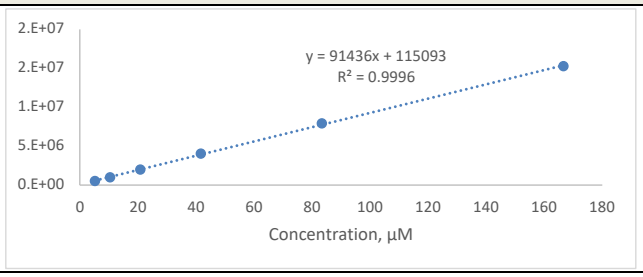

HPLC trace:

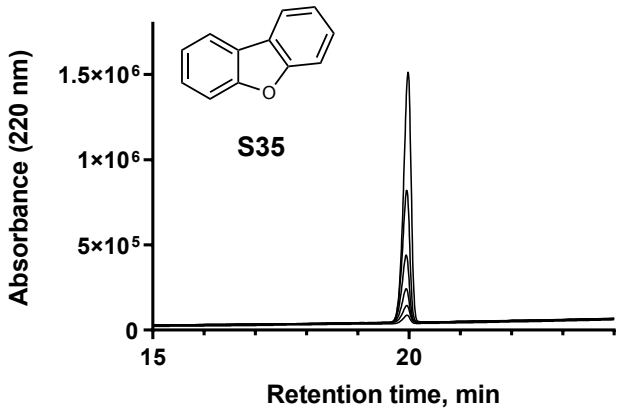

Fig. S23. HPLC calibration curve of product **S35**

HPLC Method		Calibration Curve
Method 2		
Slope	32972	
Intercept	144176	
R^2	0.9998	

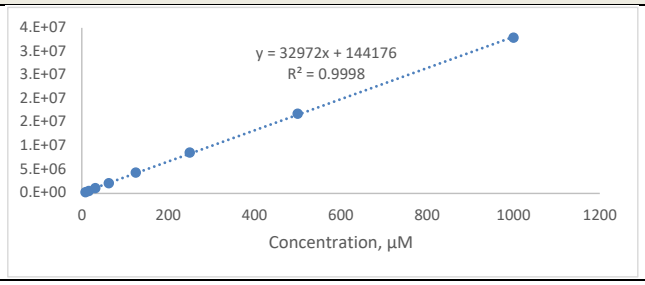

HPLC trace:

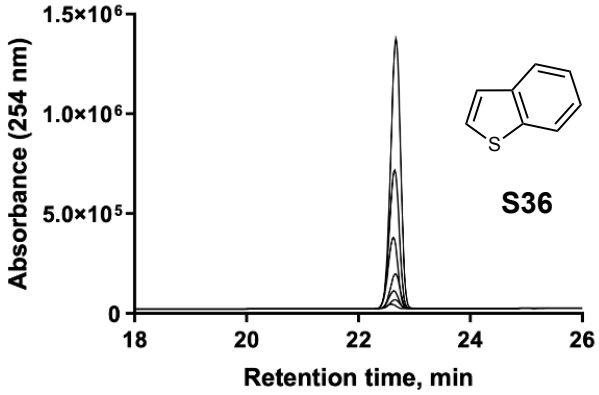

Fig. S24. HPLC calibration curve of product **S36**

HPLC Method		Calibration Curve
Method 1		
Slope	83140	
Intercept	19593	
R^2	1	

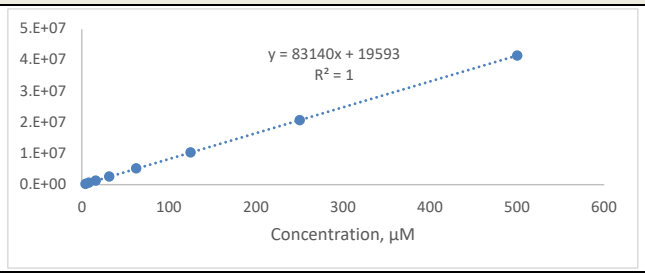

HPLC trace:

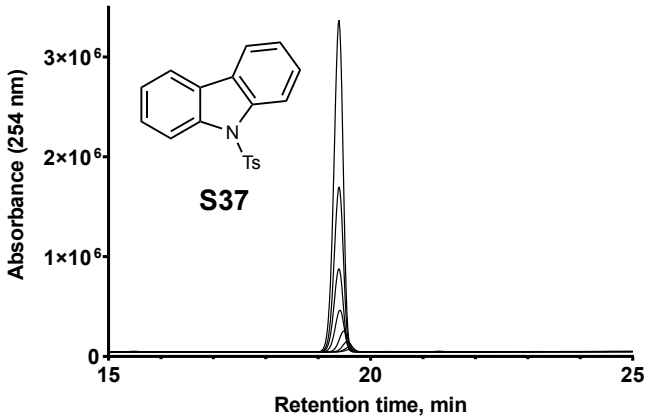

Fig. S25. HPLC calibration curve of product **S37**

HPLC Method		Calibration Curve
Method 2		
Slope	33069	
Intercept	116819	
R^2	0.9994	

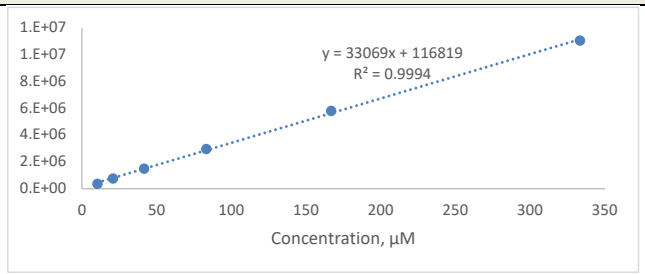

HPLC trace:

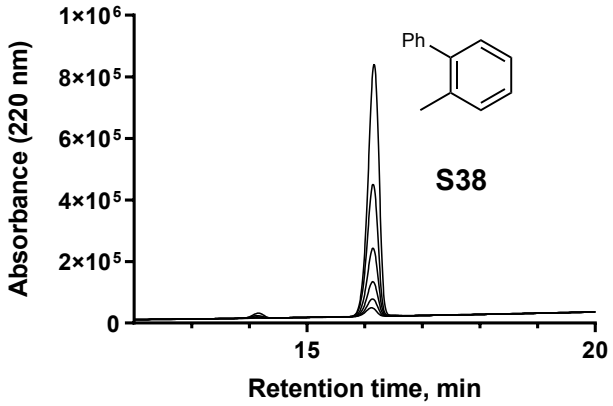

Fig. S26. HPLC calibration curve of product **S38**

HPLC Method		Calibration Curve
Method 1		
Slope	78881	
Intercept	165408	
R^2	0.9995	

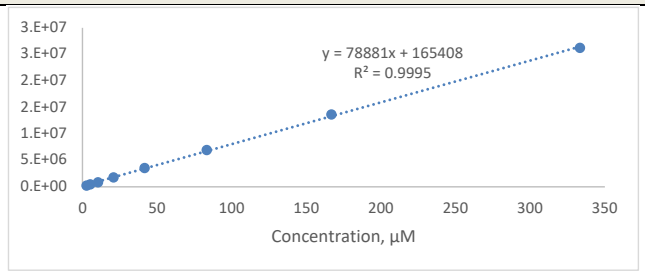

HPLC trace:

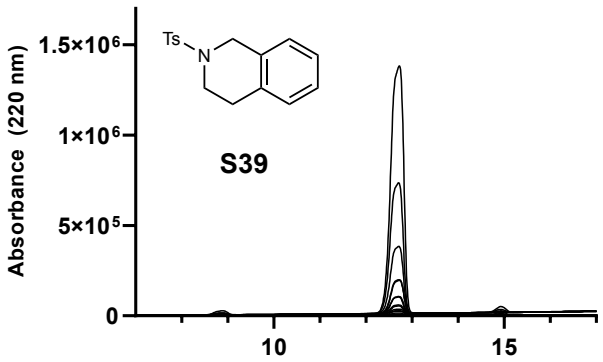

Fig. S27. HPLC calibration curve of product **S39**

HPLC Method		Calibration Curve
Method 1		
Slope	54322	
Intercept	344704	
R^2	0.9991	

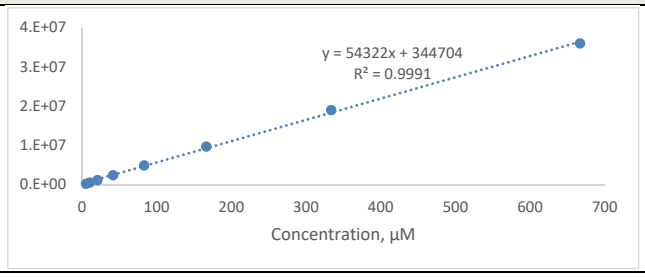

HPLC trace:

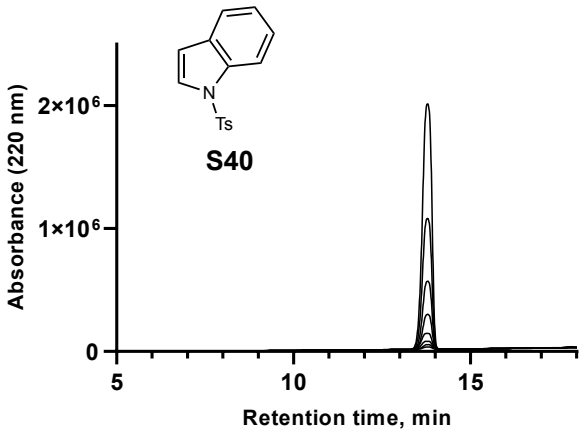

Fig. S28. HPLC calibration curve of product **S40**

HPLC Method		Calibration Curve
Method 1		
Slope	170409	
Intercept	154919	
R^2	0.9992	

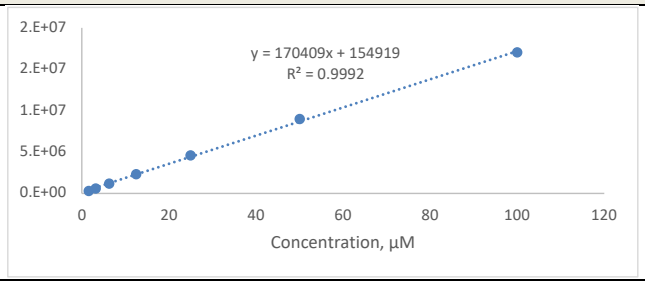

HPLC trace:

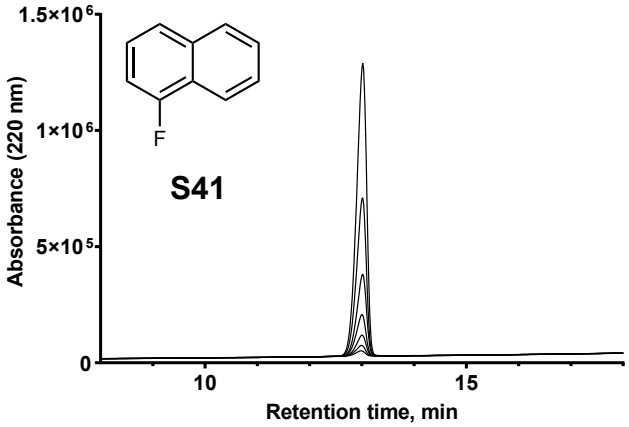

Fig. S29. HPLC calibration curve of product **S41**

HPLC Method		Calibration Curve
Method 1		
Slope	182801	
Intercept	798961	
R^2	0.9951	

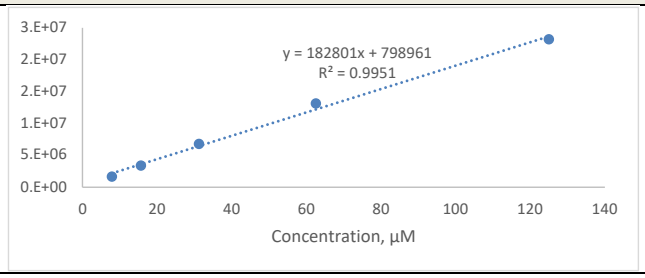

HPLC trace:

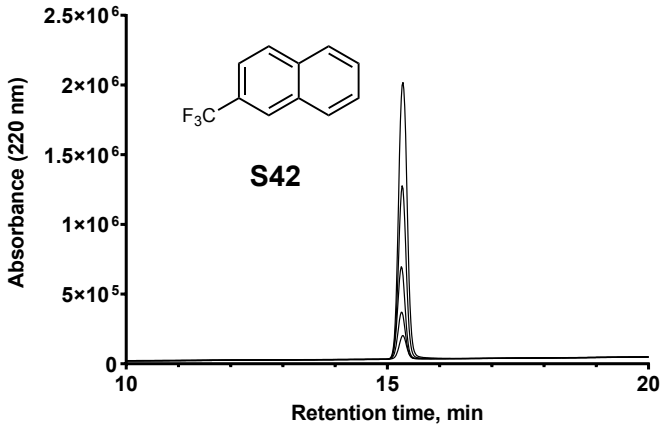

Fig. S30. HPLC calibration curve of product **S42**

HPLC Method		Calibration Curve
Method 3		
Slope	140955	
Intercept	288691	
R^2	0.9995	

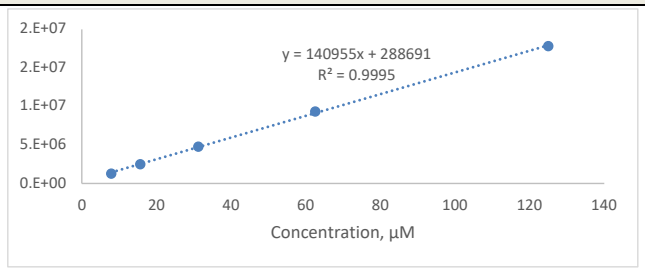

HPLC trace:

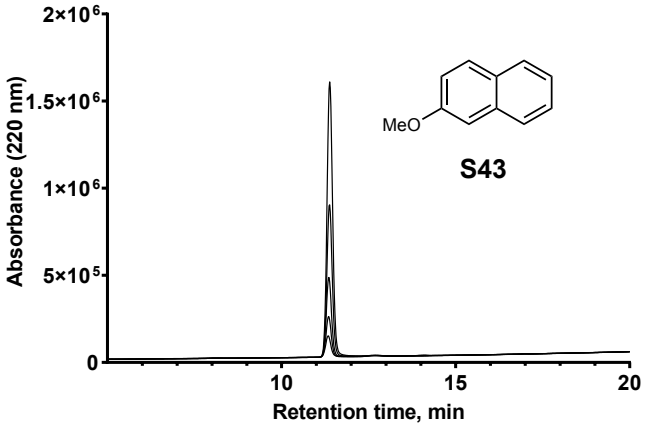

Fig. S31. HPLC calibration curve of product **S43**

HPLC Method		Calibration Curve
Method 1		
Slope	150020	
Intercept	346844	
R^2	0.9962	

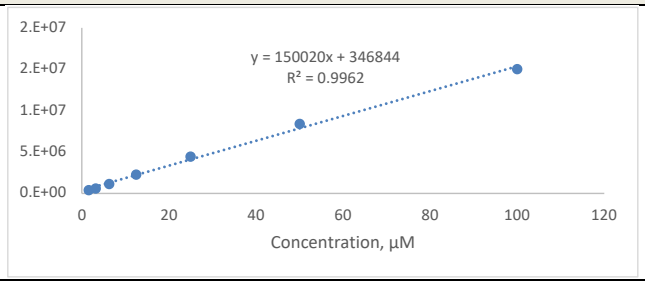

HPLC trace:

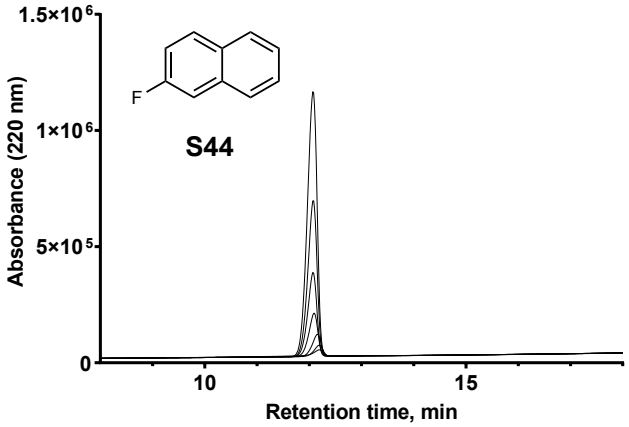

Fig. S32. HPLC calibration curve of product **S44**

HPLC Method		Calibration Curve
Method 1		
Slope	185615	
Intercept	215988	
R^2	0.9999	

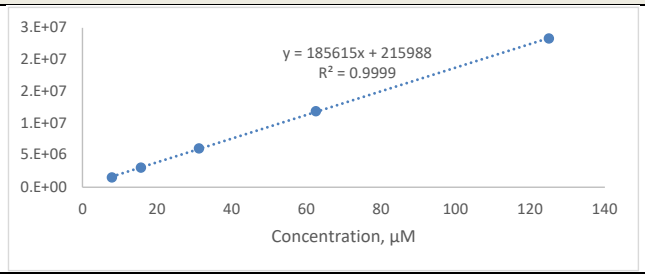

HPLC trace:

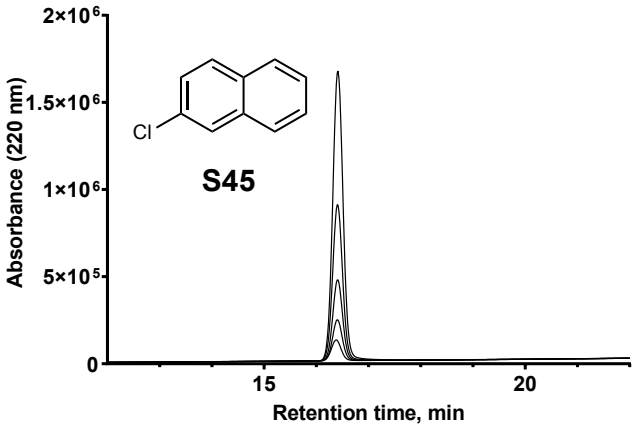

Fig. S33. HPLC calibration curve of product **S45**

HPLC Method		Calibration Curve
Method 1		
Slope	94043	
Intercept	-152025	
R^2	0.9999	

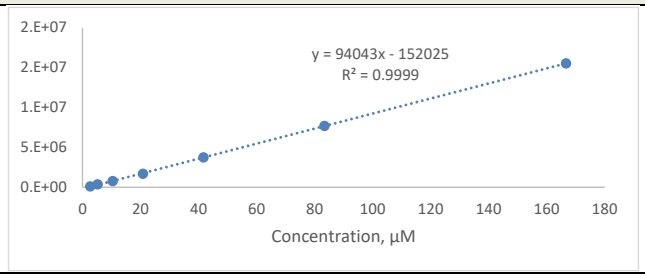

HPLC trace:

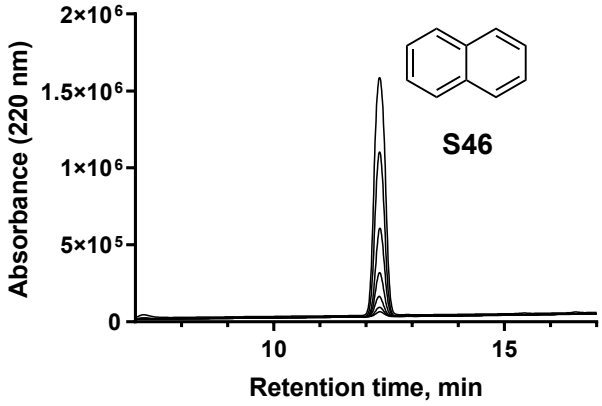

Fig. S34. HPLC calibration curve of product **S46**

HPLC Method		Calibration Curve
Method 2		
Slope	14066	
Intercept	122536	
R^2	0.9933	

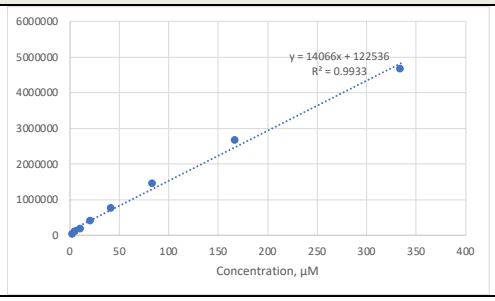

HPLC trace:

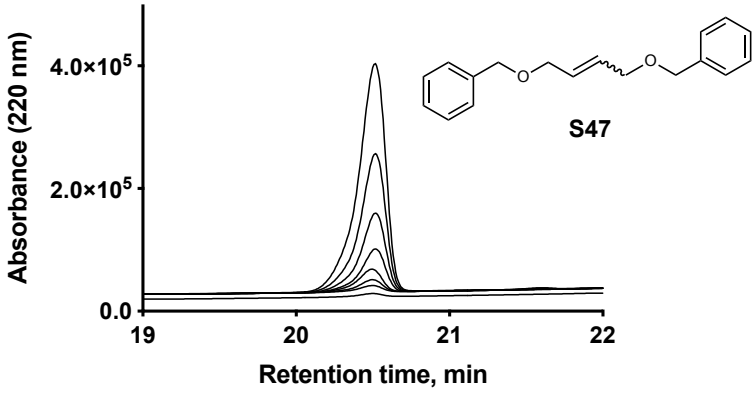

Fig. S35. HPLC calibration curve of product **S47**

HPLC Method		Calibration Curve
Method 4		
Slope	89276	
Intercept	441062	
R^2	0.9978	

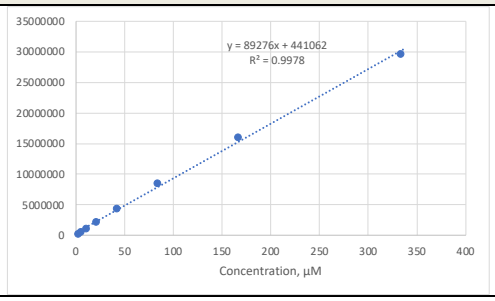

HPLC trace:

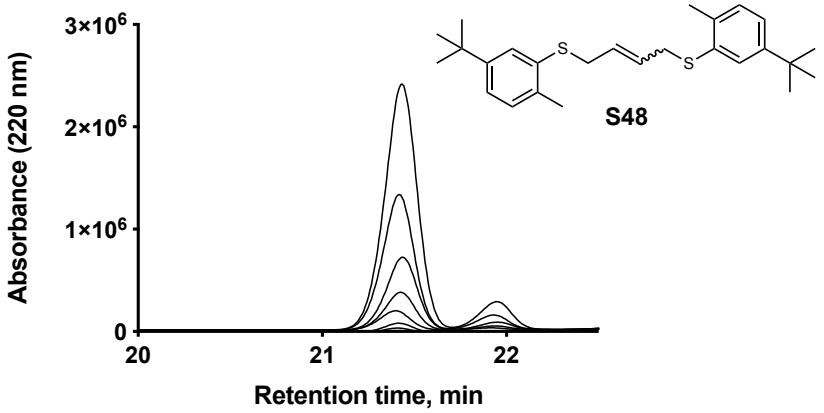

Fig. S36. HPLC calibration curve of product **S48**

HPLC Method		Calibration Curve
Method 2		
Slope	53337	
Intercept	160942	
R^2	0.9994	

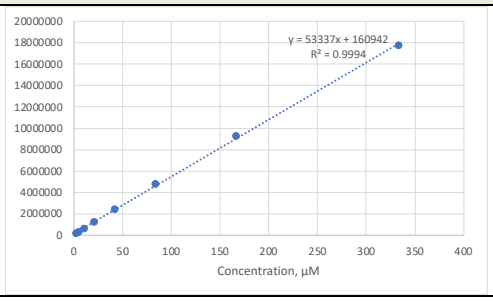

HPLC trace:

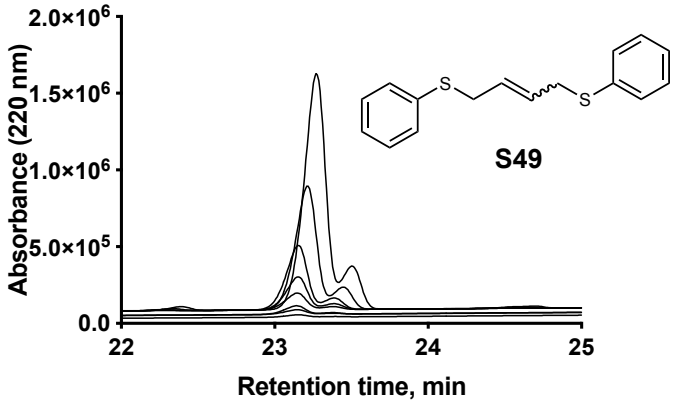

Fig. S37. HPLC calibration curve of product **S49**

HPLC Method		Calibration Curve
Method 6		
Slope	63015	
Intercept	-136816	
R^2	0.9949	

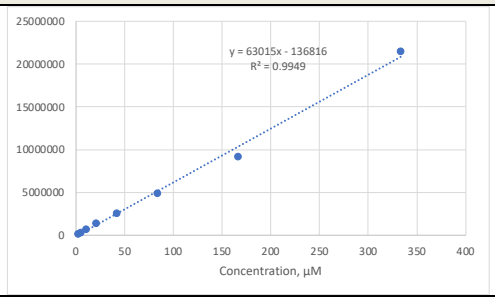

HPLC trace:

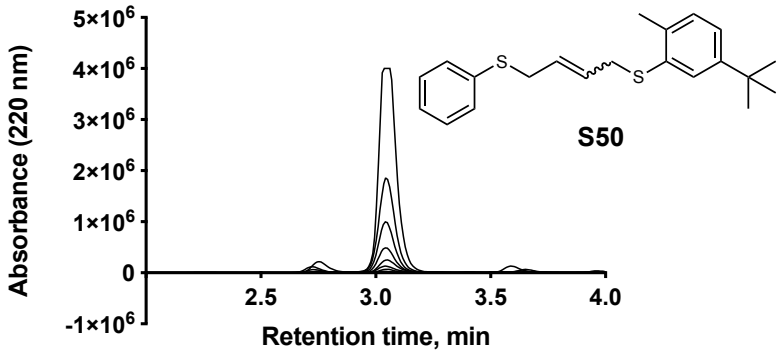

Fig. S38. HPLC calibration curve of product **S50**

HPLC Method		Calibration Curve
Method 2		
Slope	45332	
Intercept	238519	
R^2	0.9979	

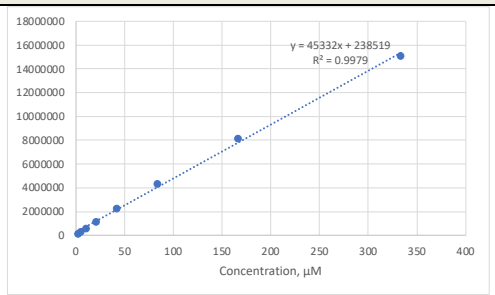

HPLC trace:

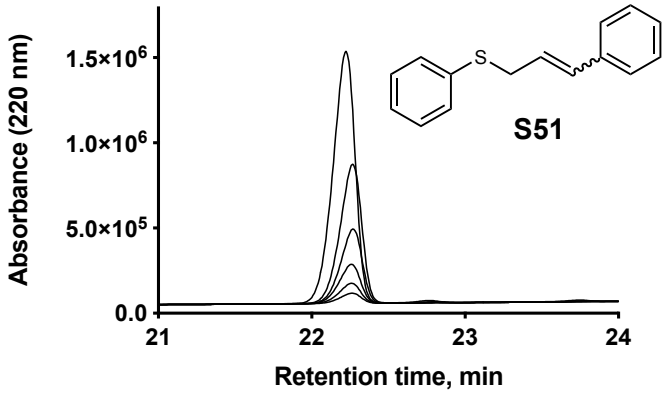

Fig. S39. HPLC calibration curve of product **S51**

HPLC Method		Calibration Curve
Method 2		
Slope	23658	
Intercept	103555	
R^2	0.9991	

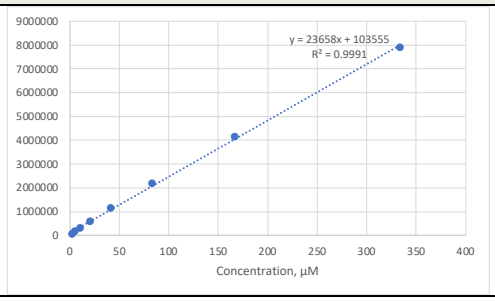

HPLC trace:

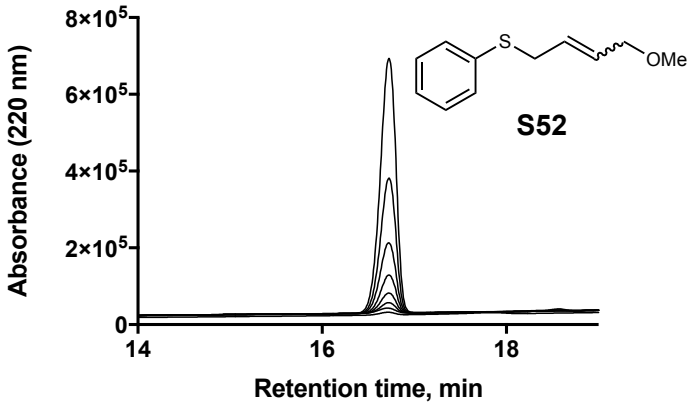

Fig. S40. HPLC calibration curve of product **S52**

HPLC Method		Calibration Curve
Method 5		
Slope	15202	
Intercept	54697	
R^2	0.9986	

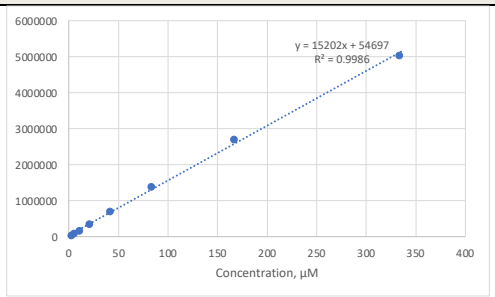

HPLC trace:

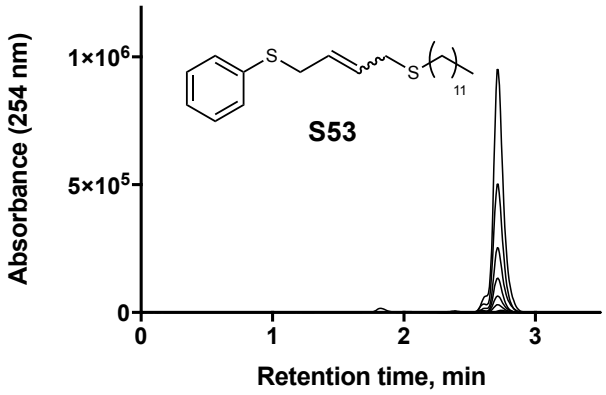

Fig. S41. HPLC calibration curve of product **S53**

HPLC Method		Calibration Curve
Method 1		
Slope	102962	
Intercept	62662	
R^2	0.9999	

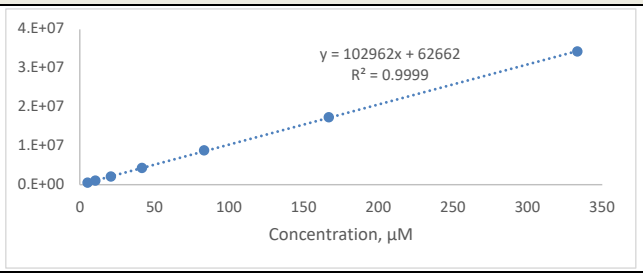

HPLC trace:

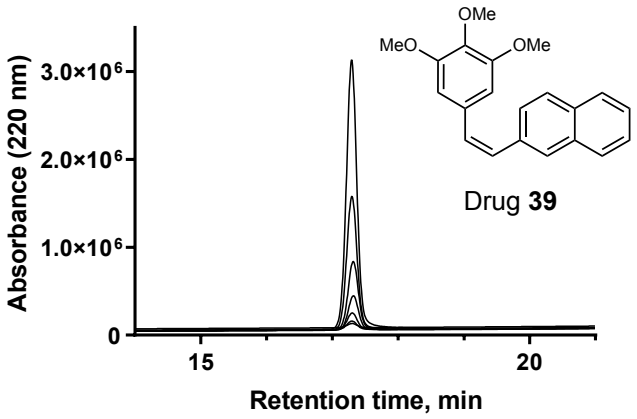

Fig. S42. HPLC calibration curve of drug **39**

Preparation of AlbRu-Cl/-I

In separated 1 mL vials, a 300 μM stock solution of human serum albumin (Alb) in PBS buffer pH 7.4 and a 400 μM stock solution of a Ru complex (Ru-I/or -Cl) in 1,4-dioxane were prepared. The reaction mixture consisted of 30 μM of Alb (50 nmol, 167 μL from 300 μM stock solution) and 40 μM of a Ru complex (66.6 nmol, 167 μL from 400 μM stock solution). The total reaction volumes were adjusted accordingly to ensure 1670 μL of 10% 1,4-dioxane in PBS buffer pH 7.4. Following initiation by the Ru complex addition, reaction mixtures were mildly mixed and incubated at 37 °C for 1 h. To remove unbound catalyst, the solution was concentrated and washed with PBS buffer using Amicon® Ultra Centrifugal Filters (30 kDa cut-off). Required concentrations of **AlbRu-Cl/-I** were then prepared accordingly. The characterization of **AlbRu-Cl/-I** was followed according to our previously reported procedures[1]. The characterization data of **AlbRu-I** was presented in the supplementary information (see Figs. S84-85)

Preparation of (cRGD)AlbRu-Cl/-I

To prepare the cRGD-functionalized artificial metalloenzyme used in this study, a solution of the cRGD peptide **40**[37] (see Fig. S86) (80.0 μmol, 200 μL in DMSO) in PBS buffer pH 7.4 (3.6 mL) was first prepared, followed by the addition of human serum albumin (Alb) (6.0 μmol, 400 μL in PBS buffer pH 7.4) and DIPEA reagent (2.4 μL). The mixture solution was incubated at 40 ºC for 16 h. To remove unreacted cRGD peptides, the solution was concentrated and washed with water using Amicon® Ultra Centrifugal Filters (30 kDa cut-off). Confirmation of cRGD peptides were made via MALDI-TOF-MS (positive mode), which detected an average molecular weight of 70 kDa (see Fig. S87). This implies that an average of 6.2 molecules of the cRGD peptide were attached to the surface of each protein. In the next stage, a solution of the prepared cRGD-functionalized Alb (120 nmol, 400 μL from 300 μM stock solution in water) in PBS buffer pH 7.4 (3.2 mL) was made. The solution of Ru complex (Ru-I/or -Cl) (160 nmol, 400 μL from 400 μM stock solution in dioxane) was then added, and the mixture was mildly mixed and incubated at 37 ºC for 1 h. To remove unbound catalyst, the solution was concentrated and washed with PBS buffer using Amicon® Ultra Centrifugal Filters (30 kDa cut-off). Required concentrations of **(cRGD)AlbRu-Cl/-I** were then prepared accordingly.

Protocols for catalytic olefin metathesis in blood

Reactions (done in triplicate) were generally carried out in Eppendorf tubes containing varying conditions of substrates (**1**-**38**) and catalyst (AquaMet catalyst, Ru-Cl/or -I, **AlbRu-Cl**/or **-I**, or **(cRGD)AlbRu-Cl**/or **-I**) in desired solutions (5:4:1 blood/PBS pH 7.4/1,4-dioxane or 8:1:1 blood/PBS pH 7.4/1,4-dioxane) The resulting mixtures were typically incubated for 3 h at 37 °C. To workup, mixtures were cooled to room temperature and then 10 mM of 1-dodecanethiol in MeOH (1 mL) was added to quench the Ru catalyst. Solutions were then centrifuged for 10 min at 16900 x *g* and the supernatants were analyzed by HPLC.

For entries 1-5 and 7 of Fig. 2A, 100 μL of sheep blood was mixed with either **AlbRu-Cl**, **AlbRu-I**, or the AquaMet catalyst (20 μL from a 0.2 mM stock solution in PBS (1 mol%); 40 μL from a 0.25 mM stock solution in PBS (2.5 mol%)), followed by dilution with PBS buffer pH 7.4 (60 or 40 μL, respectively), and adding substrate **1** (20 μL from a 20 mM stock solution in 1,4-dioxane). The resulting mixtures were incubated for specified time (3 or 24 h) at 37 °C. For entry 6 of Fig. 2A, 160 μL of sheep blood was mixed with **AlbRu-I** (20 μL from a 0.2 mM stock solution (1 mol%)) and substrate **1** (20 μL from a 20 mM stock solution 1,4-dioxane) without dilution with PBS buffer. The resulting mixture was incubated for 3 h at 37 °C.

For Fig. 2B, 100 μL of sheep blood was mixed with either **AlbRu-Cl**, **AlbRu-I**, Ru-Cl or Ru-I (**AlbRu-Cl**/or **-I** (20 μL from a 0.2 mM stock solution in PBS (1 mol%)); Ru-Cl/ or -I (10 μL from a 0.4 mM stock solution in 1,4-dioxane (1 mol%)). The resulting mixture was incubated for a specified time (0, 5, 15, 30, and 60 min for Ru-I/Cl; 0, 5, 15, 45, 120, and 360 min for **AlbRu-Cl**; and 0, 5, 15, 45, 120, 360 min, and 24 h for **AlbRu-I**) at 37 °C. After that, the mixture solution was added necessary volumes of PBS buffer pH 7.4, followed by addition of substrate **1** (20 μL from a 20 mM stock solution in 1,4-dioxane). The total reaction volume was 200 μL of 10% 1,4-dioxane and 40% PBS buffer in the blood mixture. The reaction mixture was incubated at 37 °C for additional 3 h.

For Fig. 2D and 3A-B, 100 μL of sheep blood was mixed with either **AlbRu-Cl** or **AlbRu-I** (40 μL from a 0.25 mM stock solution in PBS (2.5 mol%)), followed by dilution with PBS buffer pH 7.4 (40 μL), and adding varying substrates (**3**-**31**) (20 μL from a 20 mM stock solution in 1,4-dioxane). The obtained mixture was incubated for 3 h at 37 °C.

For Fig. 3C-I, 12.5 μL of sheep blood was mixed with **AlbRu-I** (10 μL from a 1.25 mM stock solution in PBS (5mol%)), followed by addition of varying substrates (**32**-**34**) (2.5 μL from a 100 mM stock solution in 1,4-dioxane). The obtained mixture was incubated for 3 h at 37 °C.

For Fig. 3C-II, 12.5 μL of sheep blood was mixed with **AlbRu-I** (10 μL from a 1.25 mM stock solution in PBS (5mol%)), followed by addition of stock solution of substrate **34** (1.25 μL from a 200 mM stock solution in 1,4-dioxane) and varying substrates (**33** and **35**-**37**) (1.25 μL from a 400 mM stock solution in 1,4-dioxane). The obtained mixture was incubated for 3 h at 37 °C.

For Fig. 4, 100 μL of sheep blood was mixed with either **(cRGD)AlbRu-Cl** or **(cRGD)AlbRu-I** (40 μL from a 0.25 mM stock solution in PBS (2.5 mol%)), followed by dilution with PBS buffer pH 7.4 (40 μL), and adding prodrug **38** (20 μL from a 20 mM stock solution in 1,4-dioxane). The obtained mixture was incubated for 3 h at 37 °C.

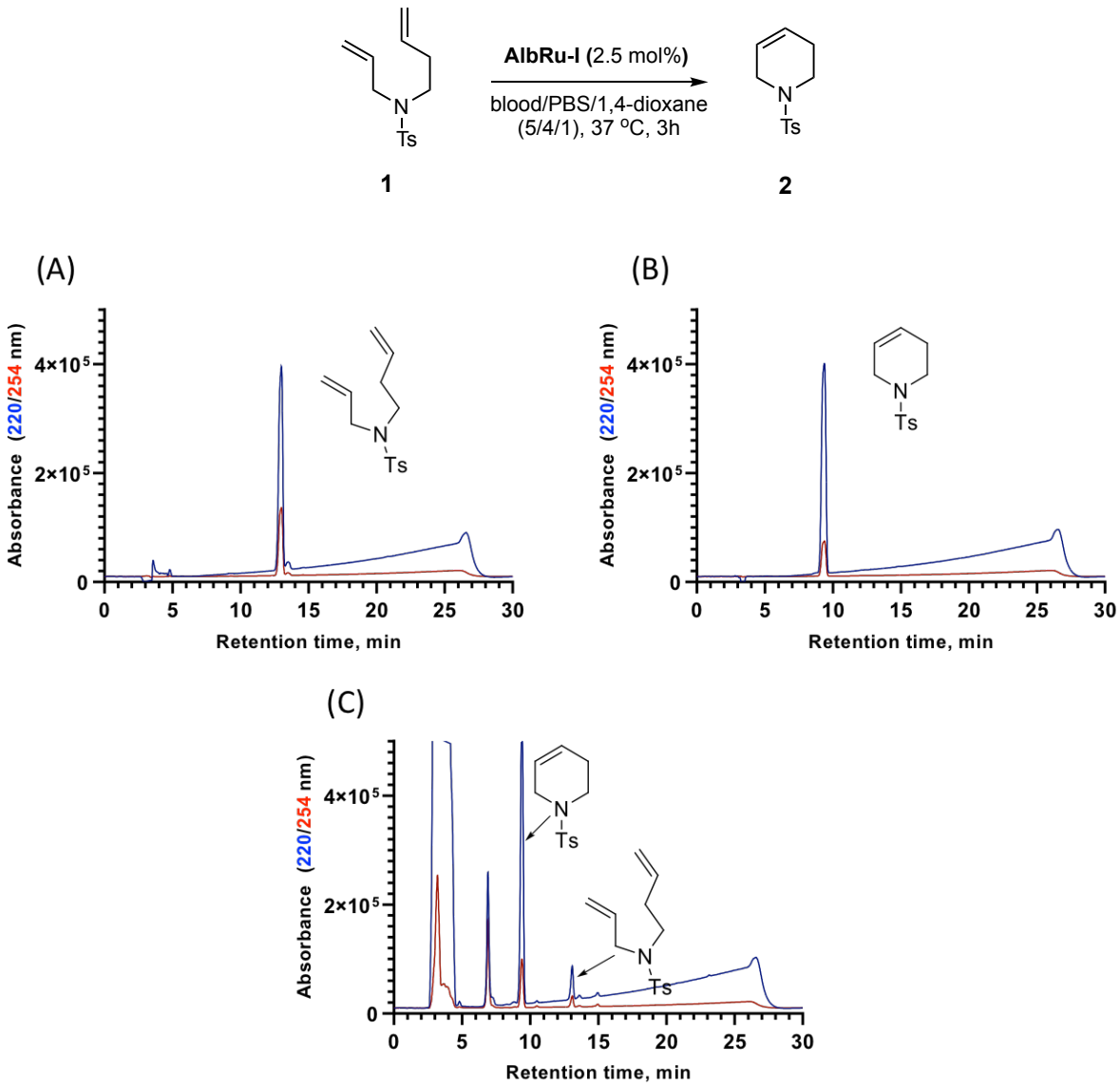

Fig. S43. Example HPLC traces of A) substrate **1**, B) product **2**, and C) analysis of reaction of **1** in blood by **AlbRu-I**.

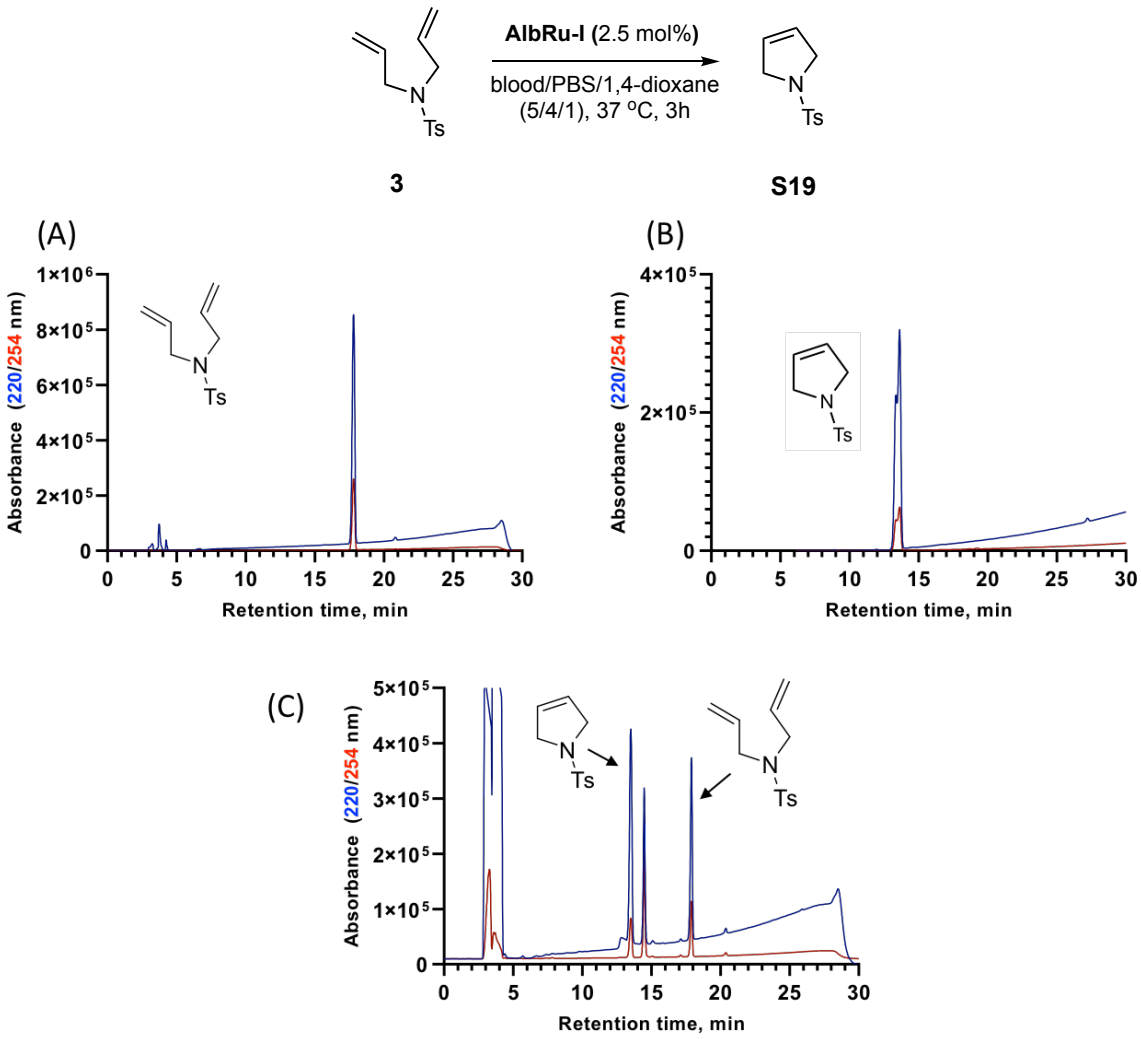

Fig. S44. Example HPLC traces of A) substrate **3**, B) product **S19**, and C) analysis of reaction of **3** in blood by **AlbRu-I**.

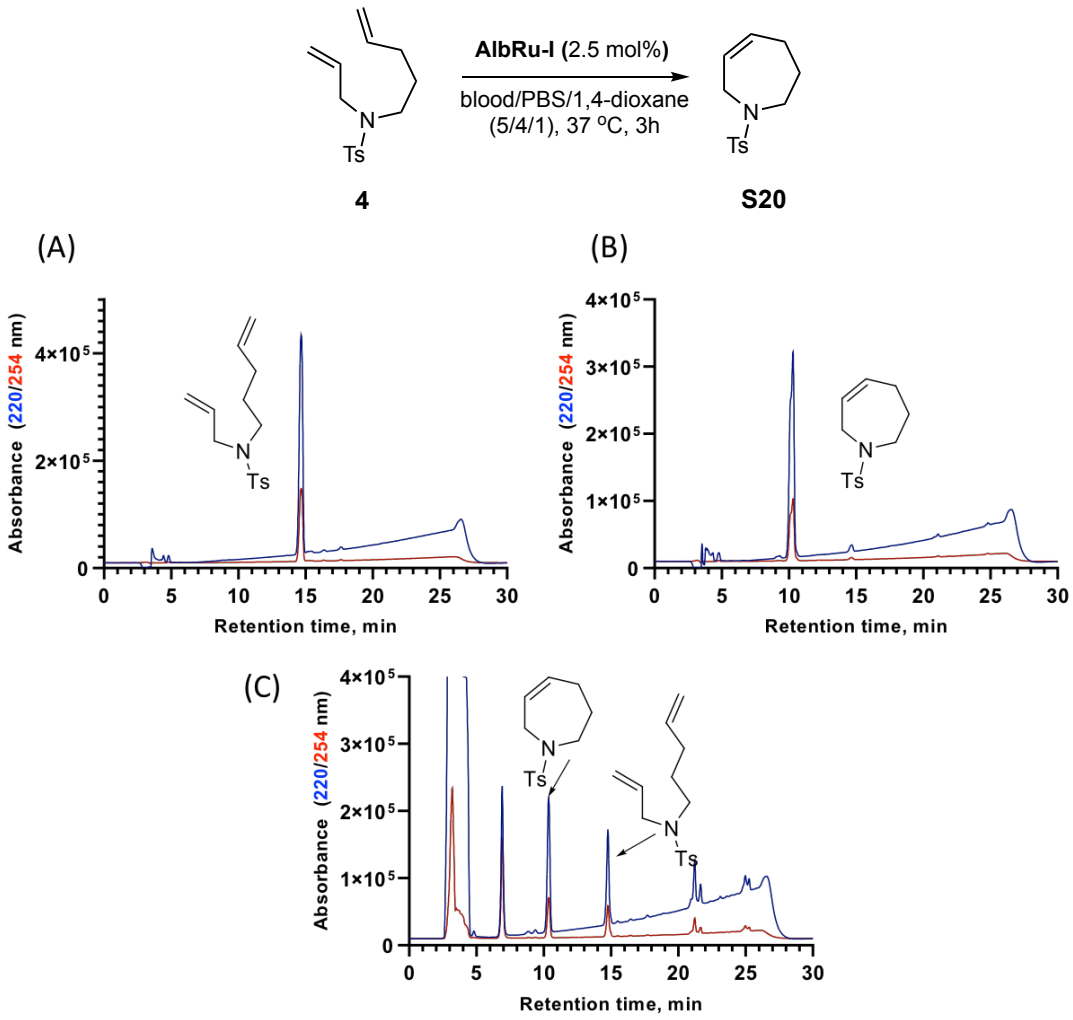

Fig. S45. Example HPLC traces of A) substrate **4**, B) product **S20**, and C) analysis of reaction of **4** in blood by **AlbRu-I**.

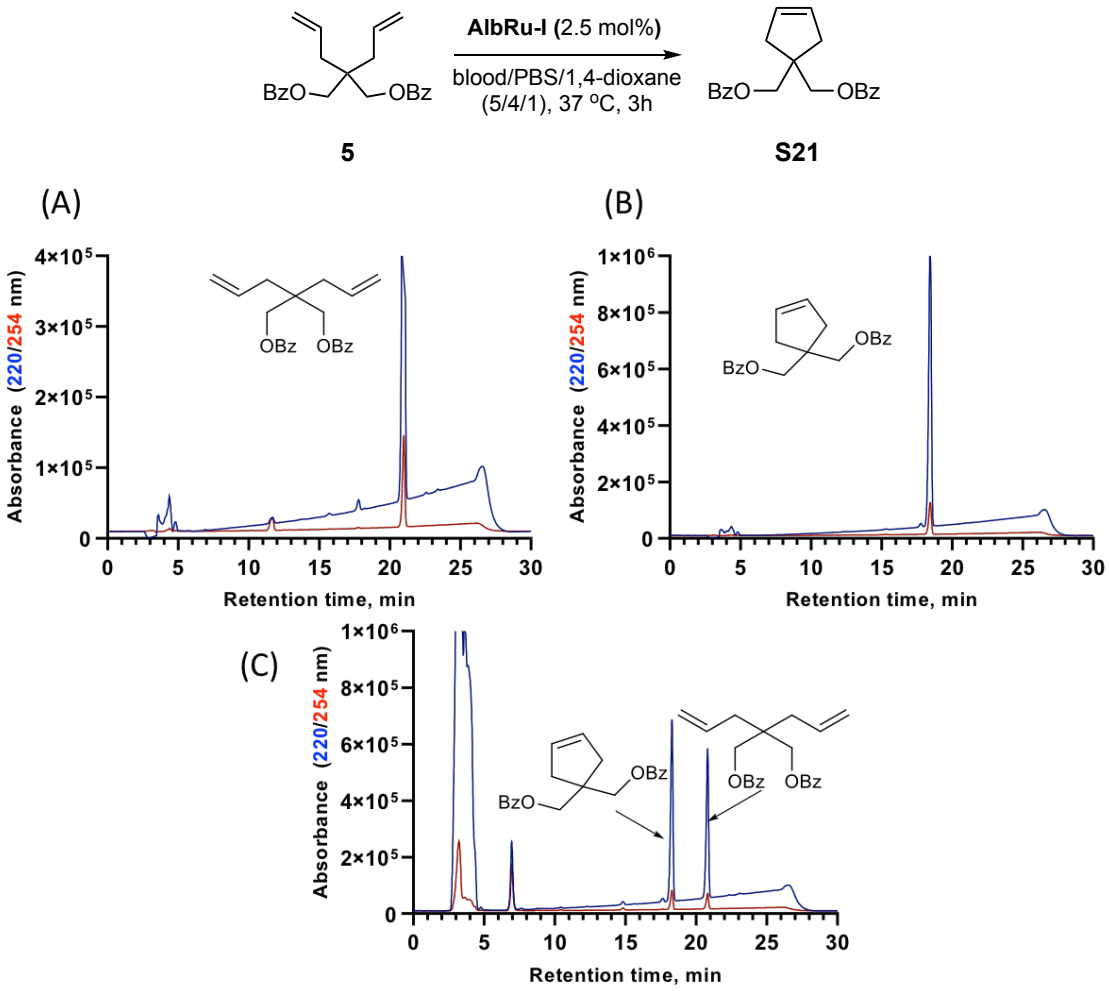

Fig. S46. Example HPLC traces of A) substrate **5**, B) product **S21**, and C) analysis of reaction of **5** in blood by **AlbRu-I**.

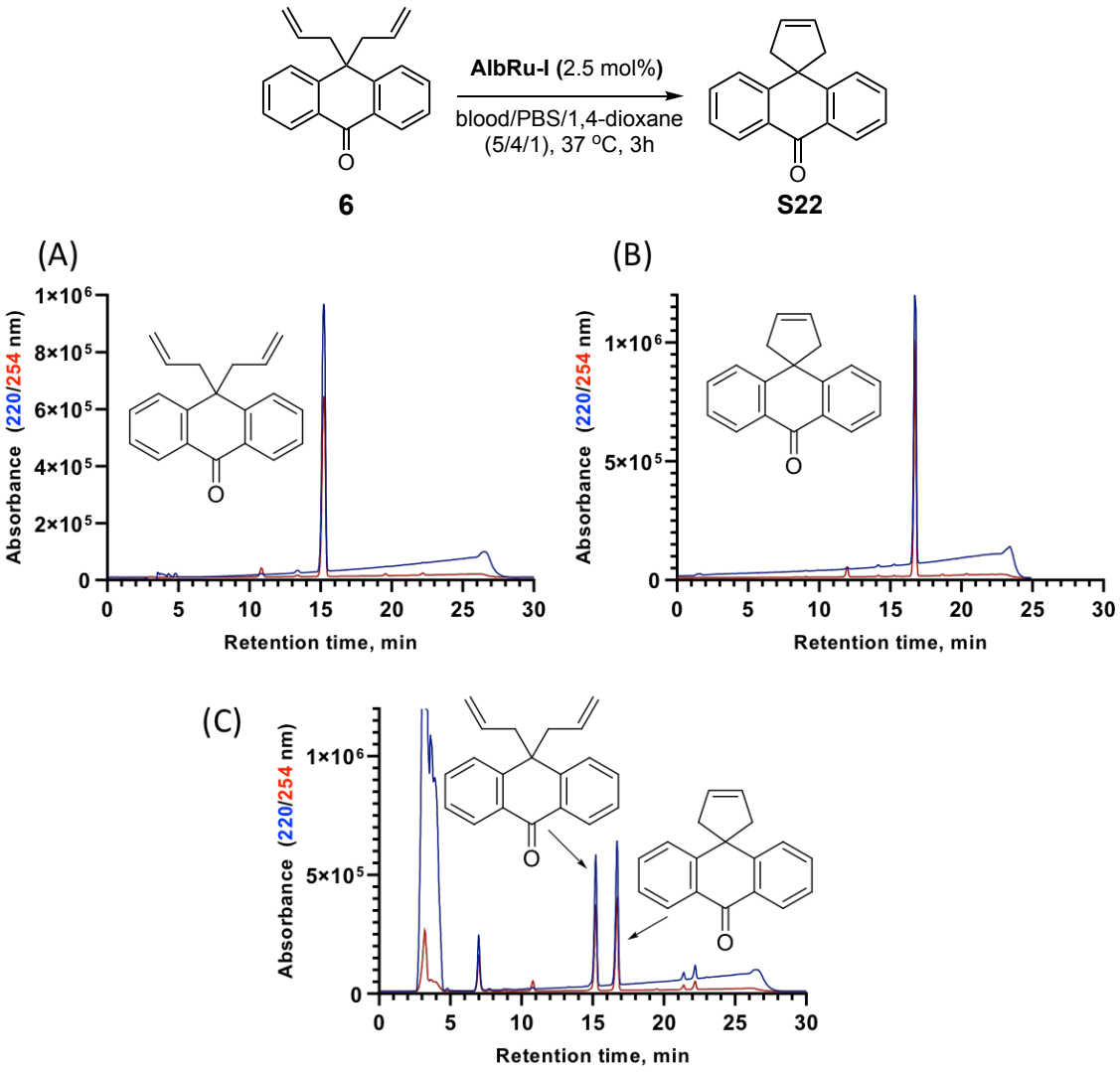

Fig. S47. Example HPLC traces of A) substrate **6**, B) product **S22**, and C) analysis of reaction of **6** in blood by **AlbRu-I**.

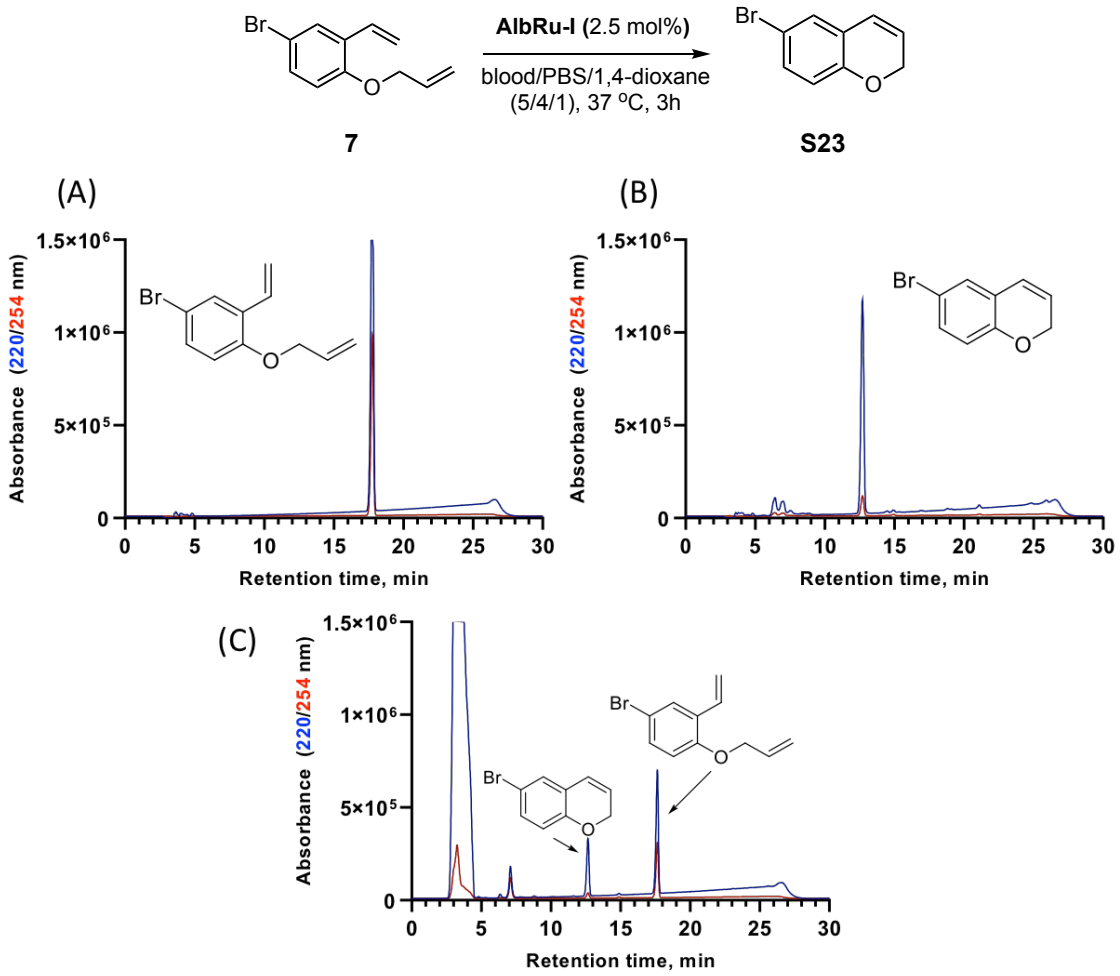

Fig. S48. Example HPLC traces of A) substrate **7**, B) product **S23**, and C) analysis of reaction of **7** in blood by **AlbRu-I**.

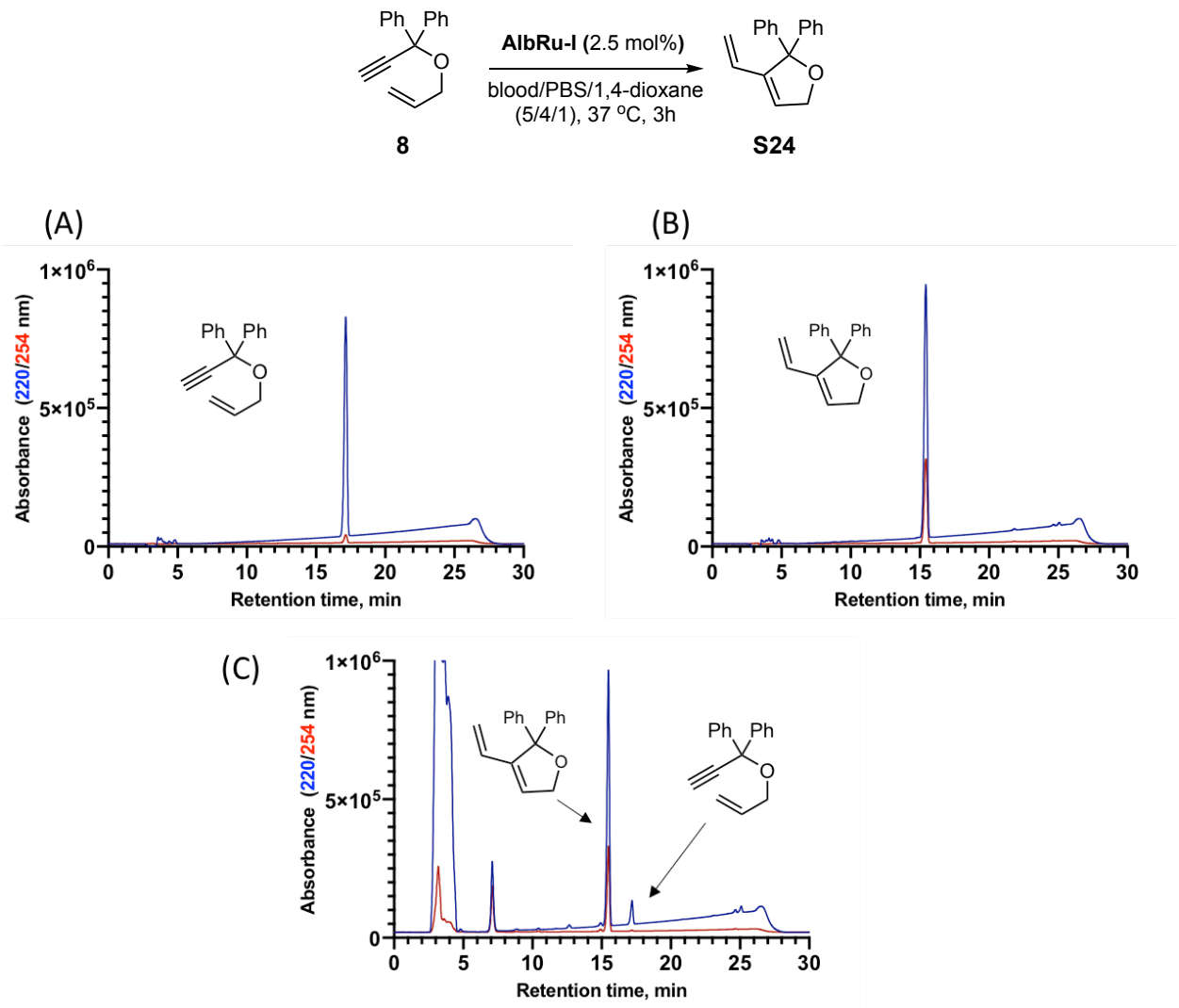

Fig. S49. Example HPLC traces of A) substrate **8**, B) product **S24**, and C) analysis of reaction of **8** in blood by **AlbRu-I**.

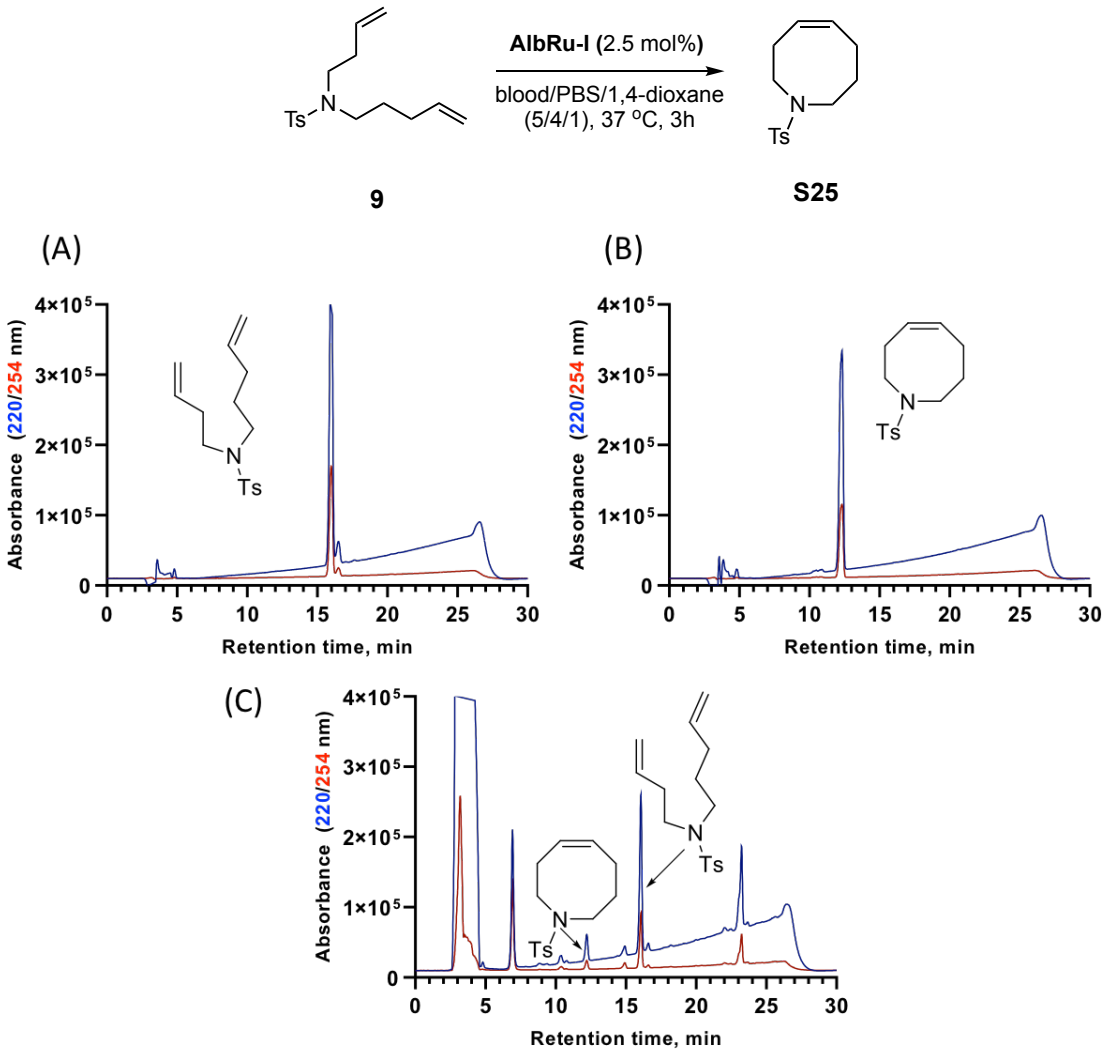

Fig. S50. Example HPLC traces of A) substrate **9**, B) product **S25**, and C) analysis of reaction of **9** in blood by **AlbRu-I**.

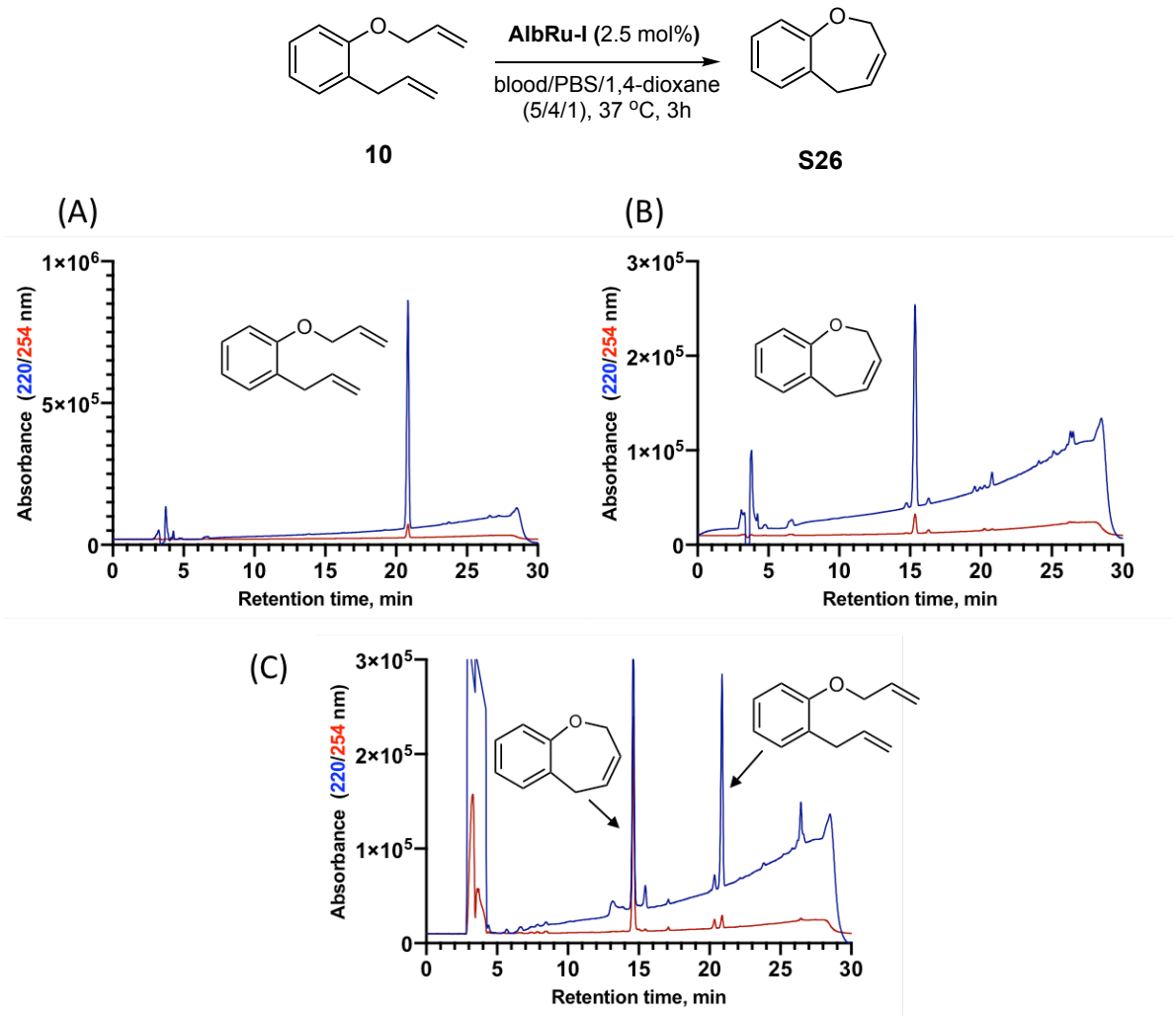

Fig. S51. Example HPLC traces of A) substrate **10**, B) product **S26**, and C) analysis of reaction of **10** in blood by **AlbRu-I**.

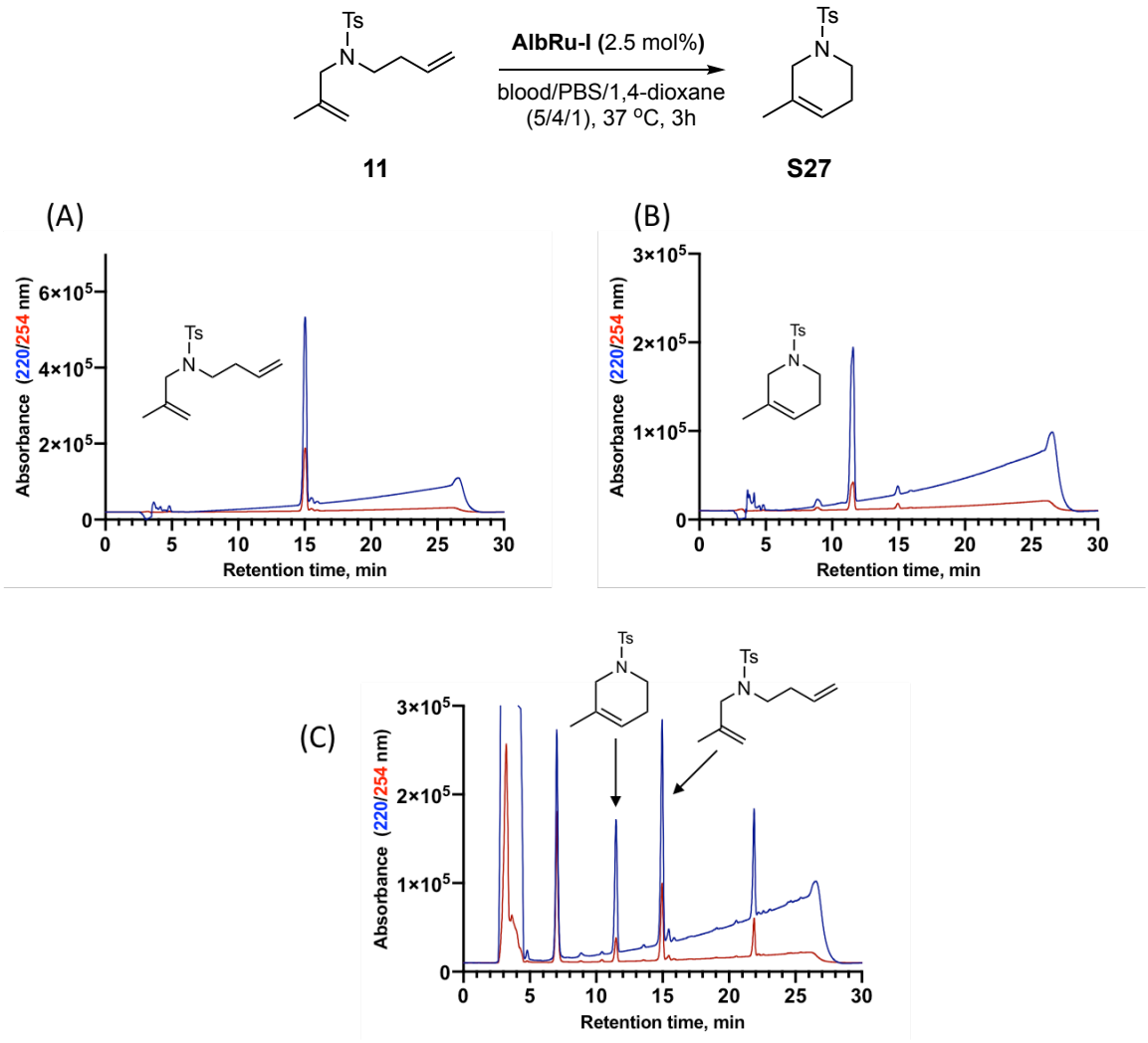

Fig. S52. Example HPLC traces of A) substrate **11**, B) product **S27**, and C) analysis of reaction of **11** in blood by **AlbRu-I**.

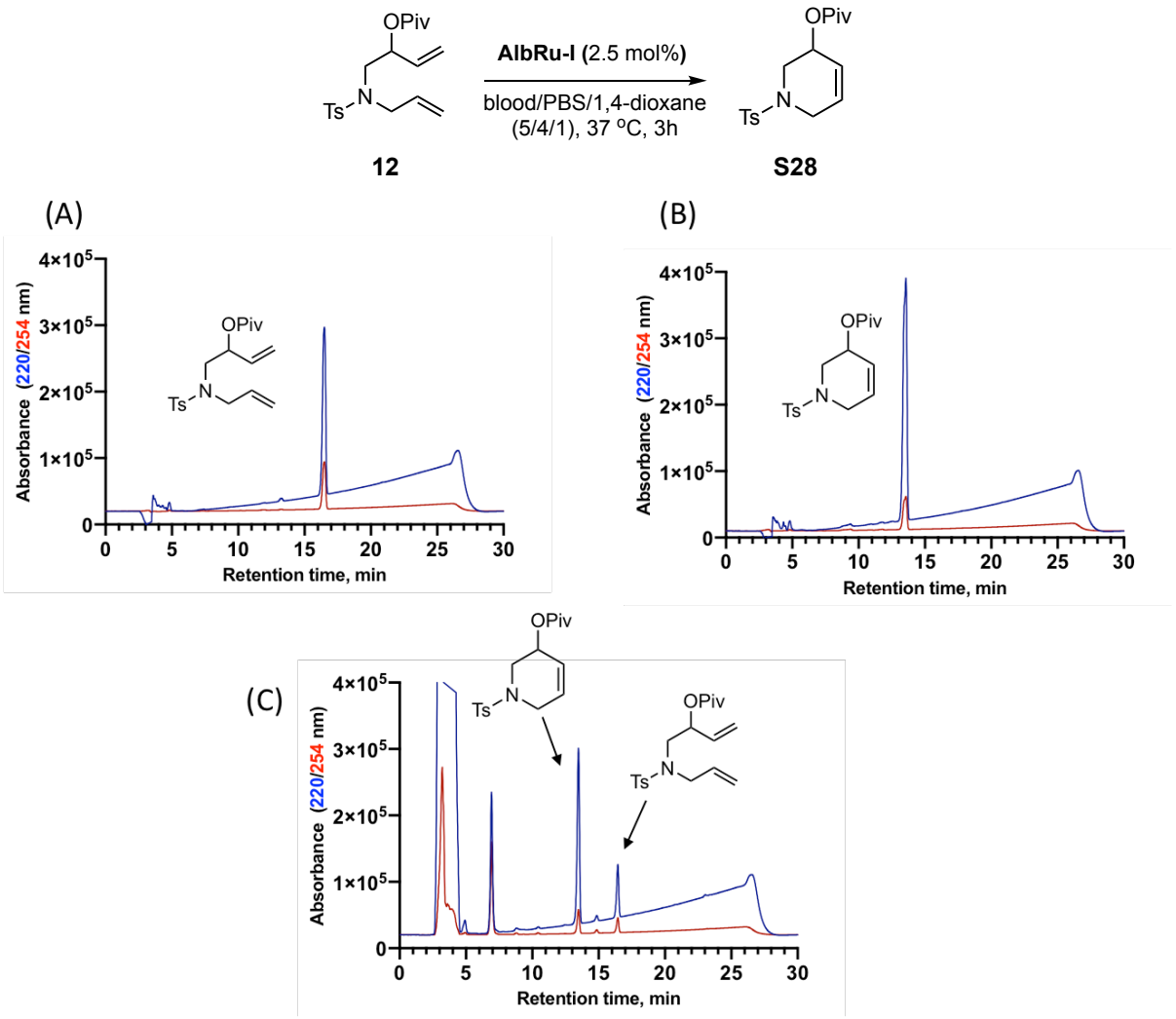

Fig. S53. Example HPLC traces of A) substrate **12**, B) product **S28**, and C) analysis of reaction of **12** in blood by **AlbRu-I**.

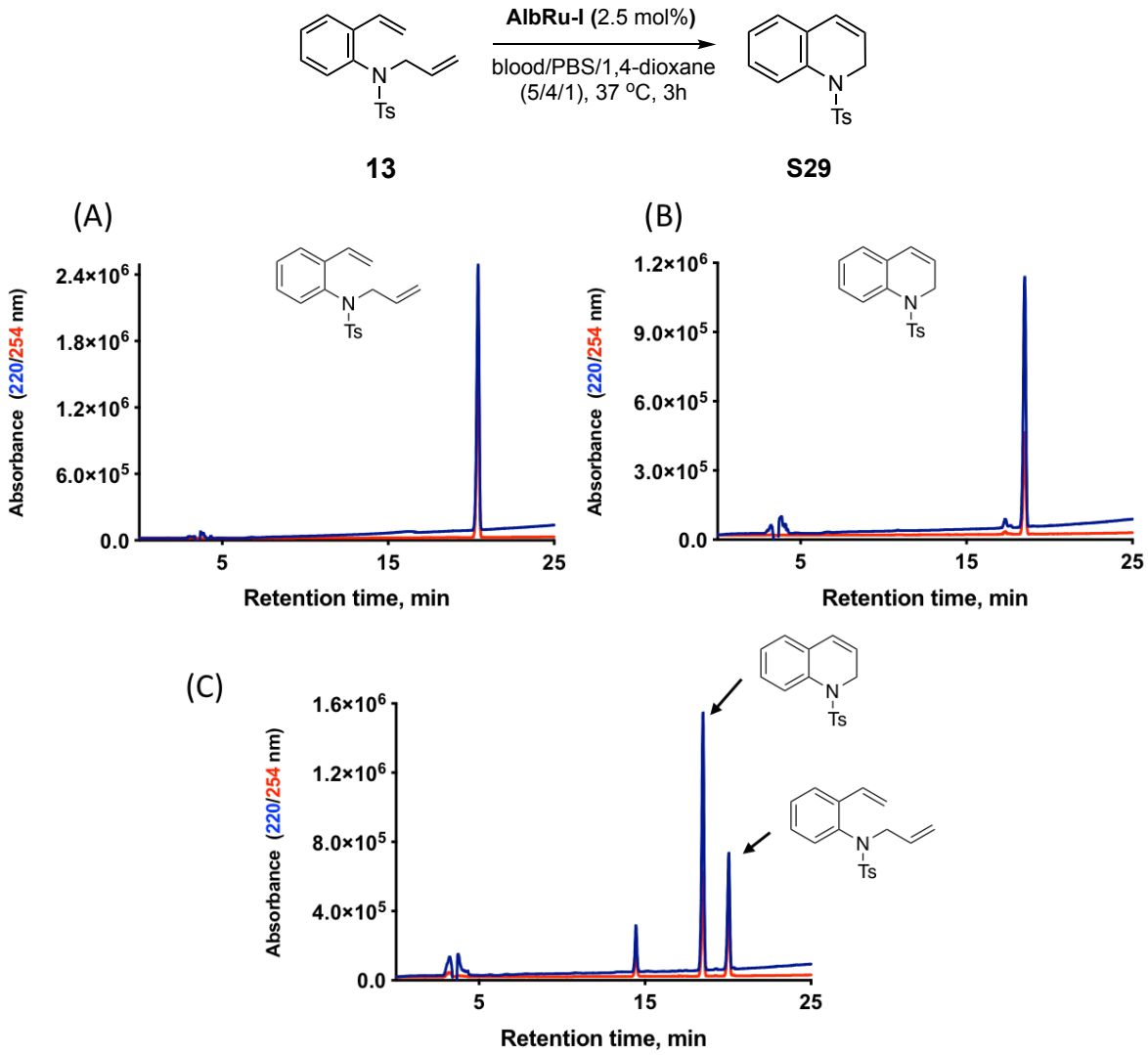

Fig. S54. Example HPLC traces of A) substrate **13**, B) product **S29**, and C) analysis of reaction of **13** in blood by **AlbRu-I**.

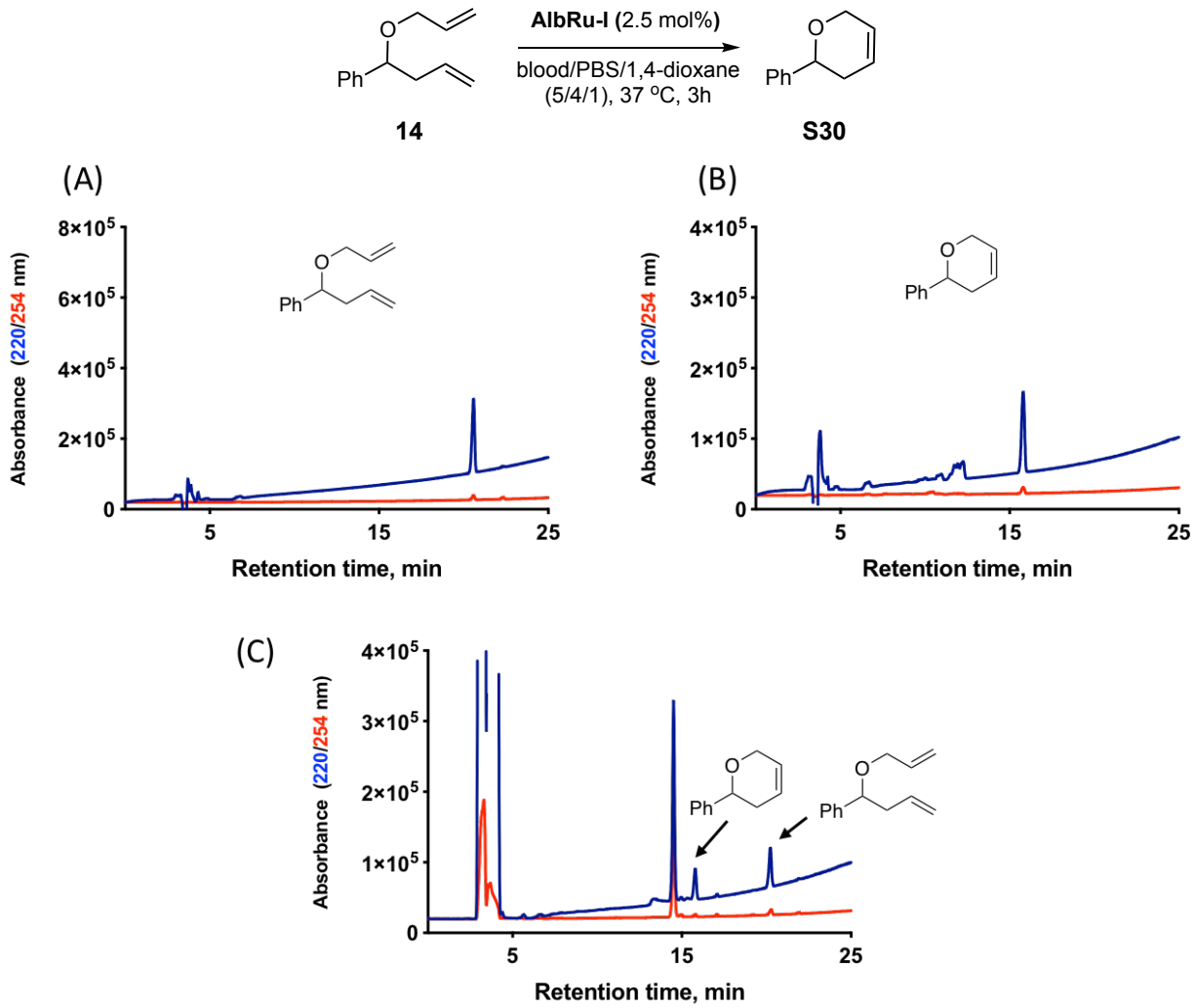

Fig. S55. Example HPLC traces of A) substrate **14**, B) product **S30**, and C) analysis of reaction of **14** in blood by **AlbRu-I**.

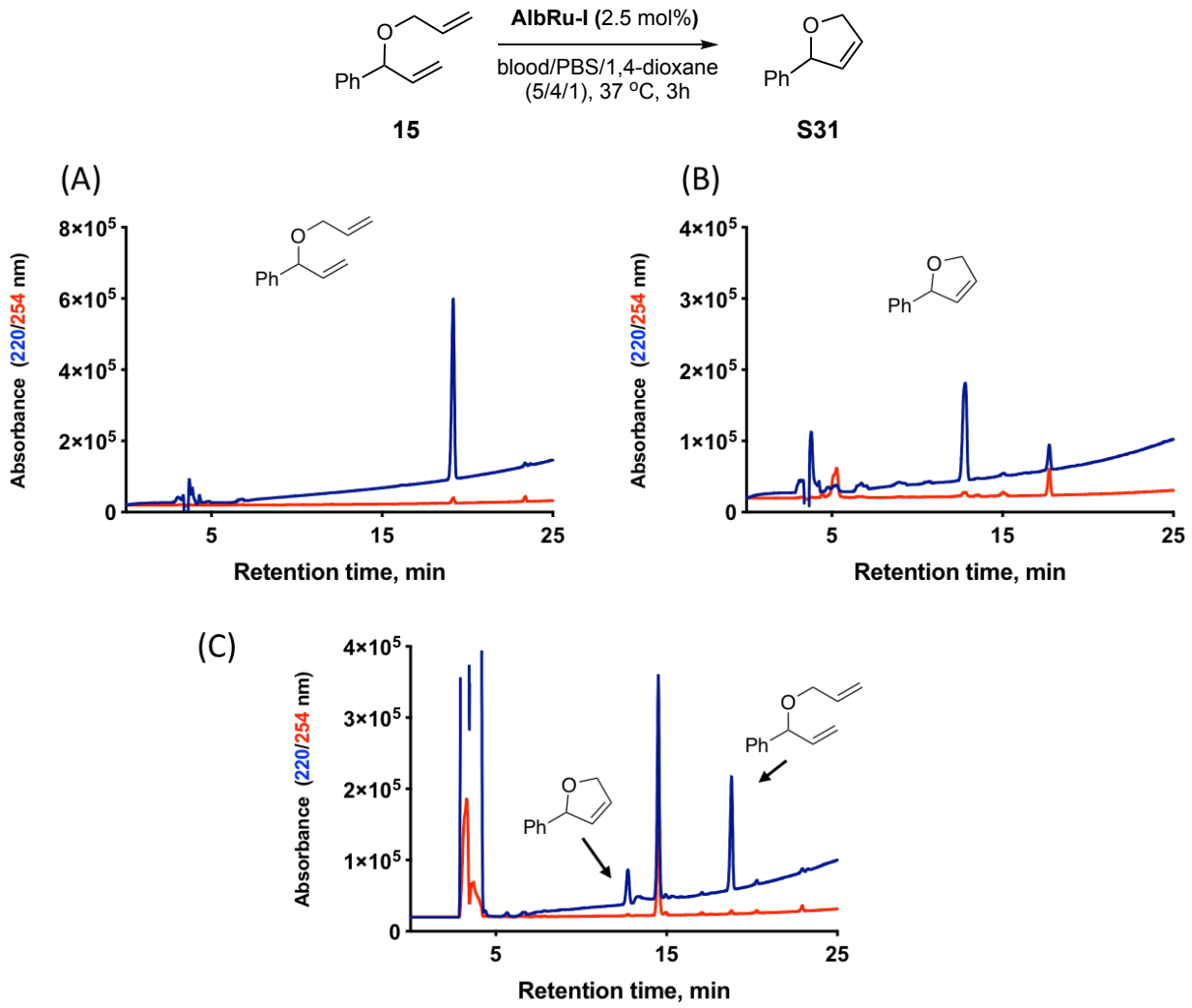

Fig. S56. Example HPLC traces of A) substrate **15**, B) product **S31**, and C) analysis of reaction of **15** in blood by **AlbRu-I**.

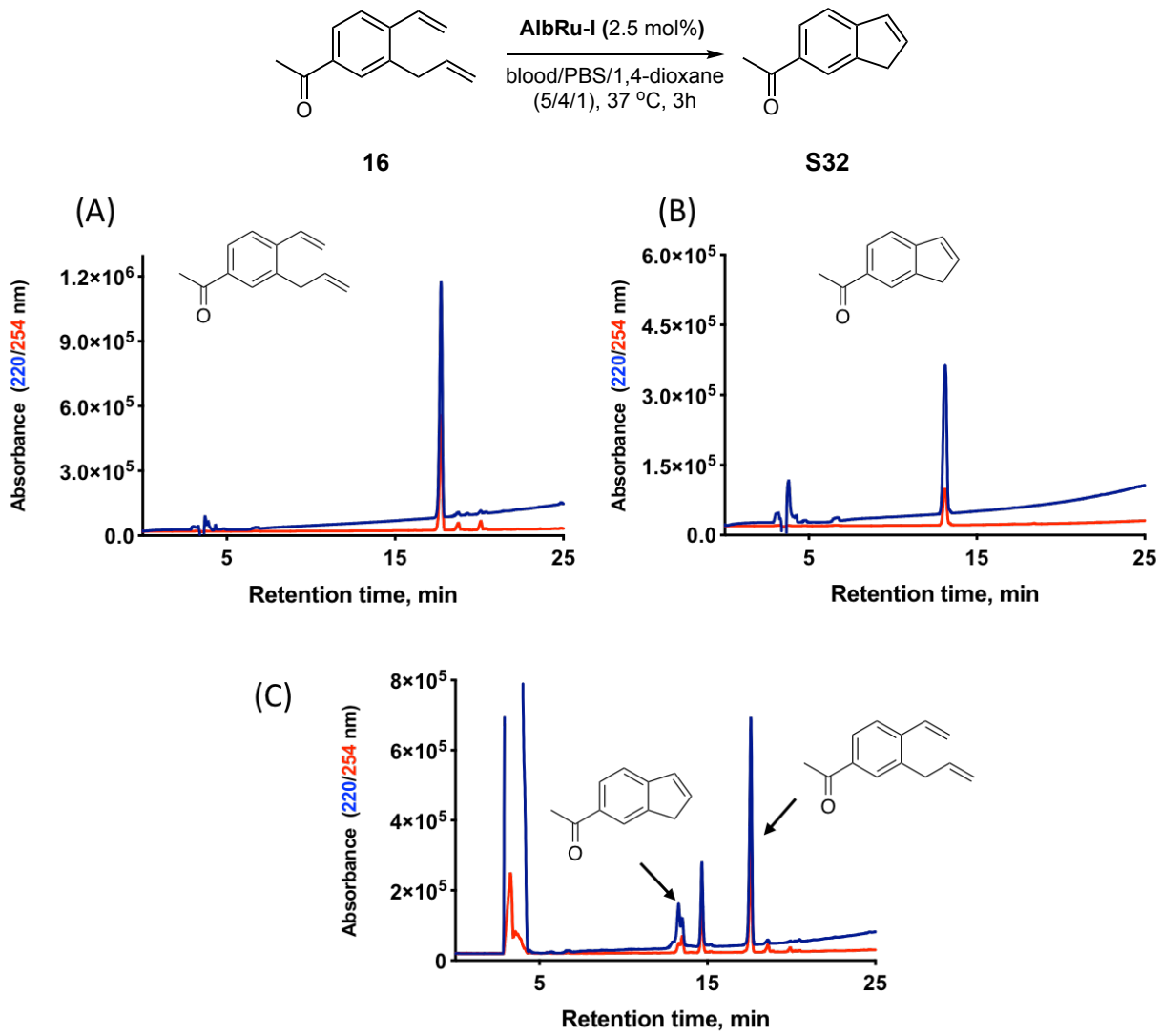

Fig. S57. Example HPLC traces of A) substrate **16**, B) product **S32**, and C) analysis of reaction of **16** in blood by **AlbRu-I**.

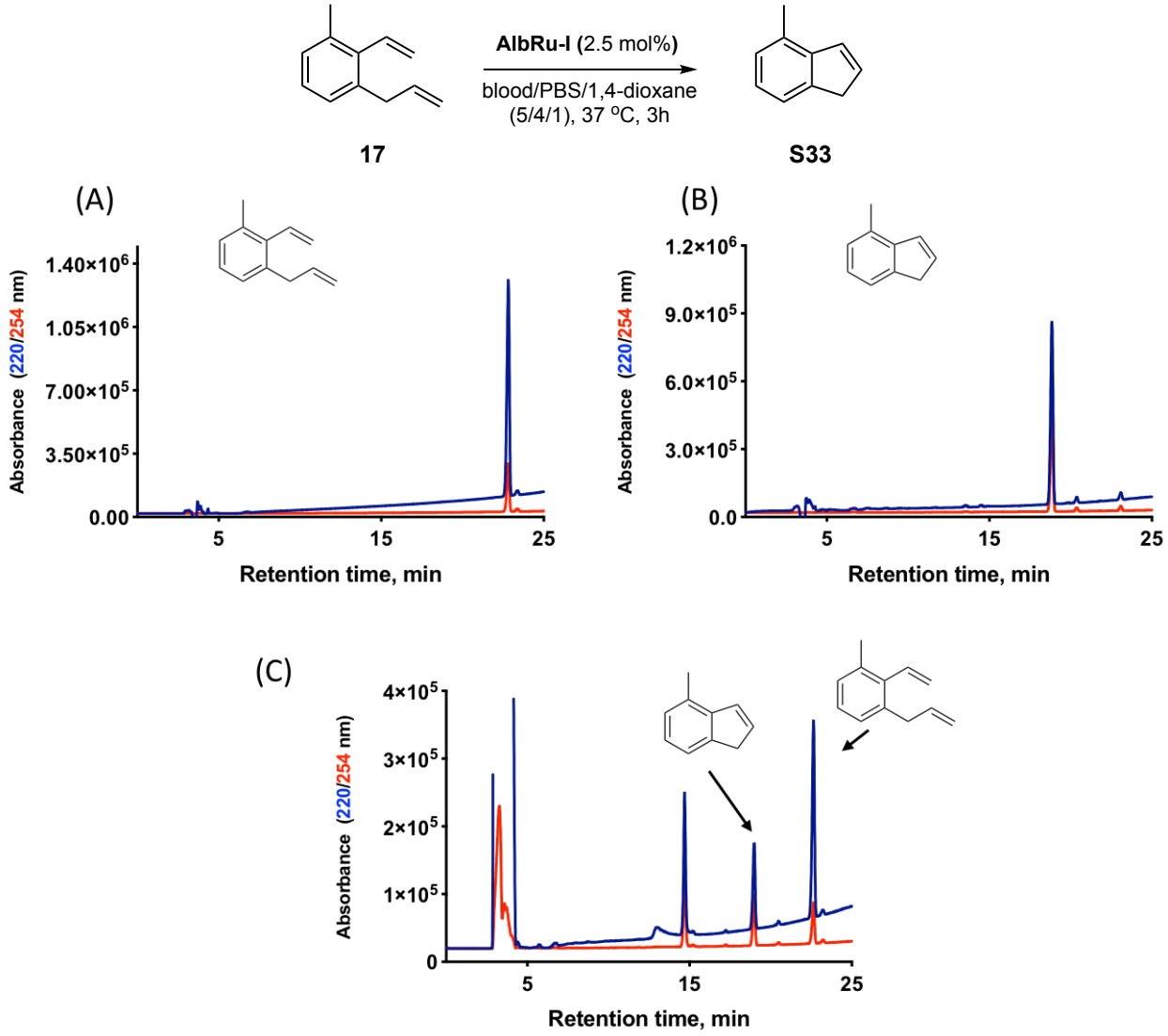

Fig. S58. Example HPLC traces of A) substrate **17**, B) product **S33**, and C) analysis of reaction of **17** in blood by **AlbRu-I**.

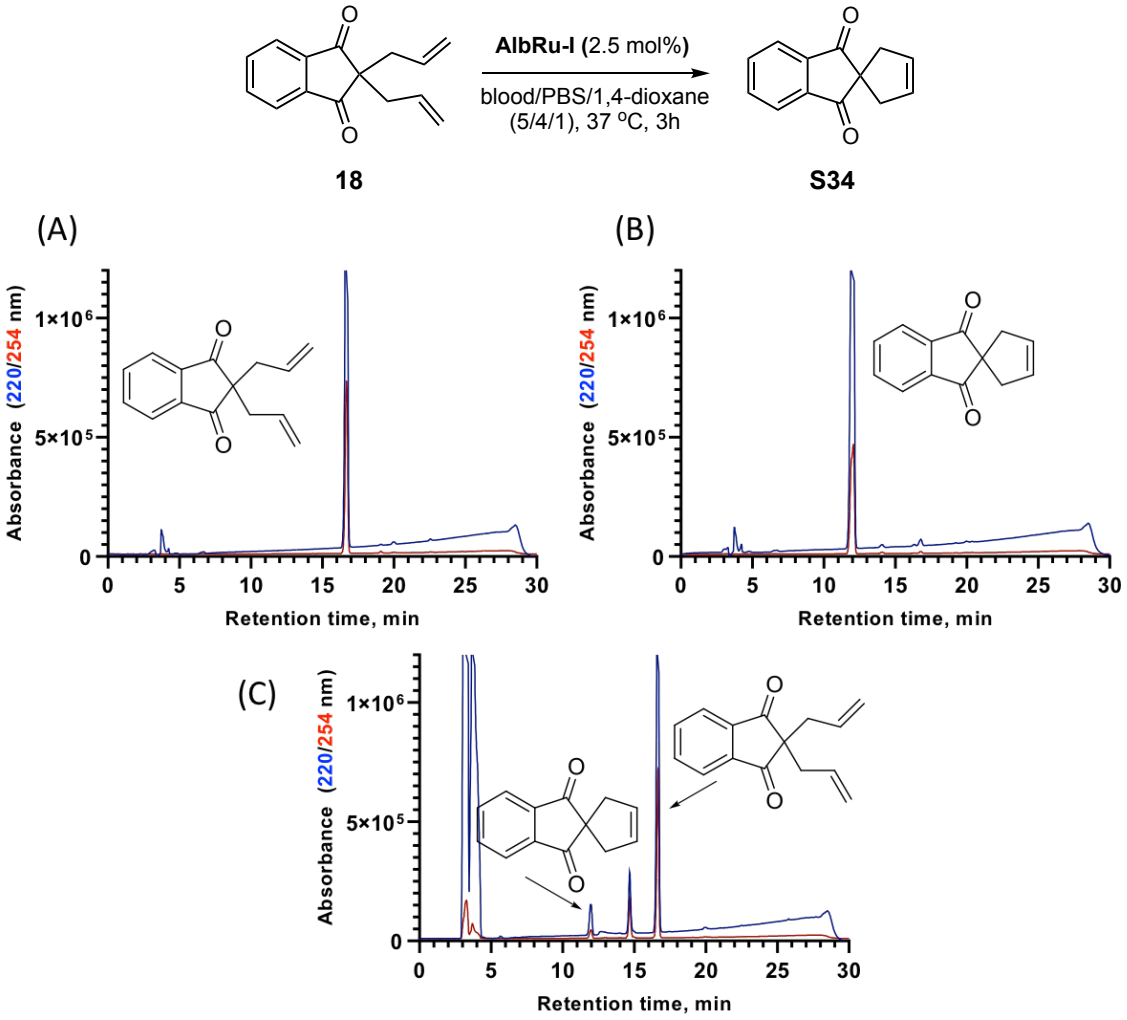

Fig. S59. Example HPLC traces of A) substrate **18**, B) product **S34**, and C) analysis of reaction of **18** in blood by **AlbRu-I**.

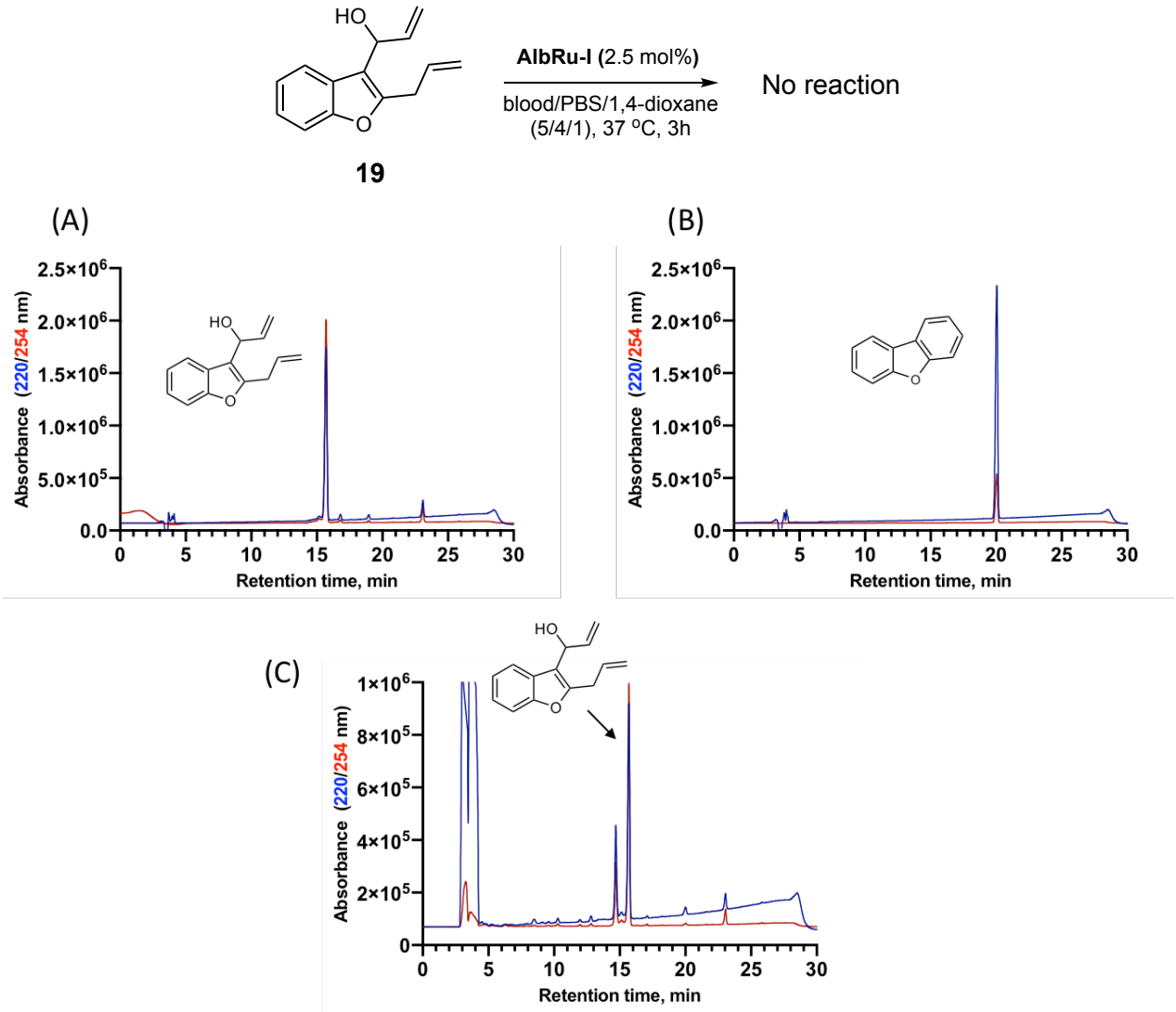

Fig. S60. Example HPLC traces of A) substrate **19**, B) product **S35**, and C) analysis of reaction of **19** in blood by **AlbRu-I**.

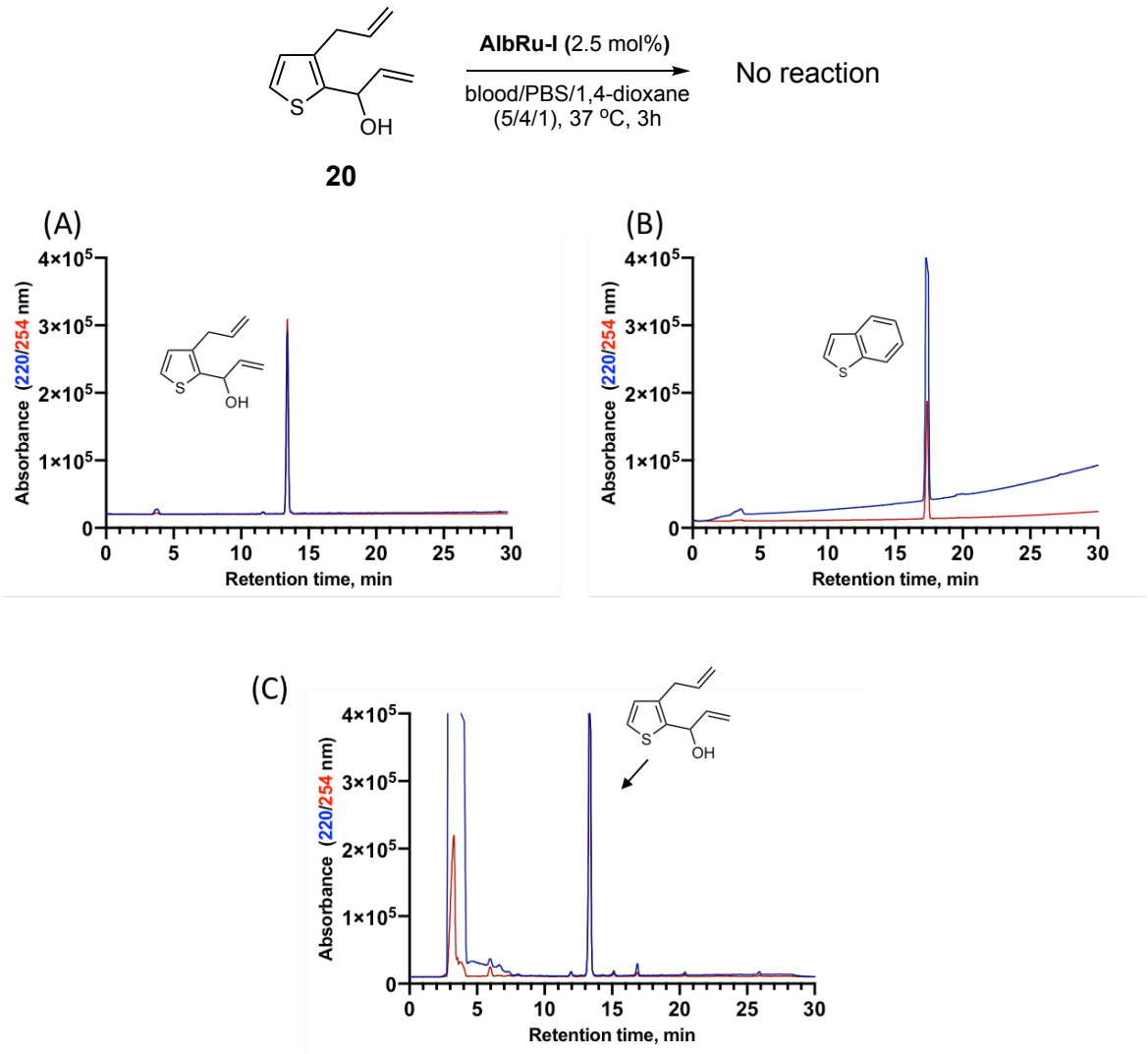

Fig. S61. Example HPLC traces of A) substrate **20**, B) product **S36**, and C) analysis of reaction of **20** in blood by **AlbRu-I**.

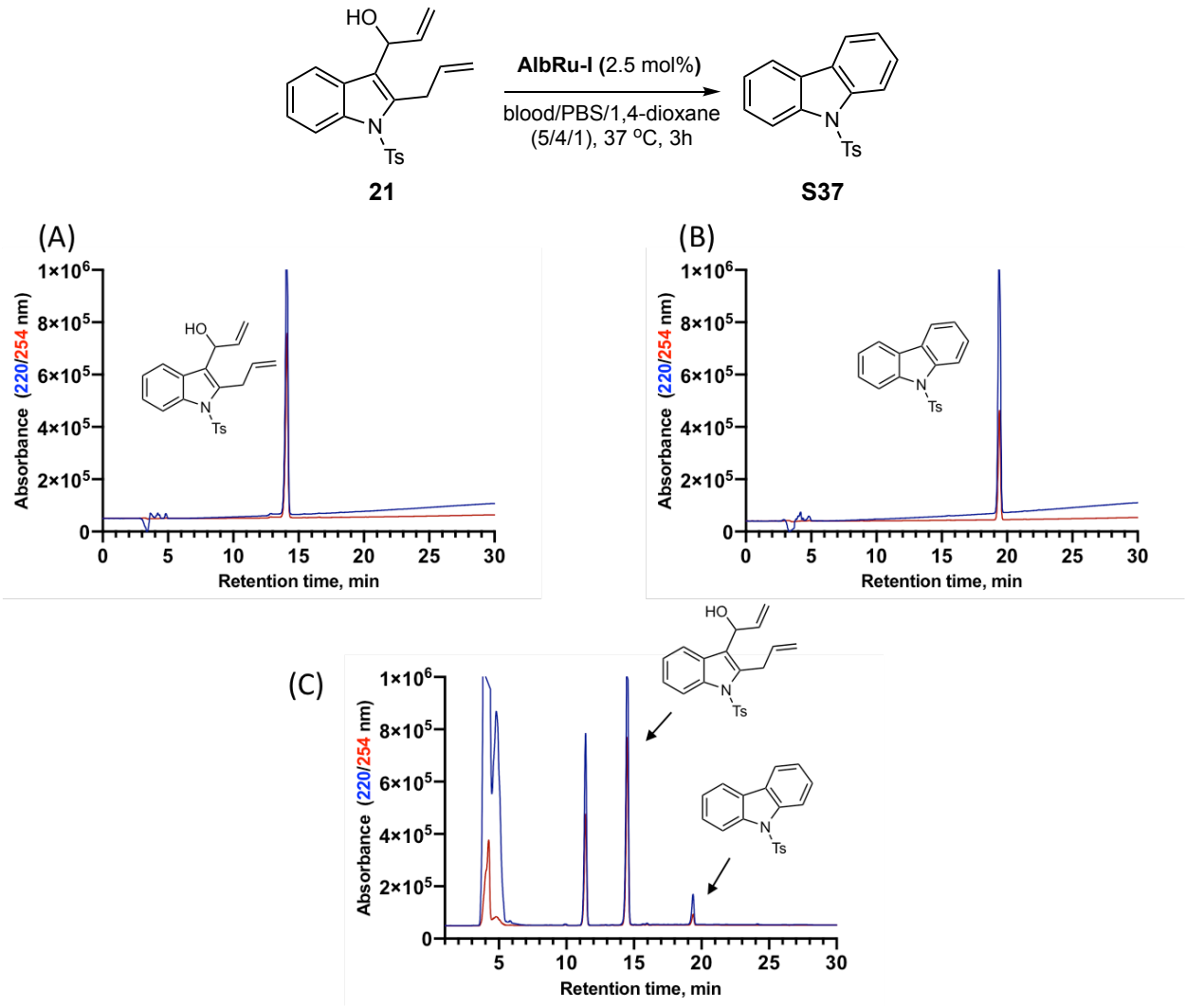

Fig. S62. Example HPLC traces of A) substrate **21**, B) product **S37**, and C) analysis of reaction of **21** in blood by **AlbRu-I**.

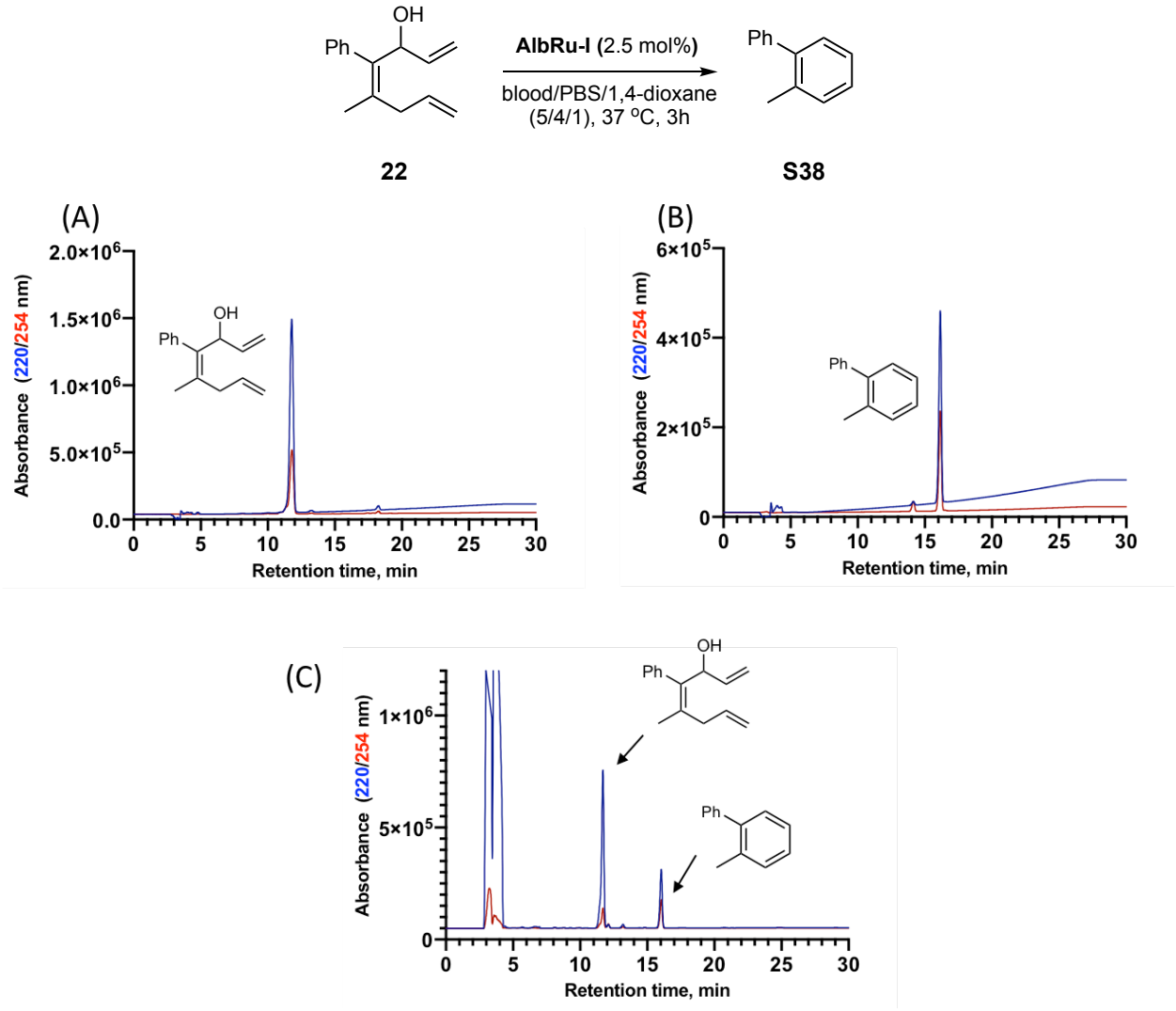

Fig. S63. Example HPLC traces of A) substrate **22**, B) product **S38**, and C) analysis of reaction of **22** in blood by **AlbRu-I**.

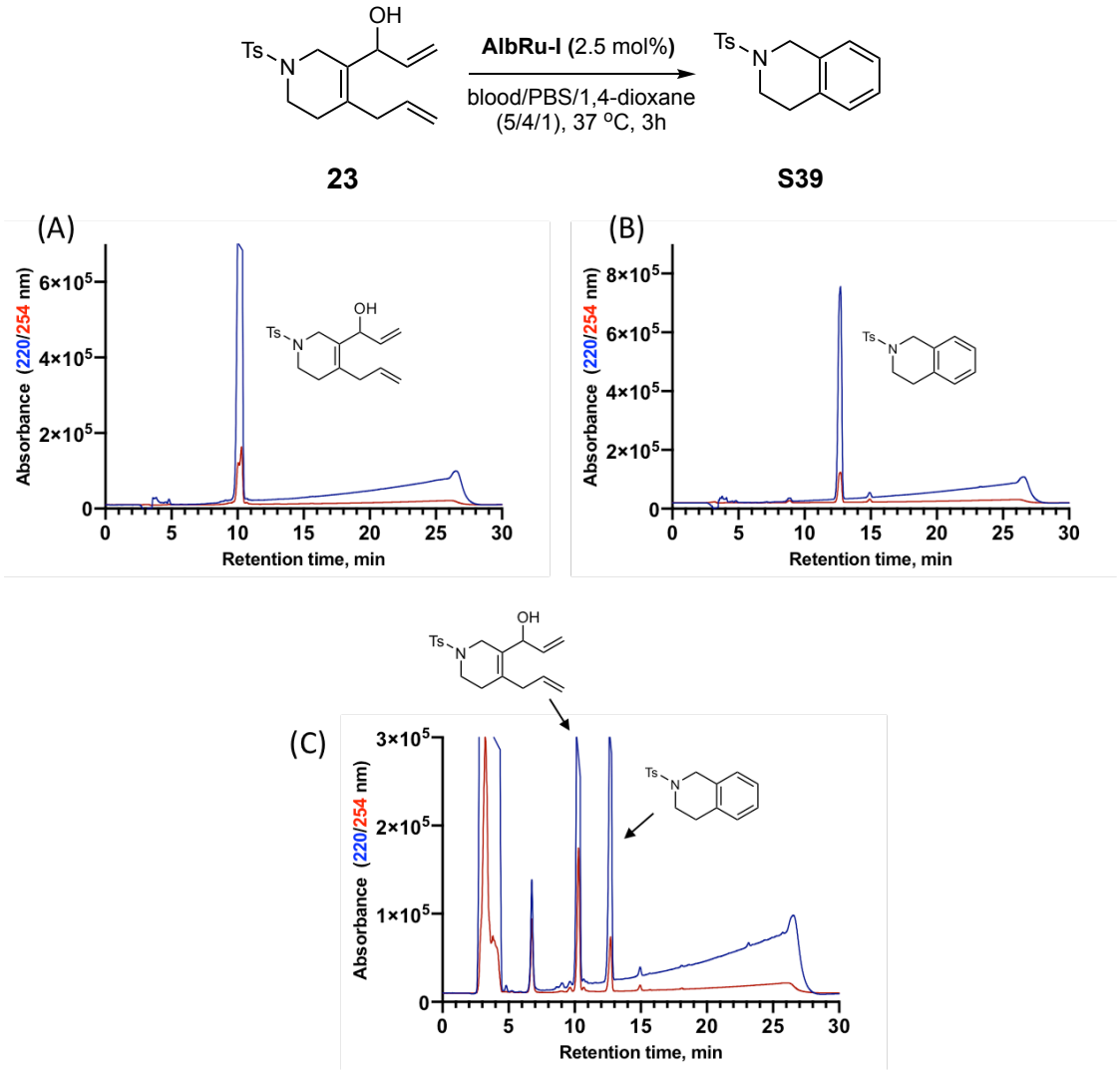

Fig. S64. Example HPLC traces of A) substrate **23**, B) product **S39**, and C) analysis of reaction of **23** in blood by **AlbRu-I**.

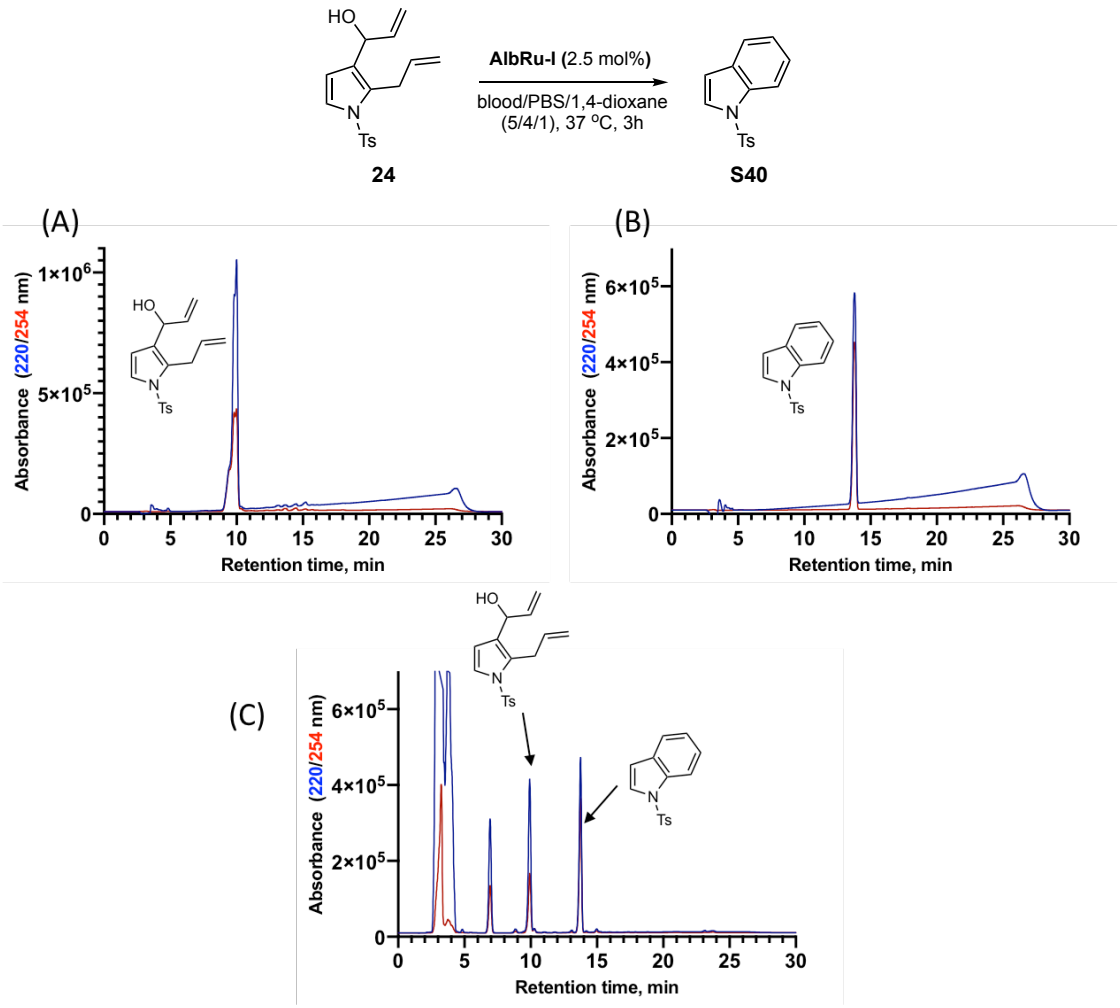

Fig. S65. Example HPLC traces of A) substrate **24**, B) product **S40**, and C) analysis of reaction of **24** in blood by **AlbRu-I**.

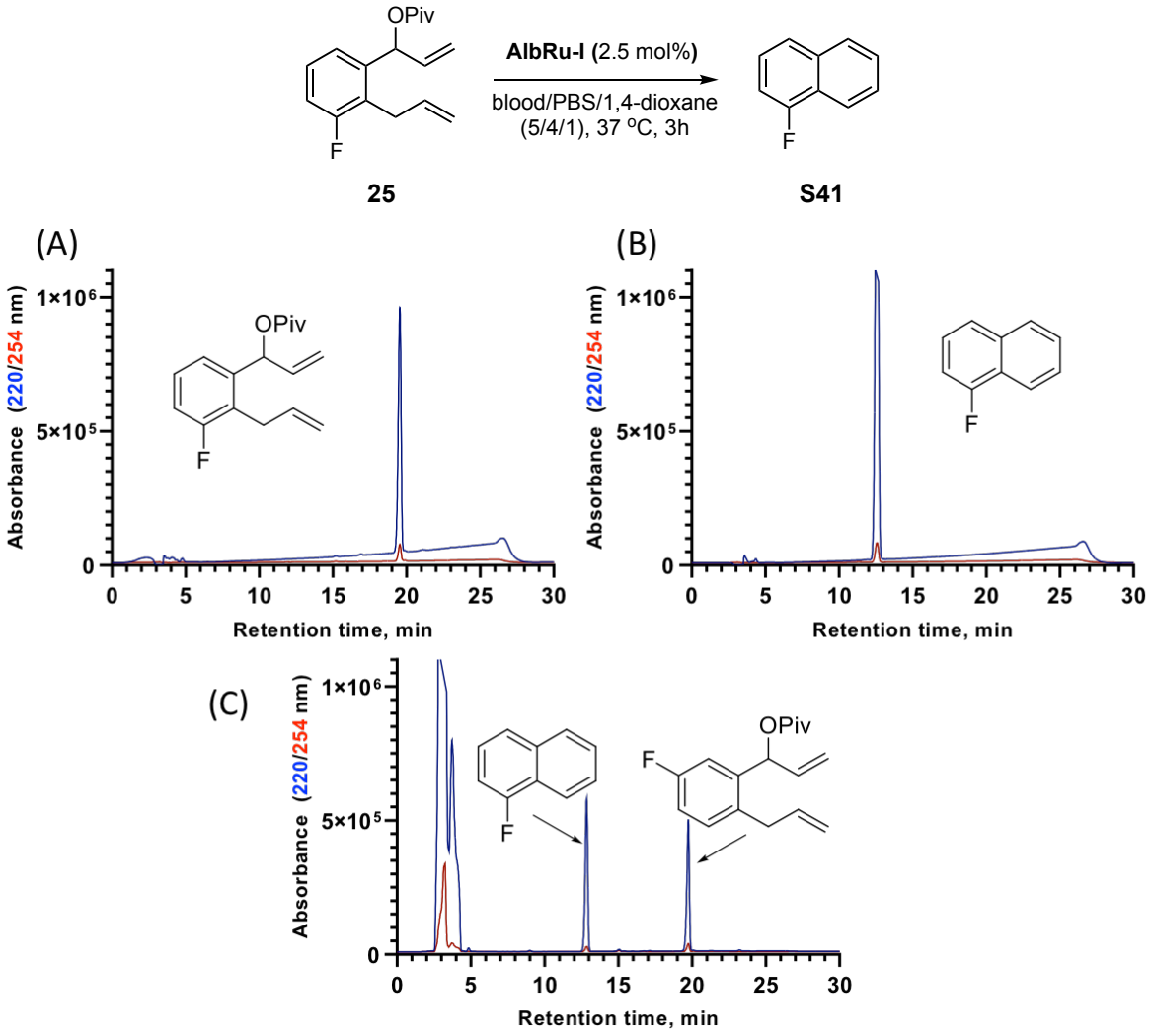

Fig. S66. Example HPLC traces of A) substrate **25**, B) product **S41**, and C) analysis of reaction of **25** in blood by **AlbRu-I**.

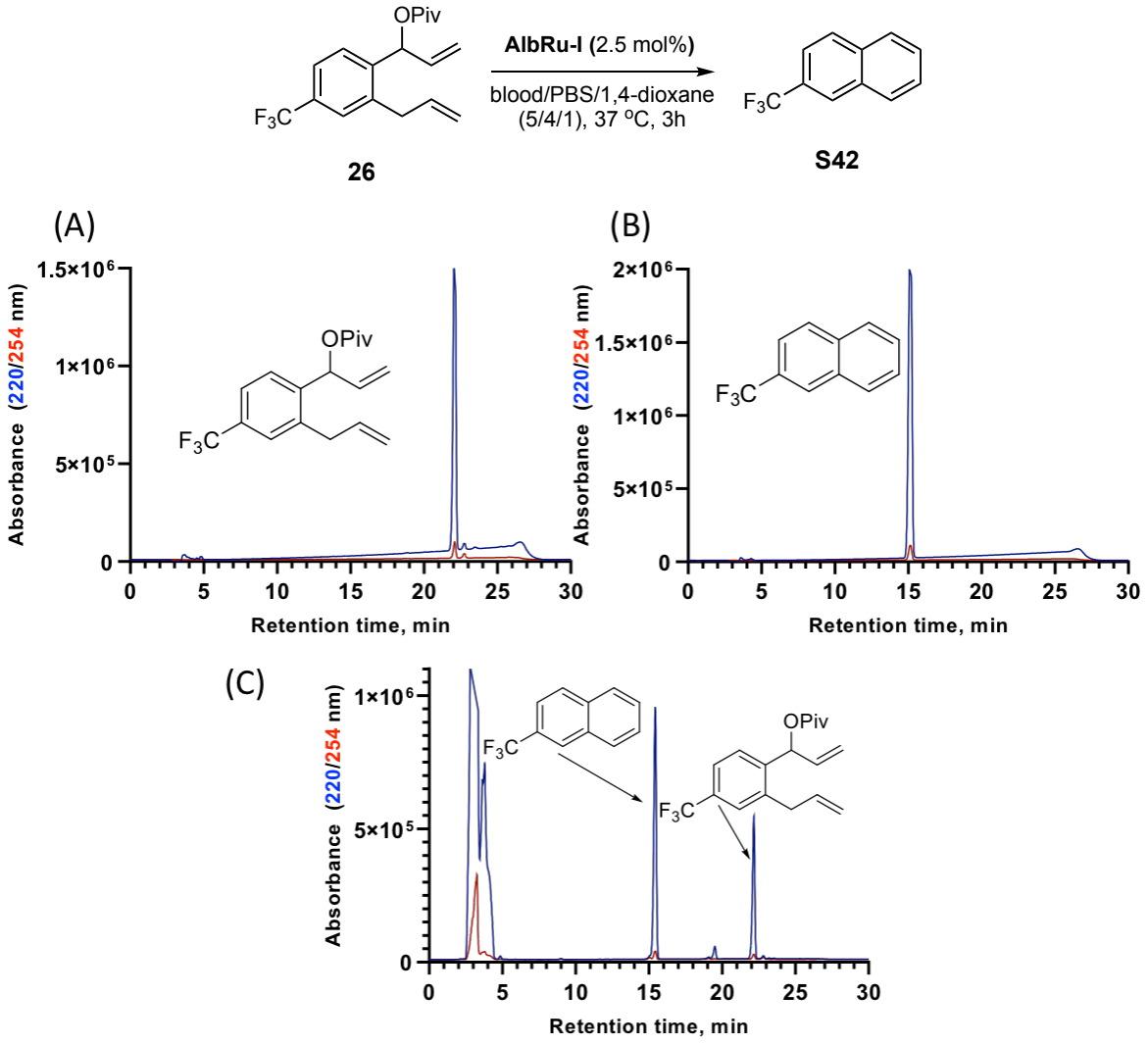

Fig. S67. Example HPLC traces of A) substrate **26**, B) product **S42**, and C) analysis of reaction of **26** in blood by **AlbRu-I**.

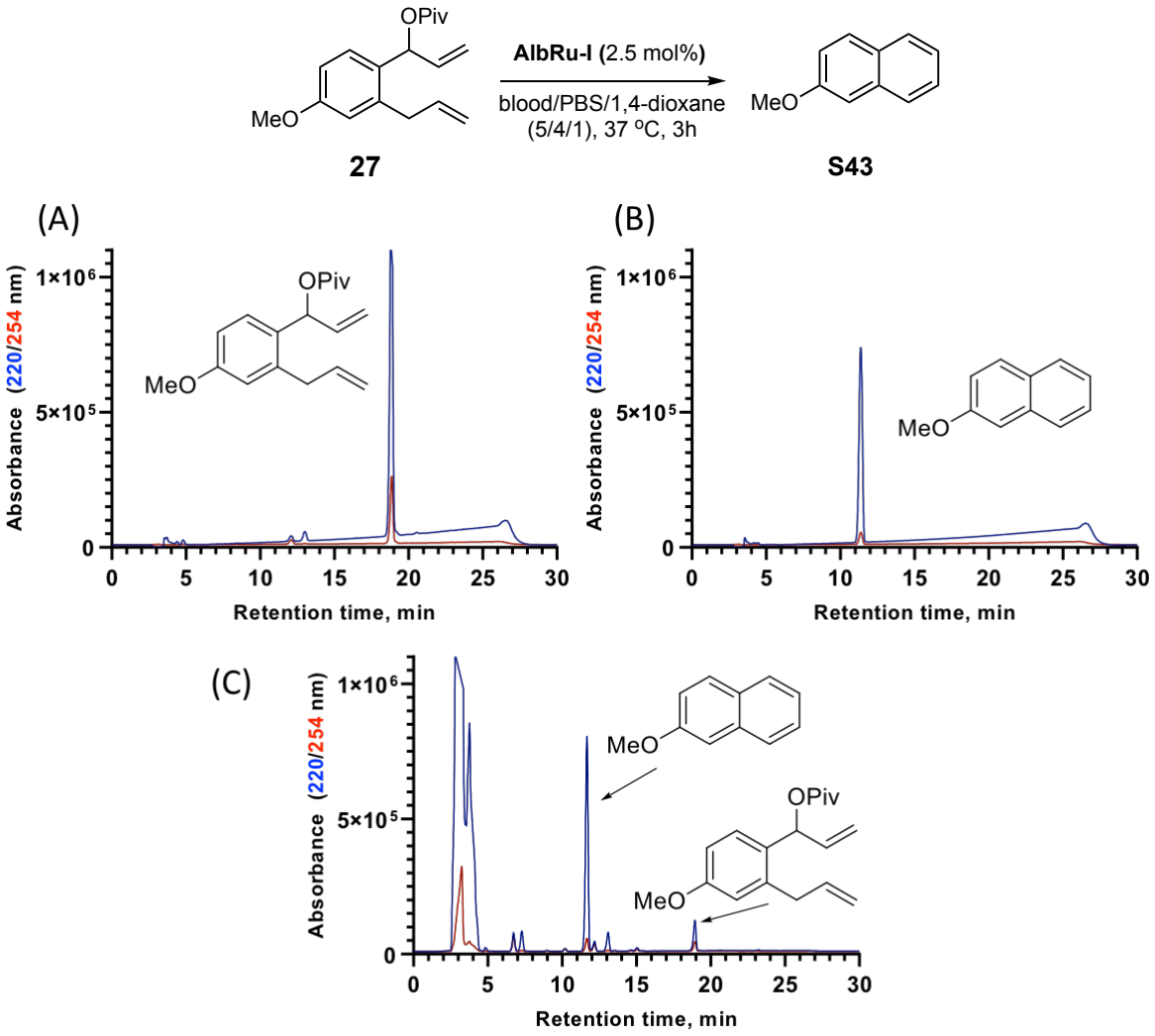

Fig. S68. Example HPLC traces of A) substrate **27**, B) product **S43**, and C) analysis of reaction of **27** in blood by **AlbRu-I**.

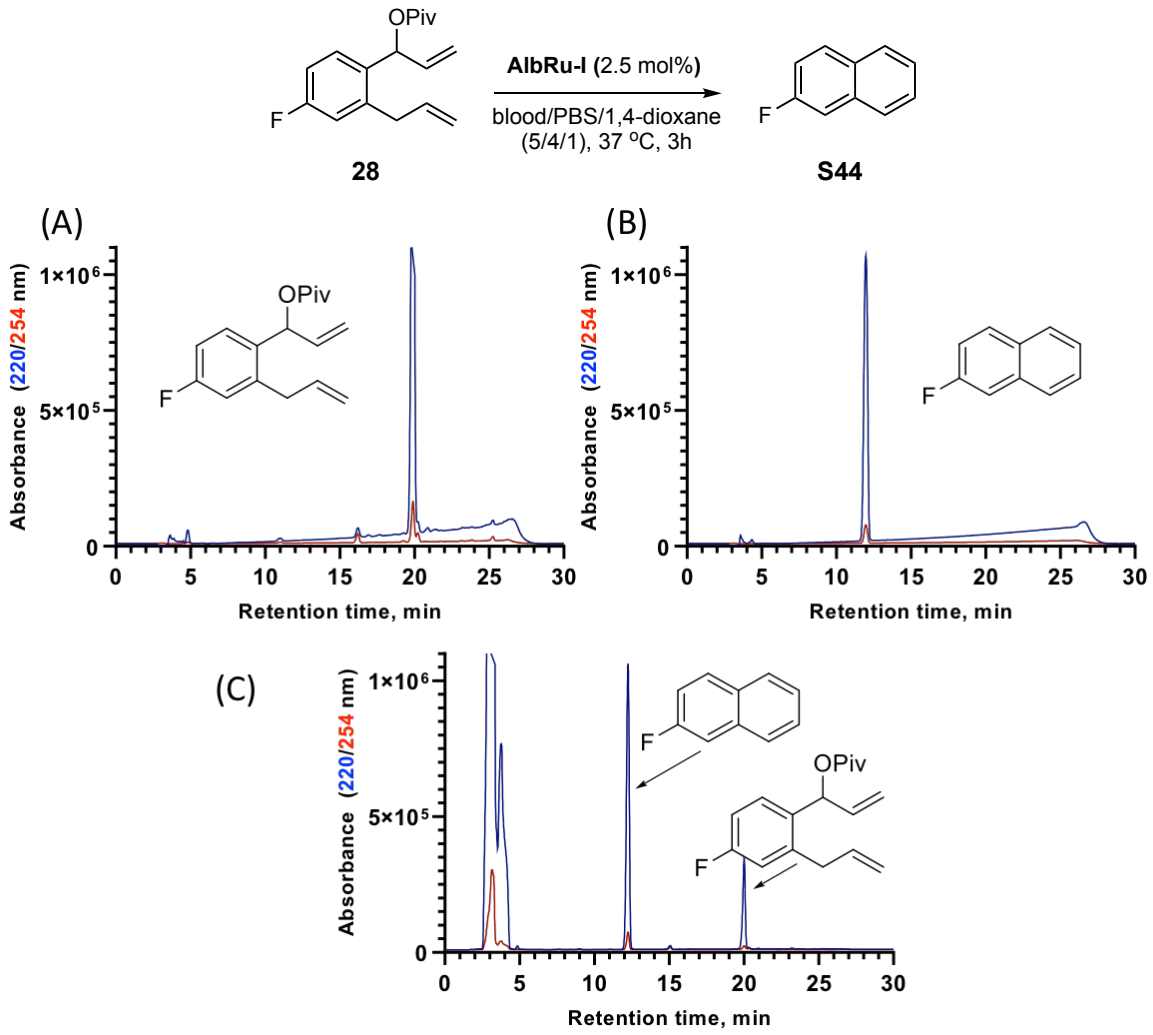

Fig. S69. Example HPLC traces of A) substrate **28**, B) product **S44**, and C) analysis of reaction of **28** in blood by **AlbRu-I**.

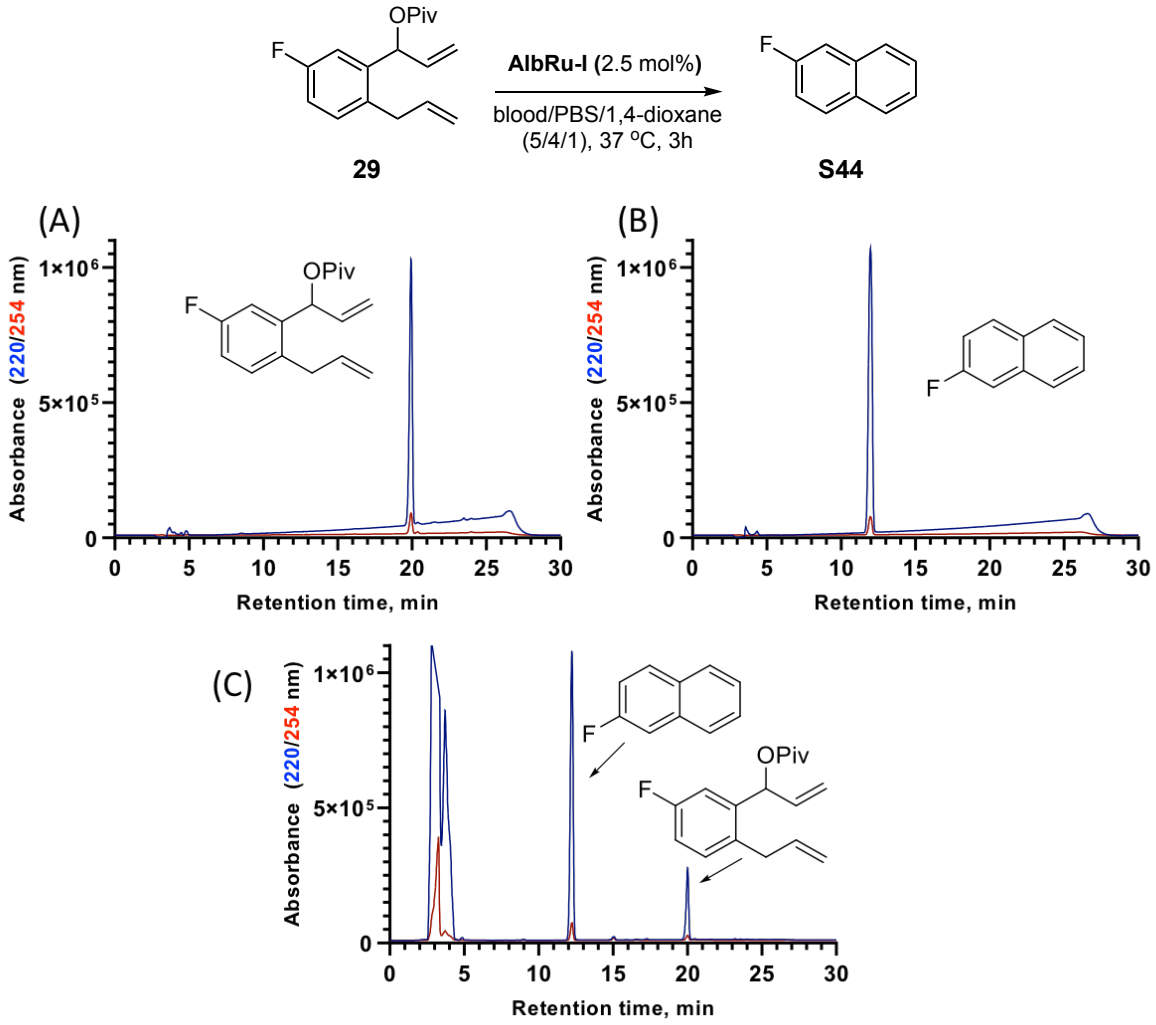

Fig. S70. Example HPLC traces of A) substrate **29**, B) product **S44**, and C) analysis of reaction of **29** in blood by **AlbRu-I**.

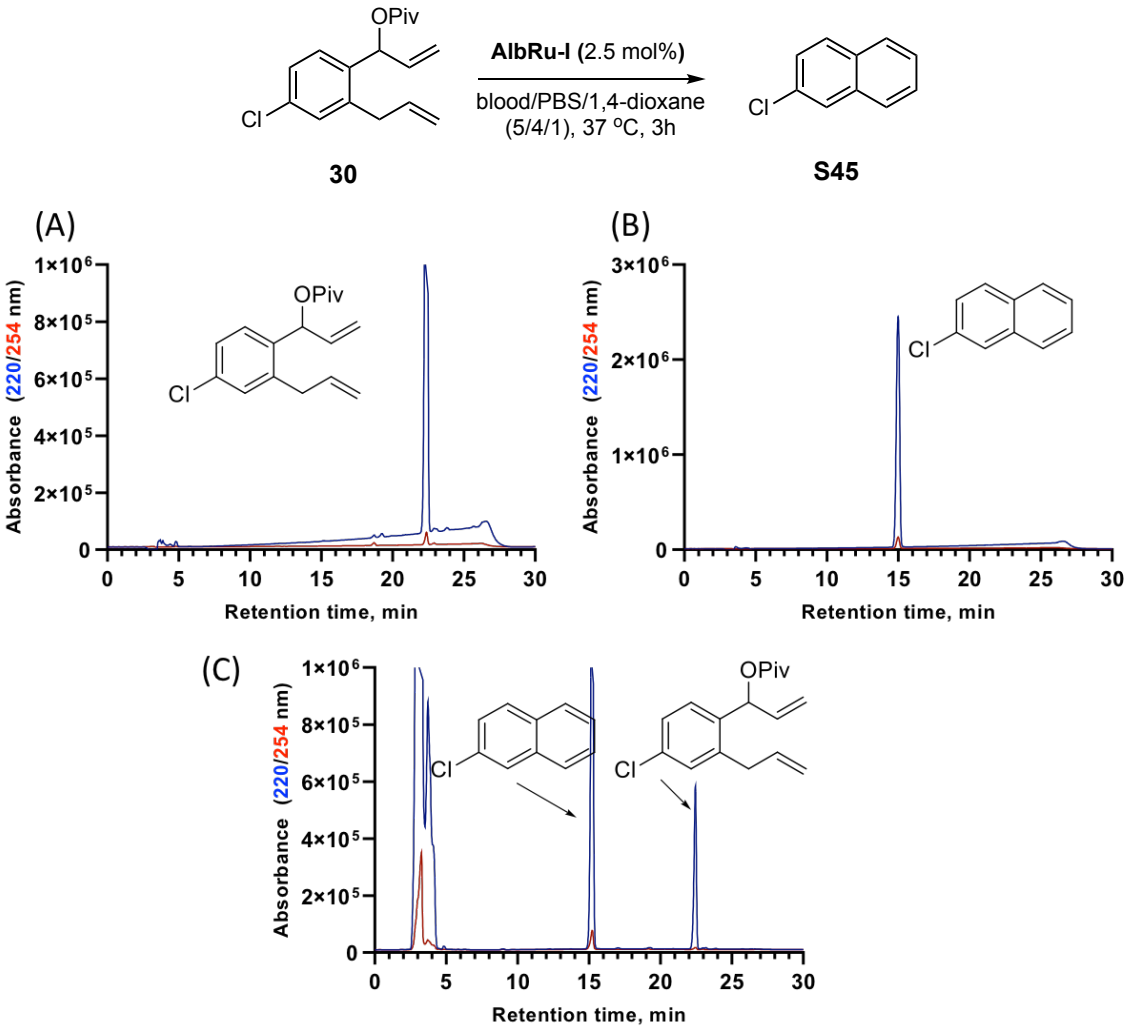

Fig. S71. Example HPLC traces of A) substrate **30**, B) product **S45**, and C) analysis of reaction of **30** in blood by **AlbRu-I**.

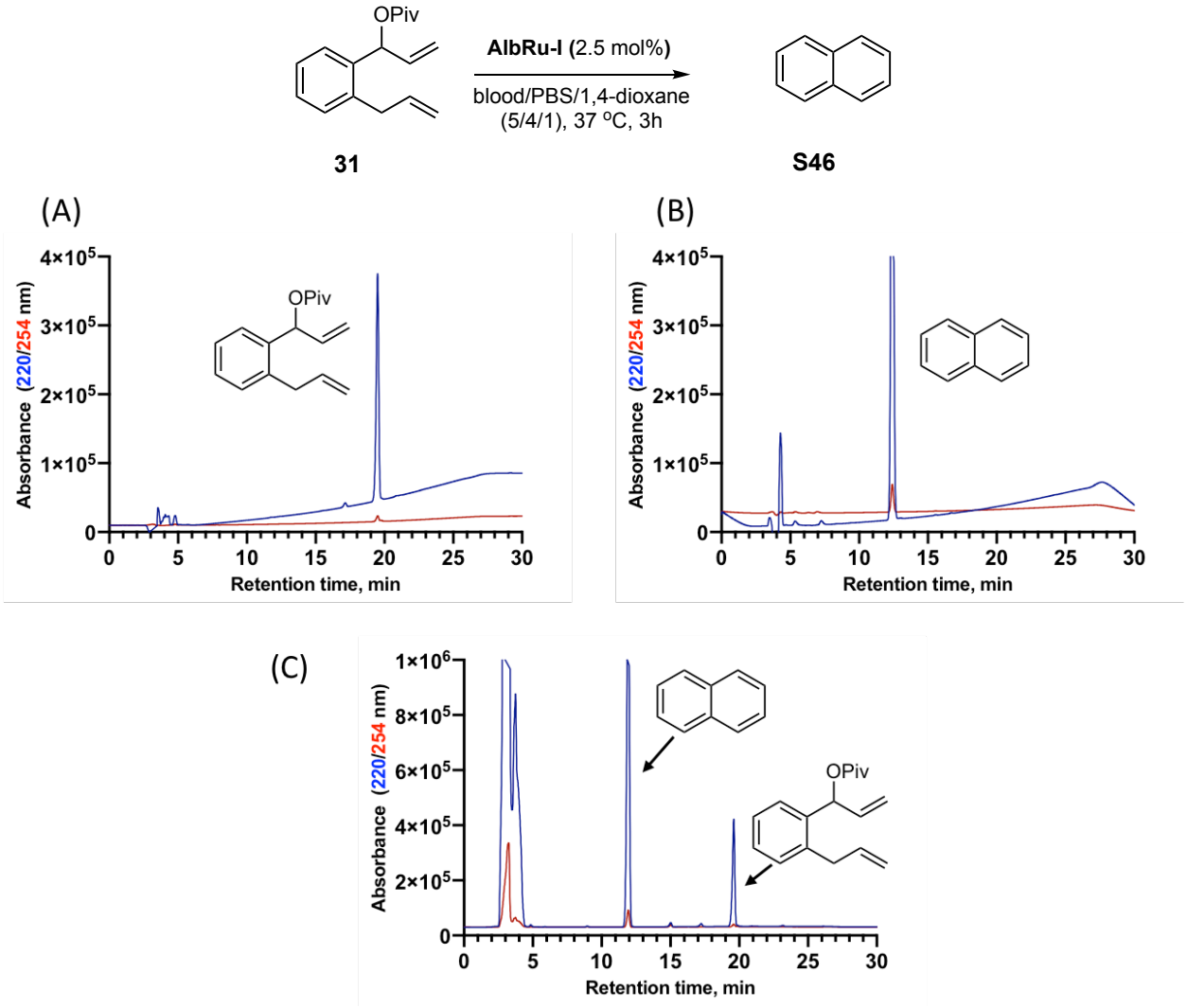

Fig. S72. Example HPLC traces of A) substrate **31**, B) product **S46**, and C) analysis of reaction of **31** in blood by **AlbRu-I**.

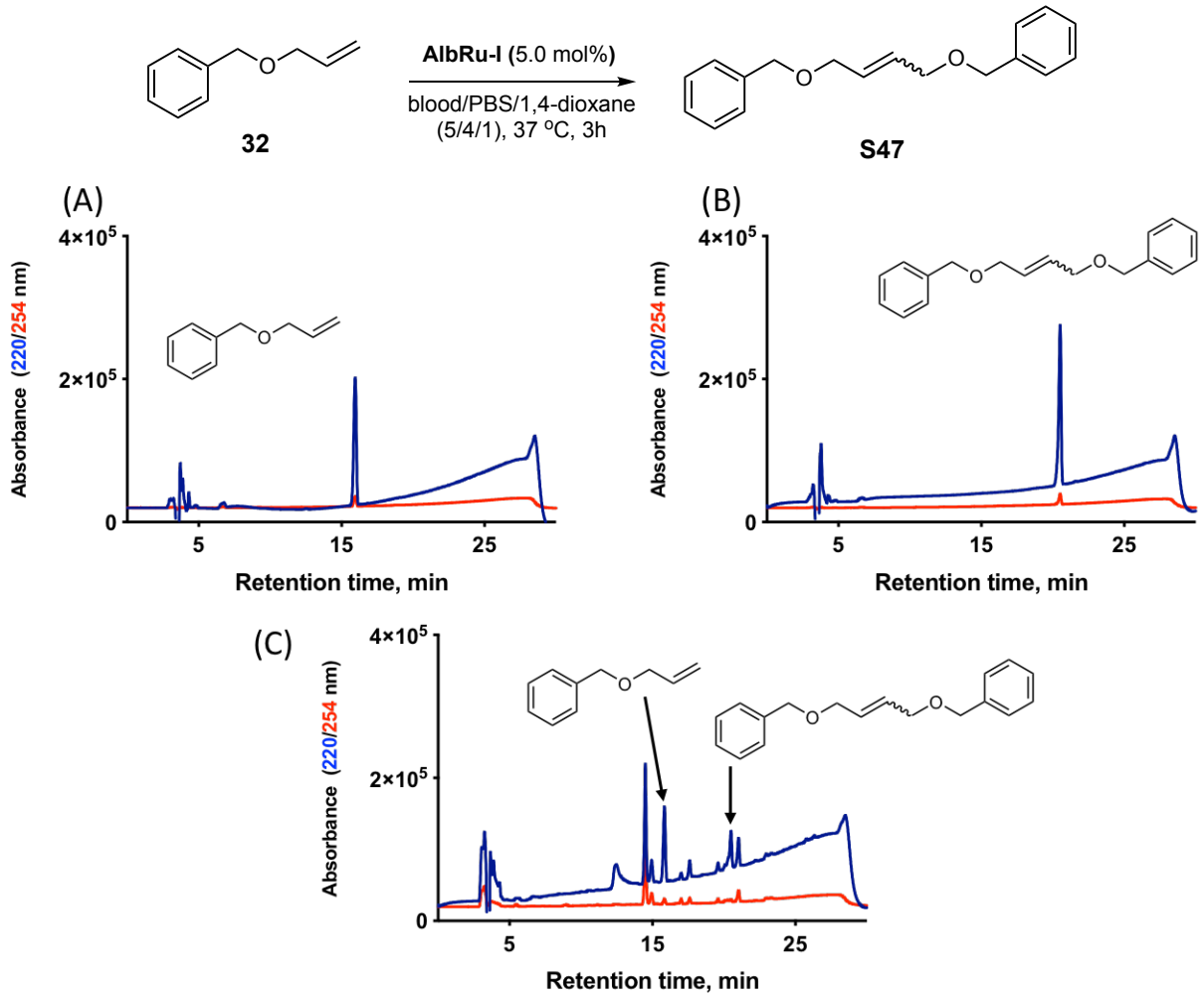

Fig. S73. Example HPLC traces of A) substrate **32**, B) product **S47**, and C) analysis of reaction of **32** in blood by **AlbRu-I**.

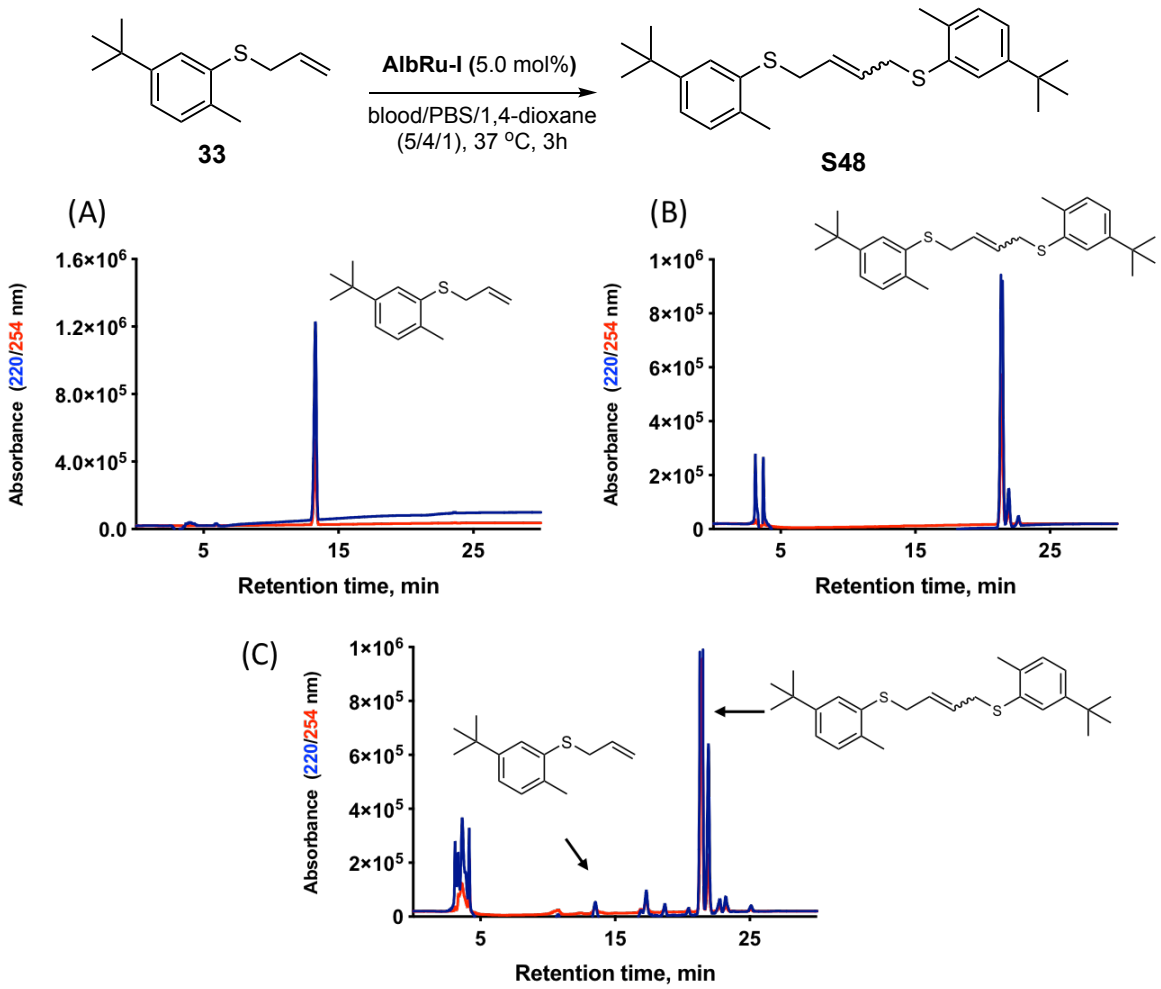

Fig. S74. Example HPLC traces of A) substrate **33**, B) product **S48**, and C) analysis of reaction of **33** in blood by **AlbRu-I**.

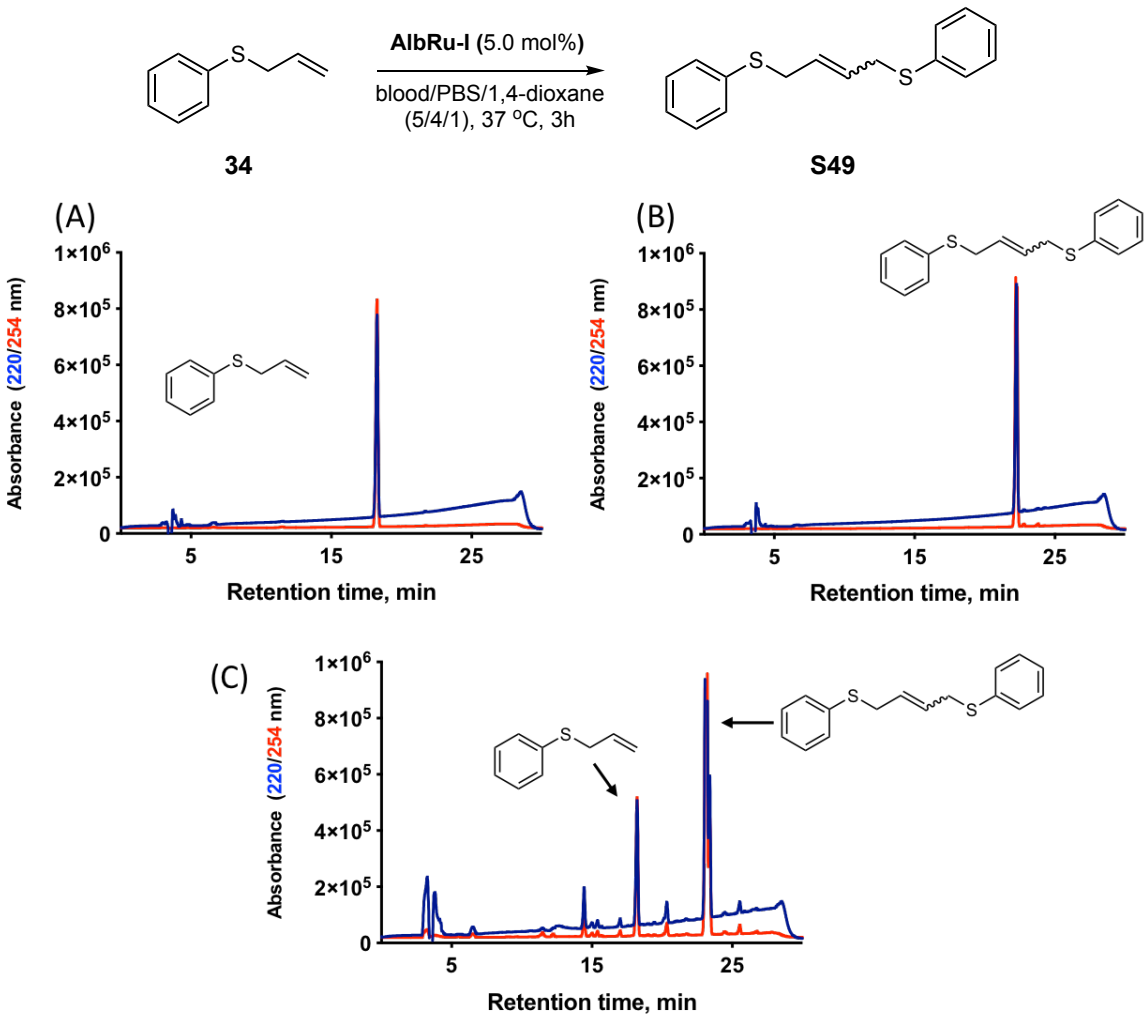

Fig. S75. Example HPLC traces of A) substrate **34**, B) product **S49**, and C) analysis of reaction of **34** in blood by **AlbRu-I**.

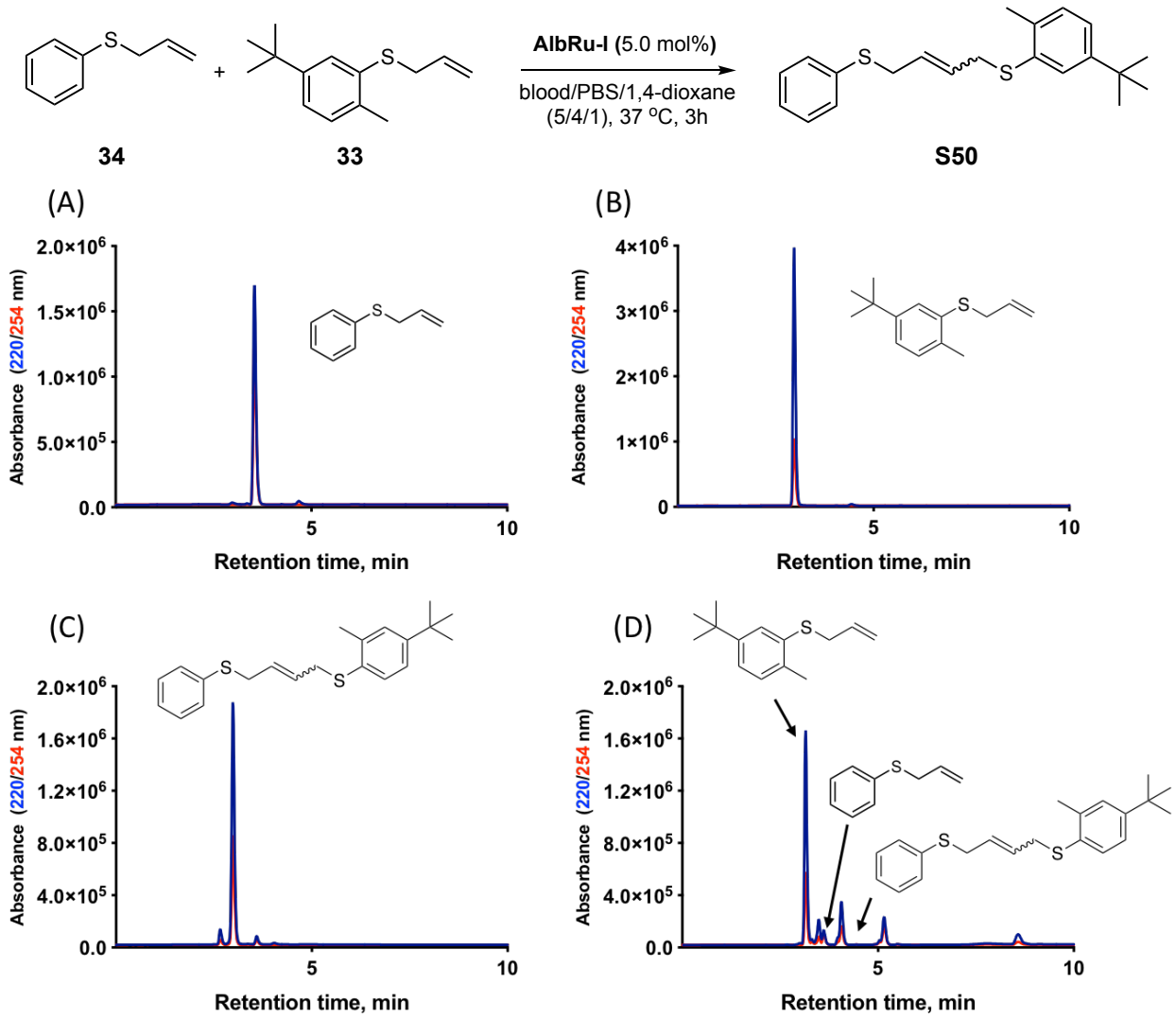

Fig. S76. Example HPLC traces of A) substrate **34**, B) substrate **33** C) product **S50**, and D) analysis of reaction of **33** with **34** in blood by **AlbRu-I**.

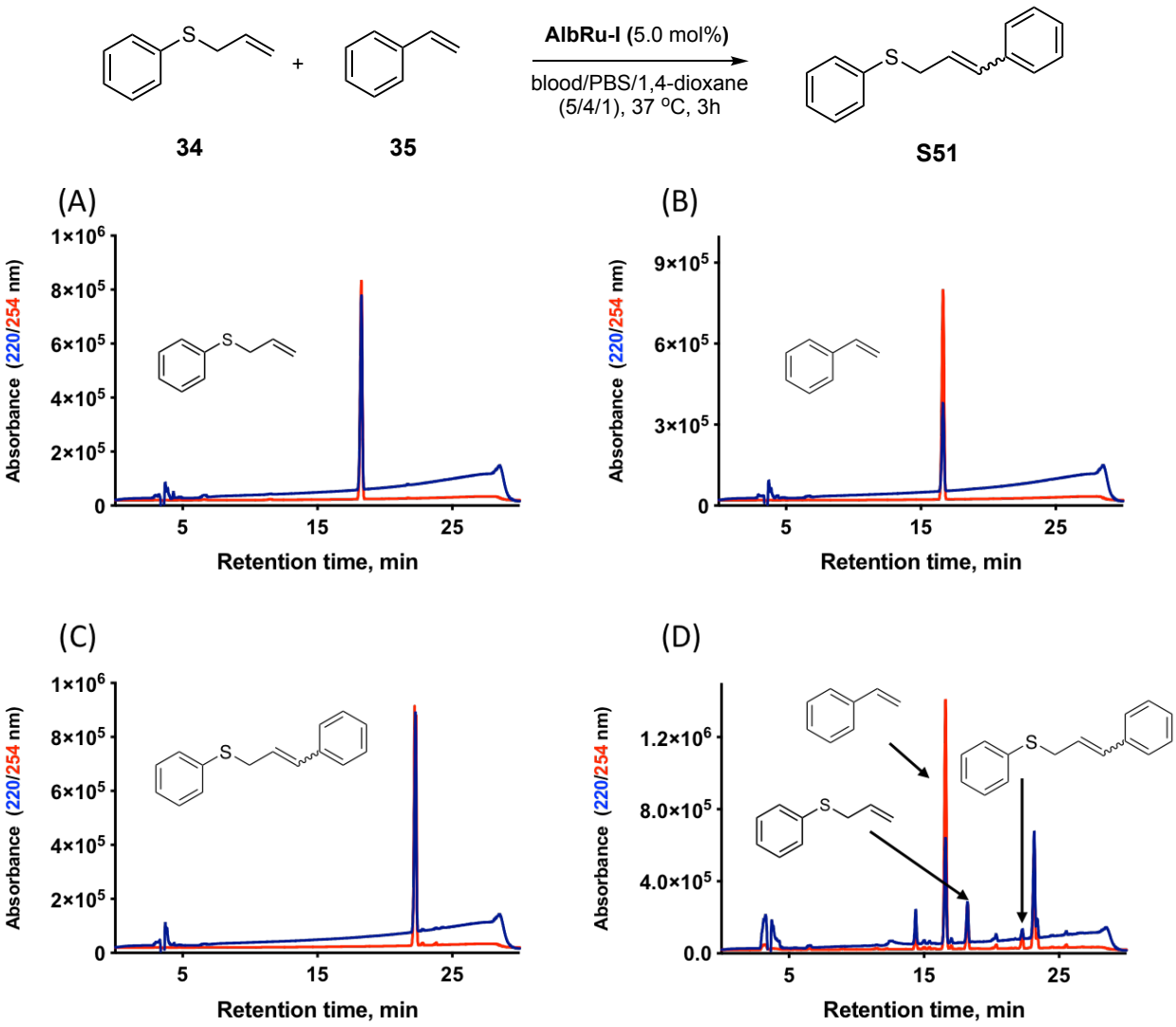

Fig. S77. Example HPLC traces of A) substrate **34**, B) substrate **35**, C) product **S51**, and D) analysis of reaction of **35** with **34** in blood by **AlbRu-I**.

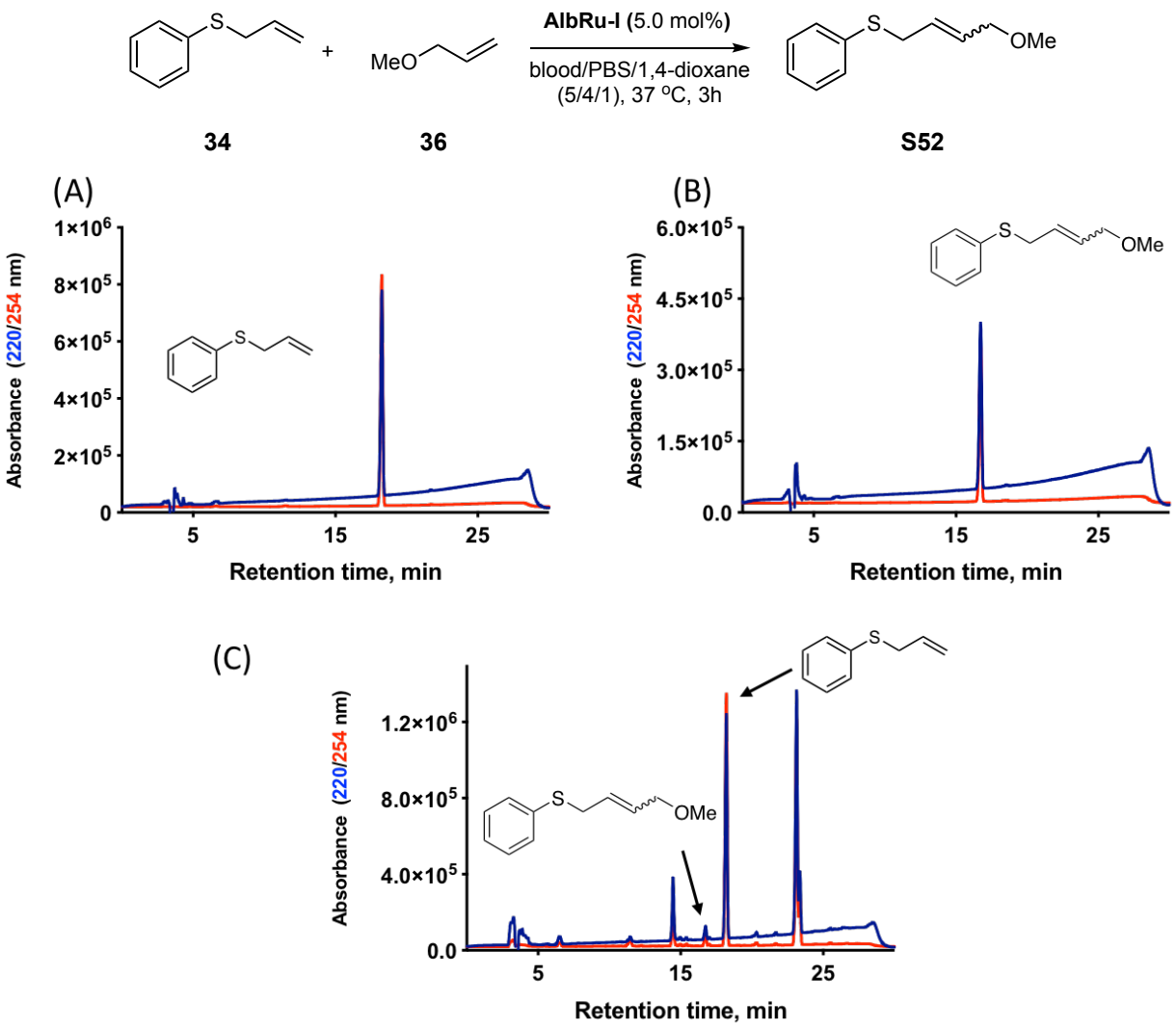

Fig. S78. Example HPLC traces of A) substrate **34**, B) product **S52**, and C) analysis of reaction of **36** with **34** in blood by **AlbRu-I**.

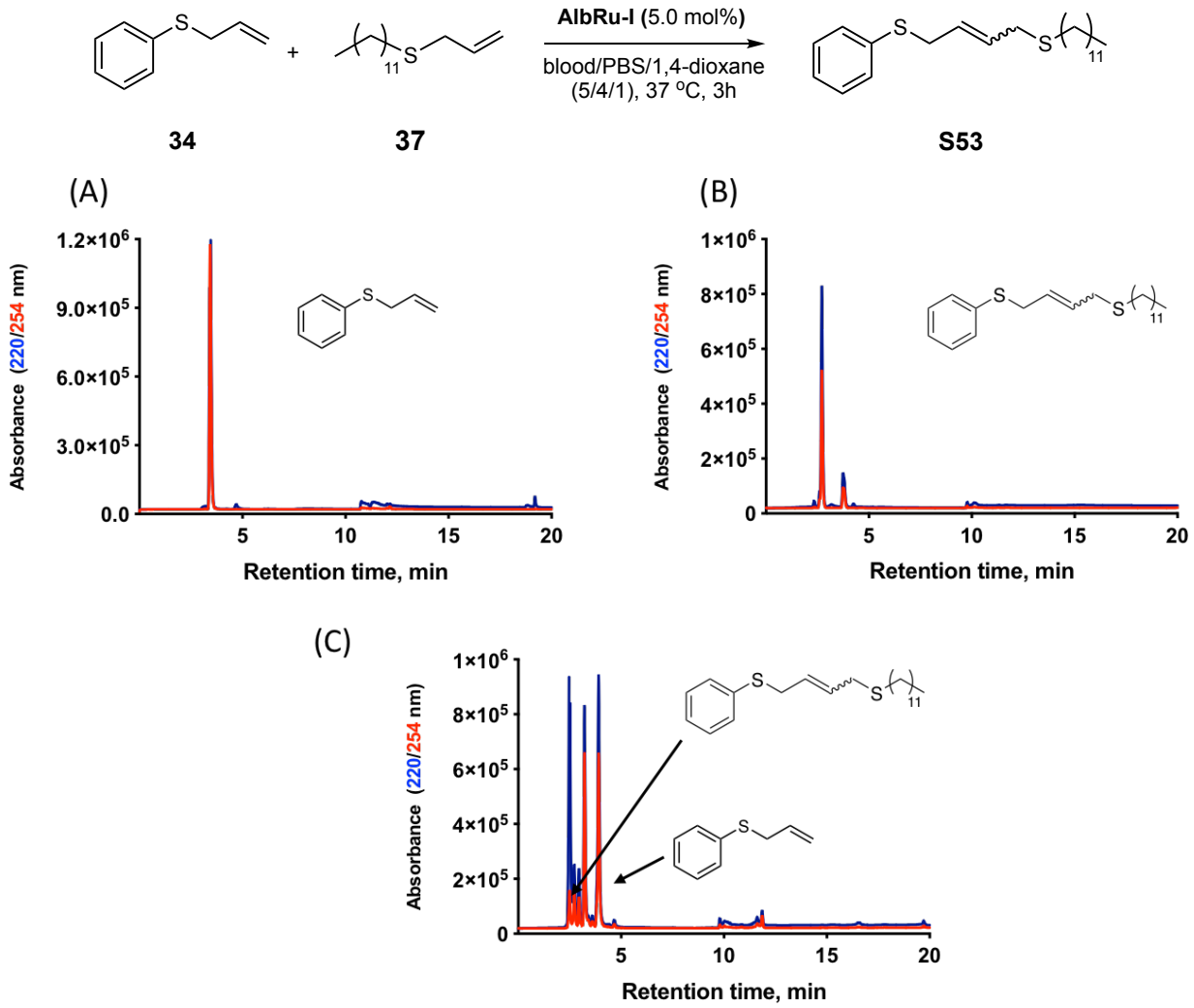

Fig. S79. Example HPLC traces of A) substrate **34**, B) product **S53**, and C) analysis of reaction of **37** with **34** in blood by **AlbRu-I**.

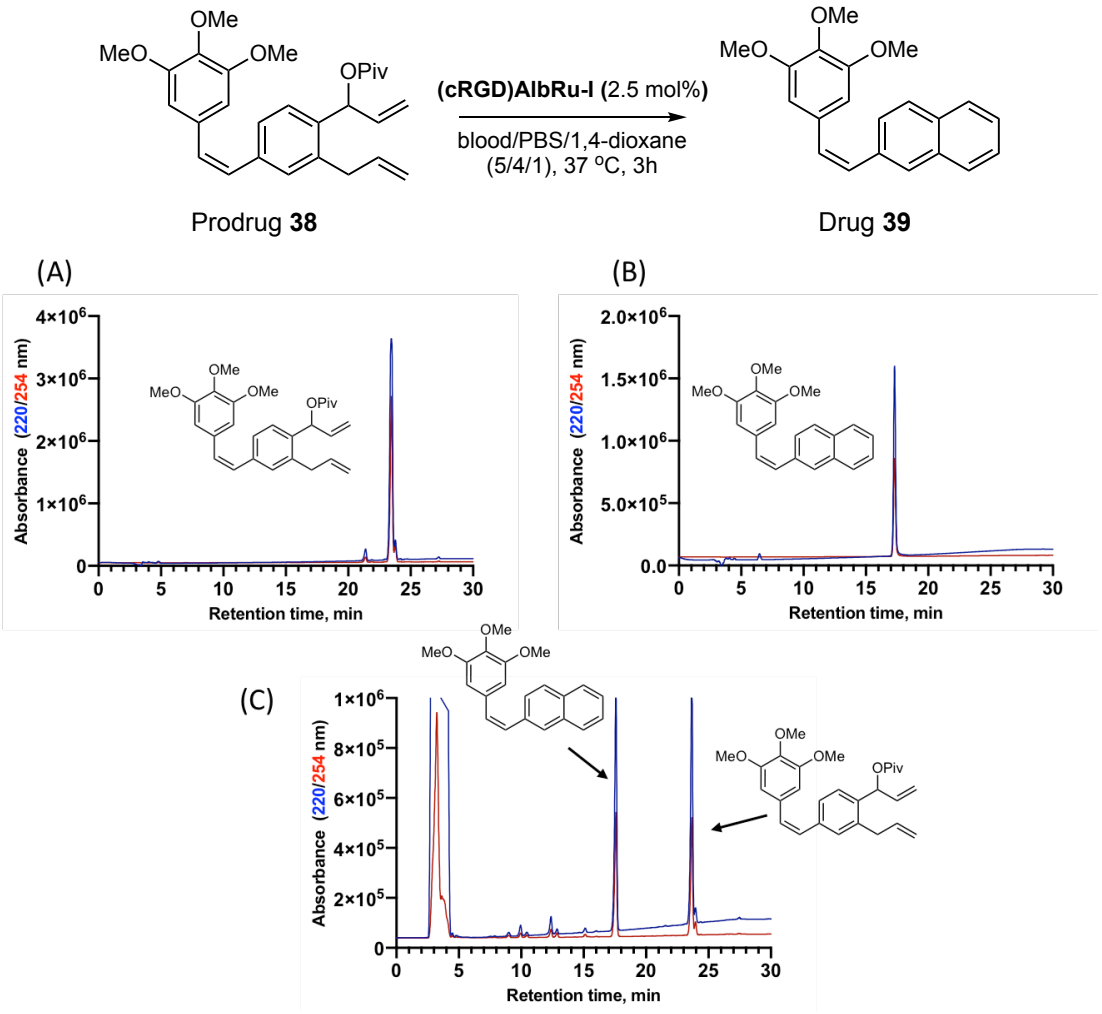

Fig. S80. Example HPLC traces of A) prodrug **38**, B) drug **39**, and C) analysis of reaction of **38** in blood by **(cRGD)AlbRu-I**.

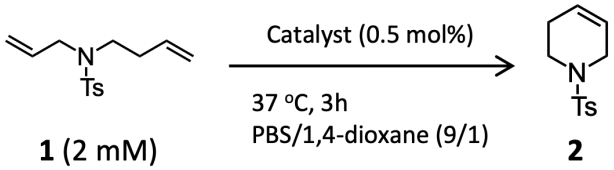

Entry	Catalyst	HPLC yield (%)
1	Ru-Cl	27.0 ± 1.2
2	Ru-I	48.9 ± 2.1

Fig. S81. Ring-closing metathesis by Ru-Cl/-I in PBS solution. Reaction conditions: substrate **1** (2 mM) and Ru-Cl/ or -I (0.5 mol%) were reacted in a mixture of PBS/1,4-dioxane (9:1). Incubations were carried out in triplicate at 37 °C for 3 h. Given HPLC yields were determined by HPLC analysis (peak retention times relative to product standards, followed by MS analysis for confirmation, and calculation of resultant yields based on product standard curves).

The result of Fig. S81 showed that by using the same loading amount (0.5 mol%), Ru-I could afford a higher yield of **2** (49%) than using Ru-Cl (27%), indicating that the iodine ligand enhanced the reactivity and stability of the Ru catalyst in aqueous media.

In a recent report by D. Fogg,[38] they found that the iodine ligand could reduce the sensitivity of the Ru-based Grubbs-Hoveyda catalyst toward moisture. Since ROH…Cl-Ru interactions have been reported for related metathesis catalysis,[39] they deduced that one probable contributor to improved tolerance toward water is the limited capacity of Ru-I catalyst to enter into hydrogen-bonding interactions with water. Our results from the reference experiment also confirmed this fact.

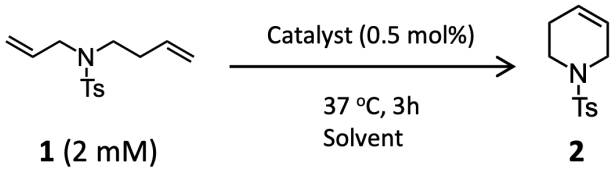

Entry	Catalyst	Solvent	HPLC yield (%)
1	**AlbRu-Cl**	PBS/1,4-dioxane (9/1)	12.1 ± 0.6
2	**AlbRu-I**	PBS/1,4-dioxane (9/1)	47.6 ± 1.5
3	**AlbRu-I**	PBS/1,4-dioxane (9/1) + NaCl (0.1 M)	51.7 ± 0.6
4	**AlbRu-Cl**	PBS/1,4-dioxane (9/1) + NaI (0.1 M)	15.2 ± 0.6

Fig. S82. Ring-closing metathesis by **AlbRu-Cl/-I** in PBS solution. Reaction conditions: substrate **1** (2 mM) and **AlbRu-Cl**/or **-I** (0.5 mol%) were reacted in various mixtures of PBS solution as indicated. Incubations were carried out in triplicate at 37 °C for 3 h. Given HPLC yields were determined by HPLC analysis (peak retention times relative to product standards, followed by MS analysis for confirmation, and calculation of resultant yields based on product standard curves).

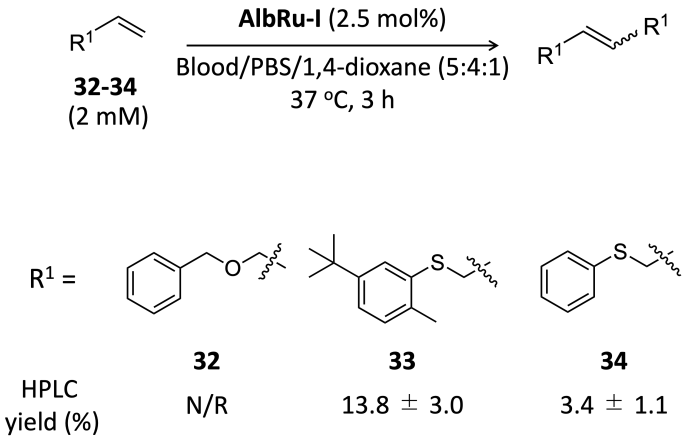

Fig. S83. Olefin metathesis by **AlbRu-I** in blood solution. Reaction conditions: substrates (2 mM) and **AlbRu-I** (2.5 mol%) were reacted in a mixture of blood/PBS/1,4-dioxane (5:4:1). Incubations were carried out in triplicate at 37 °C for 3 h. Given HPLC yields were determined by HPLC analysis (peak retention times relative to product standards, followed by MS analysis for confirmation, and calculation of resultant yields based on product standard curves).

Characterization of AlbRu-I protein complex.

As our previous study[1], a method to monitor binding of **Ru-I** with albumin was used. The approach is based on the quenching of intrinsic albumin fluorescence at λ_{EX}=280 nm/λ_{EM}=320 nm (due to aromatic amino acids like tryptophan) upon coumarin ligand of **Ru-I** binding. Binding affinity parameters obtained in this study were done through spectrofluorometric analysis via a SpectraMax iD3 multi-mode microplate reader (Molecular Devices).

Binding site confirmation

By utilizing known site marker ligands of albumin, the potential binding site for **Ru-I** can be indirectly determined. In literature, there are two well-known binding regions: Sudlow's site I (located in subdomain IIA) and Sudlow's site II (located in subdomain IIIA). Bulky, heterocyclic molecules (ex/ warfarin) are known to bind to site I while aromatic carboxylates (ex/ ibuprofen) have a preference for site II. Both warfarin and ibuprofen are known to bind albumin with low micromolar K_D.

Experimentally, a 20 μM solution of albumin was preincubated with 2 equivalents of either site marker ligand (warfarin, ibuprofen) for 1 hour at 37 ℃. The albumin/site marker ligand mixture was then added with **Ru-I** to construct saturation binding curves, which are shown in Fig. S84. From this data, it can be clearly seen that binding of **Ru-I** remains unaffected in the presence of ibuprofen, but decreases significantly with warfarin. This data suggests that the main binding site of **Ru-I** is Sudlow's site I.

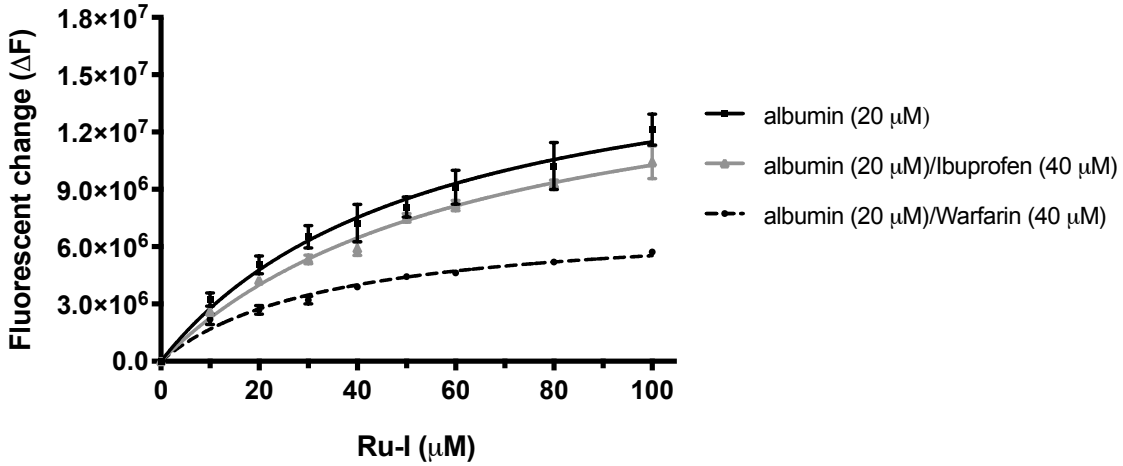

Fig. S84. Saturation binding curves based on the fluorescent quenching of albumin (black line), albumin preincubated with warfarin (dotted line), and albumin preincubated with ibuprofen (grey line). Preincubation was carried out with 20 μM of albumin and 40 μM of either PBS buffer (control), warfarin, or ibuprofen for 1 hour at 37 ℃ in 10% dioxane/PBS buffer pH 7.4. And then, an additional incubation at 37 ℃ for 1 hour was done with various concentrations of **Ru-I**. Fluorescence quenching was monitored at λ_{EX}=280 nm/λ_{EM}=320 nm. Error bars represent the standard deviation of three replicated measurements.

Dissociation constant (K_D) for Ru-I ligand

For sample preparation, 10× stock solutions of compound **Ru-I** were made in dioxane. 10× stock solutions of albumin was alternatively prepared in PBS buffer pH 7.4. For binding affinity experiments, reagents were diluted from their stock solutions to 1× final concentrations of 10% dioxane/PBS buffer. Adjustments to experimental conditions were made to albumin concentrations (10 μM), ligand concentrations (0, 5, 10, 15, 20, 25, 30, 40, 50 μM), as described. During incubations, mixtures in separated Eppendorf tubes were placed in a temperature-controlled oven at 37 ℃.

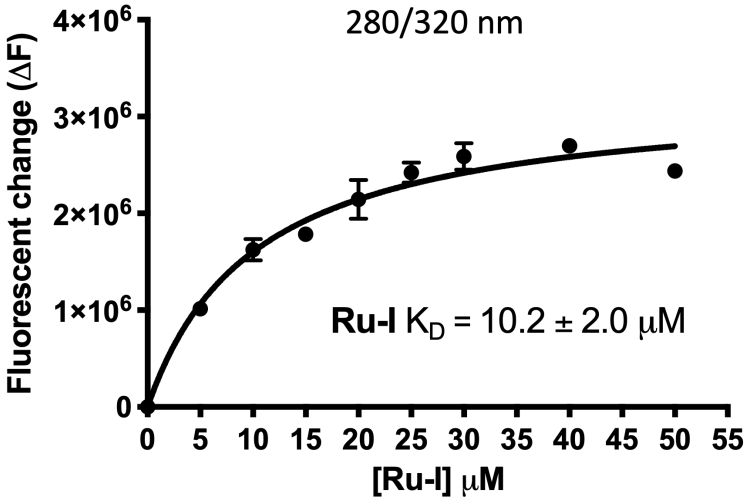

Fig. S85. Saturation binding curves based on the fluorescent quenching of albumin when bound to **Ru-I**. Experiments were conducted at albumin concentrations of 10 μM (black line). The measured equilibrium dissociation constants (K_D) were determined by non-linear regression. Incubations were performed at 37 °C for 1 hour in 10% dioxane/PBS buffer pH 7.4 and monitored at λ_{EX}=280 nm/λ_{EM}=320 nm. Error bars represent the standard deviation of three replicated measurements.

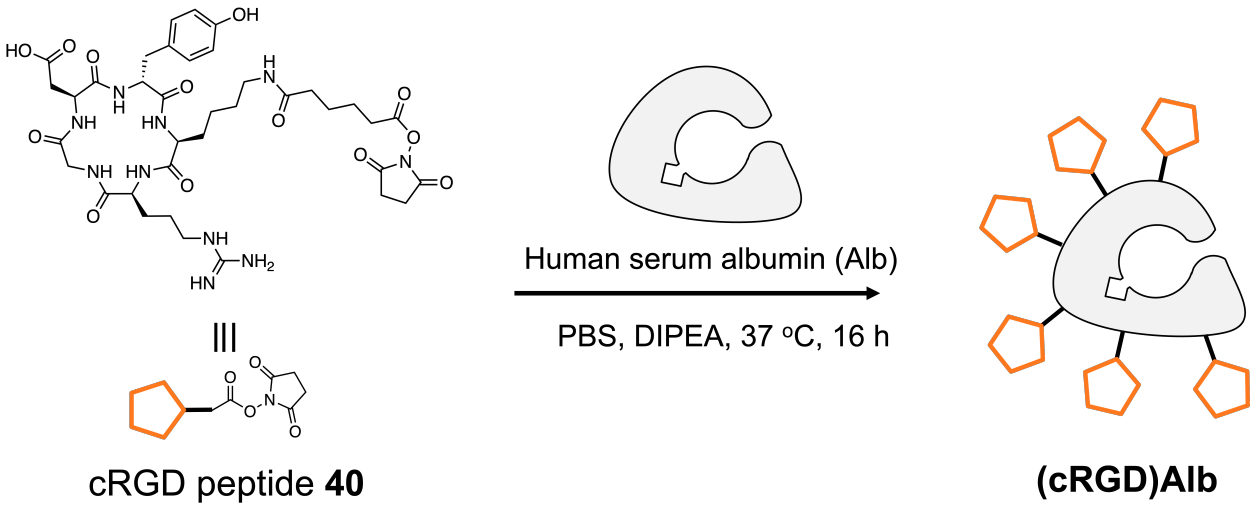

Fig. S86. Preparation of the **(cRGD)Alb**

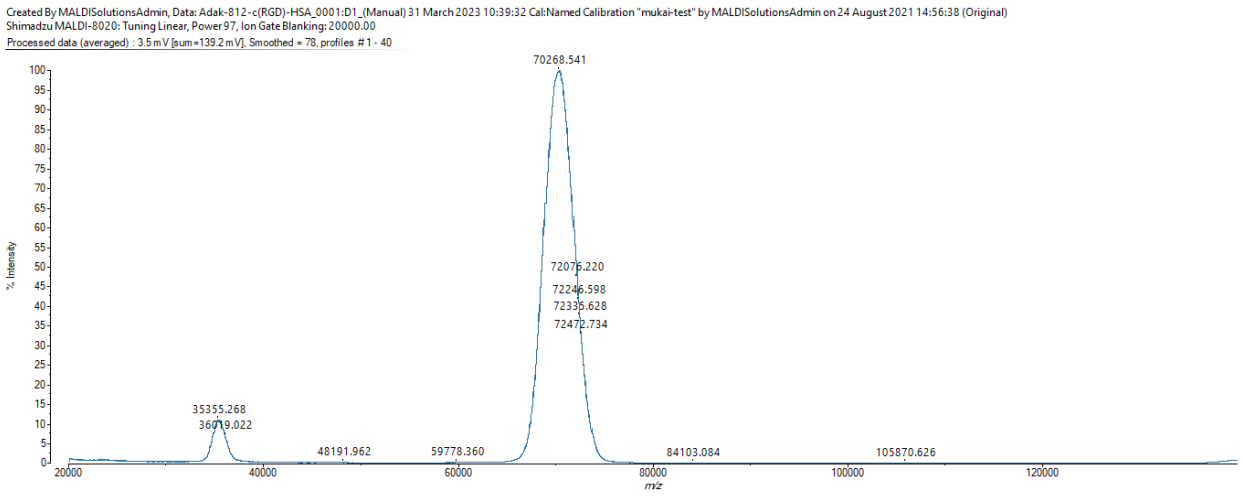

Fig. S87. MALDI-TOF-MS spectra of **(cRGD)Alb**

Cell culture

Cell line was obtained from the RIKEN Cell Bank and typically incubated at 37 °C with a 5% CO_2 humidified environment. SW620 (human colon adenocarcinoma cancer cells) was cultured in Leibovitz's L-15 medium (Wako-Fujifilm) supplemented with 10% fetal bovine serum (Biowest) and 1% penicillin-streptomycin (Gibco).

Cell viability experiments

Cell viability was determined using a MTS assay, which monitors the reduction of MTS tetrazolium salts to formazan via mitochondrial dehydrogenase of metabolically active cells. The commercial kit used in this study was the CellTiter 96® AQueous One Solution Cell Proliferation Assay (Promega, Wisconsin, USA). Based on cell titration experiments to ensure controls do not reach the stationary phase at the time of analysis, ~ 10^3 SW620 cancer cells were plated in each well of 96-well Falcon® microplates and grown overnight. The medium was then removed, followed by the incubation of compounds used in this patent. Generally, 10 μL of the compound in 10% DMSO/media solution was added to 90 μL of media, giving a final DMSO concentration of 1%.

GR_{50} values represent concentrations that gives half maximal growth rate inhibition. For evaluation of GR_{50} values for SW620 cancer cells (Fig. S88), various concentrations (0, 0.0078, 0.0156, 0.031, 0.062, 0.125, 0.25, 0.5, 1, 2, 4, 8, 16, 32, and 64 μM) of prodrug **38** and drug **39** were tested. Following an incubation period of 4 days, media was replaced with a solution of MTS reagent (20 μL) in growth media (80 μL). Following a further 2-hour incubation at 37 °C, end-point absorbance was acquired at 490 nm via a SpectraMax iD3 multi-mode microplate reader (Molecular Devices). The background control for this assay was the mixture of 20 μL MTS reagent and 80 μL medium in the absence of cells. The 100% growth was taken from cells incubated with 1% DMSO in growth medium. Obtained GR_{50} values were calculated via GraphPad Prism (version 7.0d) software using fitting based on the sigmoidal dose response equation.

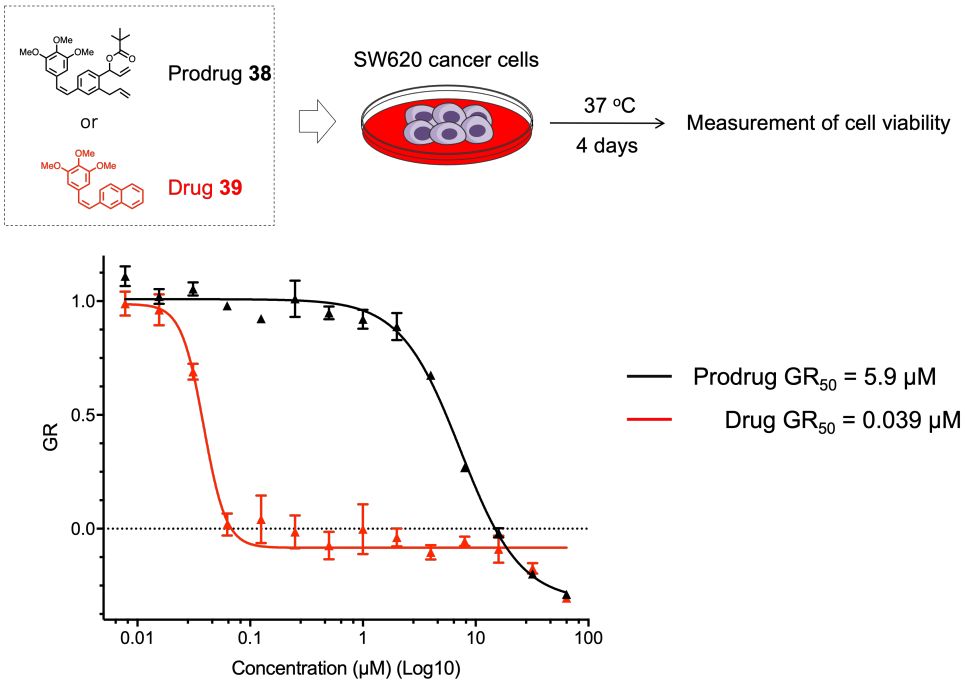

Fig. S88. Cancer cell growth curves aimed at exploring the effects (GR_{50}) of either prodrug **38** (black) and drug **39** (red) to cultures of SW620 cancer cells. GR_{50} values represent concentrations that gives half maximal growth rate inhibition.

For in cellulo prodrug activation studies by **(cRGD)Alb-I**/or **-Cl** (Fig. S89), varying concentrations (0.25, 0.5, 1.0 μM) of **(cRGD)Alb-I**/or **-Cl** were incubated with a fixed nontoxic concentration of prodrug **38** (1.0 μM). On the other hand, the concentration of prodrug **38** (1.0 μM) and various concentrations (0.25, 0.5, 1.0 μM) of **(cRGD)Alb-I**/or **-Cl** were tested as control groups. As a positive control, drug **39** (1.0 μM) was used. Following an incubation period of 4 days, media was replaced with a solution of MTS reagent (20 μL) in growth media (80 μL). Following a further 2 h incubation at 37 °C, end-point absorbance was acquired at 490 nm via a SpectraMax iD3 multi-mode microplate reader (Molecular Devices). The background control for this assay was the mixture of 20 μL MTS reagent and 80 μL medium in the absence of cells. The 100% growth was taken from cells incubated with 1% DMSO in growth medium.

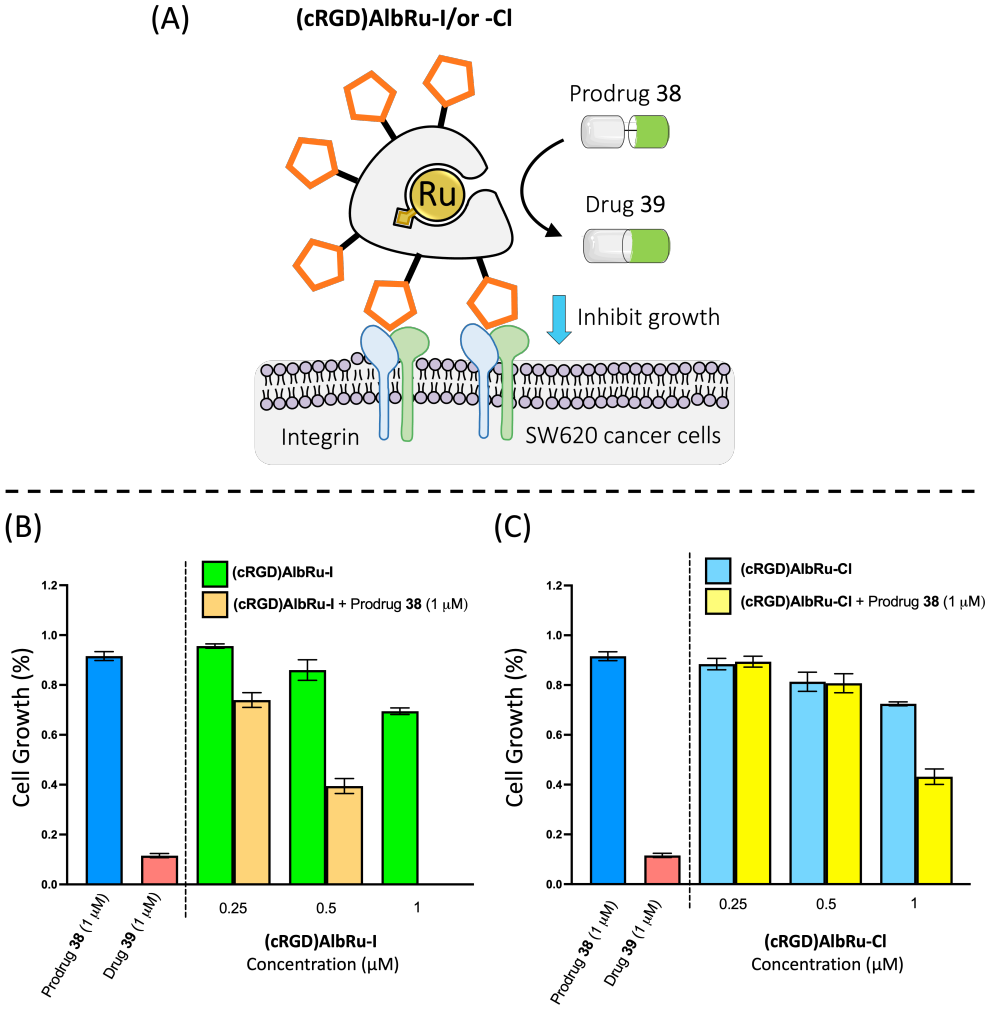

Fig. S89. Drug synthesis by the cRGD-linked ruthenium-containging artificial metalloenzymes (**(cRGD)AlbRu-I**/or **-Cl**) against SW620 cancer cells growth. (A) Schematic of cancer-targeted activation of the prodrug **38** into drug **39** using **(cRGD)AlbRu-I**/or **-Cl**. (B) Cytostatic assays were conducted using SW620 cancer cells by (B) **(cRGD)AlbRu-I** or (C) **(cRGD)AlbRu-Cl**. Error bars represent the S.D. of three replicated measurements.

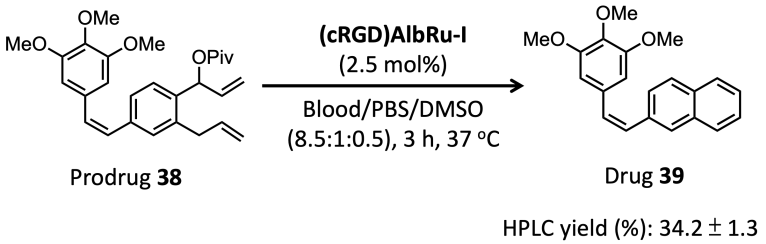

Fig. S90. Drug **39** synthesis from prodrug **38** by using **(cRGD)AlbRu-I** in a mixture of blood/PBS/DMSO (8.5/1/0.5). Reaction conditions: prodrug **38** (3 mM) and **(cRGD)AlbRu-I** (2.5 mol%) were reacted at 37 °C for 3 h. Incubations were carried out in triplicate. Given HPLC yields were determined by HPLC analysis (peak retention times relative to product standards, followed by MS analysis for confirmation, and calculation of resultant yields based on product standard curves).

Animal experiments

All animal experiments were carried out with approval by RIKEN's Animal Ethics Committee. In general, mice were anesthetized with 2.5% isoflurane in oxygen at a flow rate of 2.5-3.0 L/min. SW620 xenograft tumors were established in 6-week-old female nude mice BALB/cAJcl-nu/nu by subcutaneous injection of cells (approximately 1.0 x 10^6 cells in 100 µl of unnourished Leibovitz's L-15) into the right shoulder. Tumor growth was monitored while mice were housed in a facility with controlled temperature, salinity, aeration, and a standard 12 h light/12 h dark cycle. Stock samples were prepared as follows. For the saline stock solution, DMSO (35 µl) was added with Tween 80 (60 µl), followed by the addition of a 0.9% saline solution (505 µl). For the prodrug **38** stock solution, **38** (7.0 mg) was first dissolved in DMSO (35 µl), followed by the addition of Tween 80 (60 µl), and then a 0.9% saline solution (505 µl). For the drug **39** stock solution, **39** (3.9 mg) was first dissolved in DMSO (35 µl), followed by the addition of Tween 80 (60 µl), and then a 0.9% saline solution (505 µl). For the stock solution of **(cRGD)Ru-Cl** at a dose of 20 or 40 mg/kg, **(cRGD)Ru-Cl** was prepared in PBS (55 or 110 µl, respectively, 500 µM), followed by the addition of a 0.9% saline solution (445 or 390 µl, respectively). For the stock solution of **(cRGD)Ru-I** at a dose of 20 or 40 mg/kg, **(cRGD)Ru-I** was prepared in PBS (55 or 110 µl, respectively, 500 µM), followed by the addition of a 0.9% saline solution (445 or 390 µl, respectively). On day 1 following tumor implantation, SW620-bearing mice were randomly divided into 6 groups: saline control (group 1, n = 3); drug **39** only (group 2, n = 3); **(cRGD)Ru-Cl** at a dose of 20 mg/kg and prodrug **38** (group 3, n = 3); **(cRGD)Ru-Cl** at a dose of 40 mg/kg and prodrug **38** (group 4, n = 3); **(cRGD)Ru-I** at a dose of 20 mg/kg and prodrug **38** (group 5, n = 3); **(cRGD)Ru-I** at a dose of 40 mg/kg and prodrug **38** (group 6, n = 3). By intravenous administration, each mouse in group 1 received saline (100 µl stock solution); each mouse in group 2 received 32.5 mg/kg of drug **39** (100 µl stock solution); each mouse in group 3 received 20 mg/kg of **(cRGD)Ru-Cl** (100 µl stock solution), followed by 58 mg/kg of prodrug **38**; each mouse in group 4 received 40 mg/kg of **(cRGD)Ru-Cl** (100 µl stock solution), followed by 58 mg/kg of prodrug **38**; each mouse in group 5 received 20 mg/kg of **(cRGD)Ru-I** (100 µl stock solution), followed by 58 mg/kg of prodrug **38**; each mouse in group 6 received 40 mg/kg of **(cRGD)Ru-I** (100 µl stock solution), followed by 58 mg/kg of prodrug **38**. Treatments were done daily for 8 total injections. Tumor volume was quantified using a caliper and calculated as $width^2$ x length x 0.5. The tumor volume and body weight of the mice were recorded until day 17 post-injection.

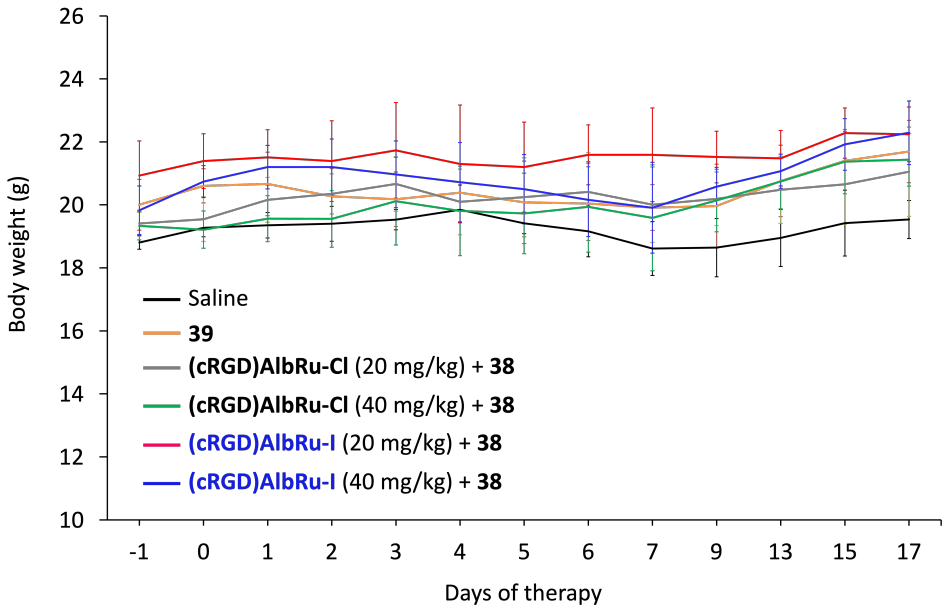

Fig. S91. Body weight (n = 3) change of various treatments group mice. Data are represented as mean value. Data are represented as mean value ± SD, n = 3 biological independent samples.

References

1. S. Eda, I. Nasibullin, K. Vong, N. Kudo, M. Yoshida, A. Kurbangalieva, K. Tanaka, Biocompatibility and therapeutic potential of glycosylated albumin artificial metalloenzymes, *Nat. Catal.* **2**, 780-792 (2019).
2. V. César, Y. Zhang, W. Kośnik, A. Zieliński, A. A. Rajkiewicz, M. Ruamps, S. Bastin, N. Lugan, G. Lavigne, K. Grela, Ruthenium catalysts supported by amino-substituted N-heterocyclic carbene ligands for olefin metathesis of challenging substrates. *Chem. Eur. J.* **23**, 1950–1955 (2017).
3. S. Chang, R. H. Grubbs, A highly efficient and practical synthesis of chromene derivatives using ring-closing olefin metathesis. *J. Org. Chem*. **63**, 864–866 (1998).
4. R. Liu, H. Ge, K. Chen, H. Xue, Selectivity in olefin-intervened macrocyclic ring-closing metathesis. *ACS Catal*. **8**, 5574–5580 (2018).
5. S. Mandal, J. Banerjee, S. Maity, S. K. Chattopadhyay, Sequential two-fold Claisen rearrangement, one-pot ring-closing metathesis and cross-metathesis as a route to substituted benzo[*b*]azepine-2-one, benzo[*b*]azepine and benzo[*b*]oxepine derivatives. *Helv. Chim. Acta*. **104**, e2000216 (2021).
6. H. Clavier, S. P. Nolan, N-Heterocyclic carbene and phosphine ruthenium indenylidene precatalysts: A comparative study in olefin metathesis. *Chem. Eur. J.* **13**, 8029–8036 (2007).
7. V. Sabatino, D. Staub, T. R. Ward, Synthesis of *N*-substituted indoles via aqueous ring-closing metathesis. *Catal. Lett*. **151**, 1–7 (2021).
8. B. Schmidt, Ruthenium-catalyzed olefin metathesis double-bond isomerization sequence. *J. Org. Chem*. **69**, 7672–7687 (2004).
9. C. Risi, F. Zhao, D. Castagnolo, Chemo-enzymatic metathesis/aromatization cascades for the synthesis of furans: disclosing the aromatizing activity of Laccase/TEMPO in oxygen-containing heterocycles. *ACS Catal*. **9**, 7264–7269 (2019).
10. A. Jana, K. Misztal, A. Żak, K. Grela, Synthesis of selectively substituted or deuterated indenes via sequential Pd and Ru catalysis. *J. Org. Chem*. **82**, 4226–4234 (2017).
11. W. Thaharn, D. Soorukram, C. Kuhakarn, V. Reutrakul, M. Pohmakotr, Synthesis of C_2-symmetric *gem*-difluoromethylenated angular triquinanes. *J. Org. Chem*. **83**, 388–402 (2018).
12. I. Nasibullin, I. Smirnov, P. Ahmadi, K. Vong, A. Kurbangaleva, K. Tanaka, Synthetic prodrug design enables biocatalytic activation in mice to elicit tumor growth suppression. *Nat. Commun.* **13**, 39 (2022).
13. Y. A. Lin, J. M. Chalker, N. Floyd, G. J. L. Bernardes, B. G. Davis, Allyl sulfides are privileged substrates in aqueous cross-metathesis: application to site-selective protein modification. *J. Am. Chem. Soc.* **130**, 9642-9643 (2008).
14. A. Jozeliūnaitė, D. Valčeckas, E. Orentas, Fullerene soot and a fullerene nanodispersion as recyclable heterogeneous off-the-shelf photocatalysts. *RSC Adv.* **11**, 4104-4111 (2021).

15. H. Takahata, Y. Suto, E. Kato, Y. Yoshimura, H. Ouchi, A new preparation of homochiral *N*-protected 5-hydroxy-3-piperidenes, promising chiral building blocks, by palladium-catalyzed deracemization of their alkyl carbonates. *Adv Synth Catal*. **349**, 685–693 (2007).

16. W. Yao, Y. Wu, G. Wang, Y. Zhang, M. Cheng, Tertiary amine mediated tandem Cross-Rauhut–Currier/Acetalization reactions: access to functionalized spiro-3,4-dihydropyrans. *Angew. Chem. Int. Ed*. **48**, 9713–9716 (2009).

17. A. R. Kelly, M. H. Kerrigan, P. J. Walsh, Addition/oxidative rearrangement of 3-furfurals and 3-furyl imines: new approaches to substituted furans and pyrroles. *J. Am. Chem. Soc*. **130**, 4097–4104 (2008).

18. W.-M. Feng, T.-Y. Li, L.-J. Xiao, Q.-L. Zhou, Nickel-catalyzed intramolecular hydroalkenylation of imines. *Org. Lett*. **23**, 7900-7904 (2021).

19. S. Fustero, E. Rodríguez, R. Lázaro, L. Herrera, S. Catalán, P. Barrio, Relay catalysis: enantioselective synthesis of cyclic benzo-fused homoallylic alcohols by chiral brønsted acid-catalyzed allylboration/ring closing metathesis. *Adv. Synth. Catal*. **355**, 1058–1064 (2013).

20. A. Tada, Y. Tokoro, S. Fukuzawa, Palladium/ClickFerrophos-catalyzed asymmetric domino allylstannylation-Heck reaction of *o*-formylaryl triflate. *J. Org. Chem*. **79**, 7905–7909 (2014).

21. Y. Hoshimoto, Y. Hayashi, H. Suzuki, M. Ohashi, S. Ogoshi, Synthesis of five- and six-membered benzocyclic ketones through intramolecular alkene hydroacylation catalyzed by Nickel(0)/*N*-heterocyclic carbenes. *Angew. Chem. Int. Ed*. **51**, 10812–10815 (2012).

22. A. Matviitsuk, S. E. Denmark, Enantio- and diastereoselective, Lewis base catalyzed, cascade sulfenoacetalization of alkenyl aldehydes, *Angew. Chem. Int. Ed*. **58**, 12486–12490 (2019).

23. M. Dąbrowski, P. Wyrębek, D. Trzybiński, K. Woźniak, K. Grela, In a quest for selectivity paired with activity: a ruthenium olefin metathesis catalyst bearing an unsymmetrical Phenanthrene-based N-heterocyclic carbene. *Chem. Eur. J.* **26**, 3782–3794 (2020).

24. Y. Wang, M. Jimenez, A. S. Hansen, E.-A. Raiber, S. L. Schreiber, D. W. Young, Control of olefin geometry in macrocyclic ring-closing metathesis using a removable silyl group. *J. Am. Chem. Soc*. **133**, 9196–9199 (2011).

25. Y. Zhang, J. H. Sim, S. N. MacMillan, T. H. Lambert, Synthesis of 1,2-dihydroquinolines via hydrazine-catalyzed ring-closing carbonyl-olefin metathesis, *Org. Lett.* **22**, 6026-6030 (2020).

26. Z. Liu, R. C. Larock, Synthesis of carbazoles and dibenzofurans via cross-coupling of *o*-iodoanilines and *o*-iodophenols with silylaryl triflates and subsequent Pd-catalyzed cyclization. *Tetrahedron* **63**, 347–355 (2007).

27. G. Barker, S. Webster, D. G. Johnson, R. Curley, M. Andrews, P. C. Young, S. A. Macgregor, A.-L. Lee, Gold-catalyzed proto- and deuterodeboronation, *J. Org. Chem*. **80**, 9807–9816 (2015).

28. S.-B. Hong, L.-C. Liang, Aqueous Suzuki couplings mediated by a hydrophobic catalyst, *RSC Adv.* **12**, 28862-28866 (2022).

29. J. L. Jios, G. P. Romanelli, J. C. Autino, H. E. Giaccio, H. Duddeck, M. Wiebcke, Complete ^{1}H and ^{13}C NMR spectral assignment of *N*-aralkylsulfonamides, *N*-sulfonyl-1,2,3,4-tetrahydroisoquinolines and *N*-sulfonyl-2,3,4,5-tetrahydro-1H-2-benzazepines. Conformational analysis of *N*-[((3′,4′-dichlorophenyl)methyl)sulfonyl]-3-methyl-2,3,4,5-tetrahydro-1*H*-2-benzazepin. *Magn. Reson. Chem*. **43**, 1057–1062 (2005).

30. M. Arisawa, Y. Terada, K. Takahashi, M. Nakagawa, A. Nishida, Development of isomerization and cycloisomerization with use of a ruthenium hydride with N-heterocyclic carbene and its application to the synthesis of heterocycles. *J. Org. Chem*. **71**, 4255–4261 (2006).

31. T. Furuya, T. Ritter, Fluorination of boronic acids mediated by silver(I) triflate, *Org. Lett.* **11**, 2860–2863 (2009).

32. A. Marhold, E. Klauke, A new method for the trifluoromethylation of aromatics. *J. Fluor. Chem*. **18**, 281–291 (1981).

33. O. M. Demuchuk, B. Yoruk, T. Blackburn, V. Snieckus, A mixed naphthyl-phenyl phosphine ligand motif for Suzuki, Heck, and hydrodehalogenation reactions, *Synlett* **18**, 2908–2913 (2006).

34. S. D. Schimler, M. A. Cismesia, P. S. Hanley, R. D. J. Froese, M. J. Jansma, D. C. Bland, M. S. Sanford, Nucleophilic deoxyfluorination of phenyls via aryl fluorosulfonate intermediates, *J. Am. Chem. Soc*. **139**, 1452–1455 (2017).

35. C. Zarate, M. Nakajima, R. Martin, A mild and ligand-free Ni-catalyzed silylation via C-OMe cleavage, *J. Am. Chem. Soc*. **139**, 1191–1197 (2017).

36. X. Xi, T. Chen, J.-S. Zhang, L.-B. Han, Efficient and selective hydrogenation of C-O bonds with a simple sodium formate catalyzed by nickel, *Chem. Commun.* **54**, 1521–1524 (2018).

37. P. Ahmadi, K. Muguruma, T.-C. Chang, S. Tamura, K. Tsubokura, Y. Egawa, T. Suzuki, N. Dohmae, Y. Nako, K. Tanaka, In vivo metal-catalyzed SeCT therapy by a proapoptotic peptide. *Chem. Sci.* **12**, 12266 (2021).

38. C. O. Blanco, J. Sims, D. L. Nascimento, A. Y. Goudreault, S. N. Steinmann, C. Michel, D. E. Fogg, The Impact of Water on Ru-Catalyzed Olefin Metathesis: Potent Deactivating Effects Even at Low Water Concentrations. *ACS Catal.* **11**, 893 (2021).

39. A. H. Hoveyda, P. J. Lombardi, R. V. O'Brien, A. R. Zhugralin, H-Bonding as a Control Element in Stereoselective Ru-Catalyzed Olefin Metathesis. *J. Am. Chem. Soc.* **131**, 8378 (2009).

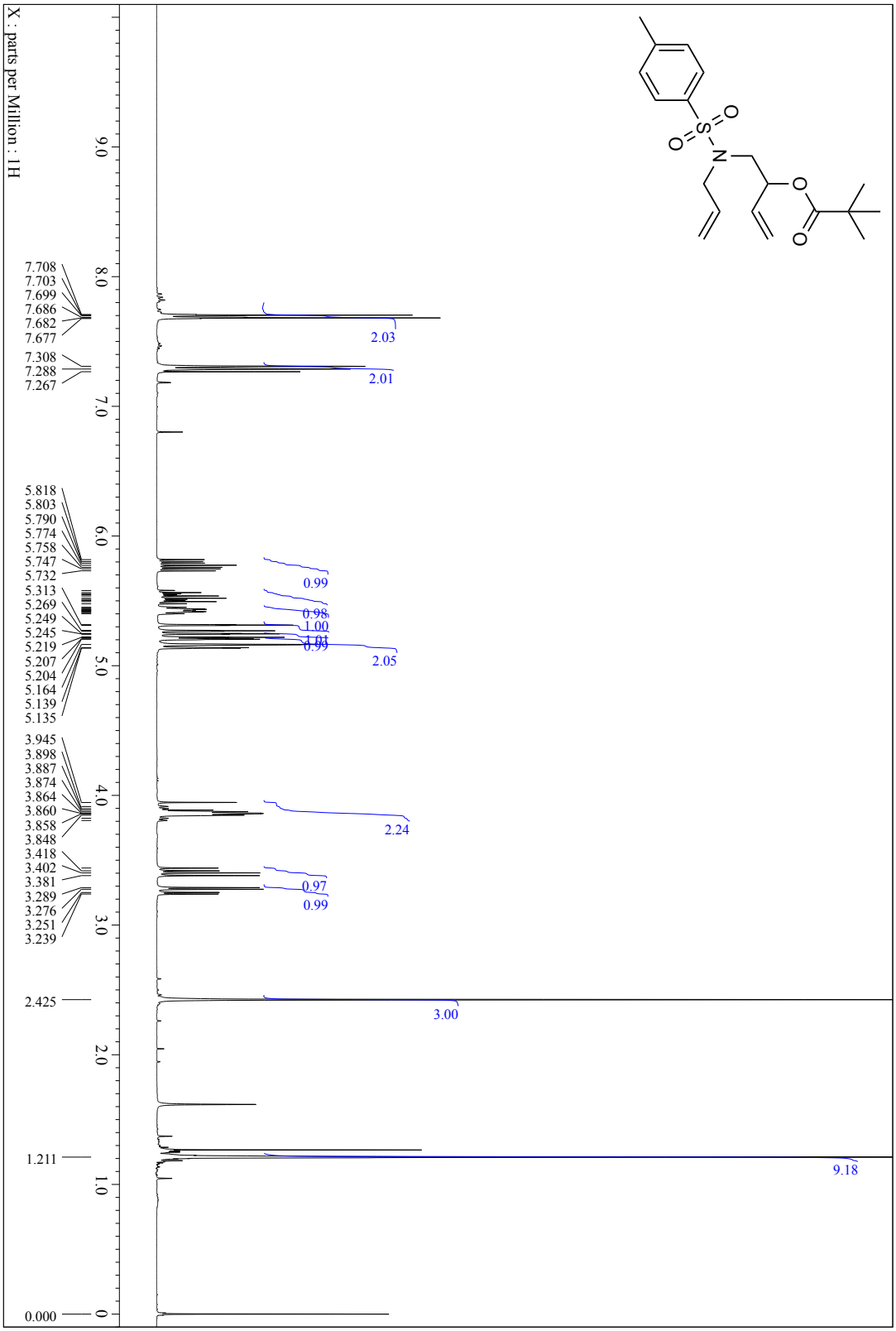

Fig. S92.

^{1}H NMR spectra of **12**

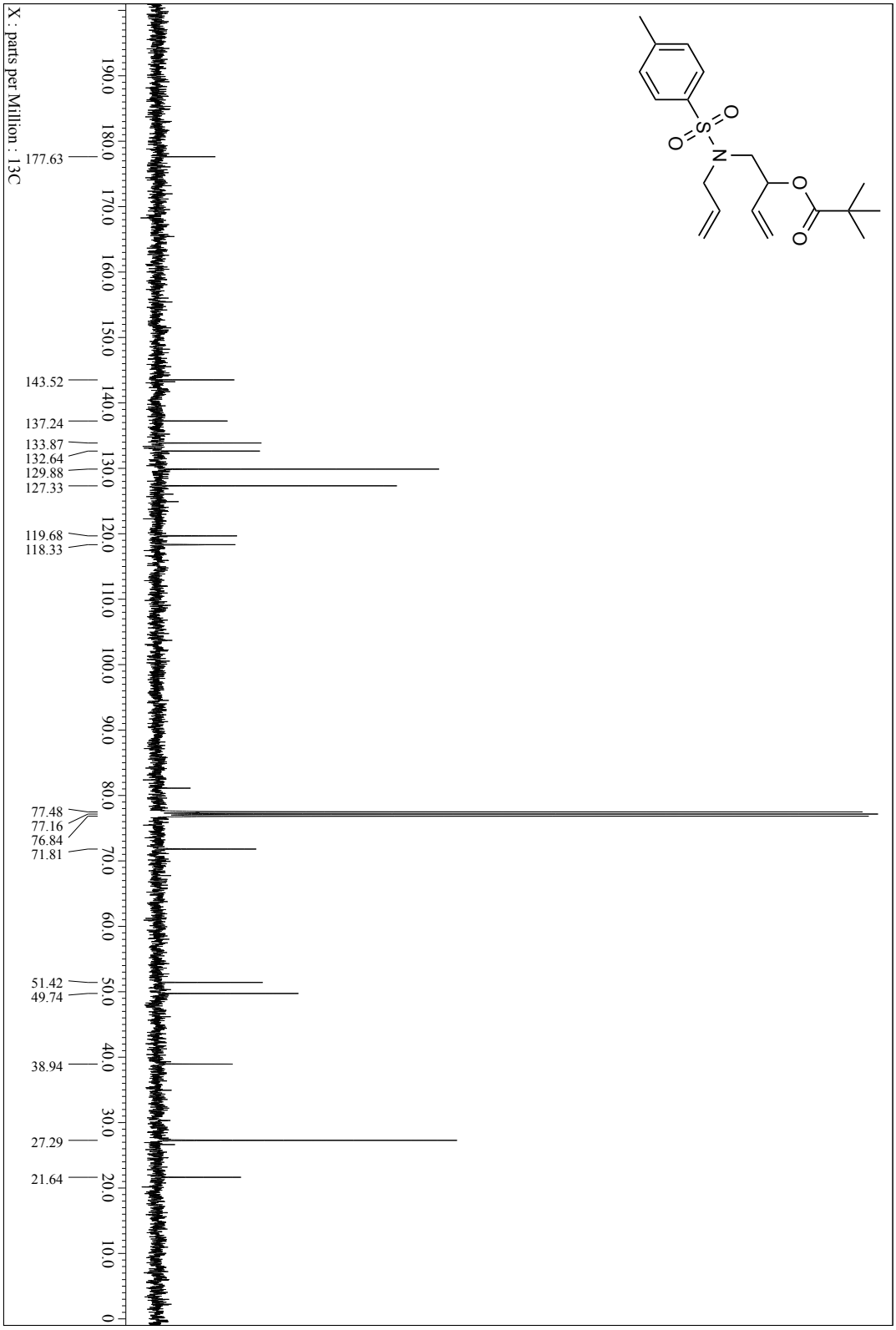

Fig. S93.

^{13}C NMR spectra of **12**

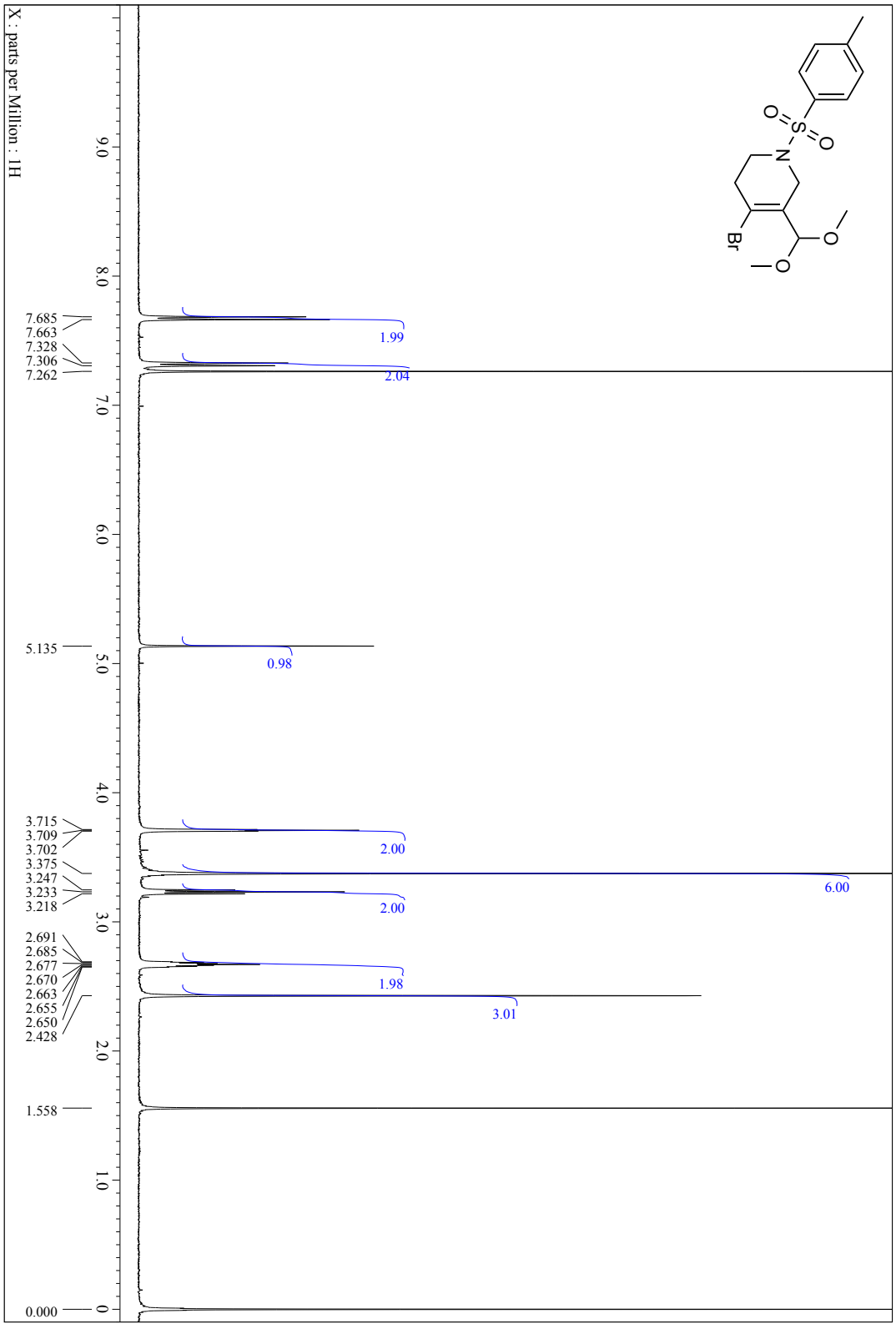

Fig. S94.

^{1}H NMR spectra of **S3**.

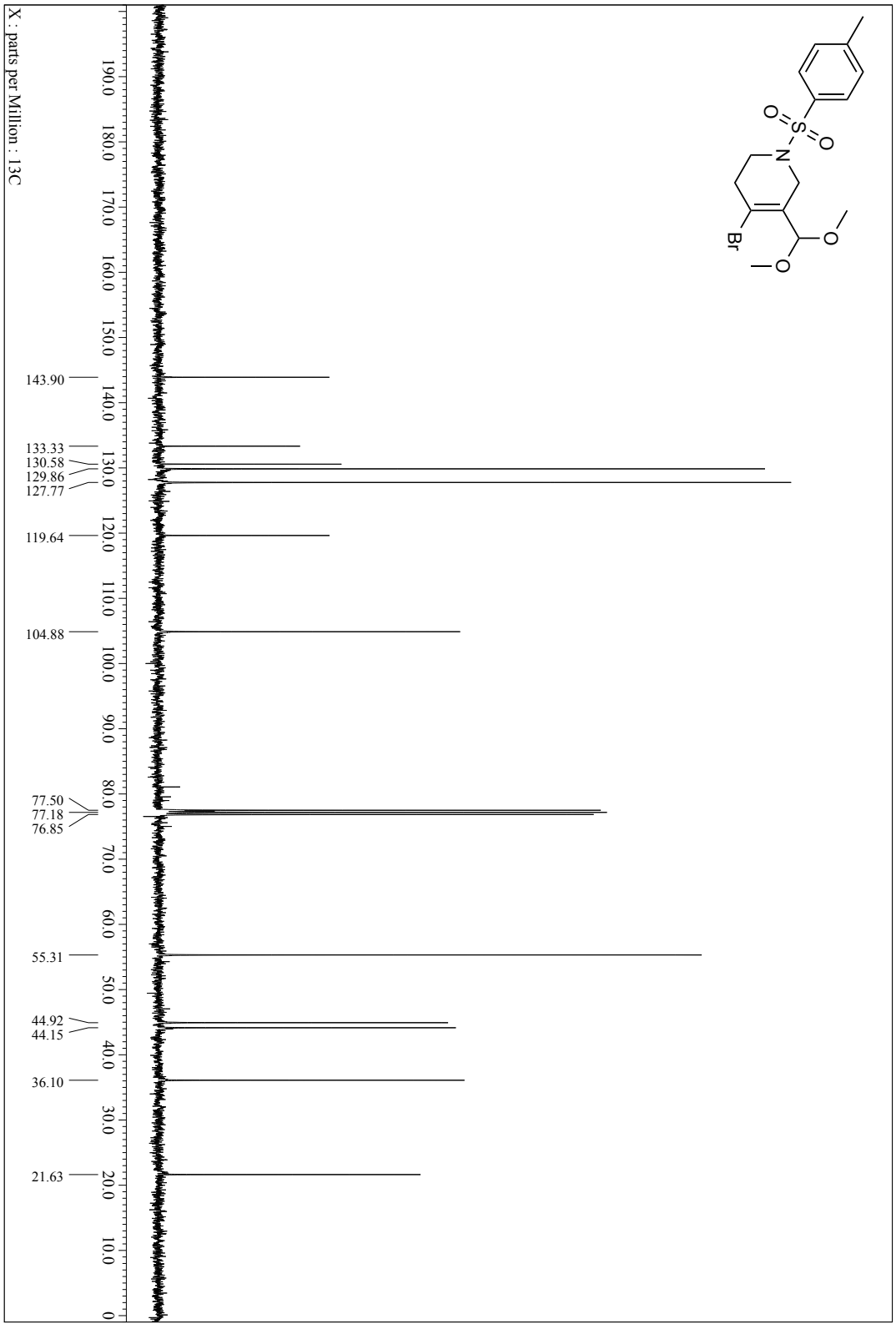

Fig. S95.

^{13}C NMR spectra of **S3**.

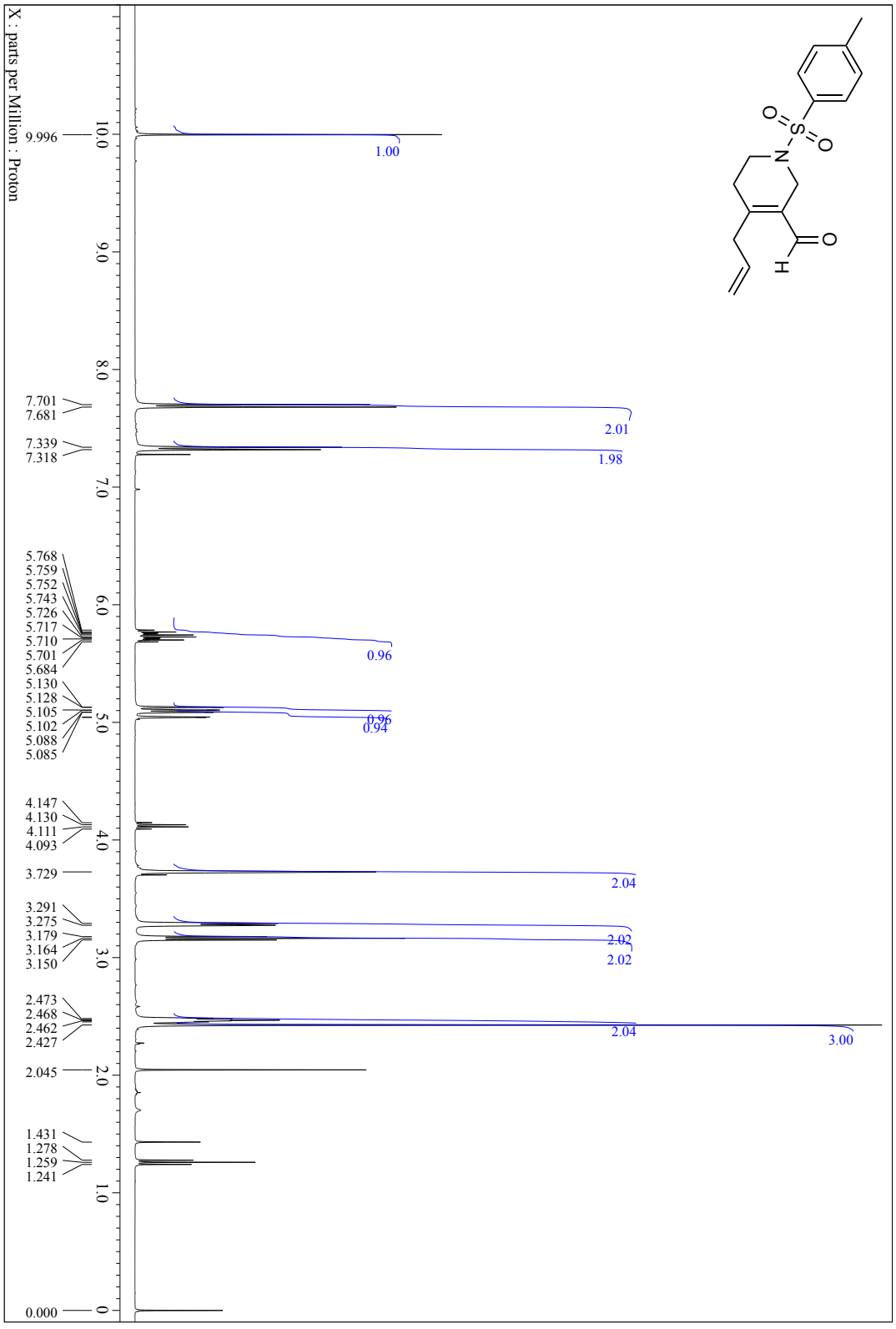

Fig. S96.

^{1}H NMR spectra of **S4**.

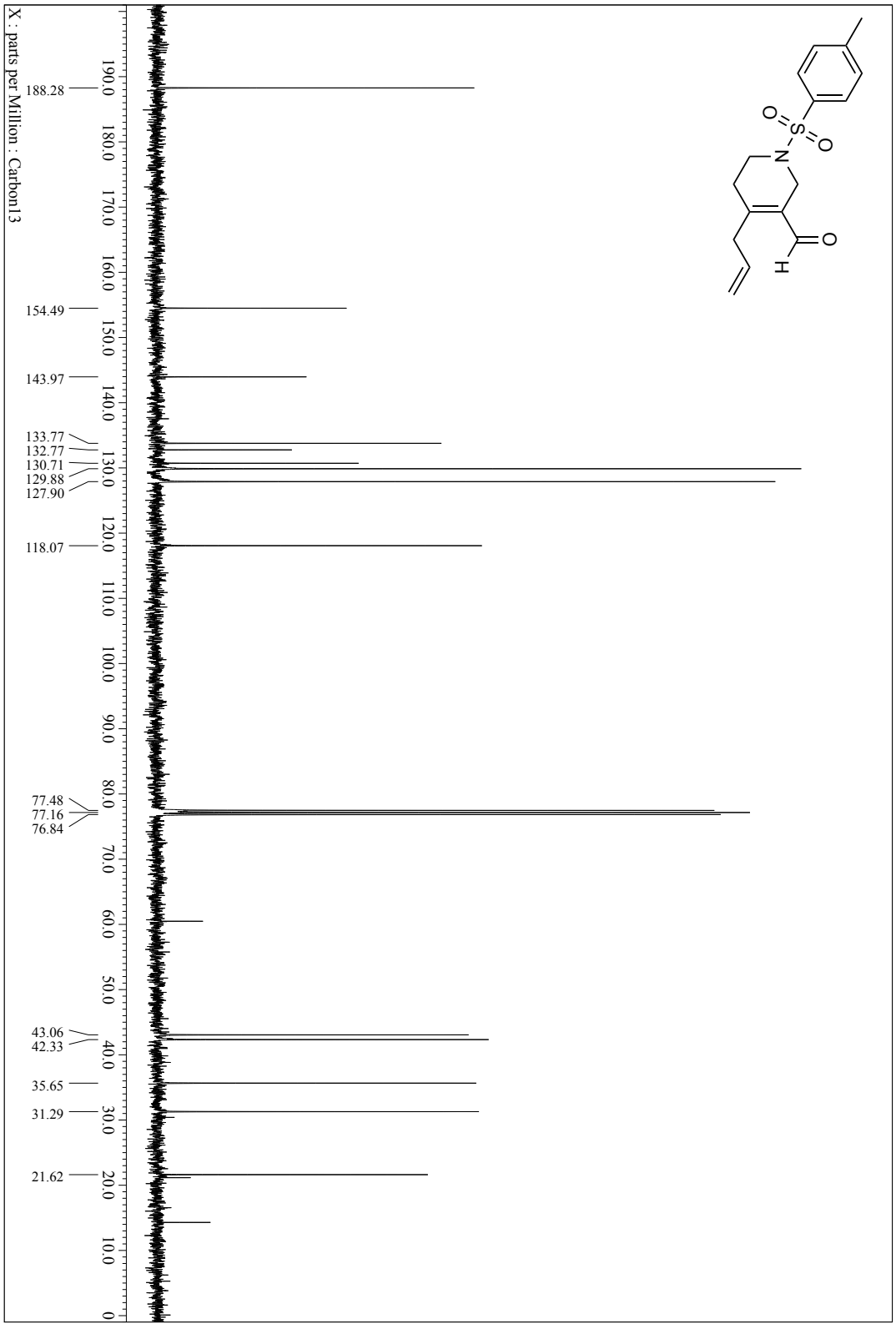

Fig. S97.

^{13}C NMR spectra of **S4**.

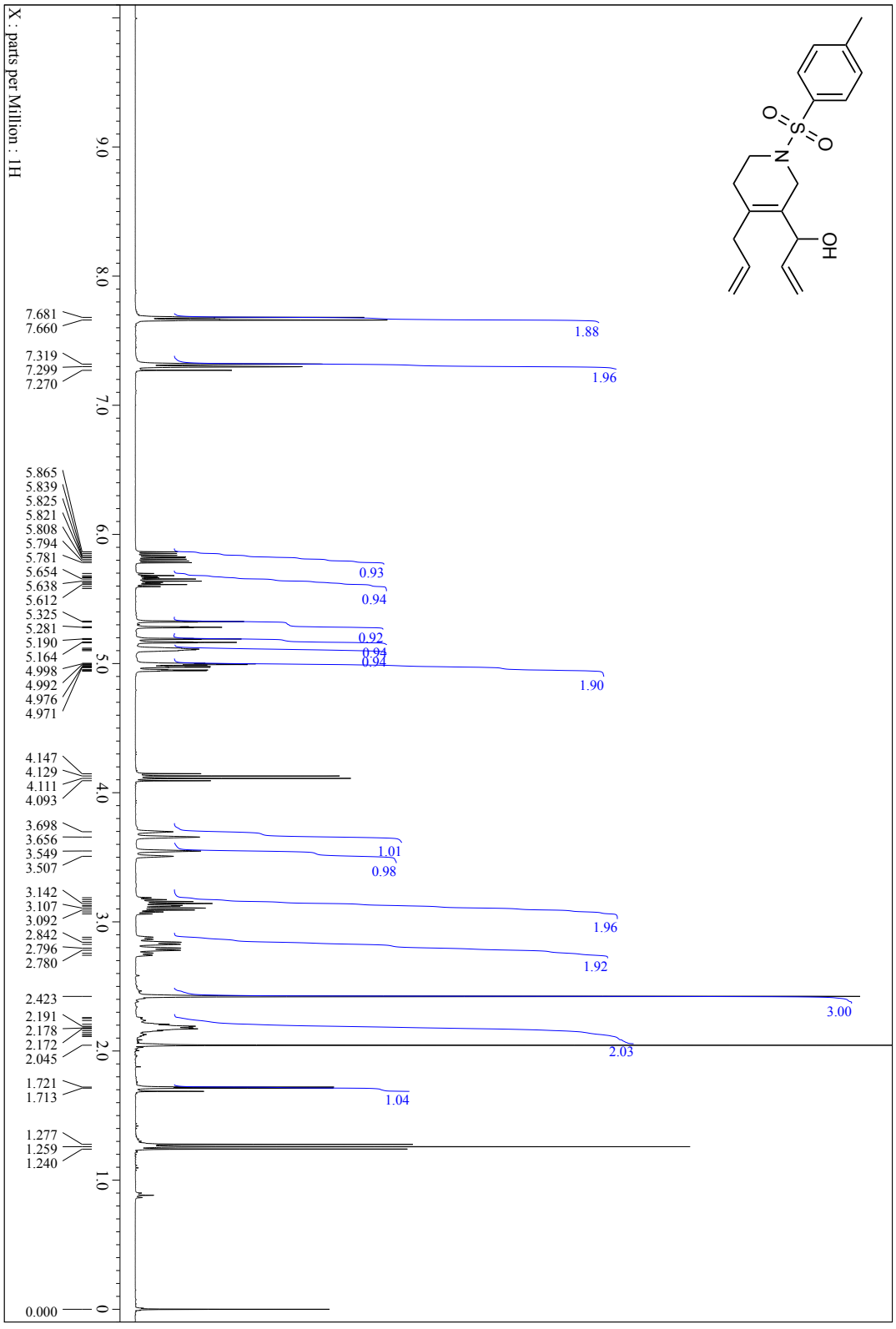

Fig. S98.

^{1}H NMR spectra of **23**.

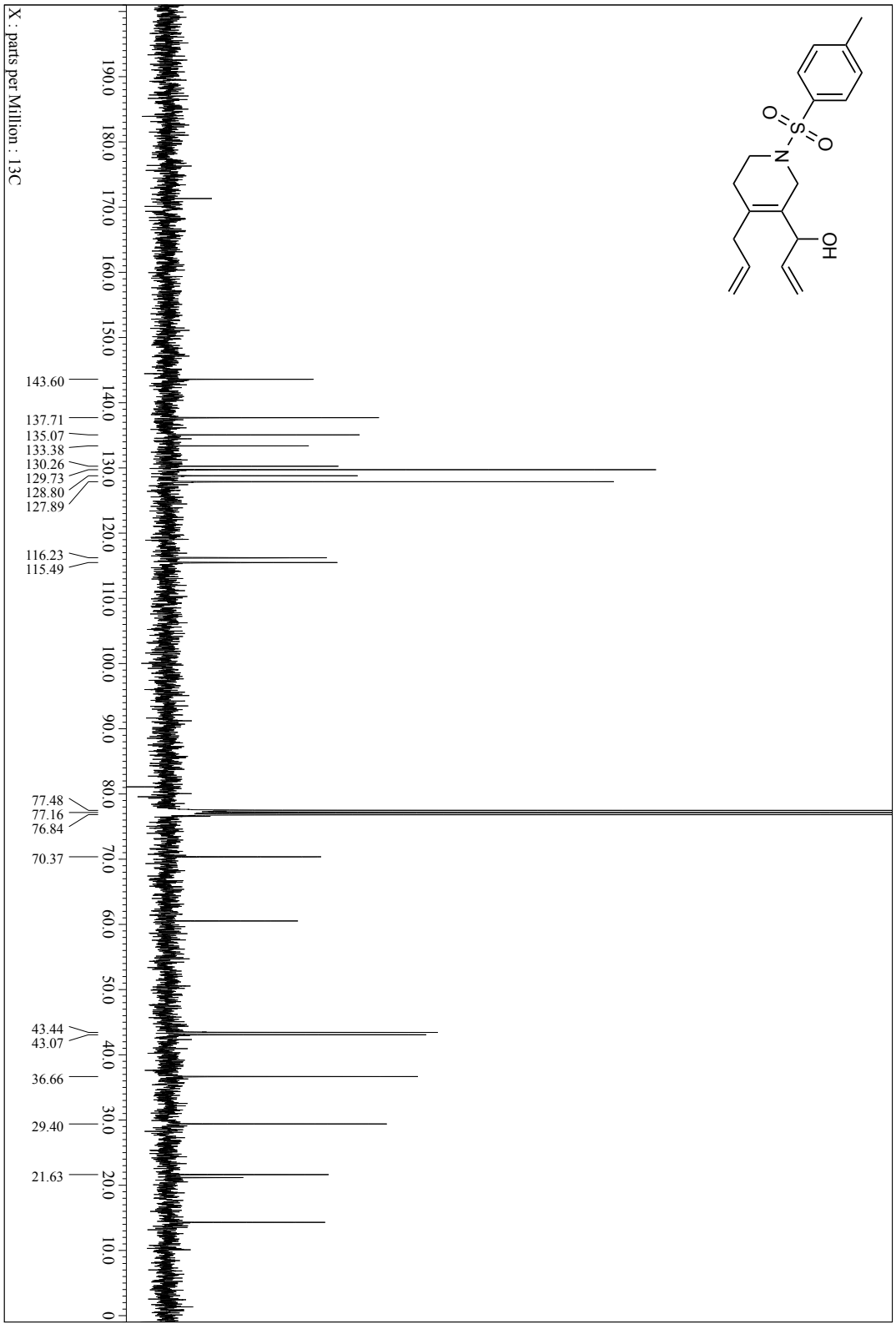

Fig. S99.

^{13}C NMR spectra of **23**.

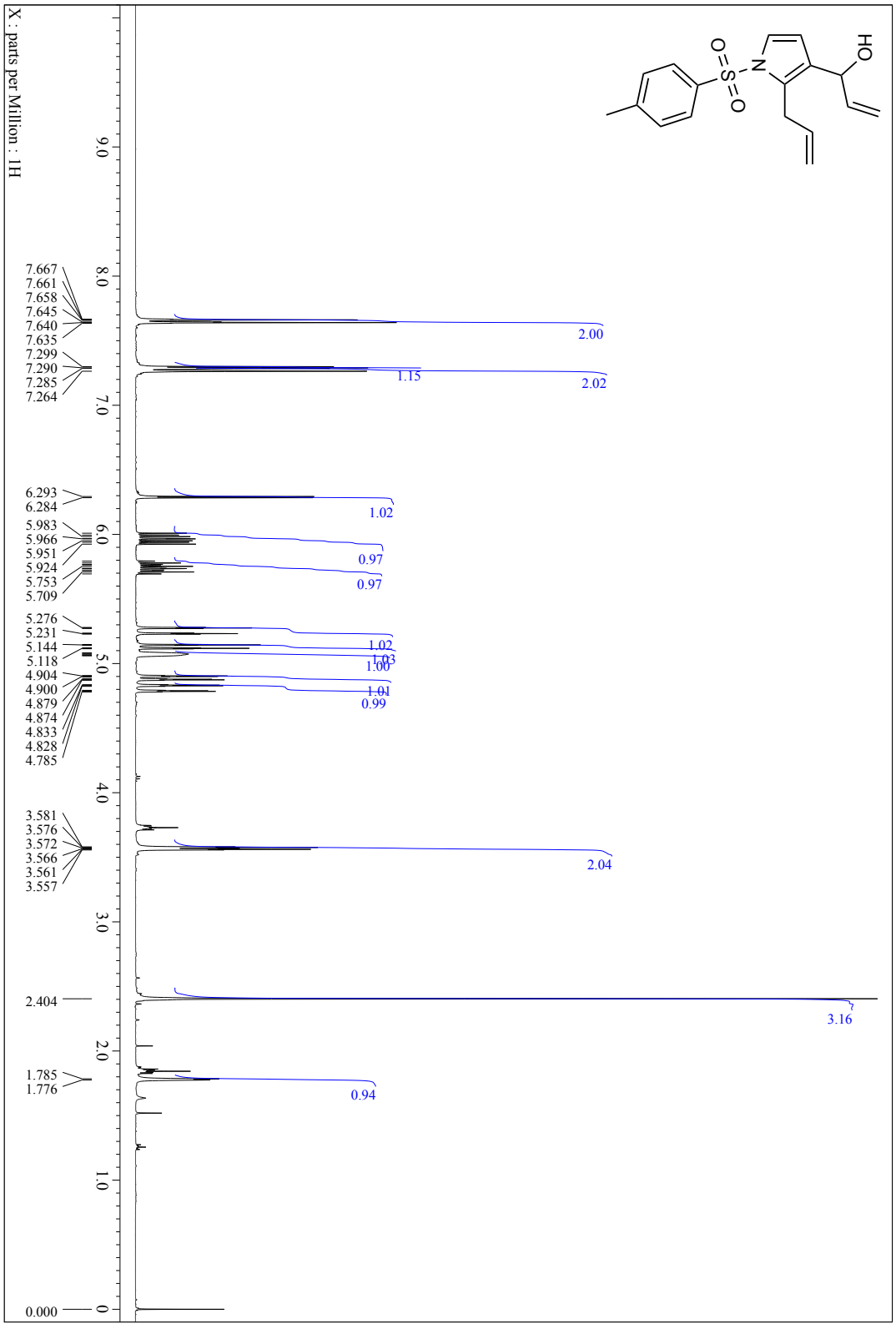

Fig. S100.

^{1}H NMR spectra of **24**.

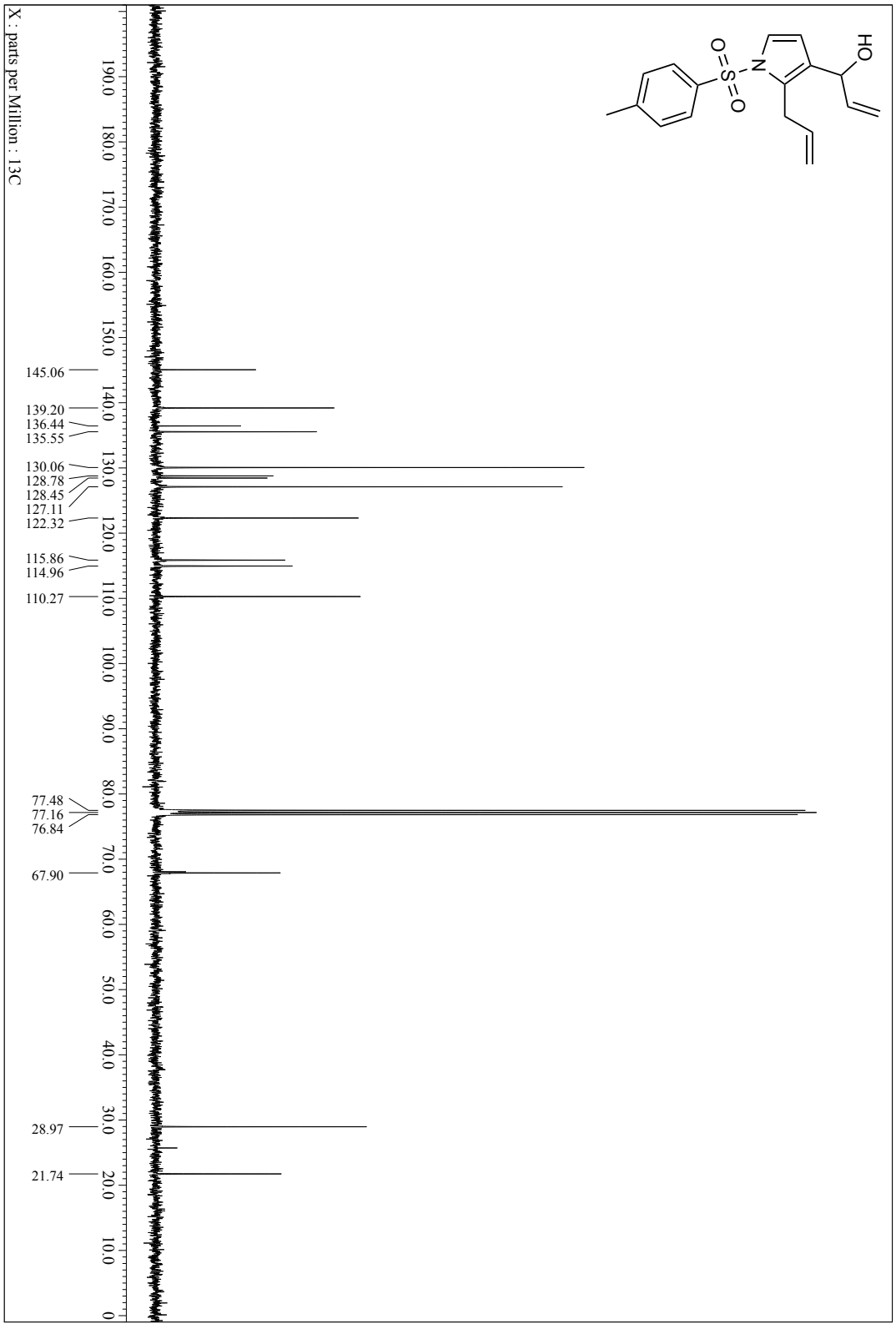

Fig. S101.

^{13}C NMR spectra of **24**.

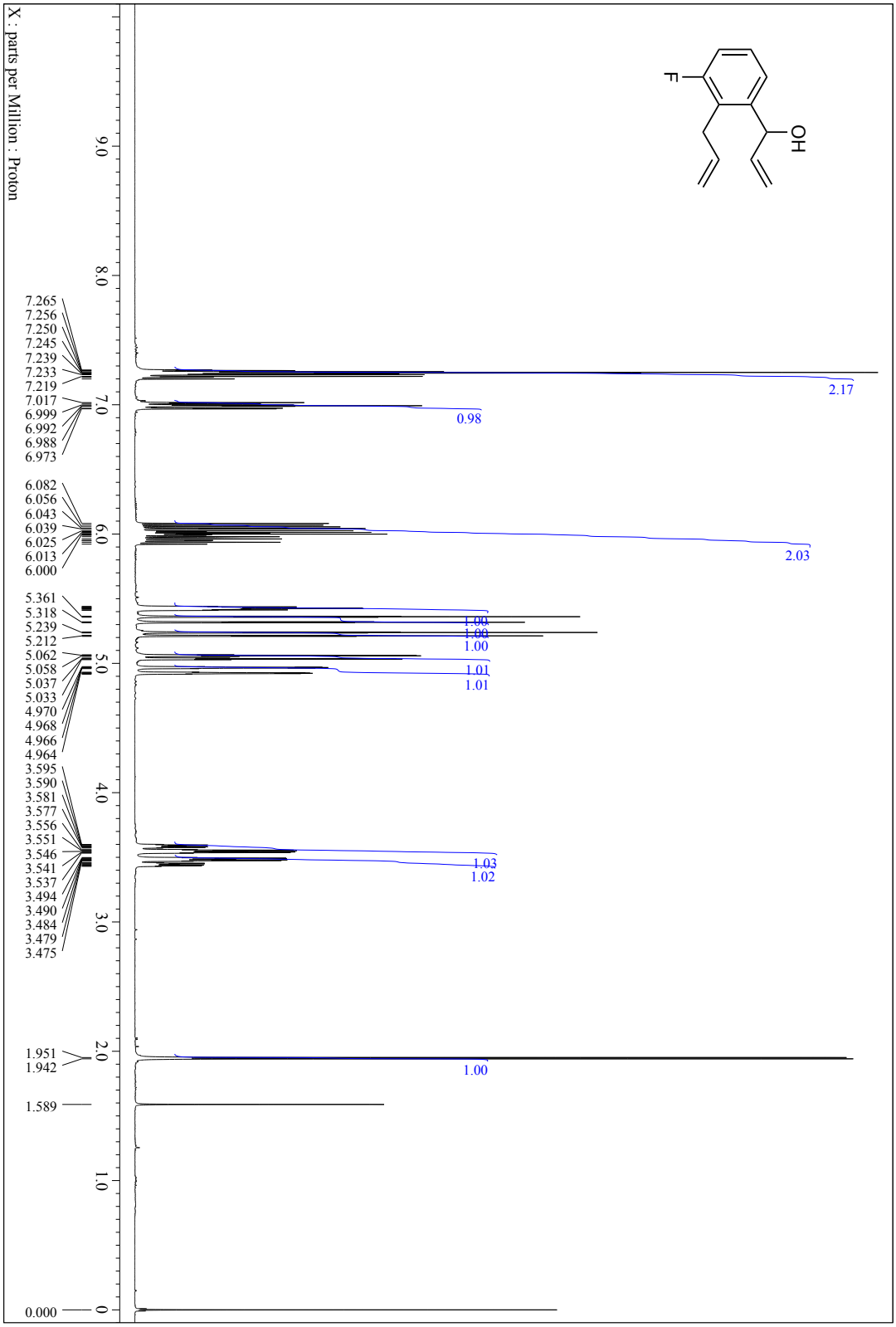

Fig. S102.

^{1}H NMR spectra of **S7**.

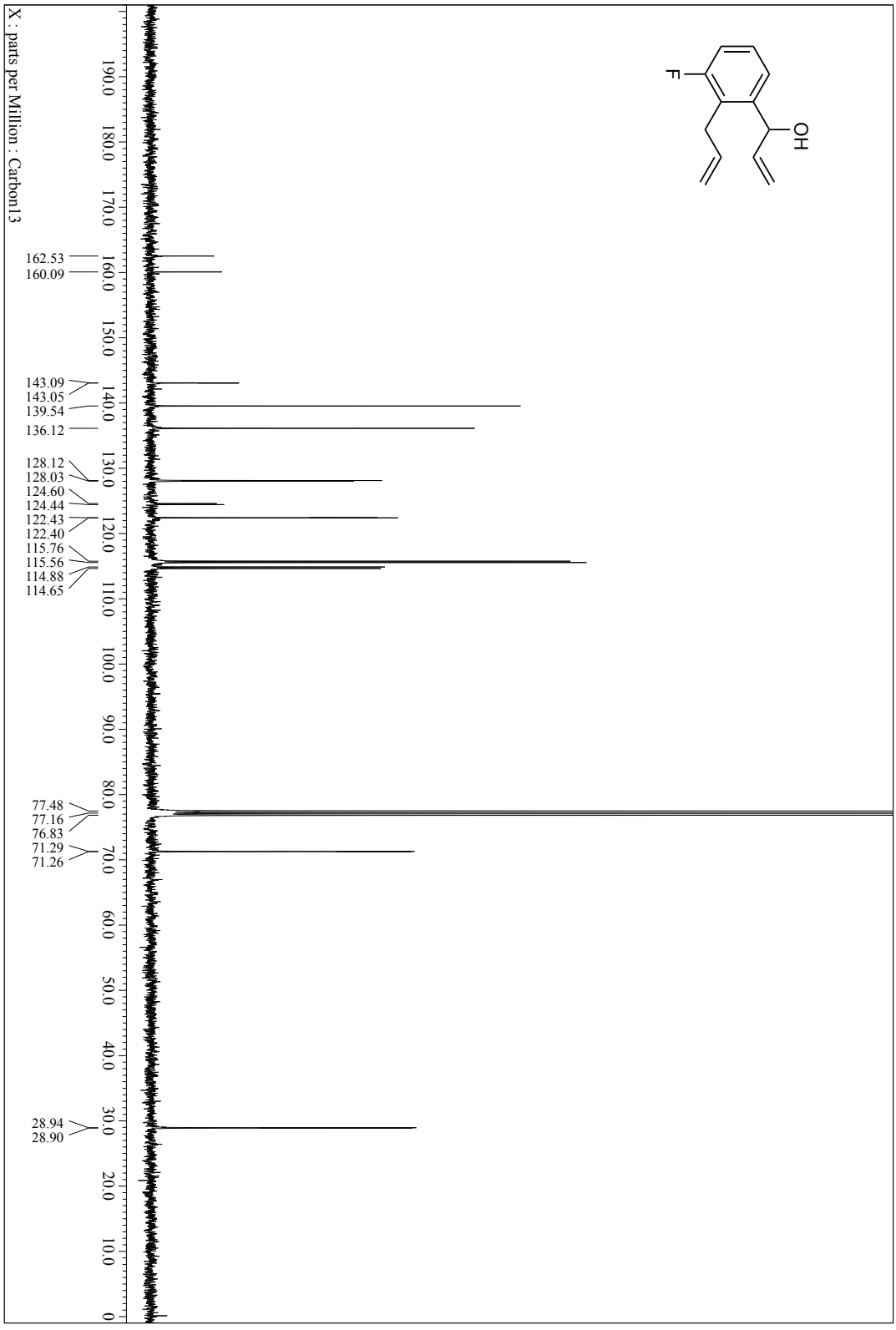

Fig. S103.

^{13}C NMR spectra of **S7**.

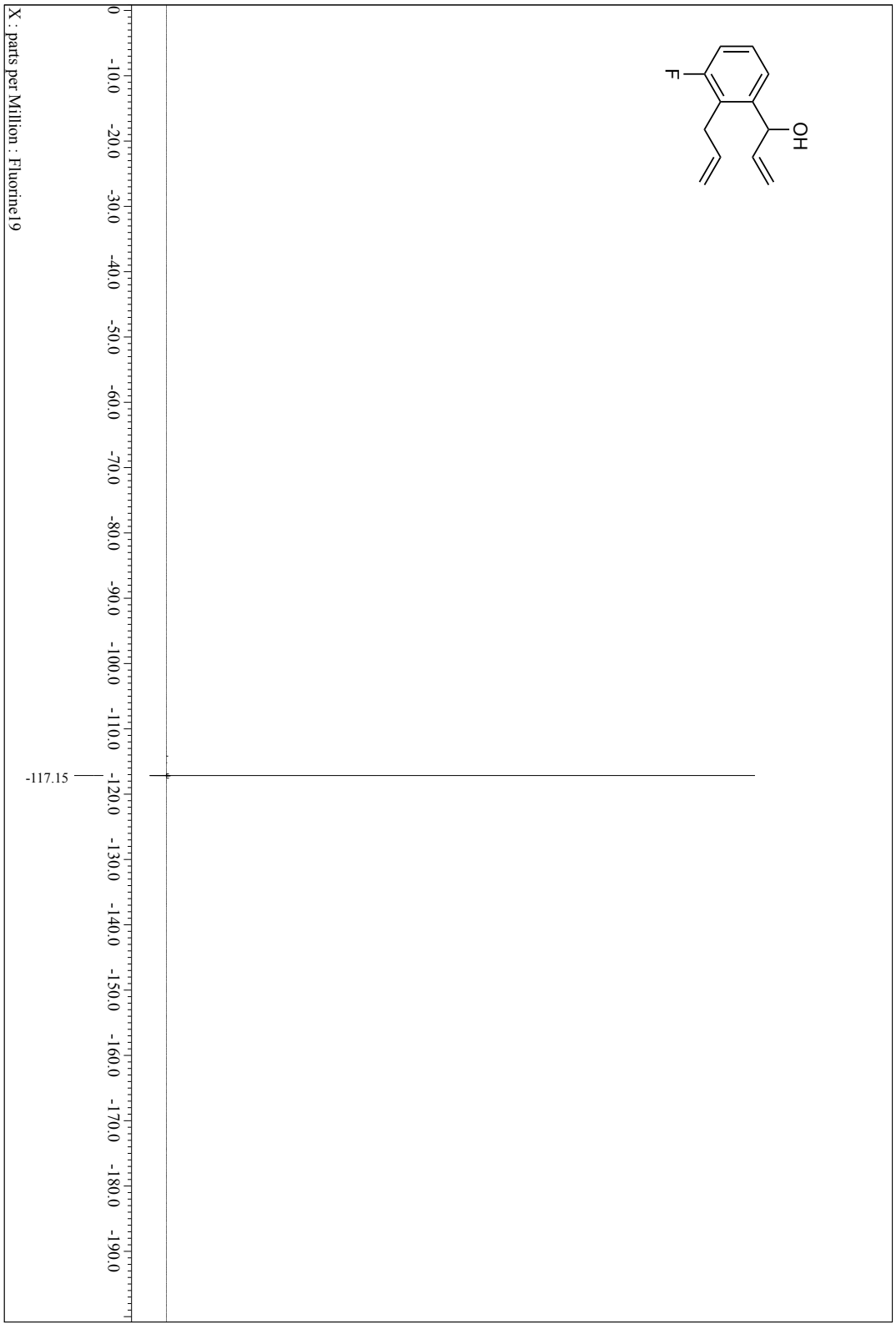

Fig. S104.

^{19}F NMR spectra of **S7**.

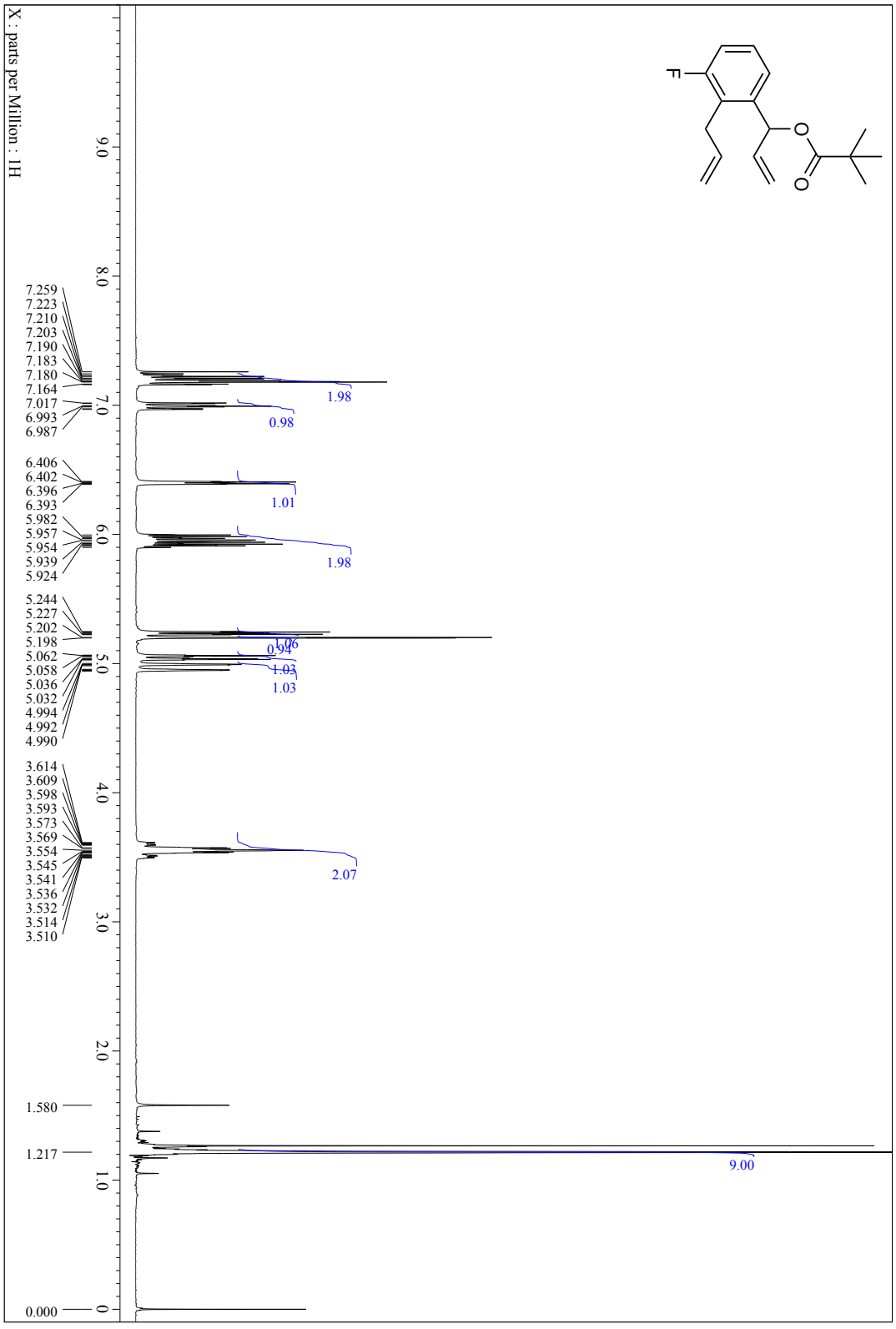

Fig. S105.

^{1}H NMR spectra of **25**.

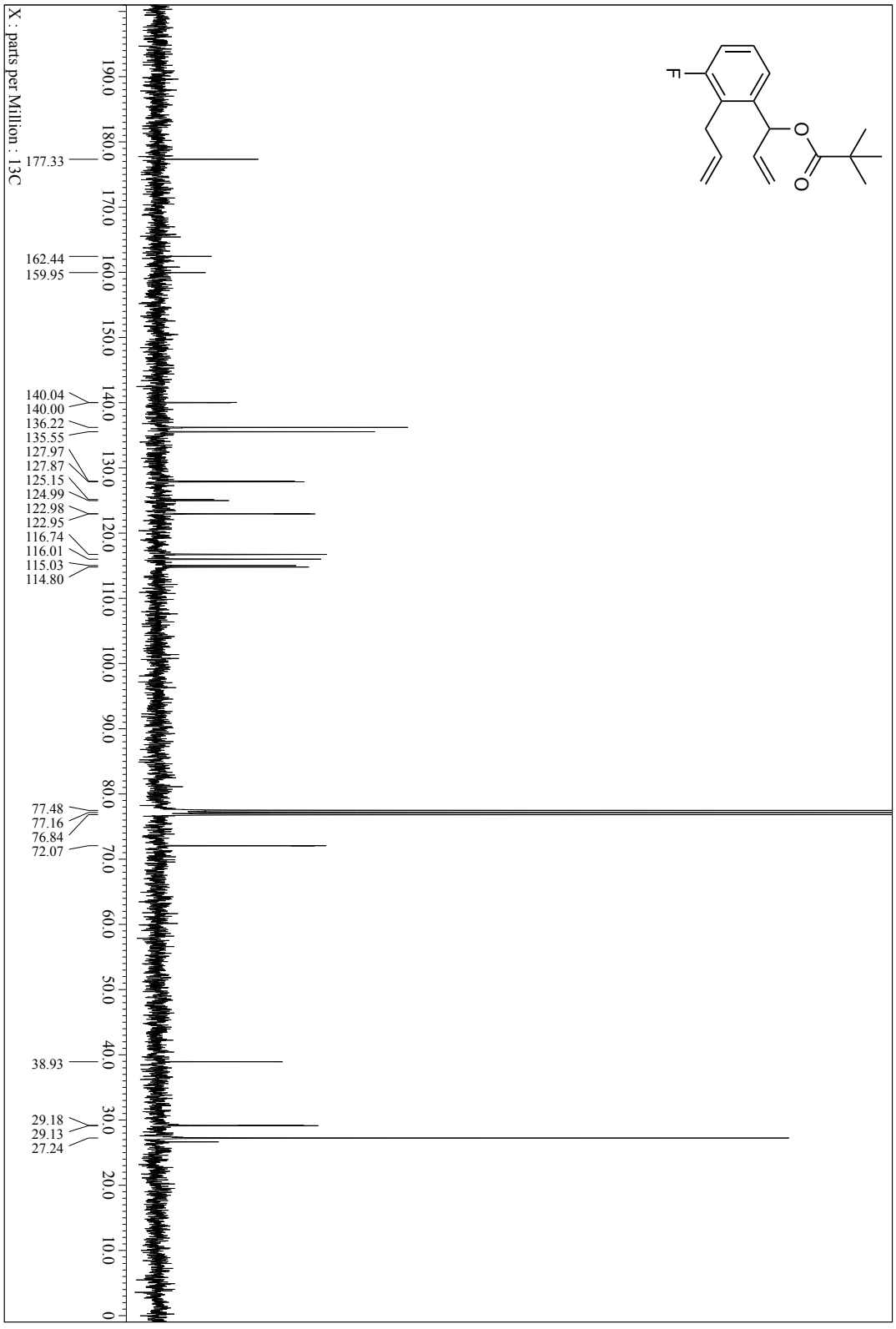

Fig. S106.

^{13}C NMR spectra of **25**.

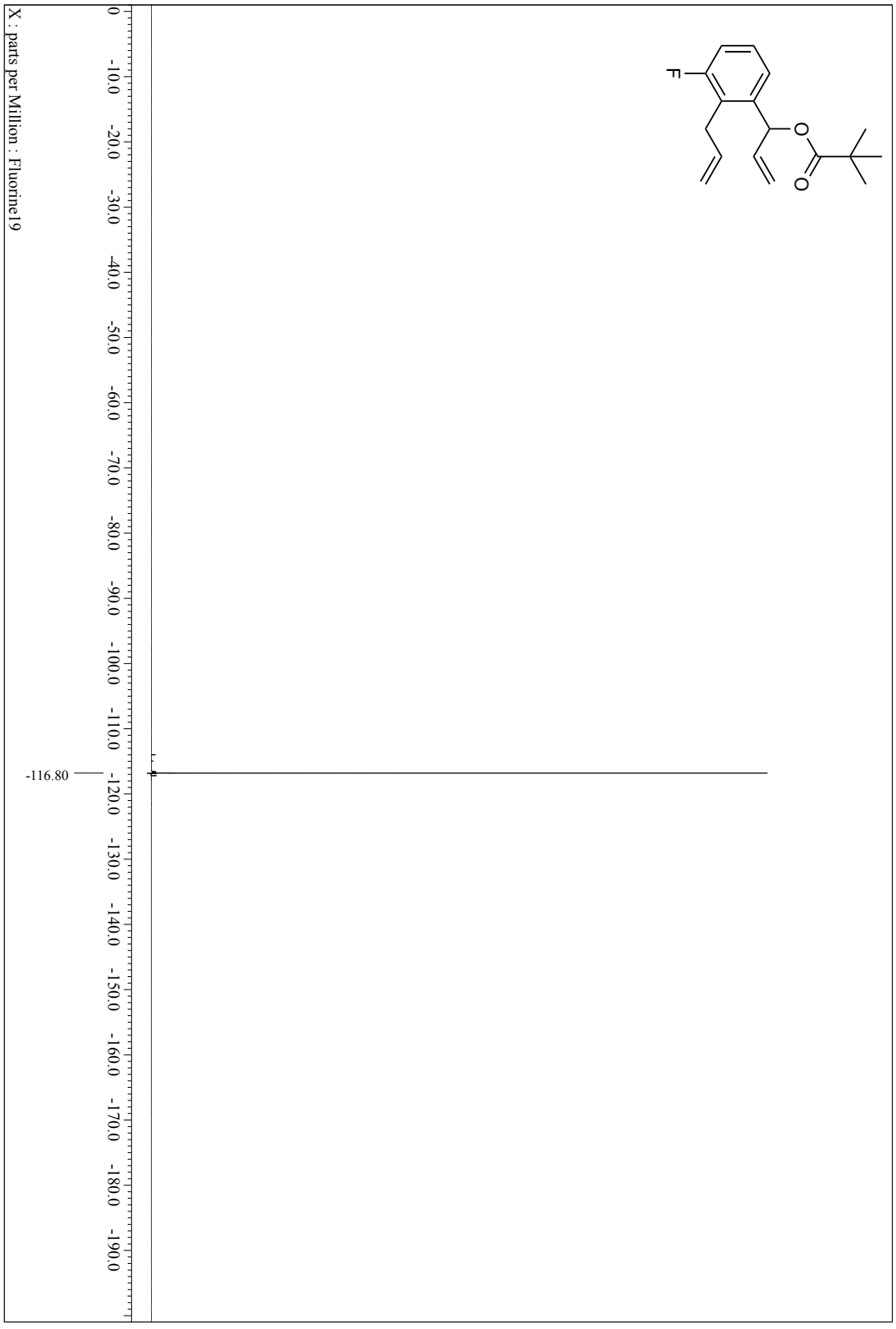

Fig. S107.

^{19}F NMR spectra of **25**.

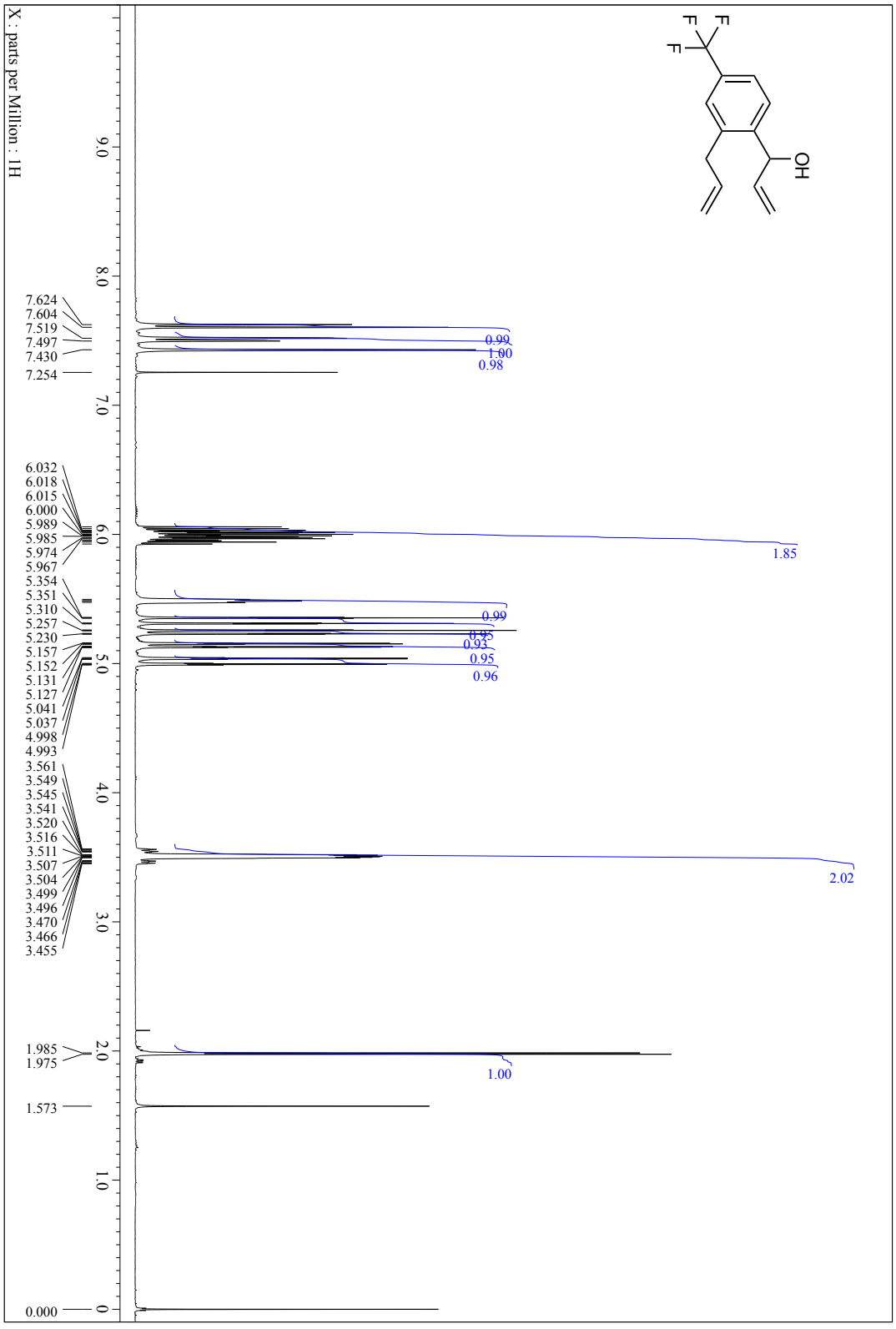

Fig. S108.

^{1}H NMR spectra of **S9**.

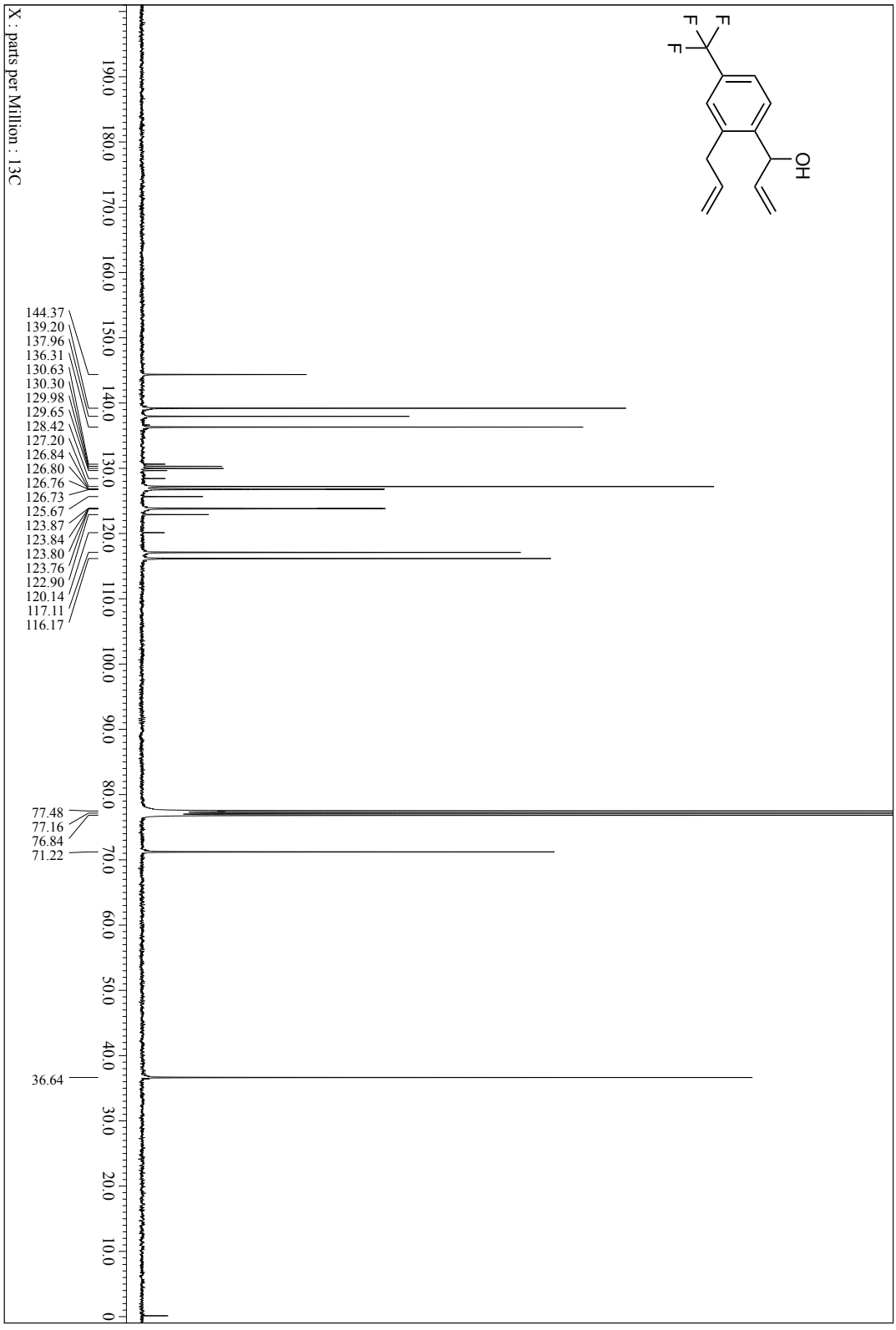

Fig. S109.

^{13}C NMR spectra of **S9**.

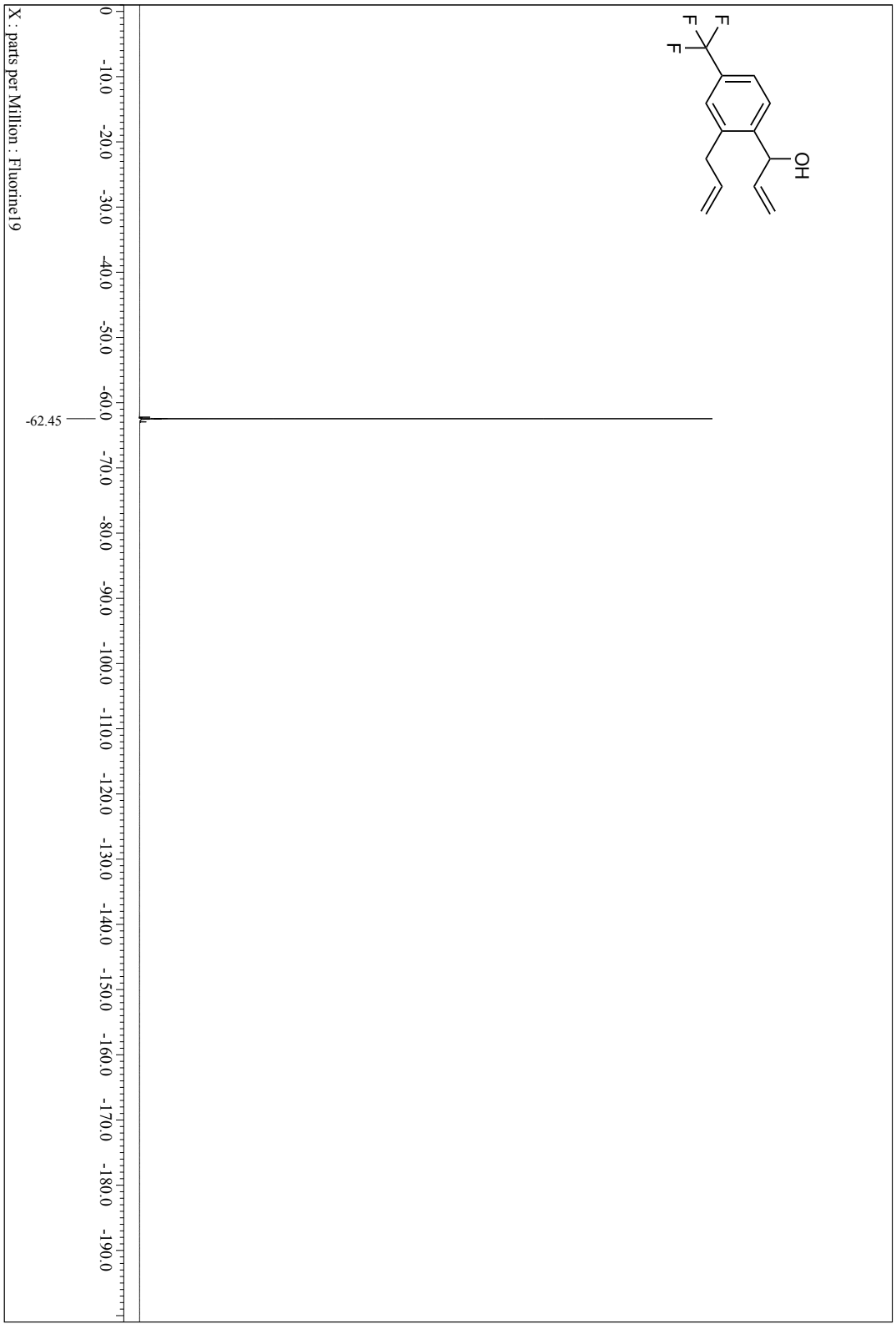

Fig. S110.

^{19}F NMR spectra of **S9**.

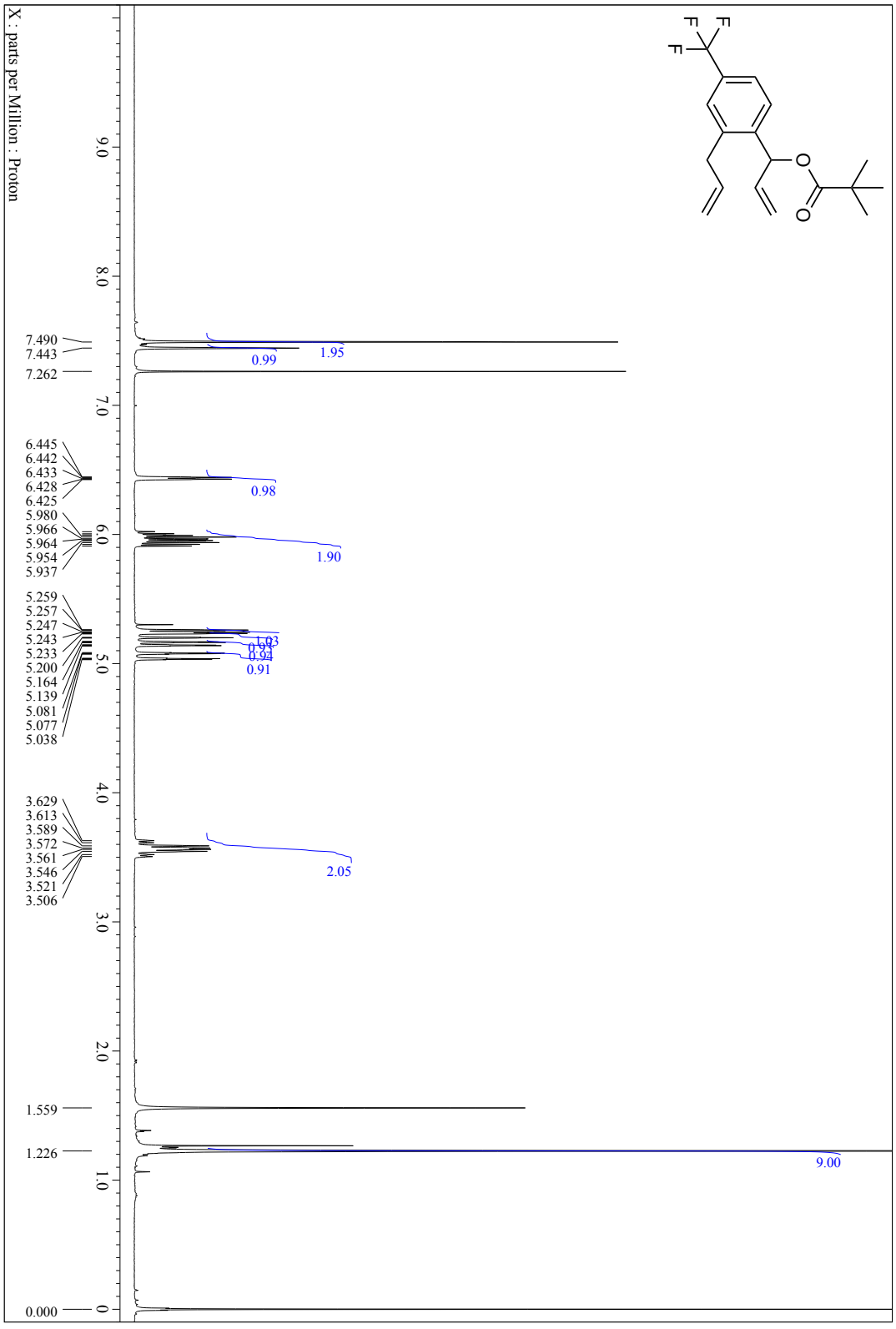

Fig. S111.

^{1}H NMR spectra of **26**.

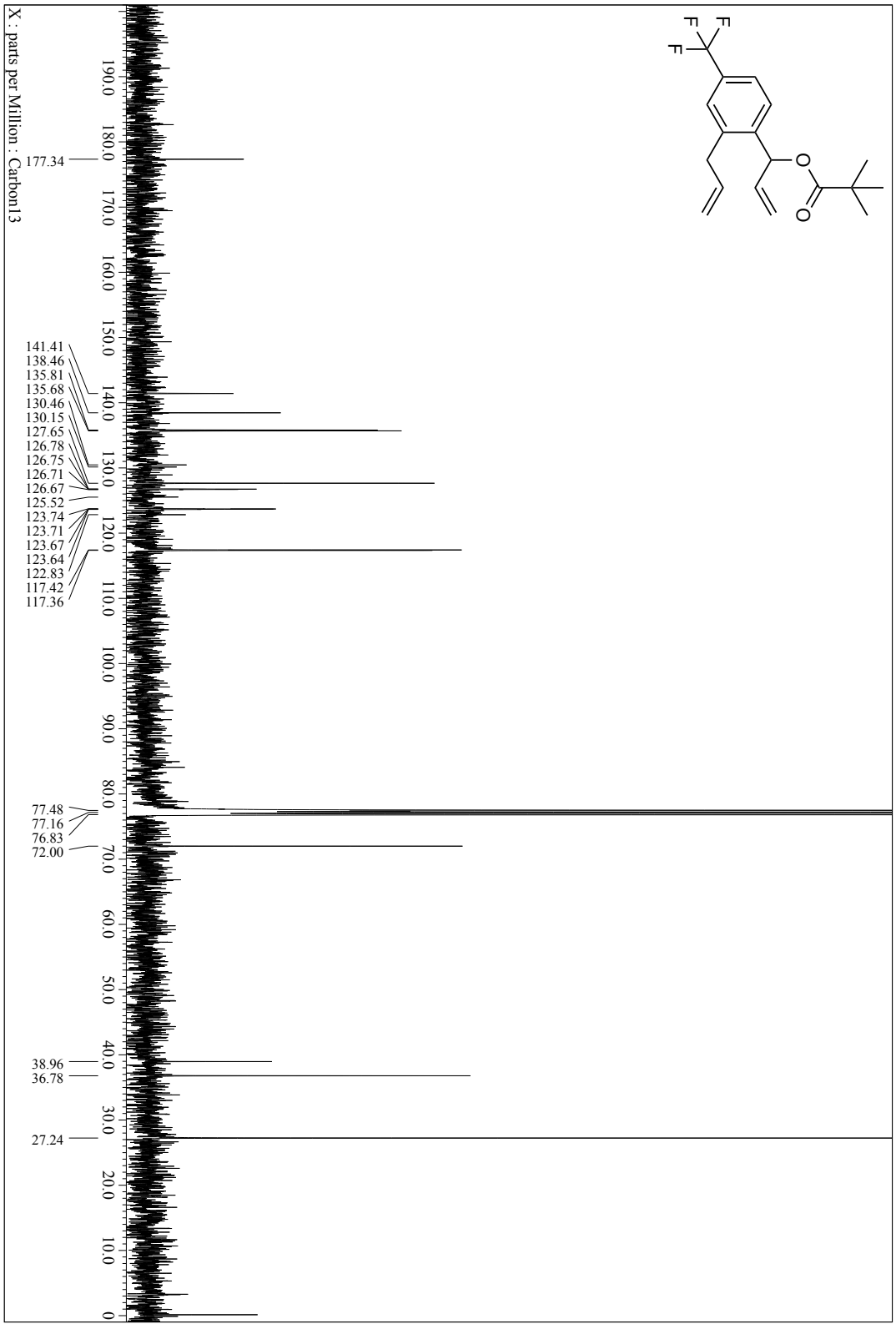

Fig. S112.

^{13}C NMR spectra of **26**.

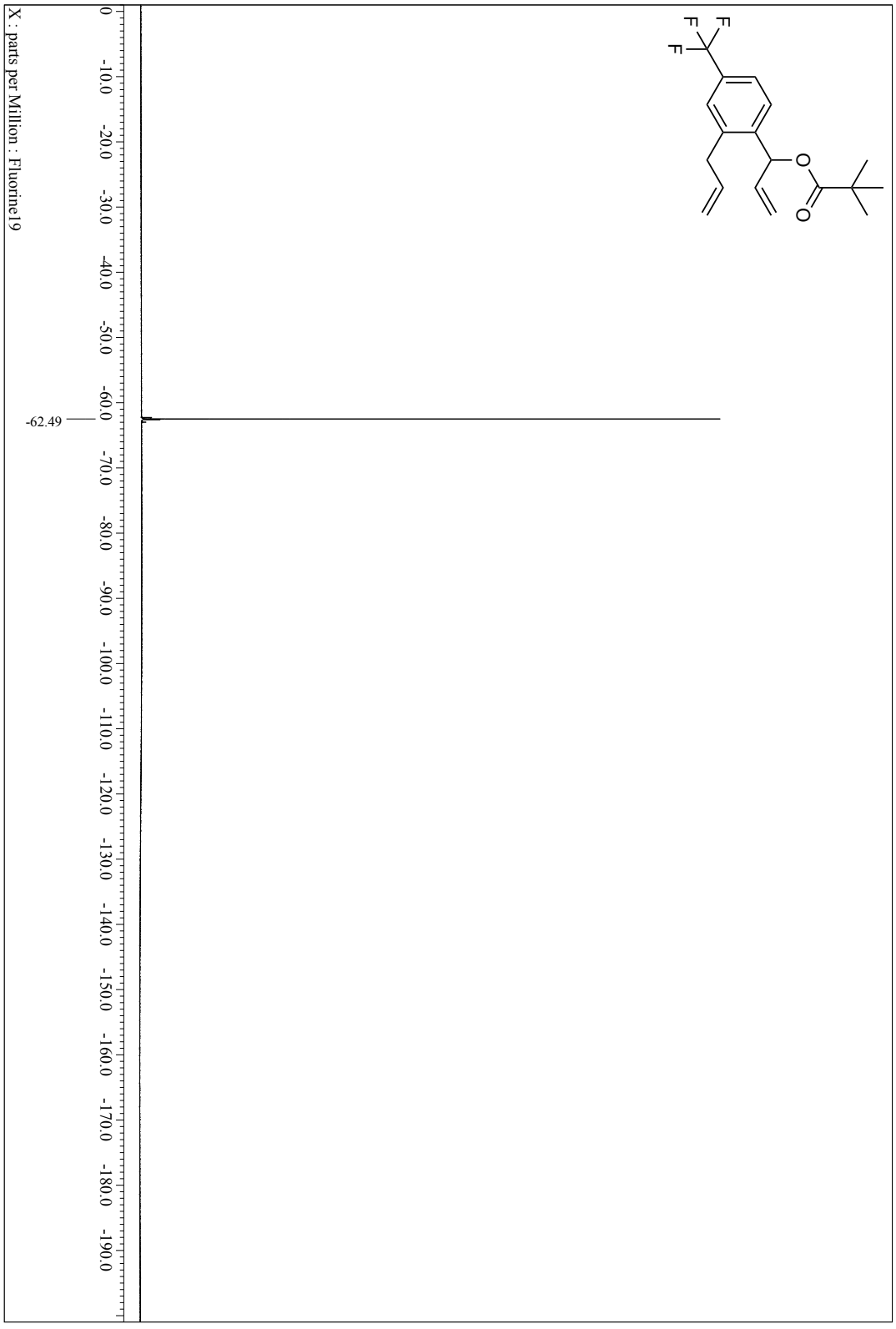

Fig. S113.

^{19}F NMR spectra of **26**.

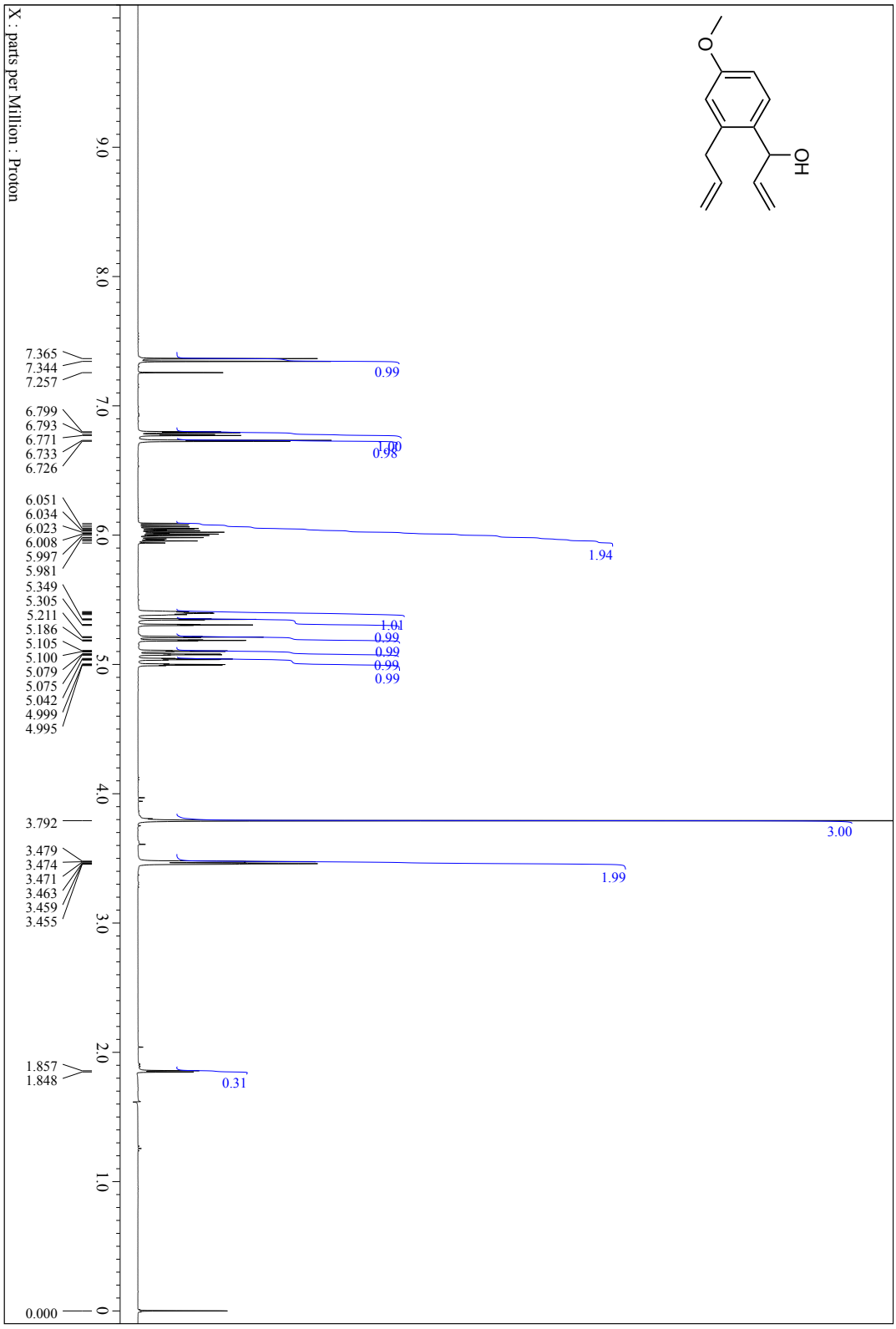

Fig. S114.

^{1}H NMR spectra of **S11**.

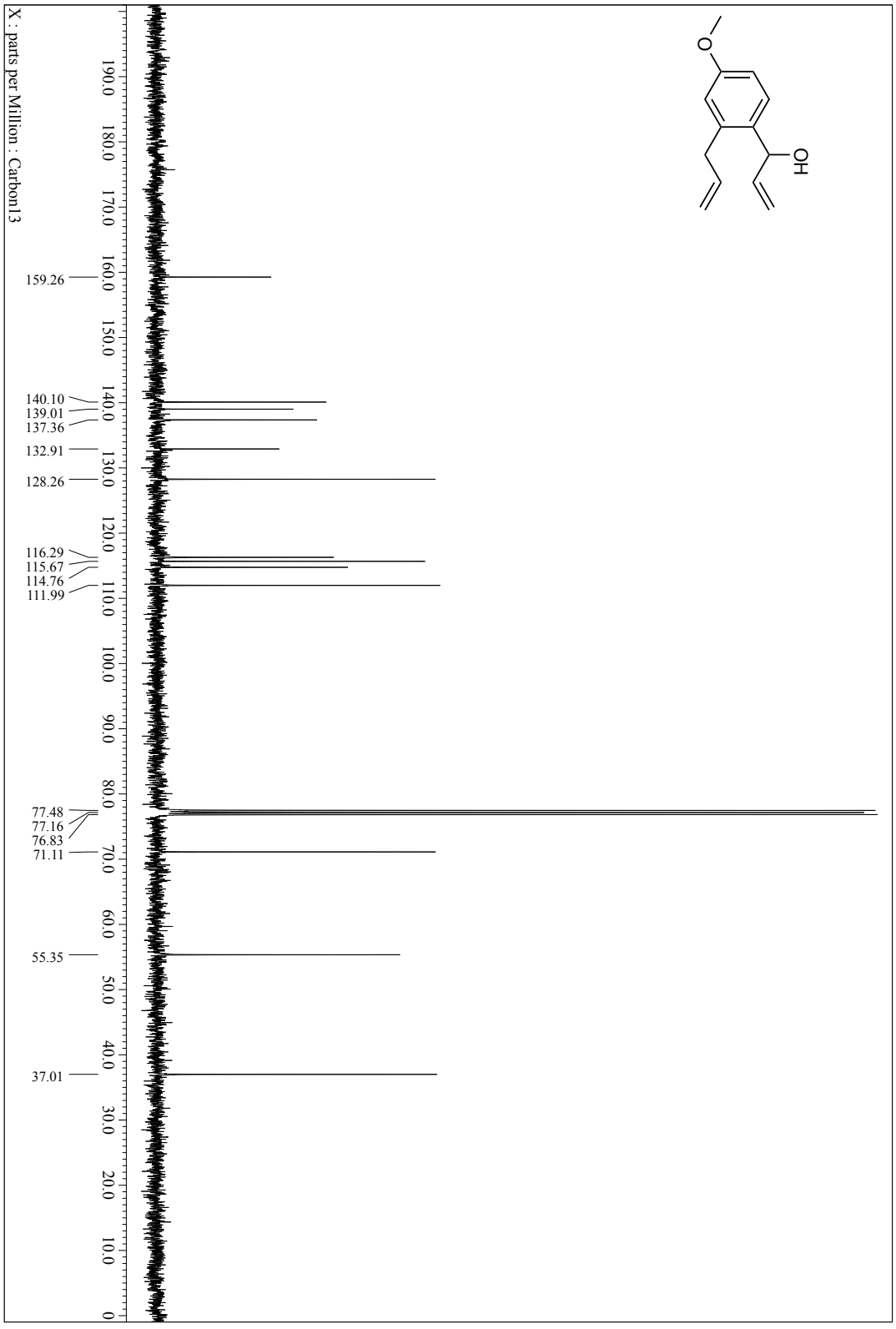

Fig. S115.

^{13}C NMR spectra of **S11**.

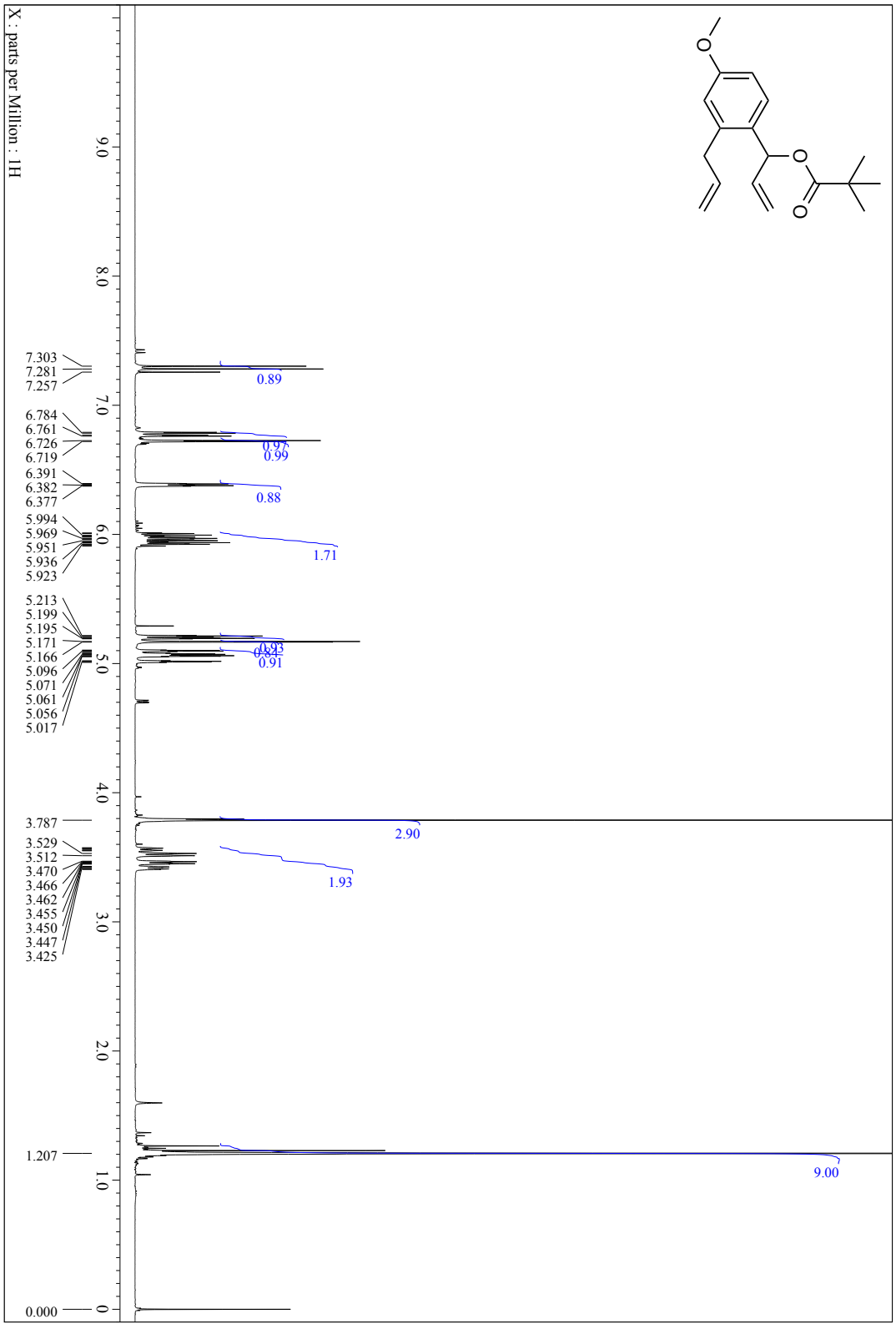

Fig. S116.

^{1}H NMR spectra of **27**.

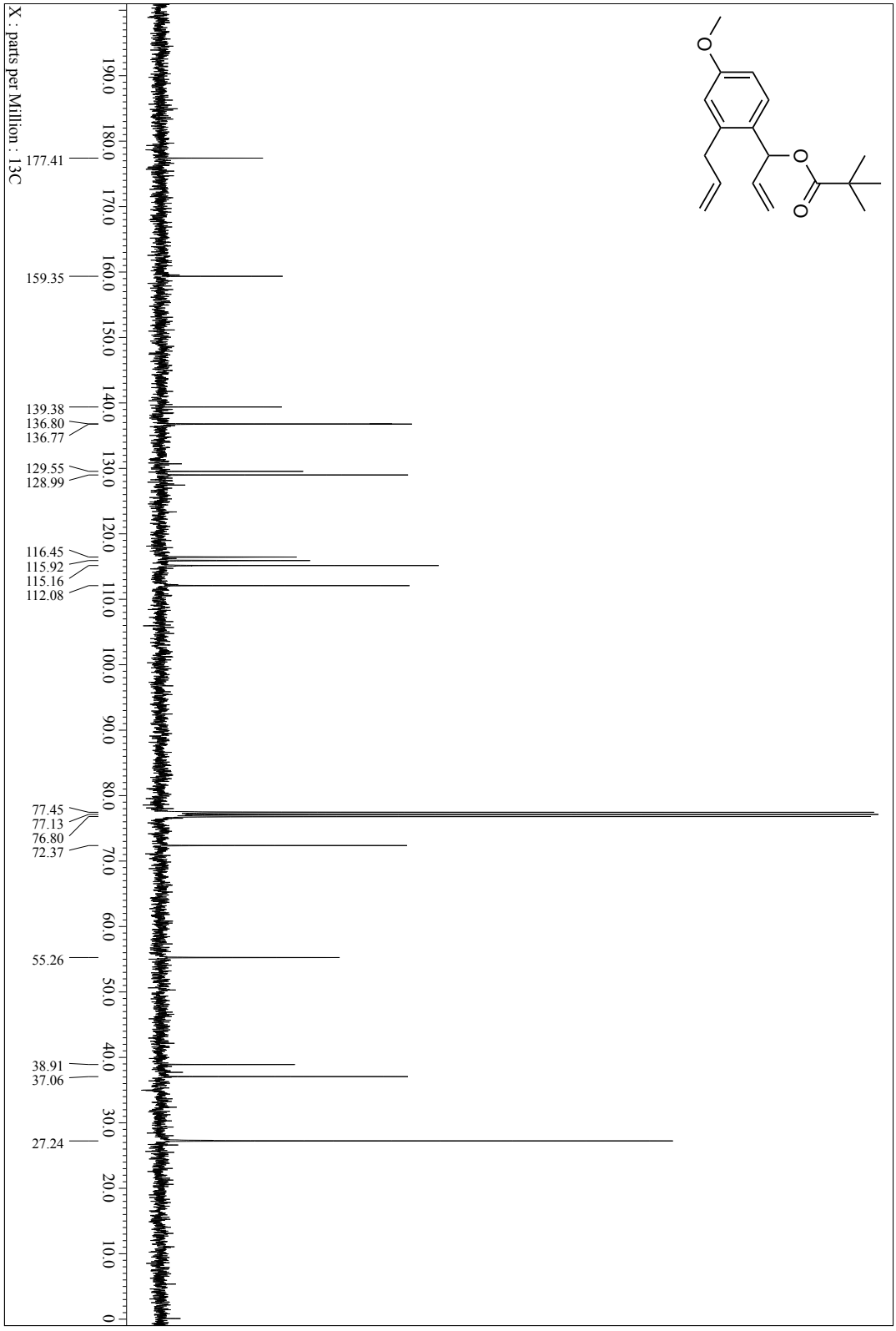

Fig. S117.

^{13}C NMR spectra of **27**.

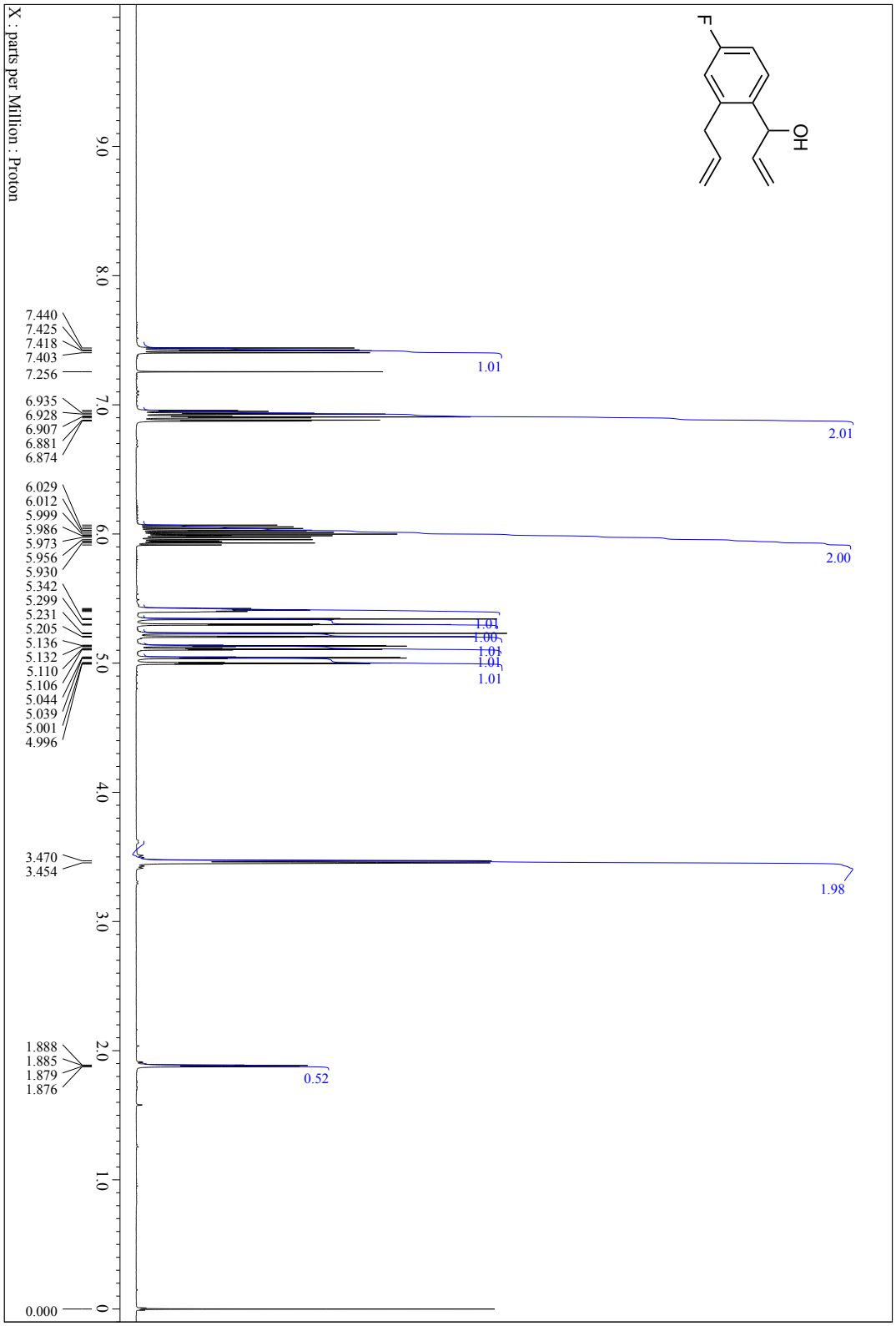

Fig. S118.

^{1}H NMR spectra of **S13**.

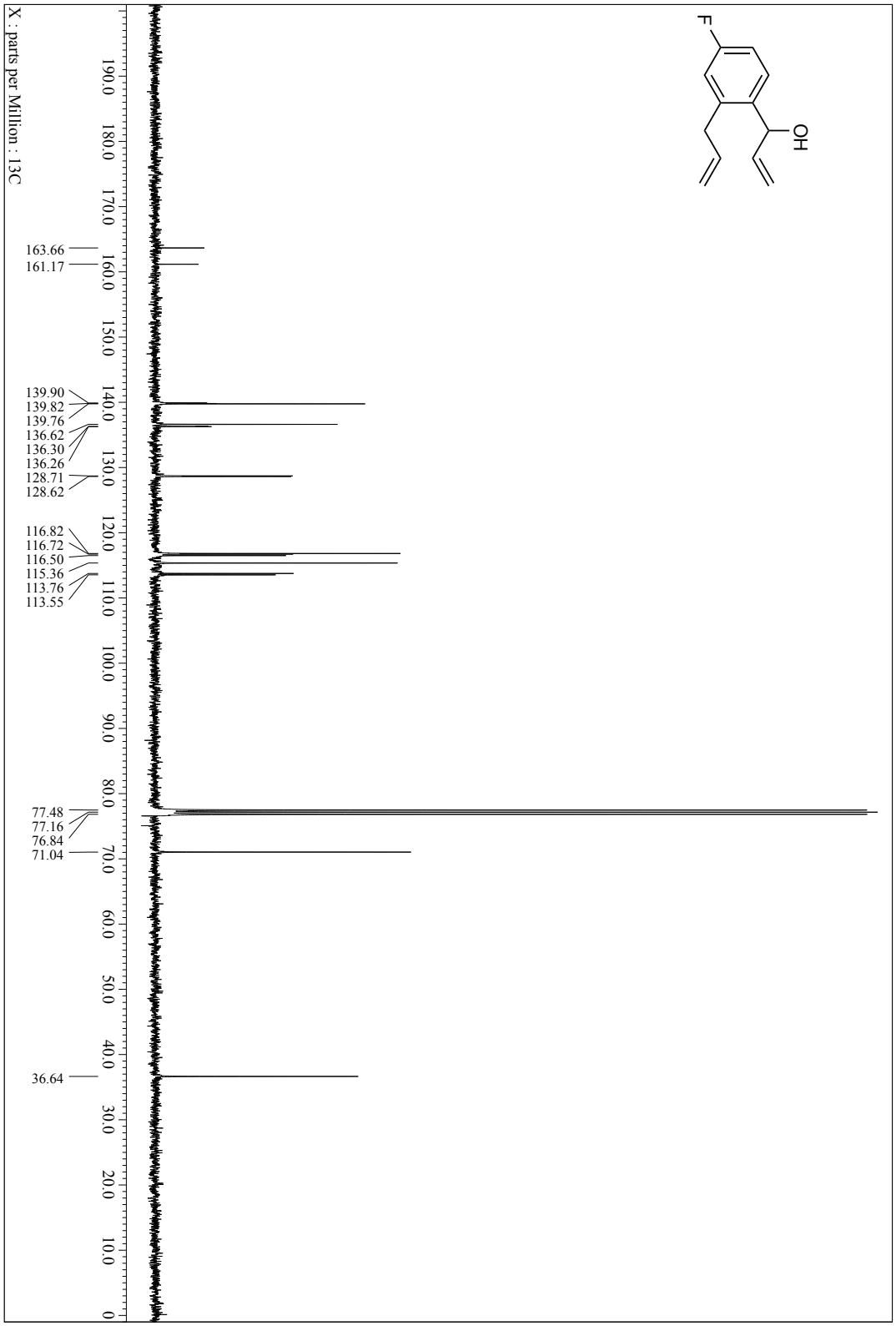

Fig. S119.

^{13}C NMR spectra of **S13**.

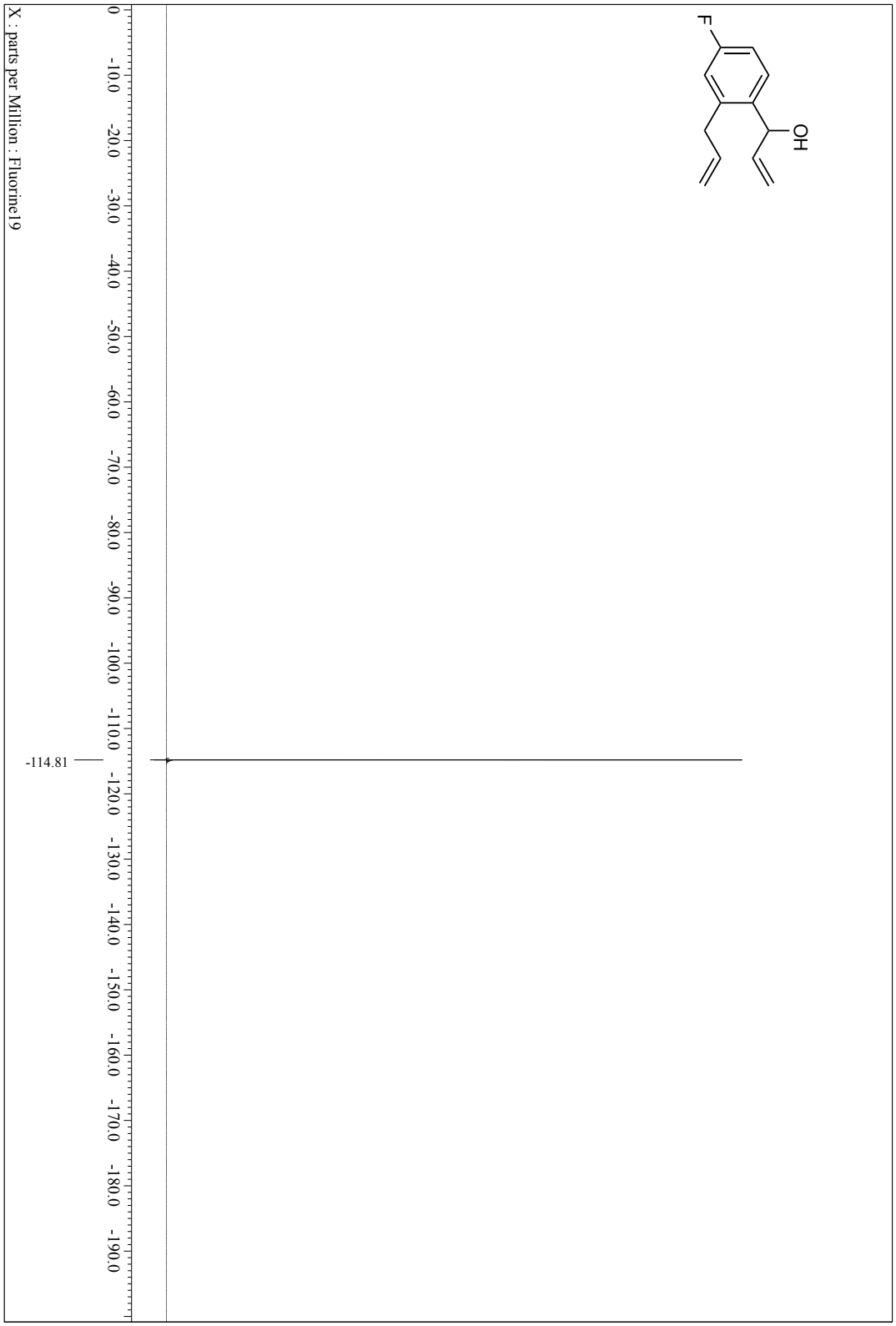

Fig. S120.

^{19}F NMR spectra of **S13**.

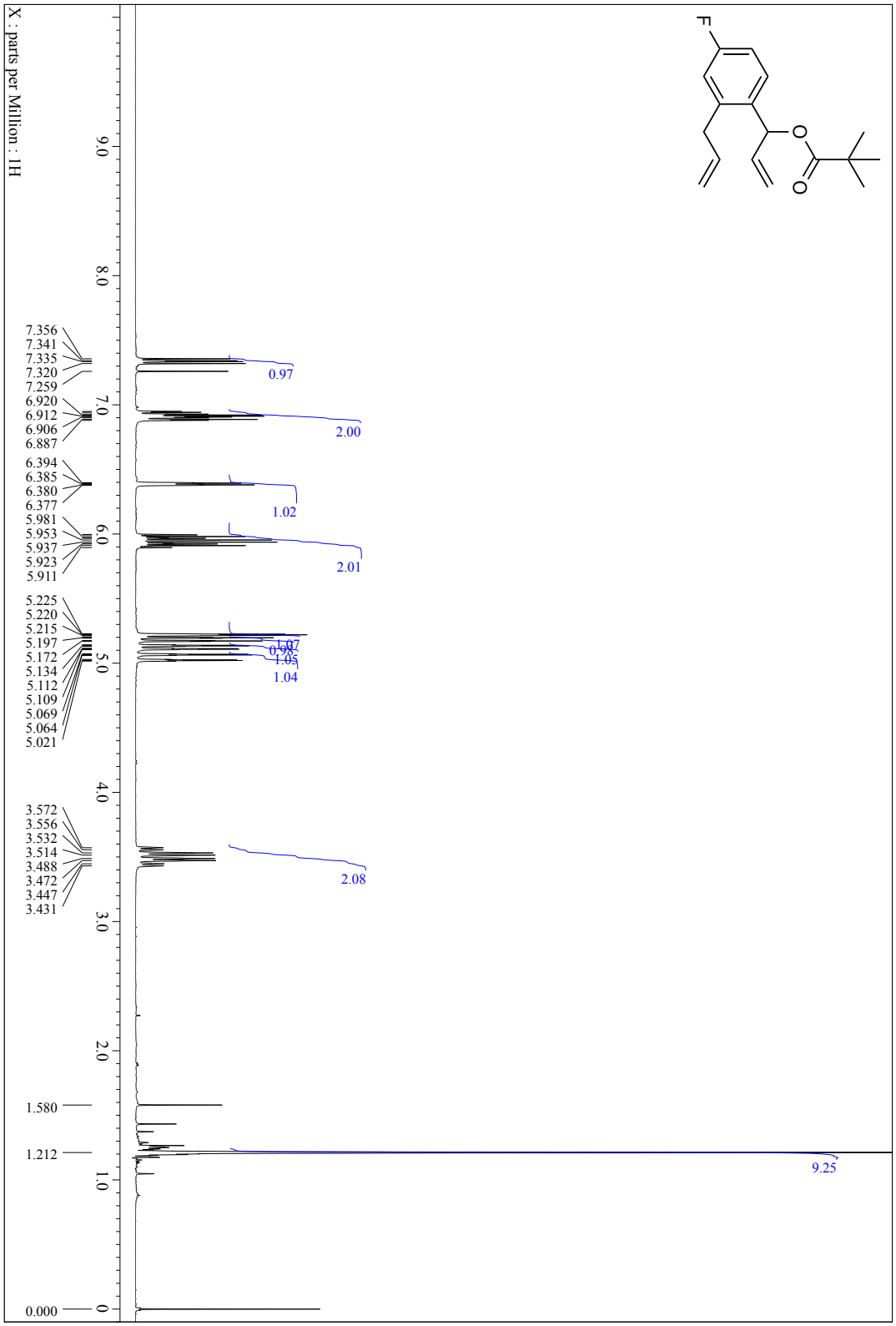

Fig. S121.

^{1}H NMR spectra of **28**.

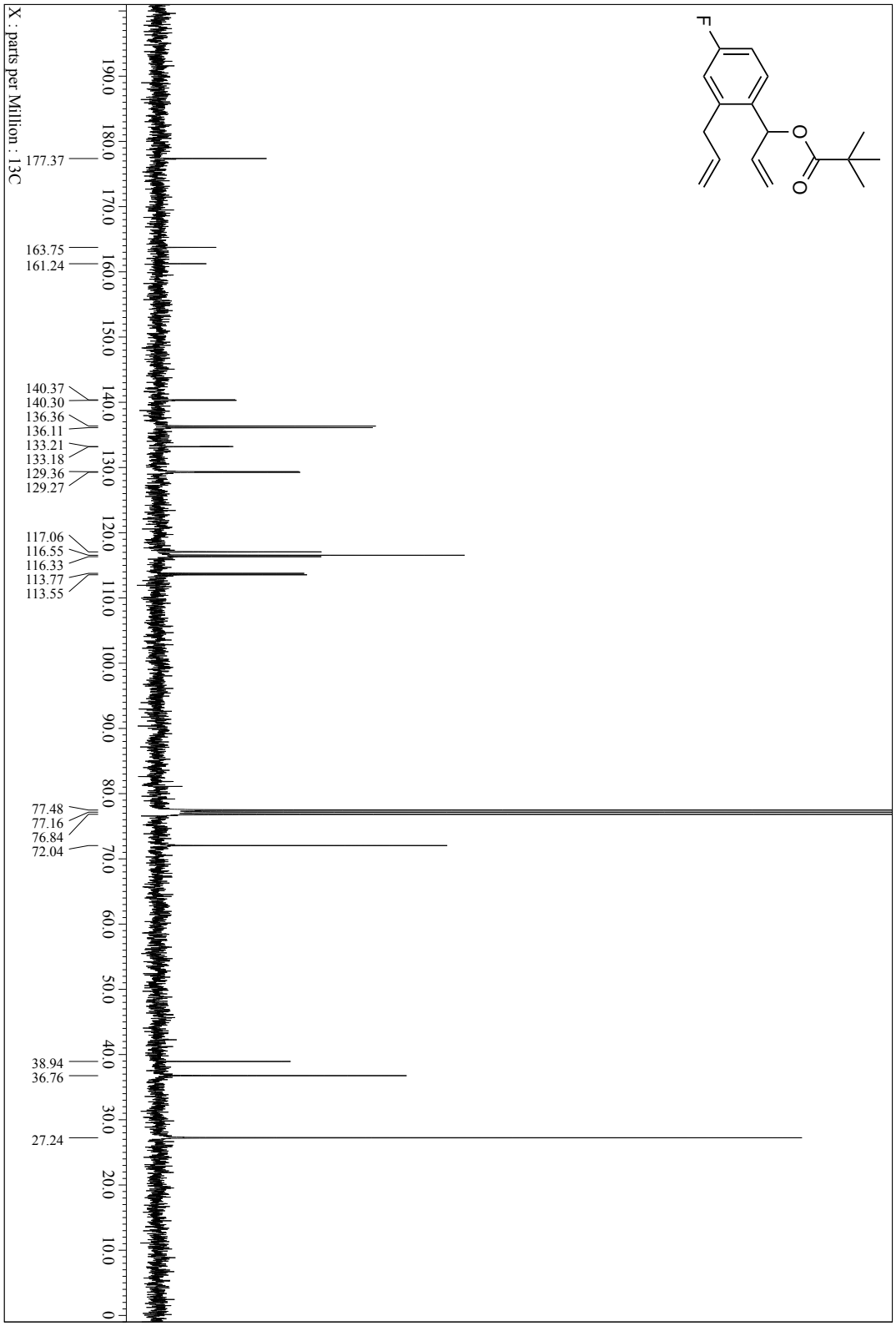

Fig. S122.

^{13}C NMR spectra of **28**.

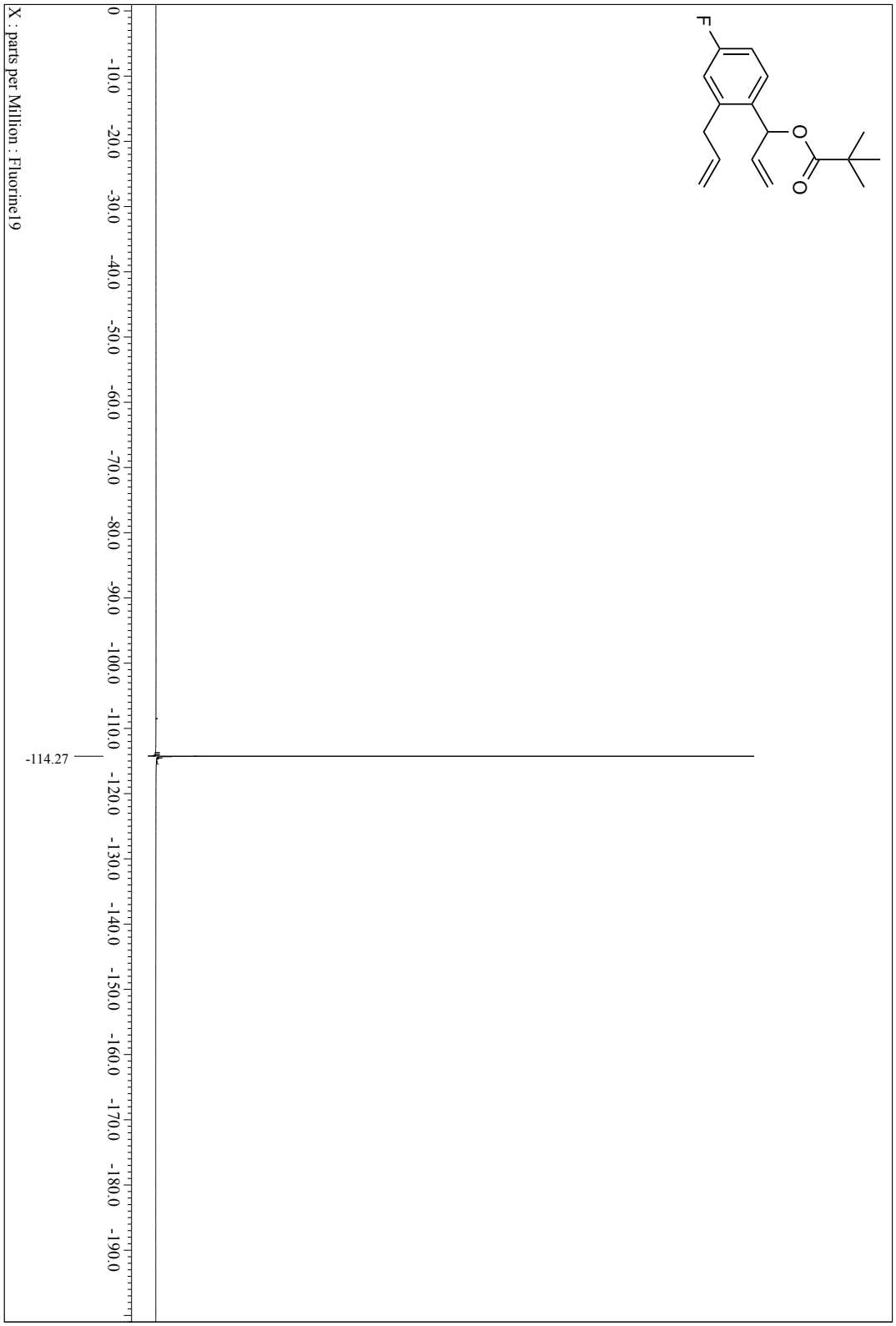

Fig. S123.

^{19}F NMR spectra of **28**.

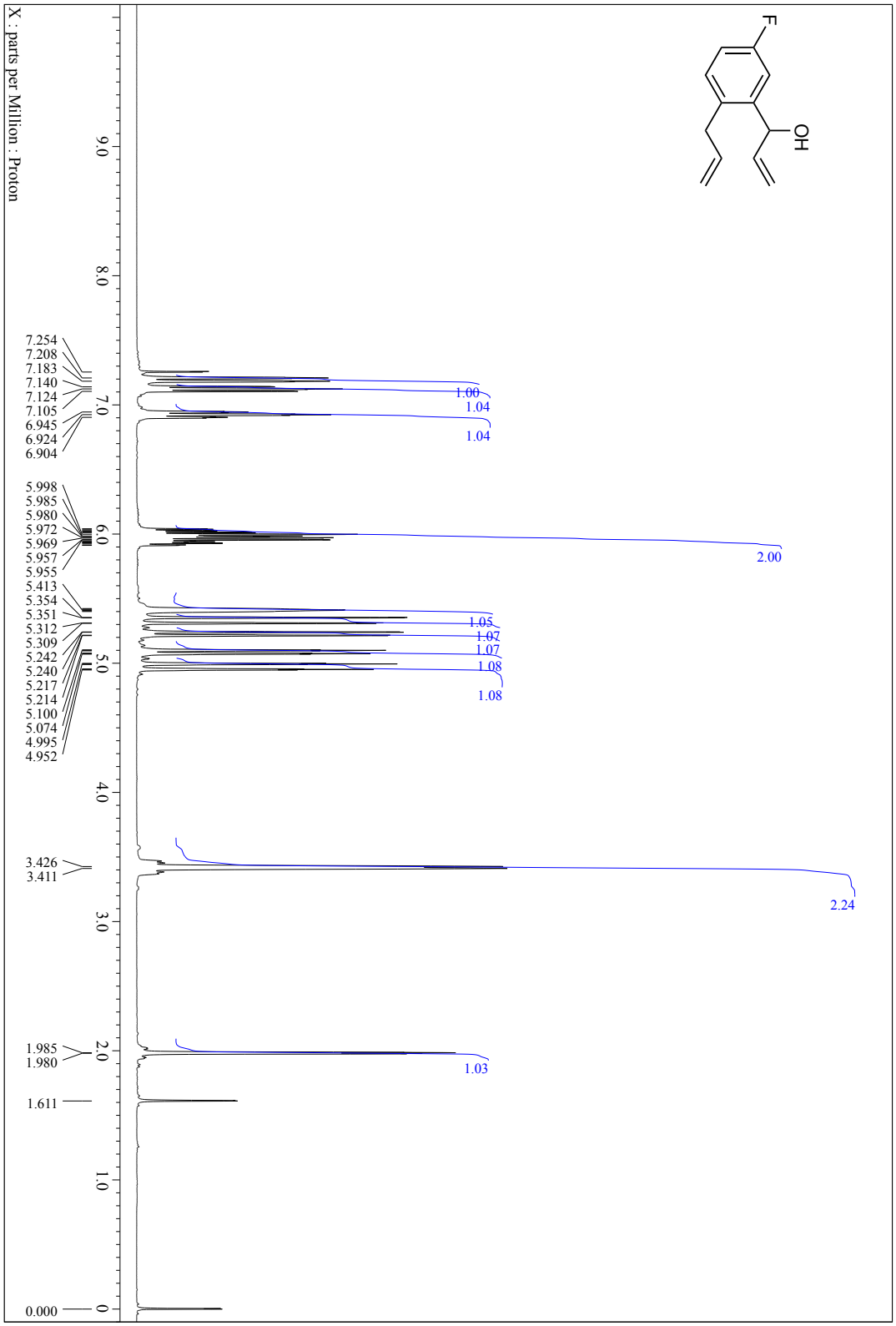

Fig. S124.

^{1}H NMR spectra of **S15**.

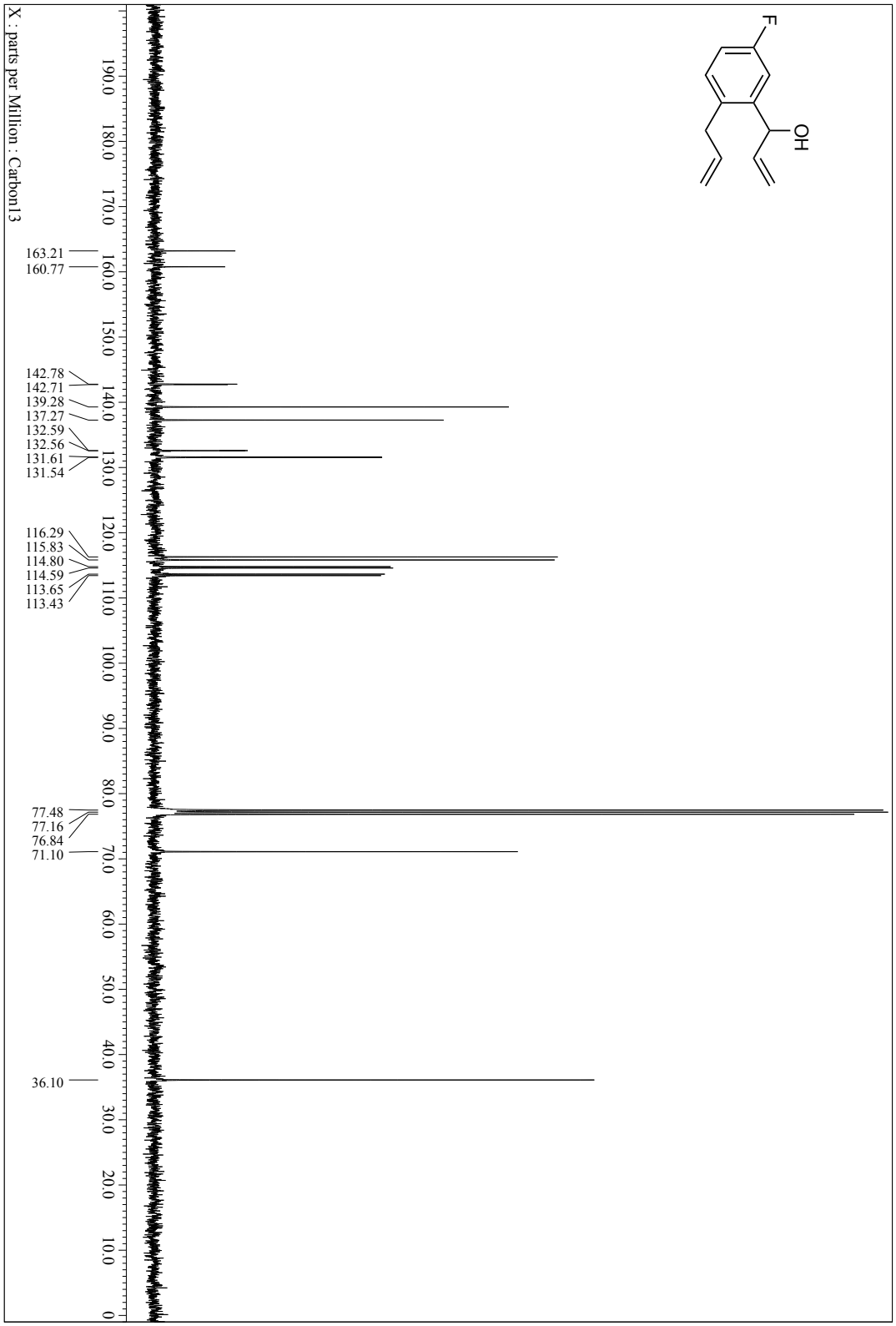

Fig. S125.

^{13}C NMR spectra of **S15**.

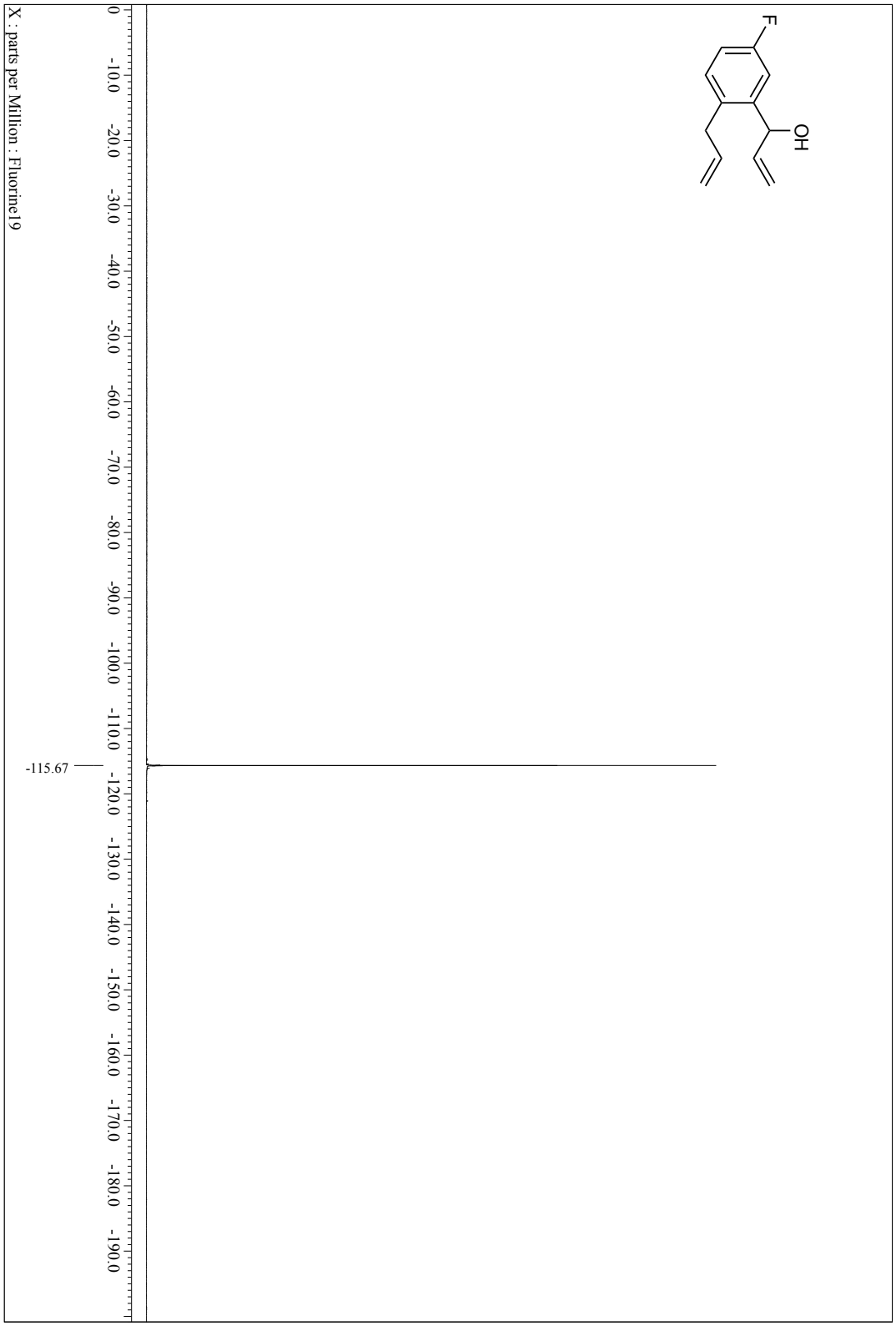

Fig. S126.

^{19}F NMR spectra of **S15**.

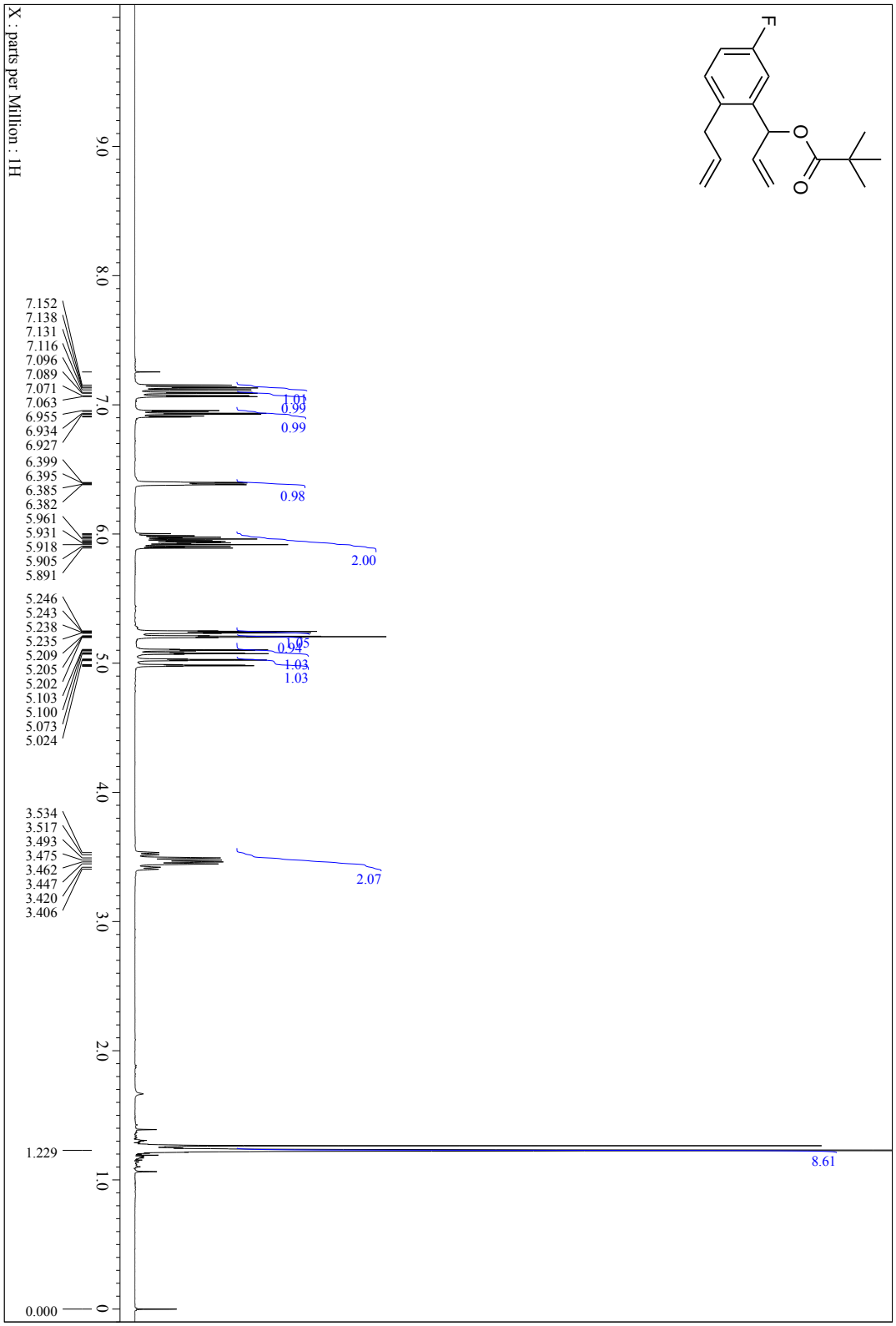

Fig. S127.

^{1}H NMR spectra of **29**.

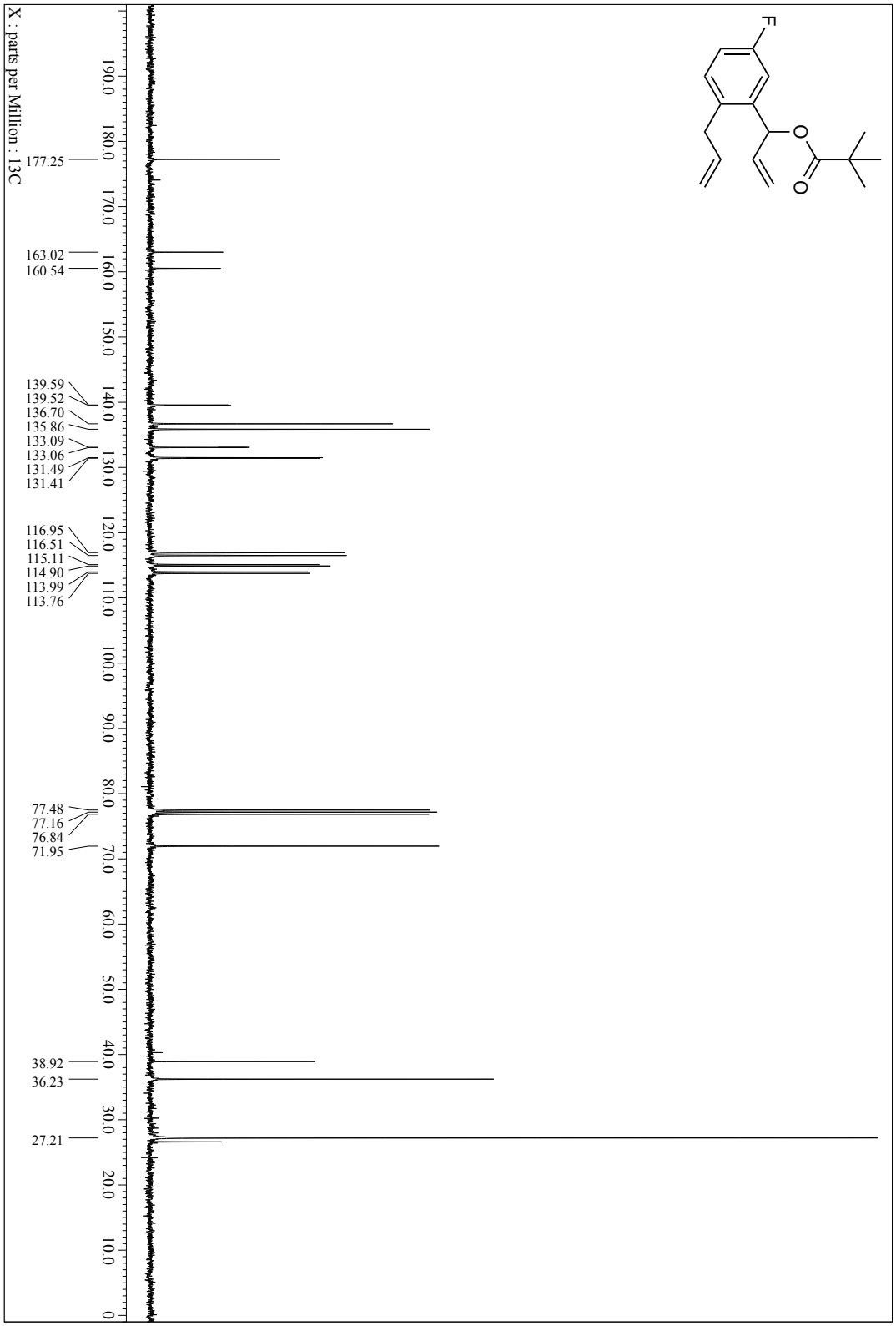

Fig. S128.

^{13}C NMR spectra of **29**.

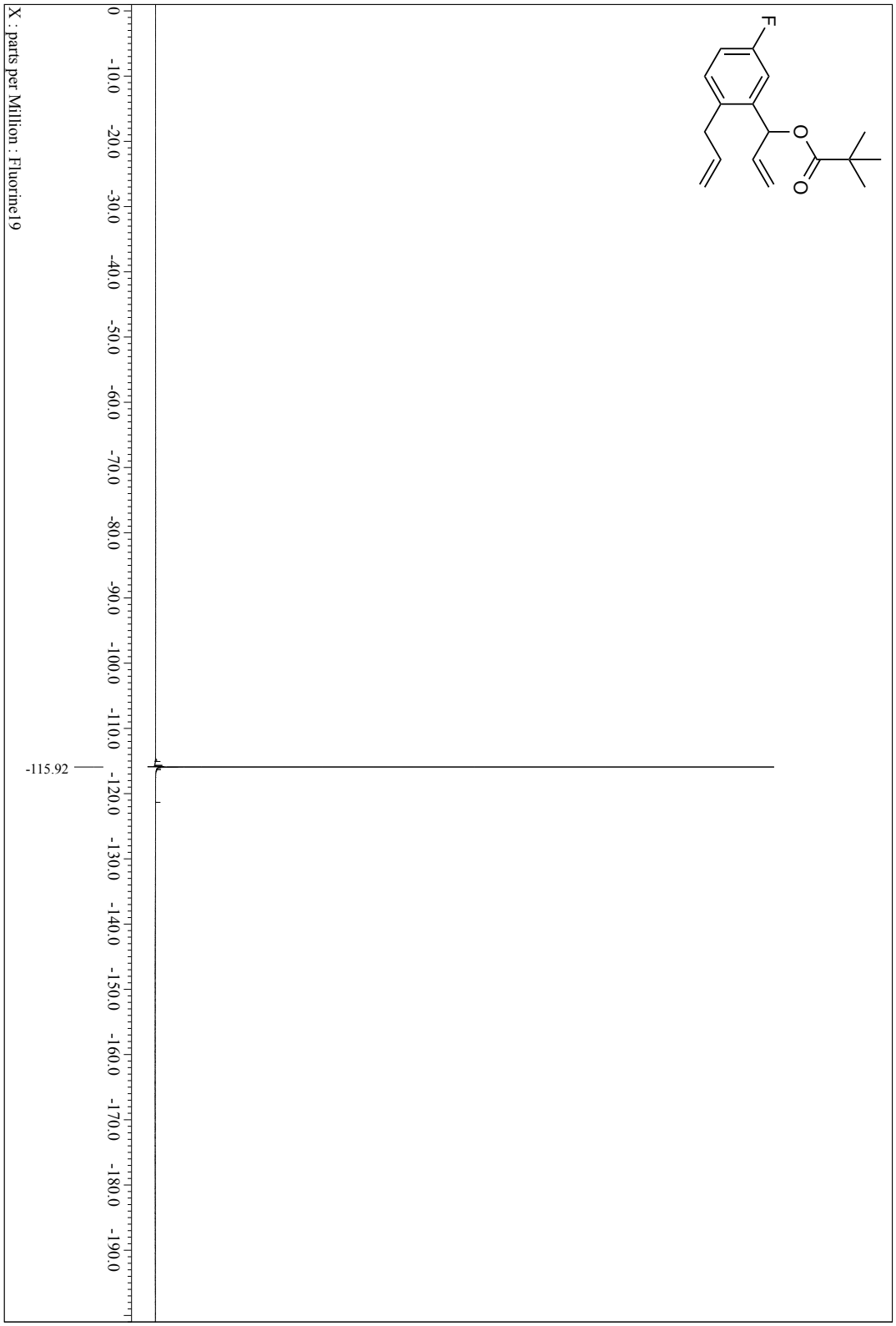

Fig. S129.

^{19}F NMR spectra of **29**.

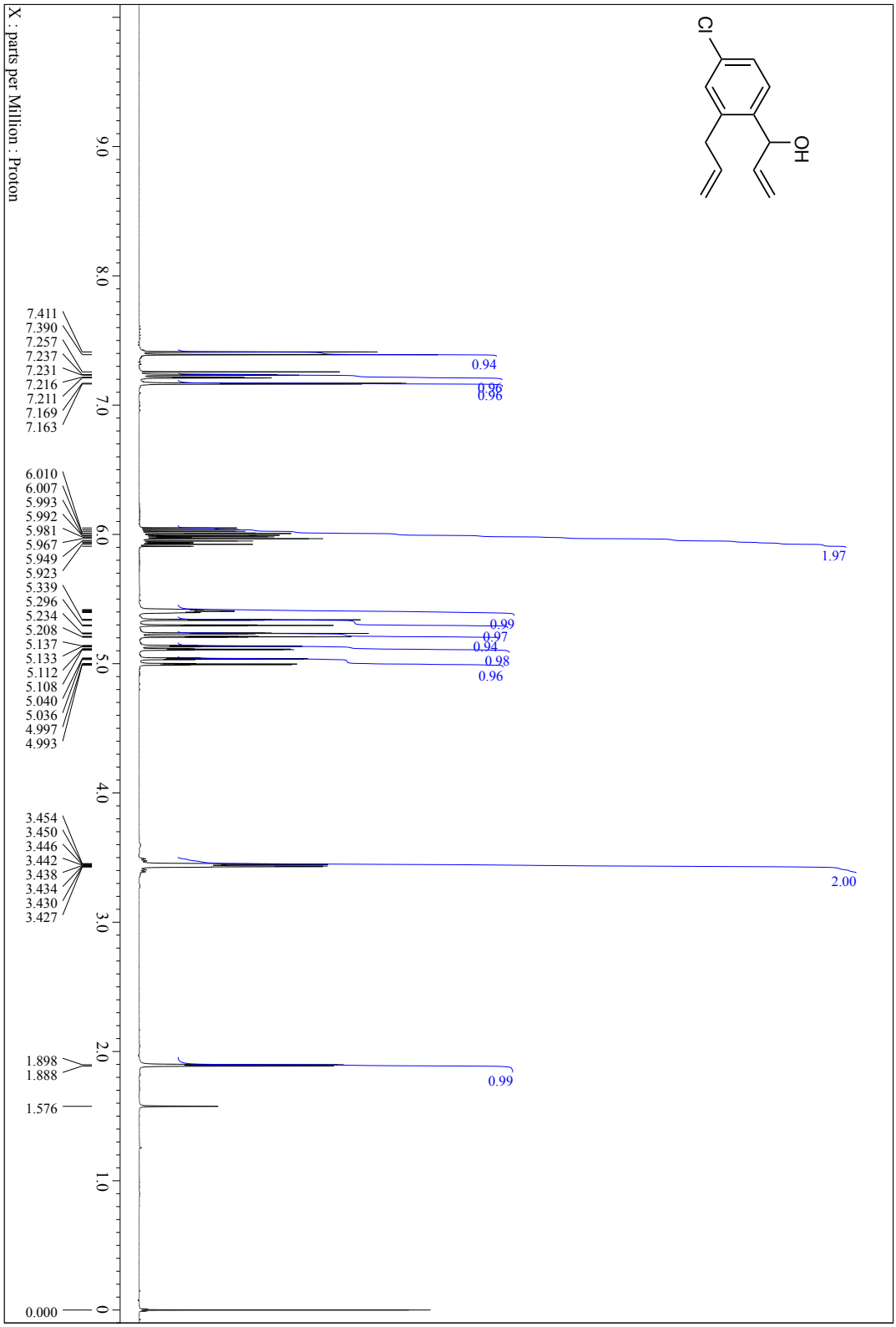

Fig. S130.

^{1}H NMR spectra of **S17**.

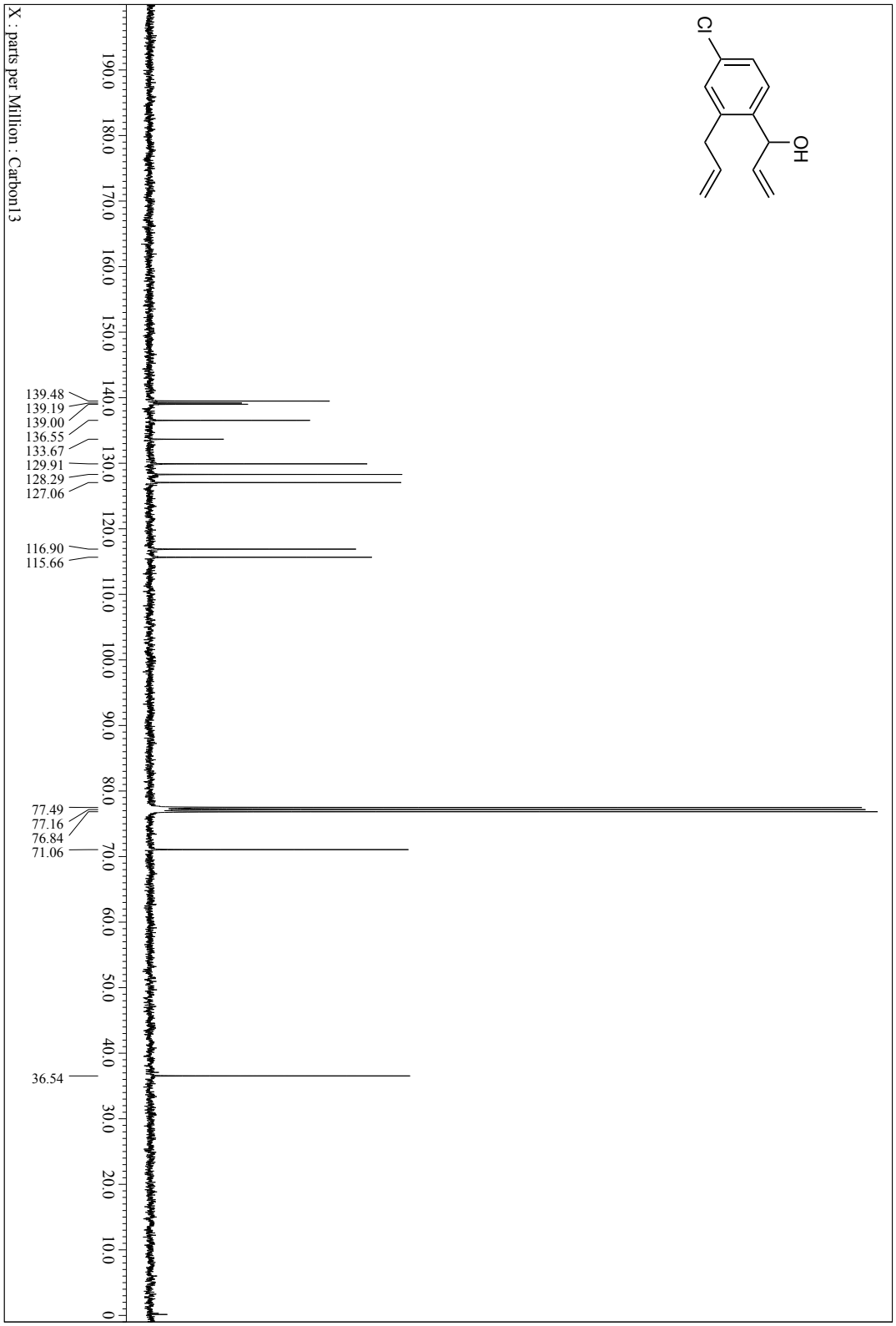

Fig. S131.

^{13}C NMR spectra of **S17**.

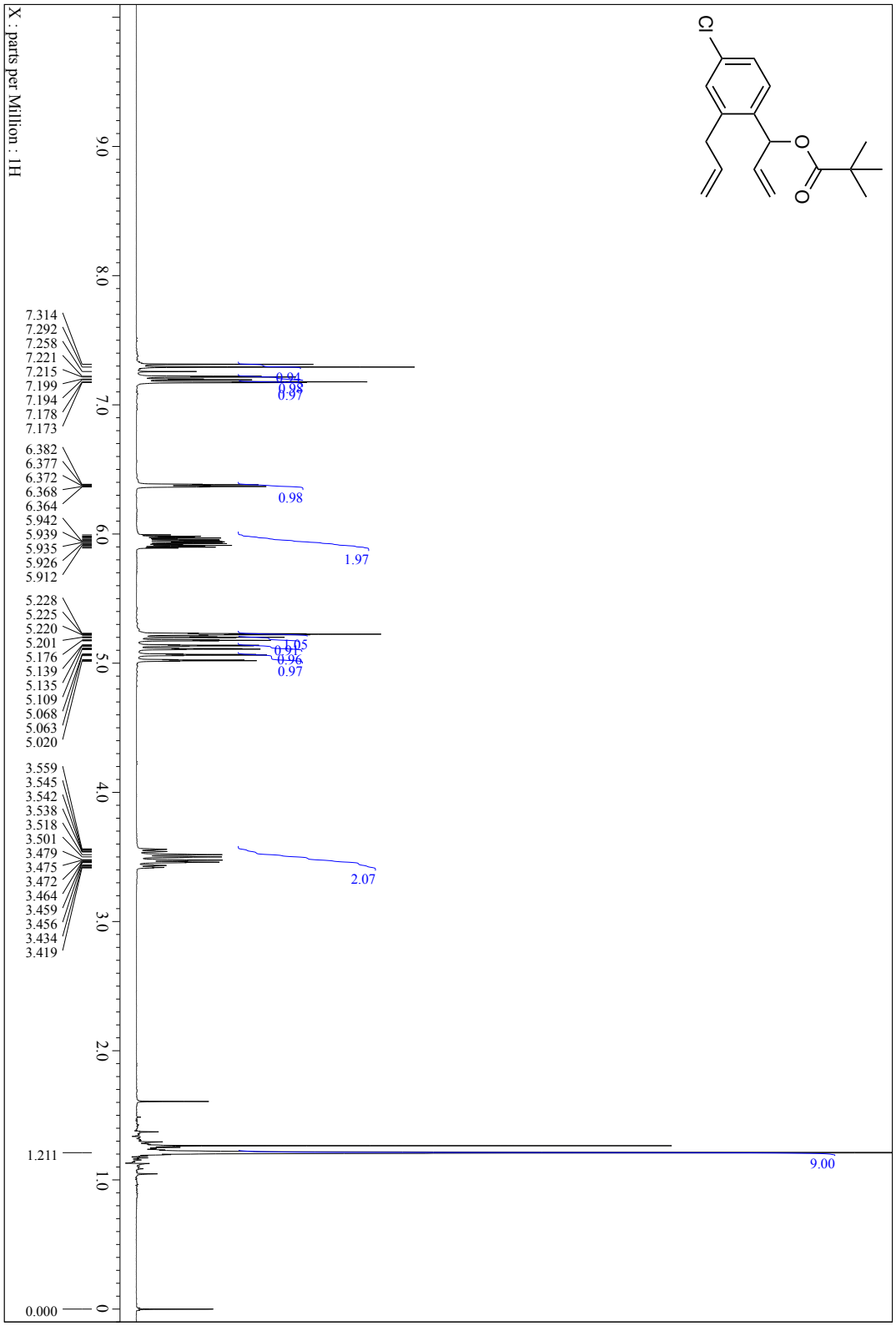

Fig. S132.

^{1}H NMR spectra of **30**.

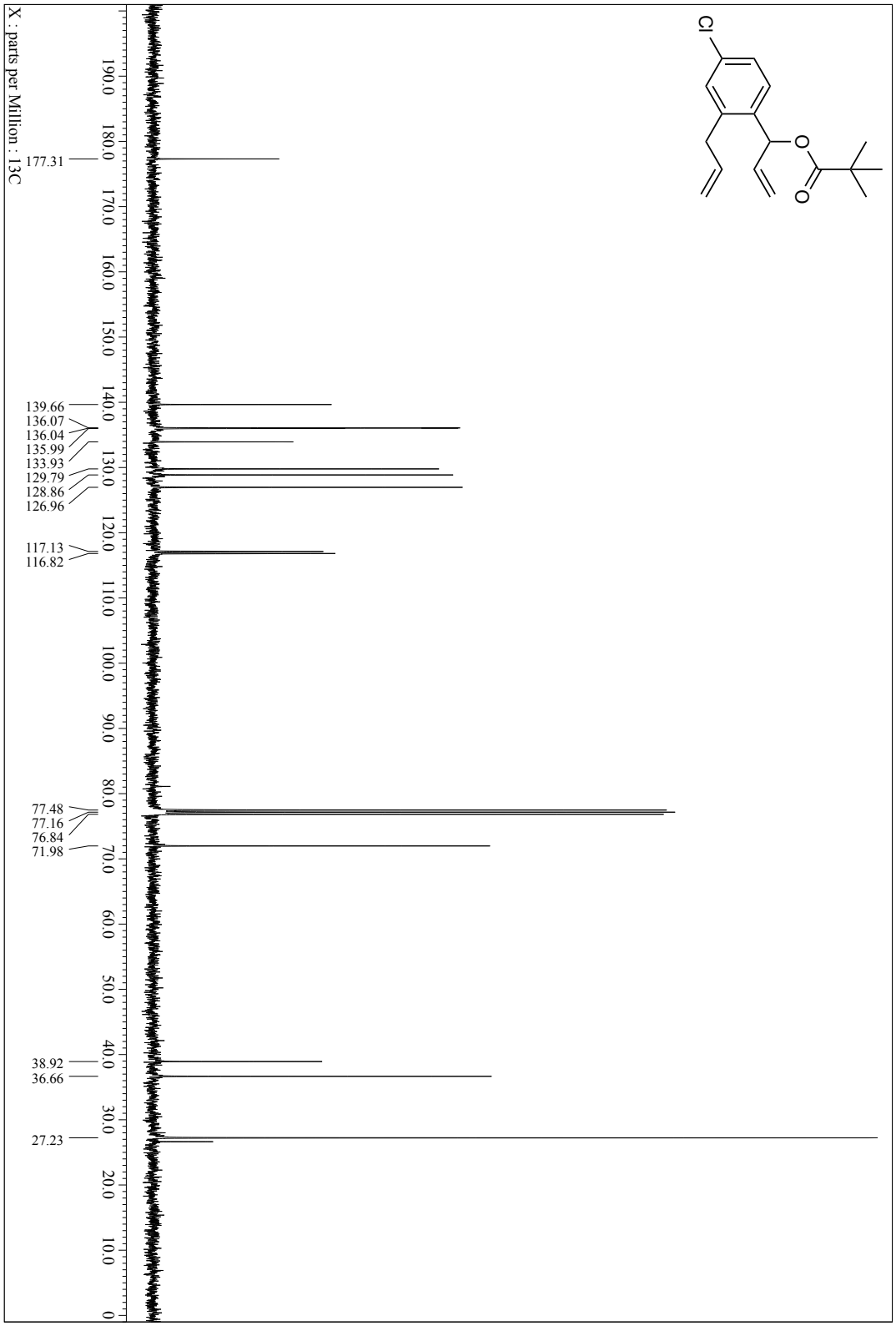

Fig. S133.

^{13}C NMR spectra of **30**.

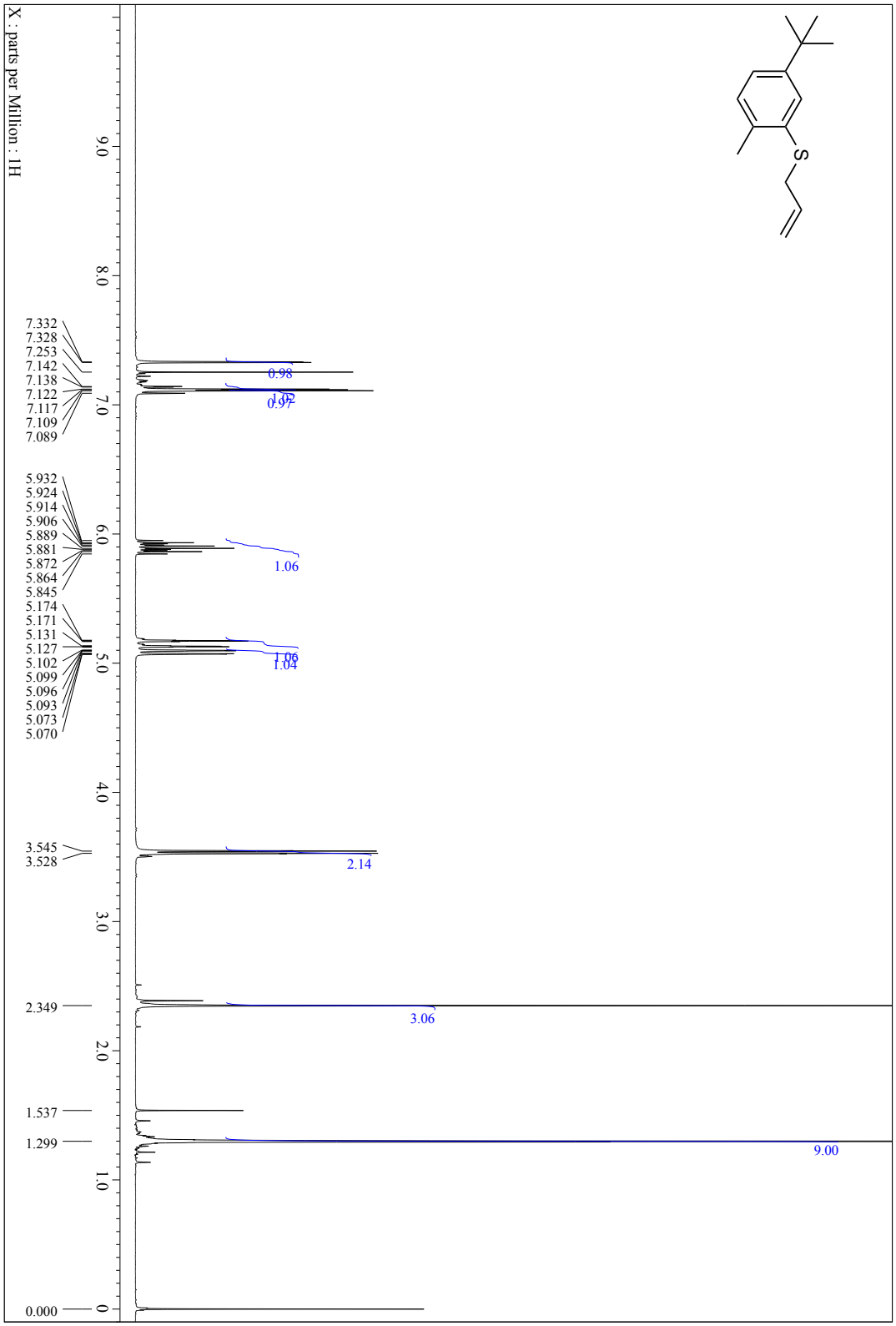

Fig. S134.

^{1}H NMR spectra of **33**.

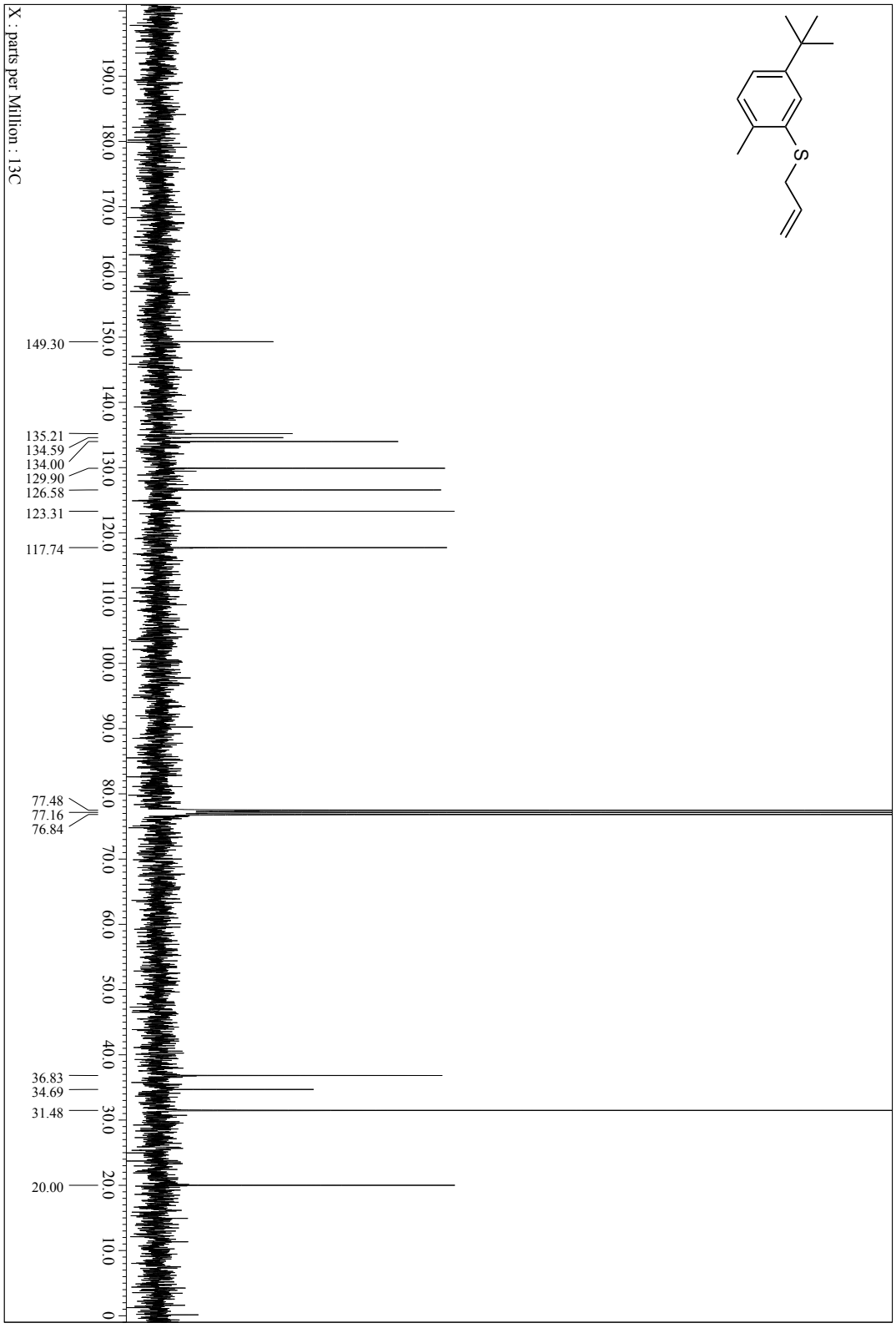

Fig. S135.

^{13}C NMR spectra of **33**.

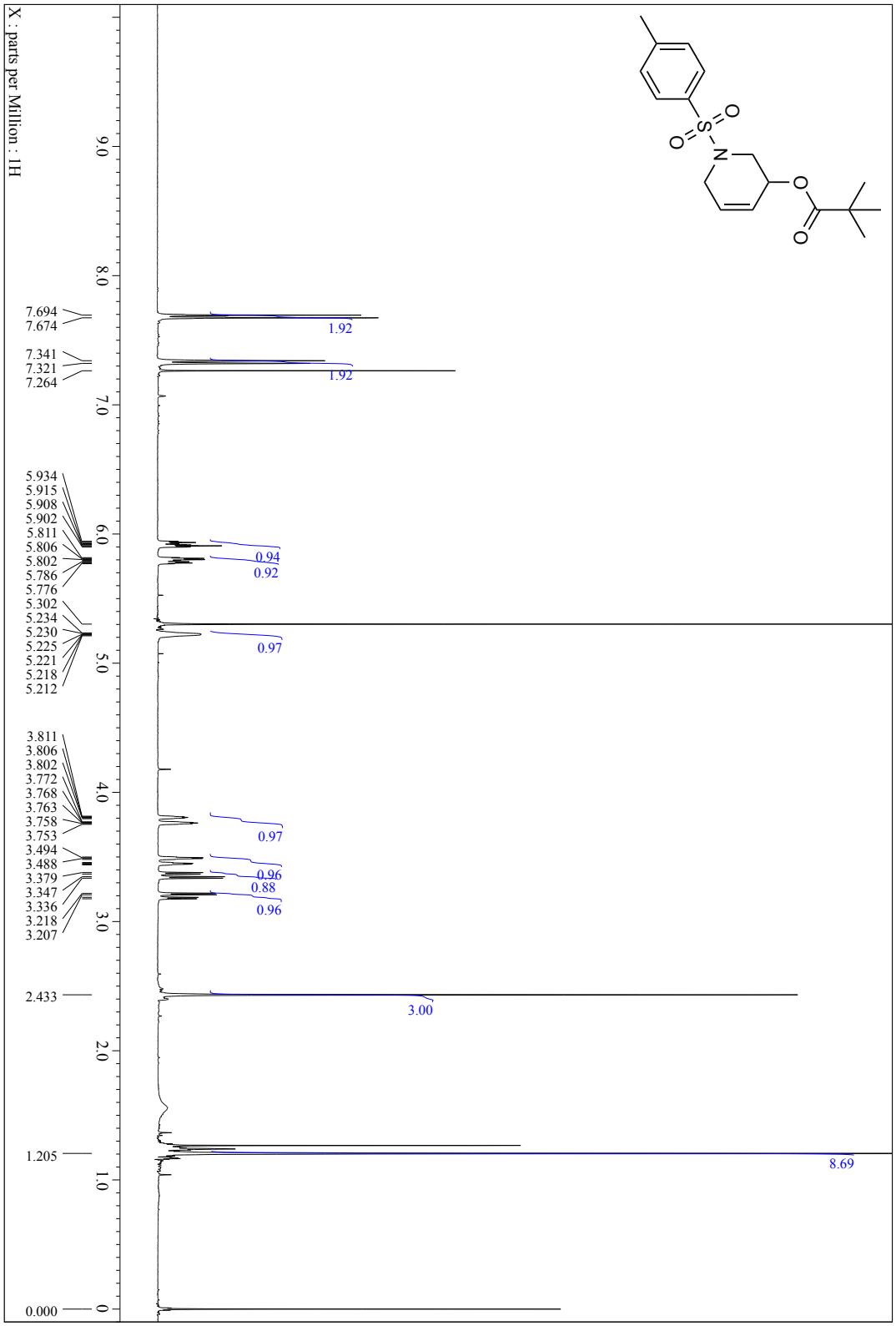

Fig. S136.

^{1}H NMR spectra of **S28**.

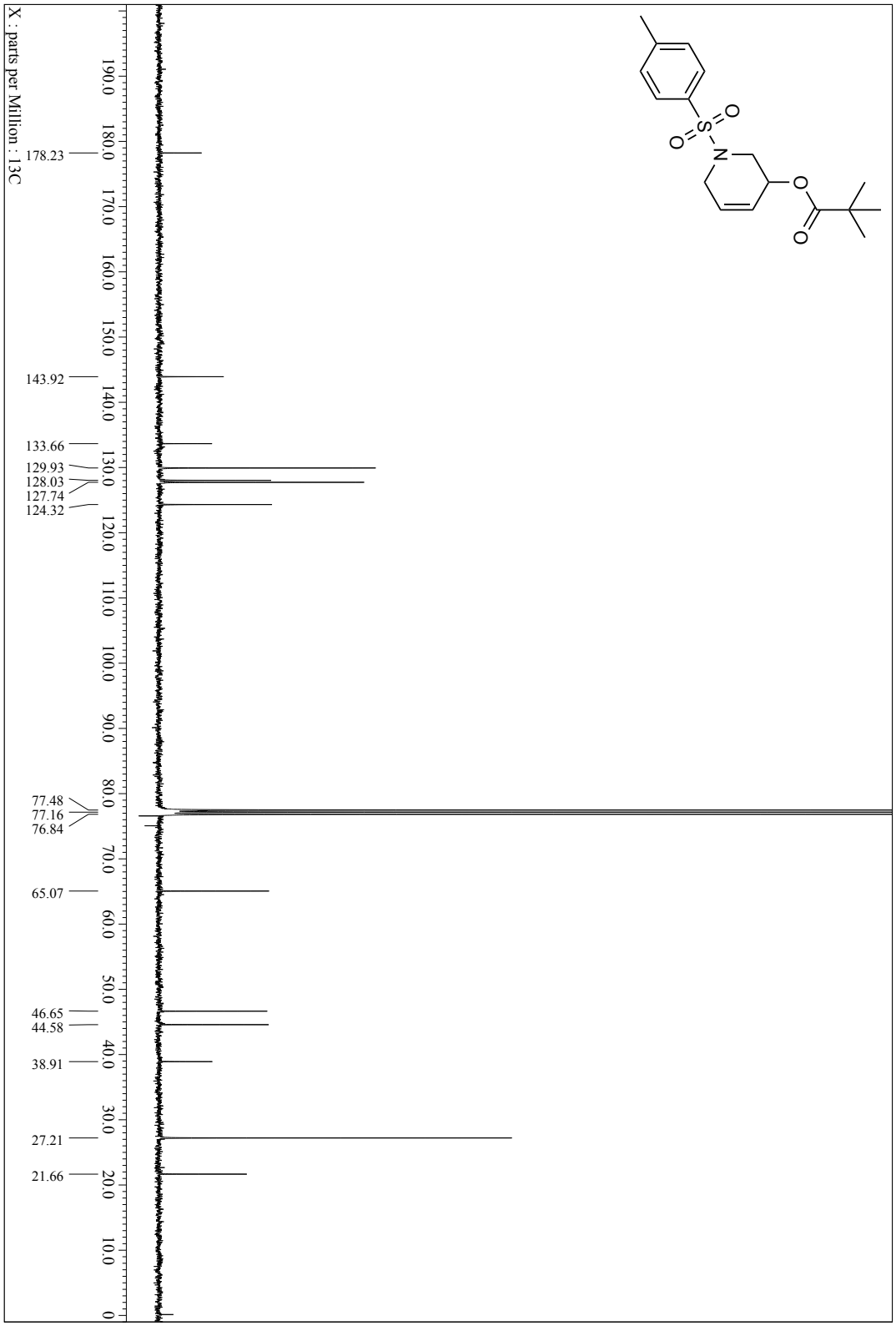

Fig. S137.

^{13}C NMR spectra of **S28**.

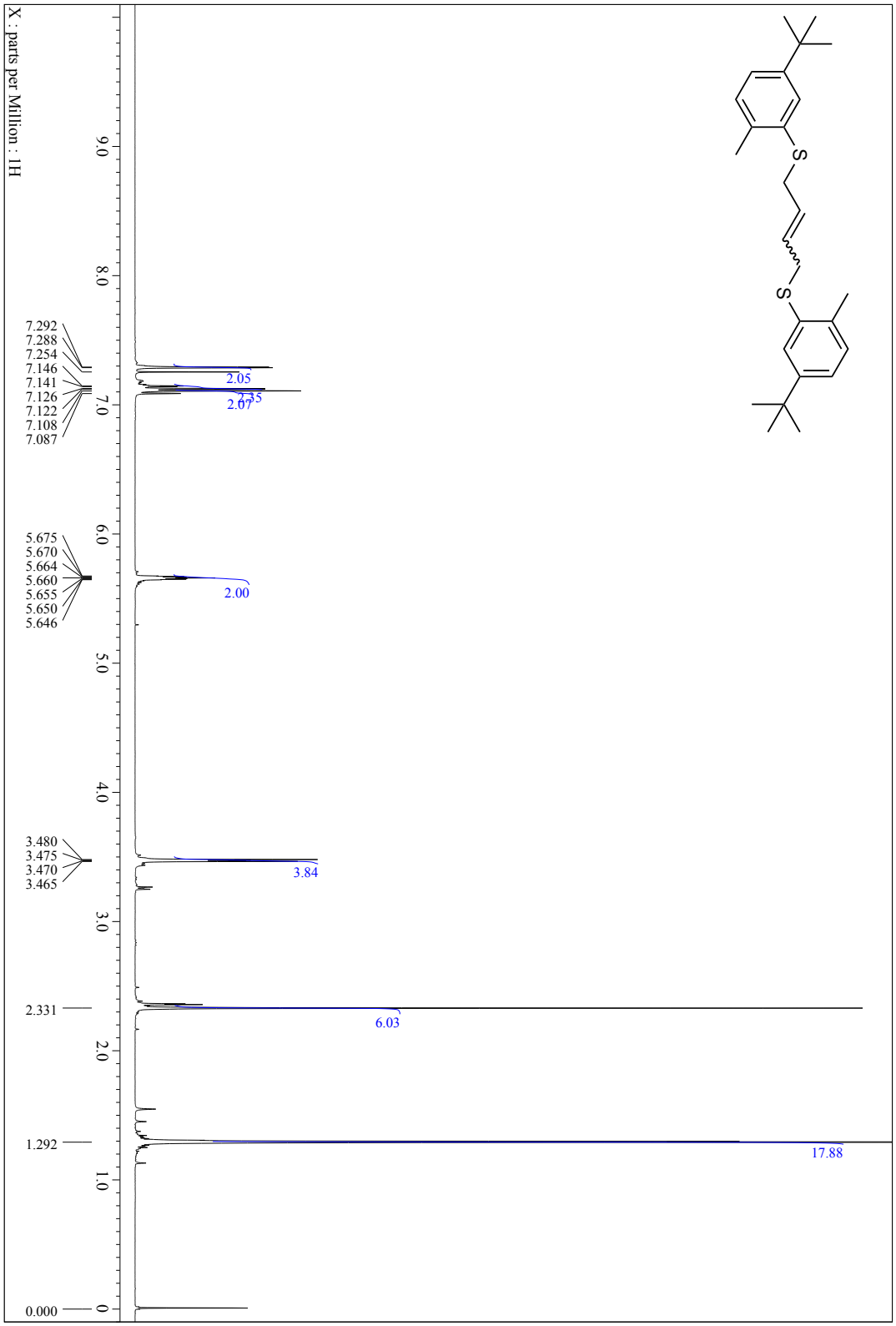

Fig. S138.

^{1}H NMR spectra of **S48**.

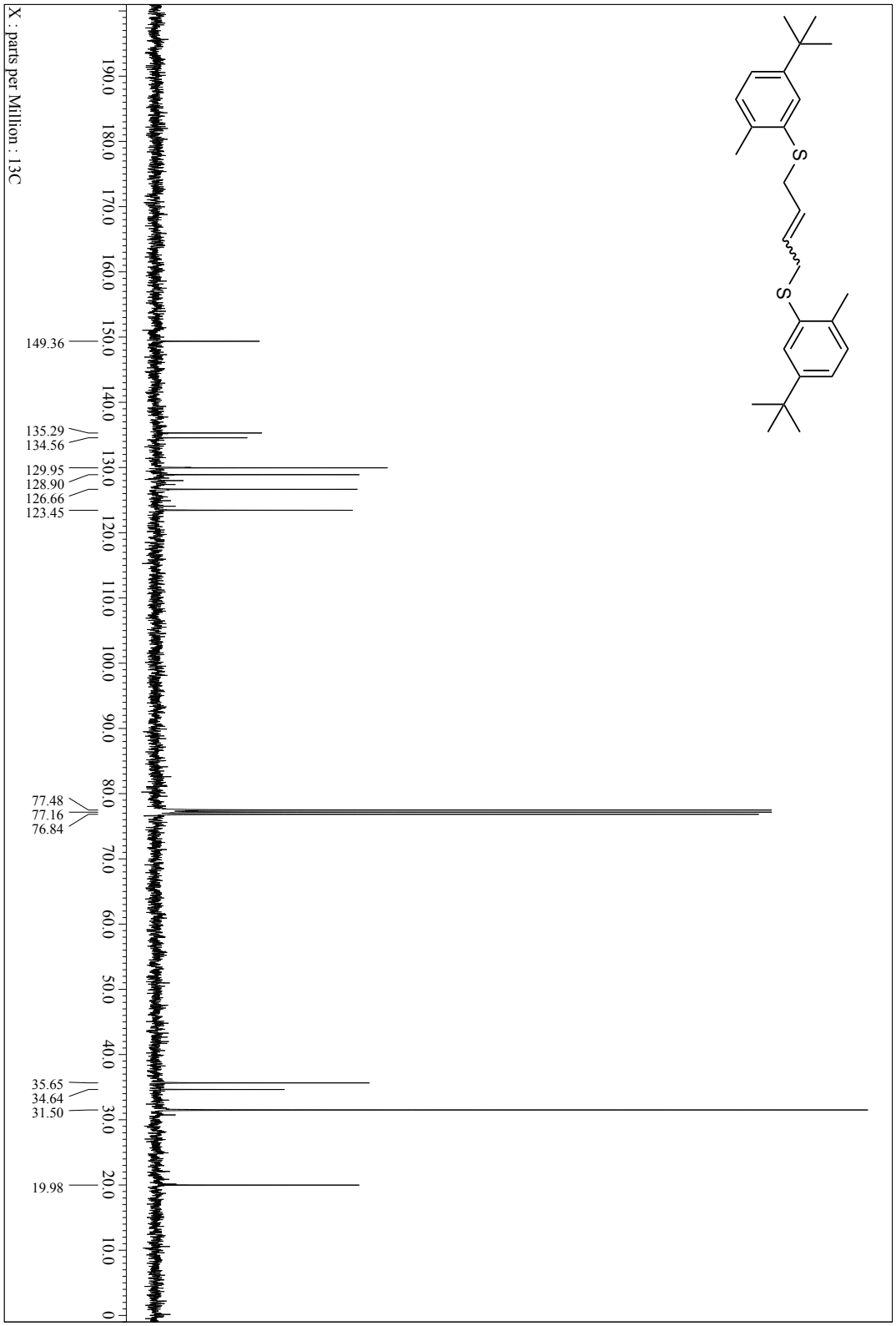

Fig. S139.

^{13}C NMR spectra of **S48**.

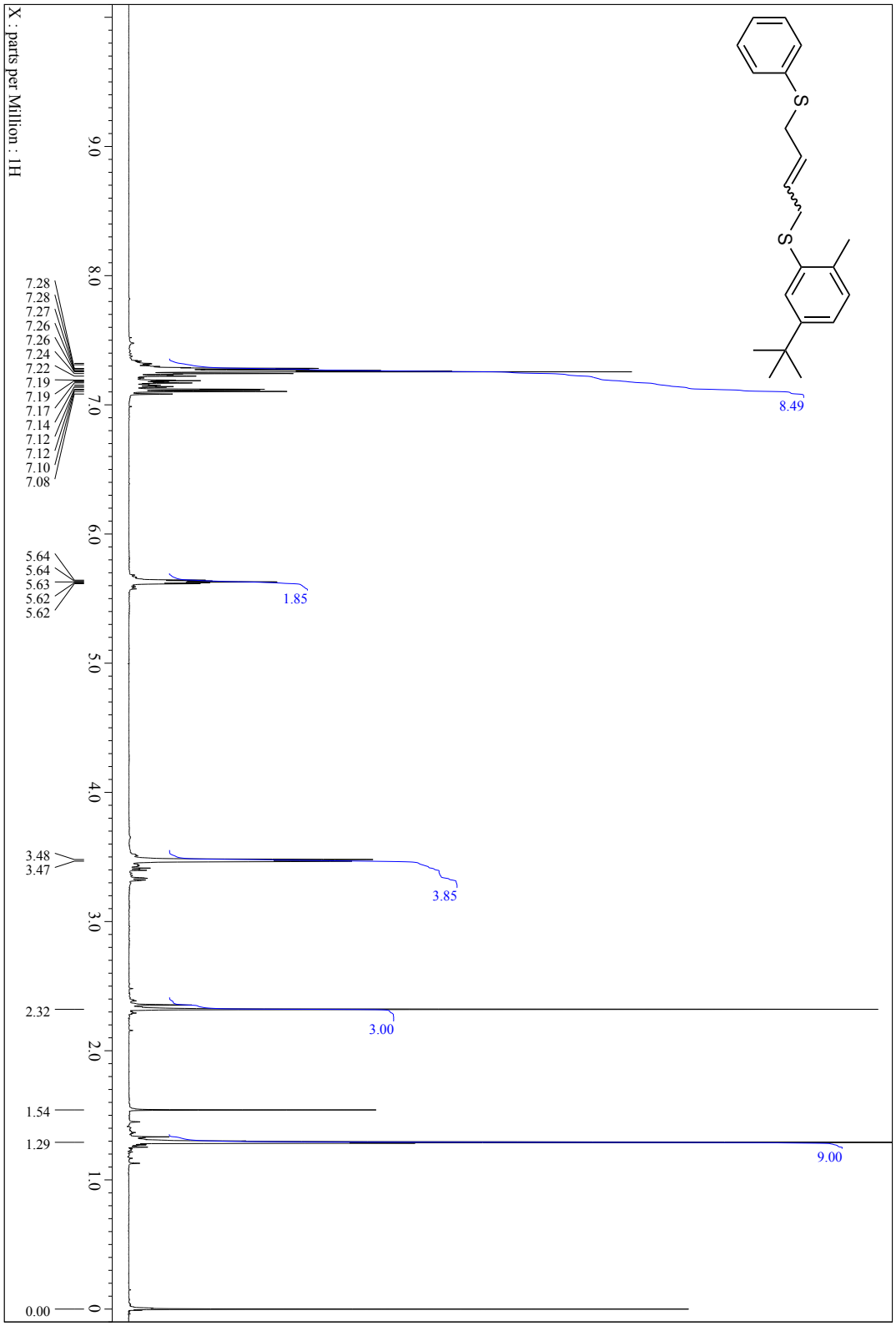

Fig. S140.

^{1}H NMR spectra of **S50**.

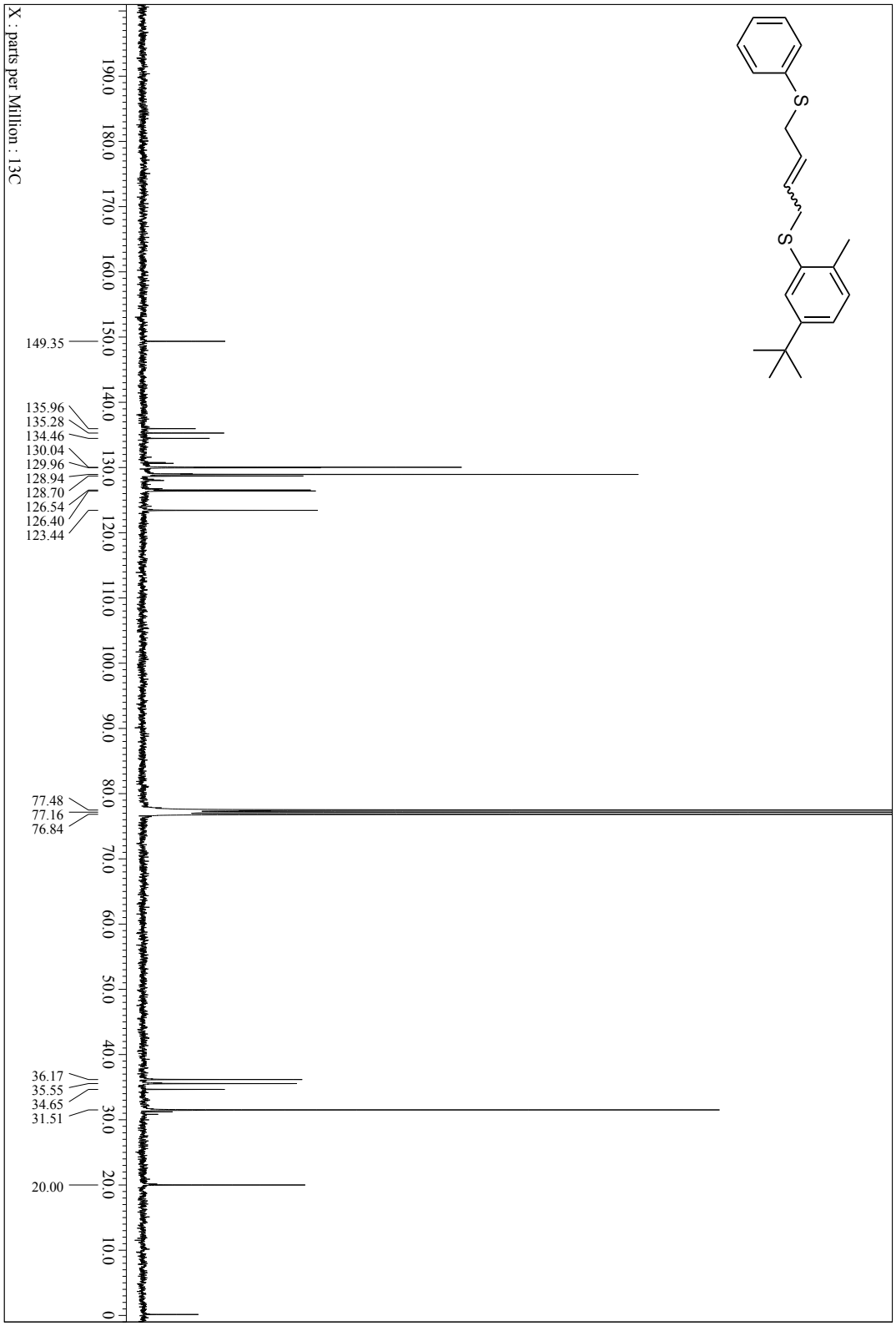

Fig. S141.

^{13}C NMR spectra of **S50**.

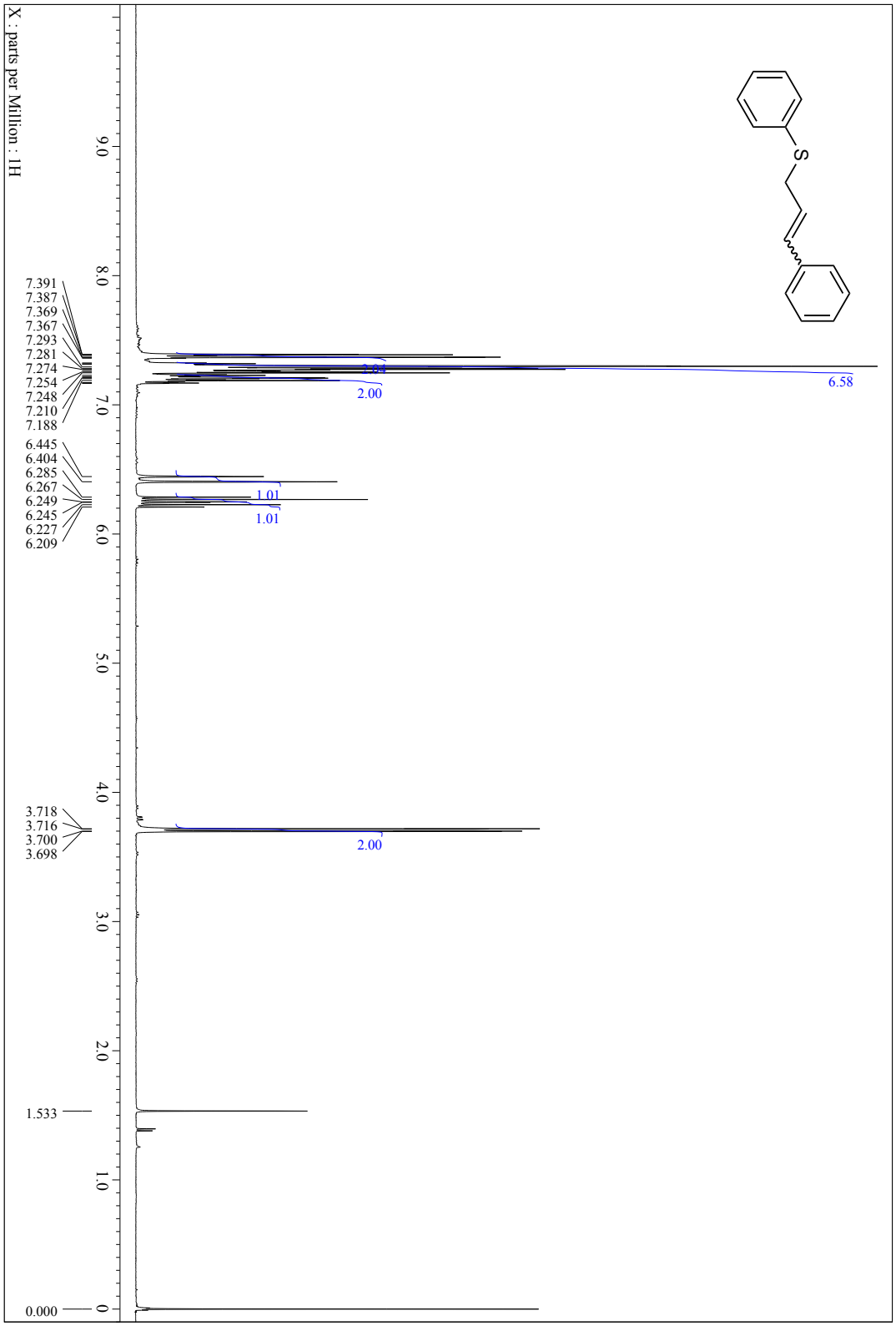

Fig. S142.

^{1}H NMR spectra of **S51**.

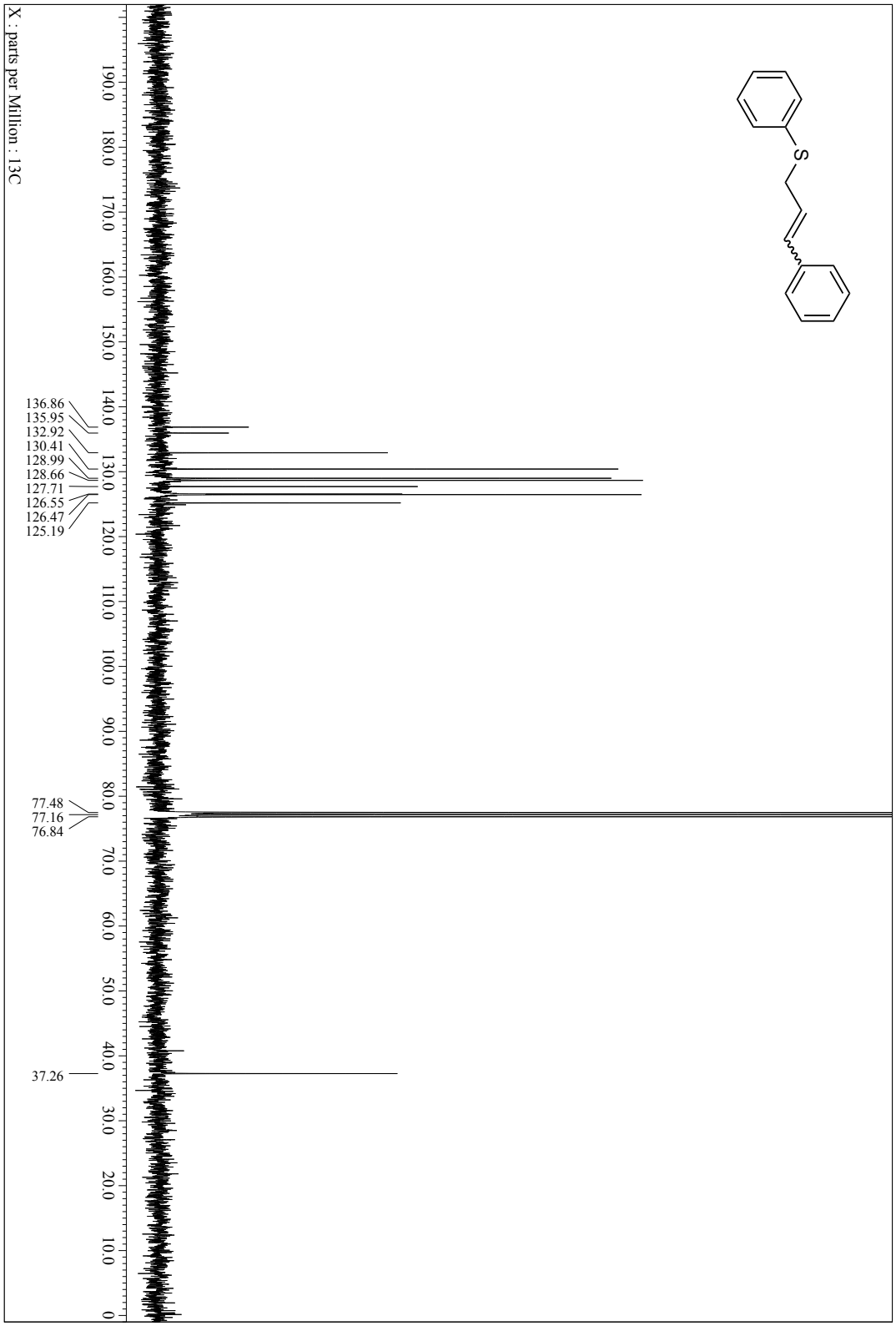

Fig. S143.

^{13}C NMR spectra of **S51**.

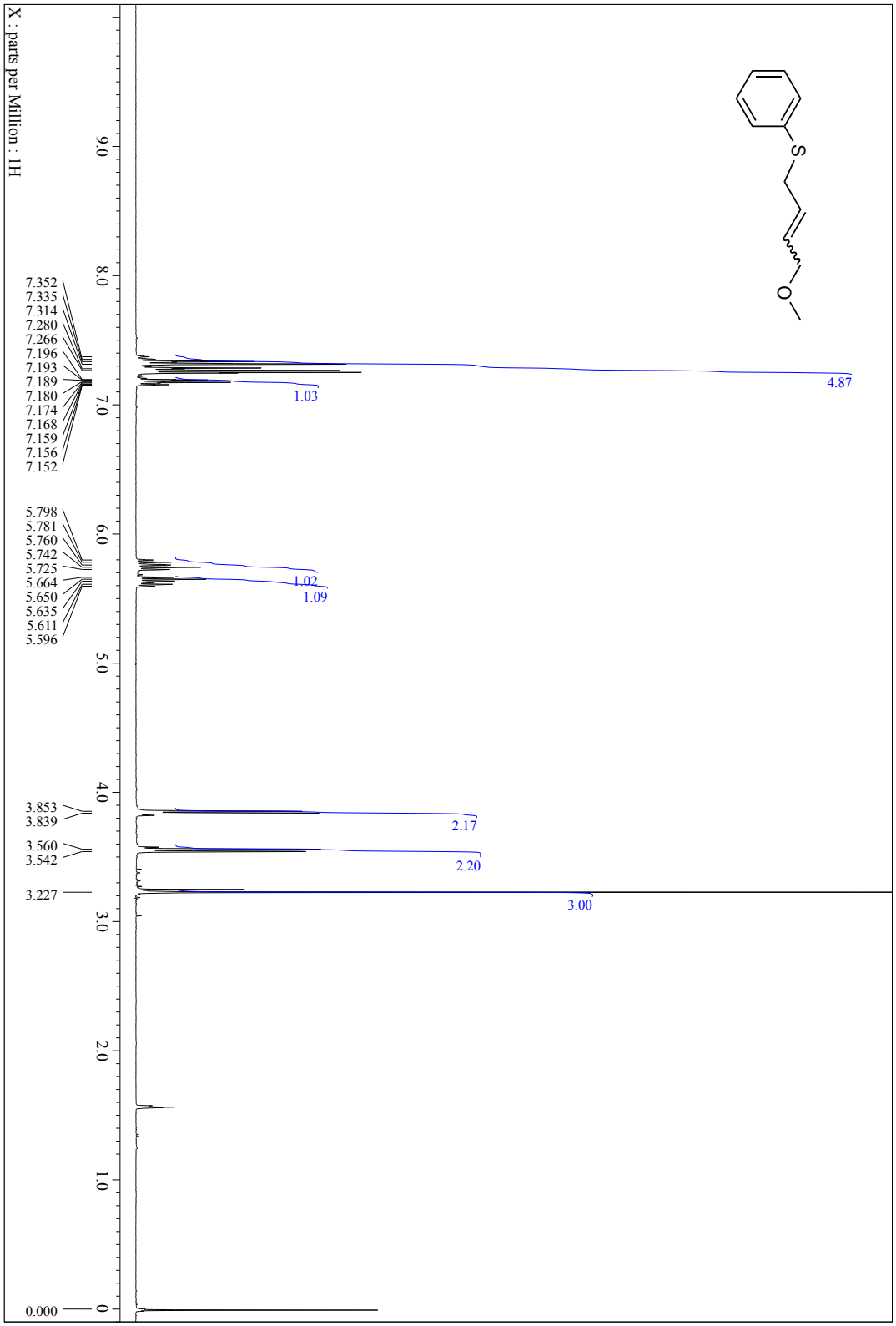

Fig. S144.

^{1}H NMR spectra of **S52**.

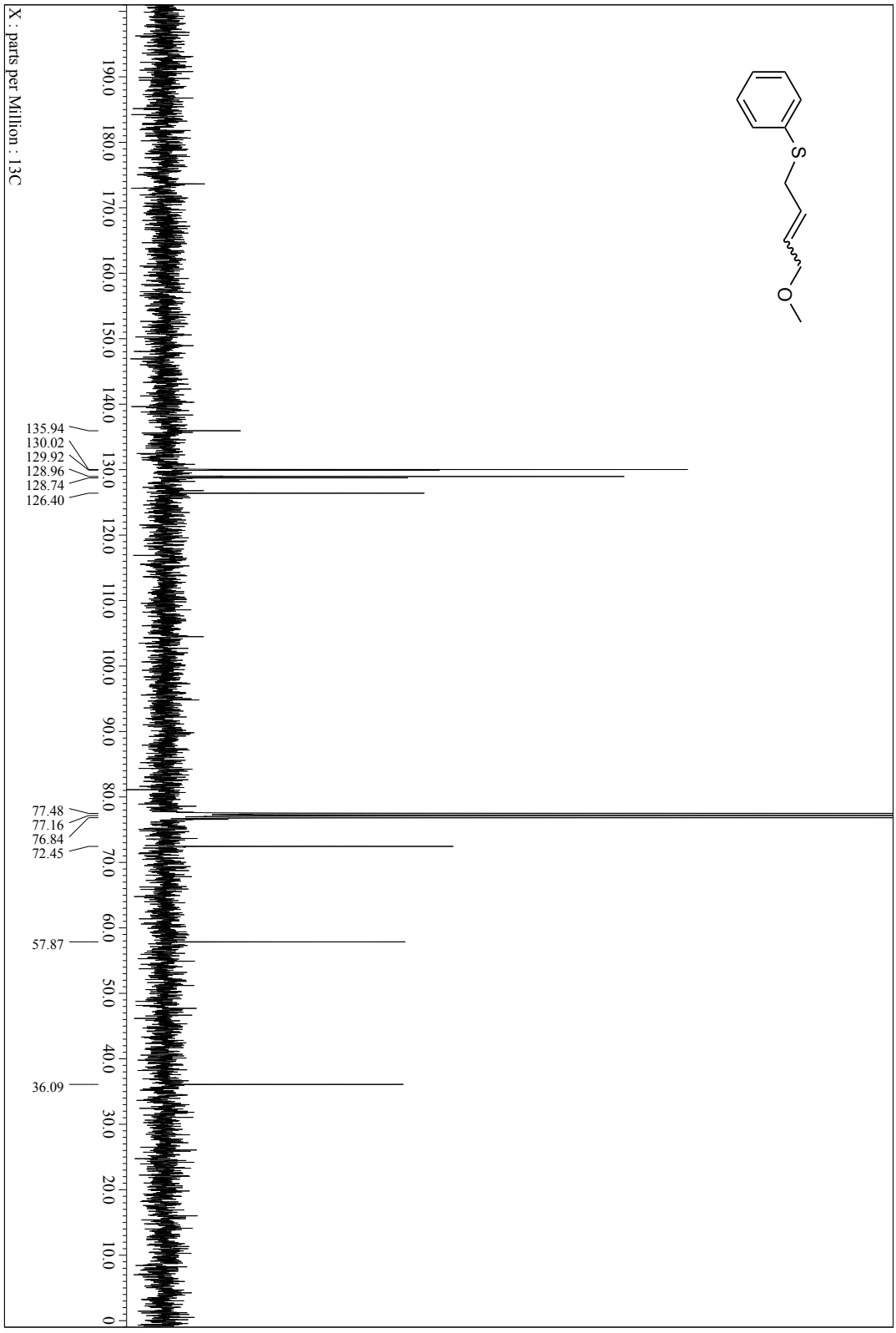

Fig. S145.

^{13}C NMR spectra of **S52**.

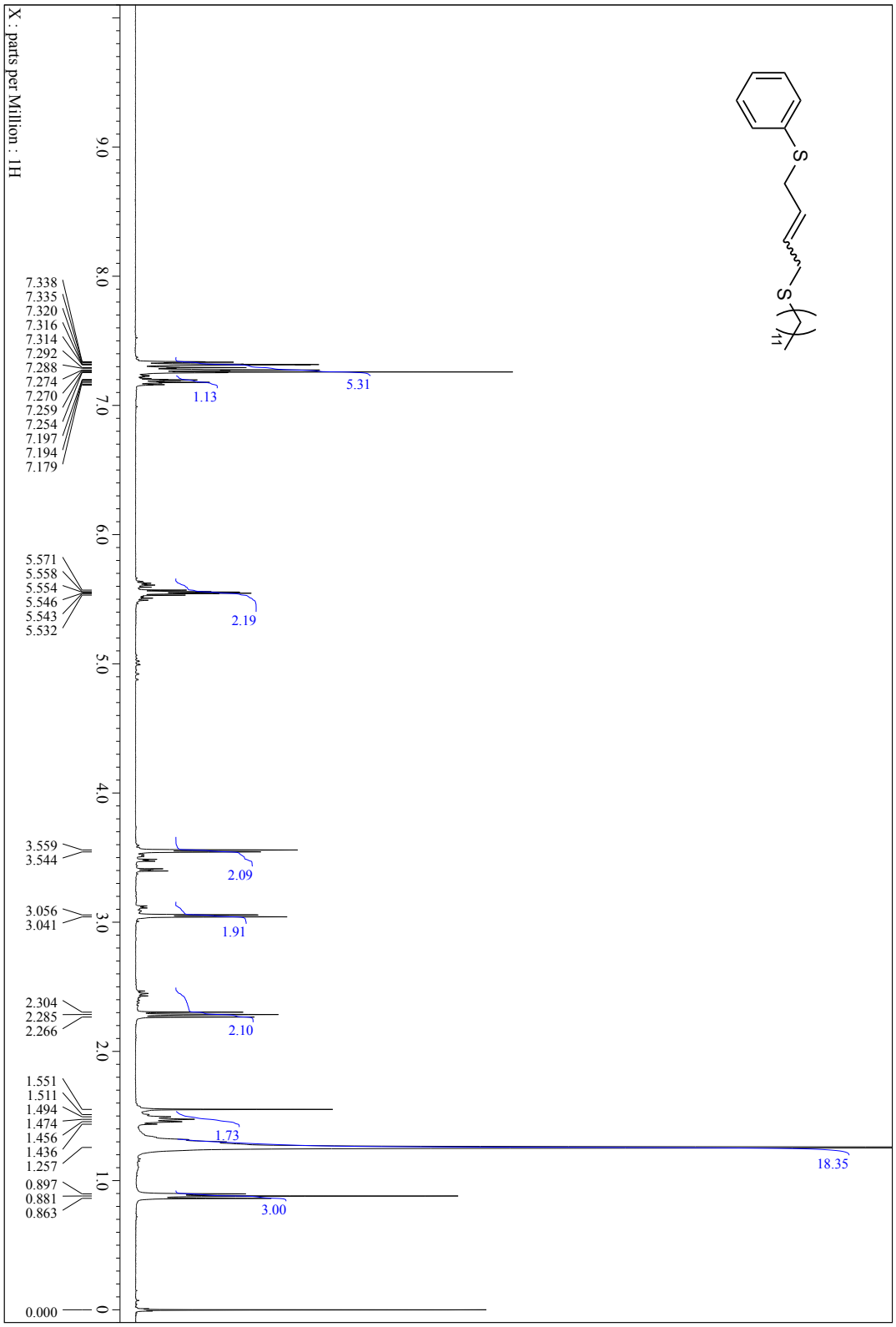

Fig. S146.

^{1}H NMR spectra of **S53**.

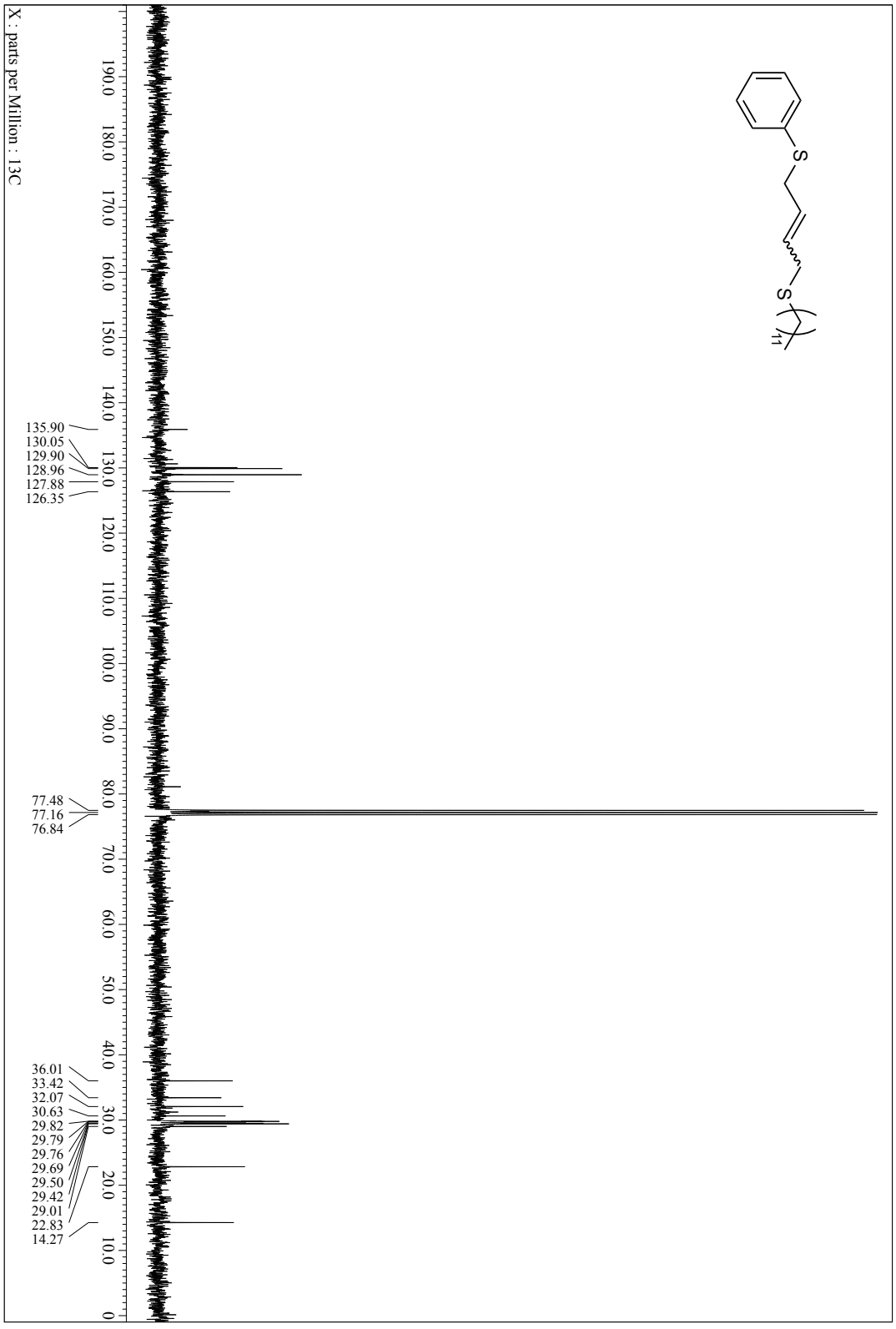

Fig. S147.

^{13}C NMR spectra of **S53**.

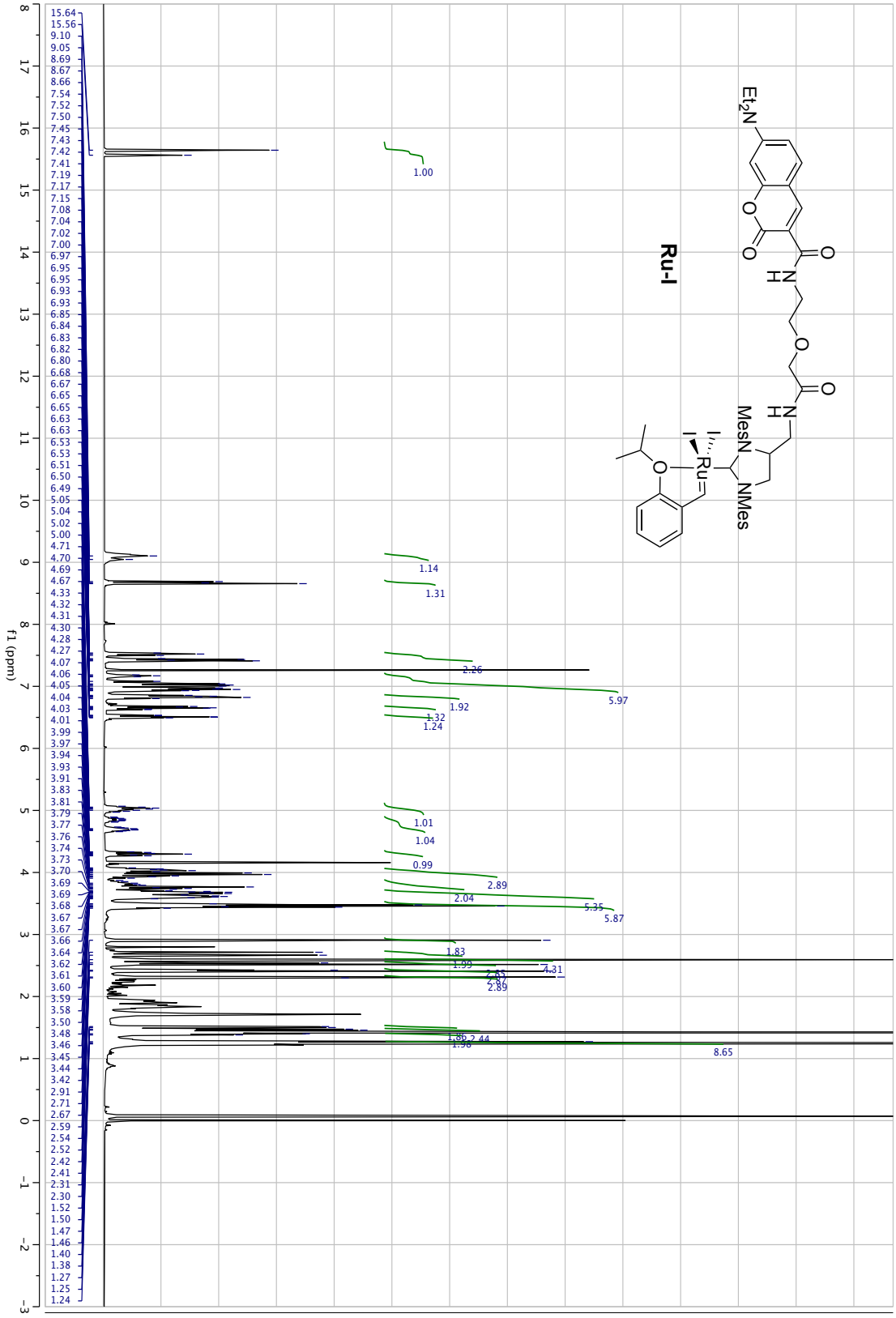

Fig. S148.

^{1}H NMR spectra of **Ru-I**.

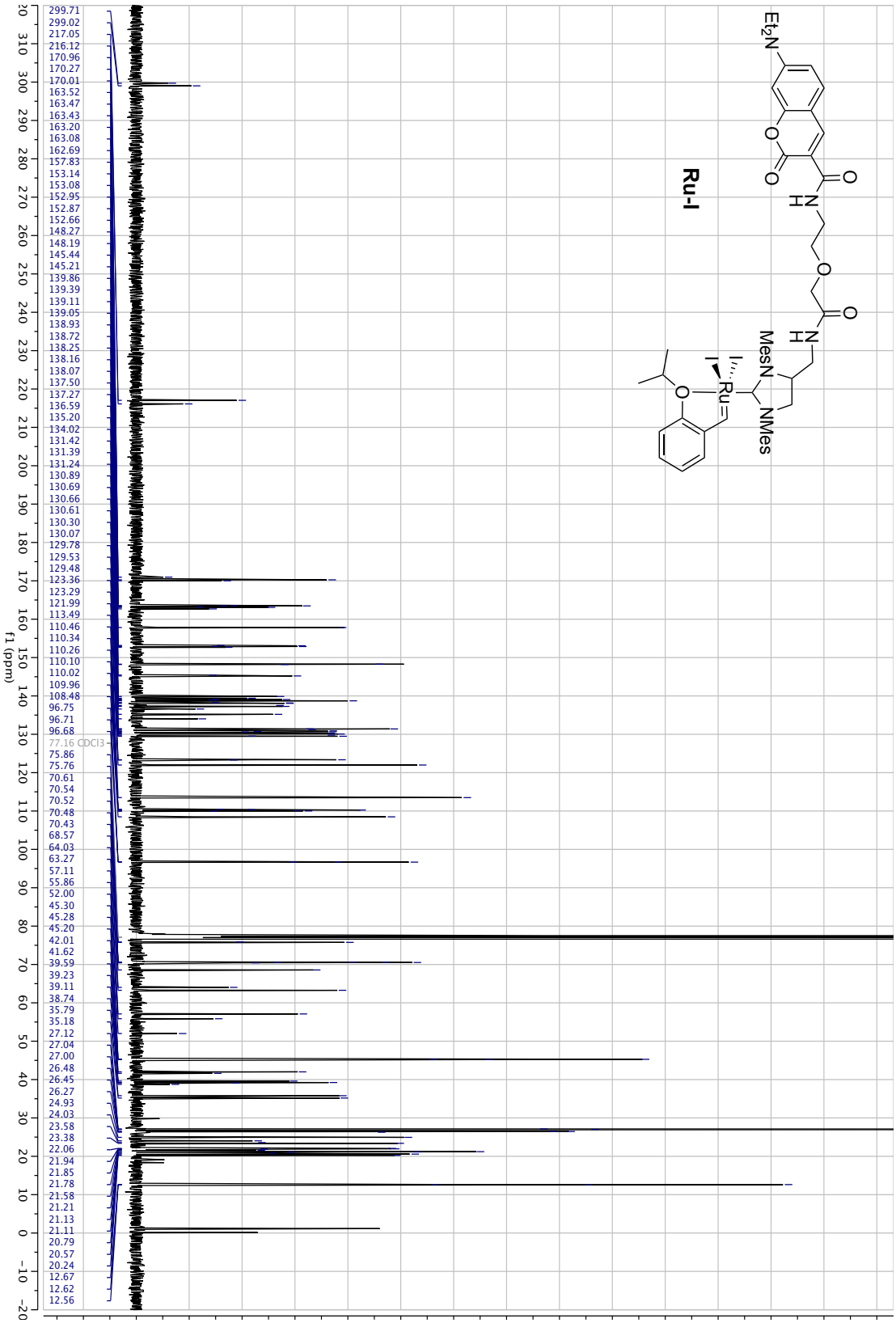

Fig. S149.

^{13}C NMR spectra of **Ru-I**.